IntechOpen

Current Topics in the Utilization of Clay in Industrial and Medical Applications

Edited by Mansoor Zoveidavianpoor

CURRENT TOPICS IN THE UTILIZATION OF CLAY IN INDUSTRIAL AND MEDICAL APPLICATIONS

Edited by **Mansoor Zoveidavianpoor**

Current Topics in the Utilization of Clay in Industrial and Medical Applications
http://dx.doi.org/10.5772/intechopen.71295
Edited by Mansoor Zoveidavianpoor

Contributors

Nazile Ural, Faheem Uddin, Mugera Gitari, Rabelani Mudzielwana, Wen-Chieh Cheng, David Mills, Seyyed Alireza Hashemi, Seyyed Mojtaba Mousavi, Ali Mohammad Amani, Abdullah Shahrani, Aziz Fihri, Gasan Alabedi, Ihsan Taie, Raluca Ianchis, Tatiana Munteanu, Claudia M Ninciuleanu, Ioana C Gifu, Elvira Alexandrescu, Silviu Preda, Bogdan Trica, Cristina L Nistor, Sabina G Nitu, Cristian Petcu, Carlos Maurício Vieira, Lucas Amaral, Sergio Monteiro

Notice

First published in London, United Kingdom, 2018 by IntechOpen
eBook (PDF) Published by IntechOpen, 2019
IntechOpen is the global imprint of INTECHOPEN LIMITED, registered in England and Wales, registration number: 11086078, The Shard, 25th floor, 32 London Bridge Street
London, SE19SG – United Kingdom
Printed in Croatia

British Library Cataloguing-in-Publication Data
A catalogue record for this book is available from the British Library

Additional hard and PDF copies can be obtained from orders@intechopen.com

Current Topics in the Utilization of Clay in Industrial and Medical Applications
Edited by Mansoor Zoveidavianpoor

p. cm.

Print ISBN 978-1-78923-728-3

Online ISBN 978-1-78923-729-0

eBook (PDF) ISBN 978-1-83881-554-7

Meet the editor

Dr. Mansoor Zoveidavianpoor has over 18 years of multidisciplinary oil and gas experience, built upon his technical, operational, and management roles in the industry and academia. Mansoor holds a BSc in Geology, and MSc and PhD degrees both in Petroleum Engineering. He has been involved in different disciplines such as geology, flow assurance, piping construction, artificial intelligence, environmental engineering, petroleum engineering, and project management. He has lectured several courses at the University Technology Malaysia (UTM), Petroleum University of Technology, and Islamic Azad University. He is a member of the Society of Petroleum Engineers and registered as a chartered petroleum engineer. He has published more than 50 publications in international peer-reviewed journals and conferences, has contributed to five textbooks, and served in many scientific committees. Previously he worked as an assistant professor at UTM and currently works as a senior petroleum engineer at the National Iranian Oil Company. Mansoor is actively involved in multidisciplinary studies and currently his main focus is on integrated reservoir management.

Contents

Preface

It is not surprising that due to their common availability and extraordinary properties, clays are currently receiving so much attention in science and engineering. In addition to their multidisciplinary endeavor, there is a need to bring together the scattered literature on the varied disciplines that make up clay science and engineering. This book presents recent developments and research activities that highlight the importance of clay science and engineering in the environment and medical and civil engineering. The book contains nine chapters separated into three main sections: (1) Clay for the Environment, (2) Clay in Civil Engineering, and (3) Clay in Medical Applications. There are four chapters in the first section and the focus is on topics related to an introduction to the natural sources and chemical structure of one of the important clay types, montmorillonite. The application of waste recycling and the removal of arsenic and fluoride are the focus of the next two chapters. In addition, a technique for corrosion protection is presented as the fourth chapter within this section. In the second section, special emphasis has been placed on the importance and application of clay in civil engineering, which is demonstrated in two chapters. In the third section, new research and development in utilizing clay minerals in medical applications is presented. Intended for readers wishing to acquire an understanding of the current trends in clay science and engineering and comprehension of the issue, this book addresses exciting topics in this field.

Mansoor Zoveidavianpoor, PhD
Sr. Petroleum Engineer
National Iranian Oil Company (NIOC)—Arvandan Oil and Gas Company (AOGC)
Khorramshahr, Khuzestan, Iran

Section 1

Clay for the Environment

Chapter 1

Montmorillonite: An Introduction to Properties and Utilization

Faheem Uddin

Additional information is available at the end of the chapter

http://dx.doi.org/10.5772/intechopen.77987

Abstract

Clay mineral is an important material available in nature. With an increasing understanding of clay structure, montmorillonite is realized viable for an enhanced performance in a variety of materials and products in the areas of catalysis, food additive, antibacterial function, polymer, sorbent, etc. Significant development in the use and application of montmorillonite is seen in recent time. This chapter provides an overview of montmorillonite, structure, and properties and particularly discusses its recent utilization in important materials. Montmorillonite is introduced in terms of its natural sources, chemical structure, physical and chemical properties, and functional utilization. The important physical and chemical properties are summarized as particle and layered structure, molecular structure and cation exchange effect, barrier property, and water sorption. This is followed by the important functional utilizations of montmorillonite based on the effects of its chemical structure. The important functional utilization of montmorillonite includes food additive for health and stamina, for antibacterial activity against tooth and gum decay, as sorbent for nonionic, anionic, and cationic dyes, and the use as catalyst in organic synthesis. The environment concerns, to date, do not indicate the adversity for particles used as additive. Studies will be useful which are clearly based on any montmorillonite structure to describe environmental effects.

Keywords: clay, montmorillonite, bentonite, water, cationic exchange

1. Introduction

Historically, clay mineral has long benefitted human life and civilization. Being an integral part of earth, its history is older than the creation of man. The divine script of Holy Quran confirmed that man was created using clay. This indicates that clay mineral was present before

the human life began on earth. The ancient Greek philosophy and culture consider clay an important component of life. Currently, the twenty-first century is in the process of appreciating the even growing number of clay applications in material science.

In times when technology was not at the core of human civilization, clay mineral was used as an important form of material to form a variety of products. Its softness, plasticity, porosity, tangibility, pliability, and climatic adaptability, all at affordable cost, were viable characteristics to recognize its usefulness, and introduced several products.

Today, when nanotechnology is the hallmark of scientific world, the contribution of clay mineral is significantly visible as highly useful fillers or additives in polymers for desired effects. Nanoclays, based on montmorillonite, are currently used to modify the polymer performance.

The science of clay was introduced since prehistoric times. Ceramists used nanoparticles since antiquity [1]; however, nanotechnology is the knowingly scientific utilization of nanoparticles. The use of kaoline may be traced back to the third century BC in China. China clay, a traditional name of kaoline, is a mixture of minerals generally containing kaolinite, quartz, mica, feldspar, illite, and montmorillonite [2].

Historically, the use of clay is known in architecture, industry, and agriculture. The production of sun-dried and fired bricks for building construction still follows century-old procedures. Floor tiles, ceramics, earthenware, and pipes for drainage are examples of clay-based products used since ages. An interesting behavior of clay, in producing products, is its ability to swell and to mold in water, and retain the shape of a container when dry.

A common characteristic of clay mineral is a fine-grained natural structure in a sheet-like geometry. The sheet-structured hydrous silicates are generally called phyllosilicates [3]. The natural clay particle is smaller than 0.004 mm in diameter that may range from 0.002 to 0.001 mm for quartz, mica, feldspar, iron, and aluminum oxides [4]. Colloidal clay particles are finer and found in layered silicates (<0.001 mm in diameter).

Clay minerals may be grouped in four types, shown in **Table 1**. The group members vary mainly in the layered structure. These include the kaolinite group, the smectite group (montmorillonite group), the illite group, and the chlorite group [5].

The kaolinite group has three members including kaolinite, dickite, and nacrite; the formula for kaolinite group is $Al_2Si_2O_5(OH)_4$.

The illite group is represented by mineral illite, the only common clay type. The general formula for illite is $(K, H)Al_2\ (Si, Al)_4O_{10}(OH)_2 \cdot XH_2O$. It is an important rock-forming mineral and main component of shales. The structure of this group is similar to the montmorillonite group with silicate layers sandwiching an aluminum oxide/hydroxide layer in the same stacking sequence.

The chlorite group is relatively large. This group is not necessarily considered as part of clays; therefore, it is placed as a separate group in phyllosilicate. The members in chlorite group are mesite, chamosite, cookeite, and daphnite with varying formulas and structures. There is no general formula.

The variety of clay minerals is based on the arrangement of tetrahedral and octahedral sheets. For example, 1:1 clay mineral would have one tetrahedral and one octahedral sheet per clay

S. no	Group name	Member minerals	General formula	Remarks
1.	Kaolinite	Kaolinite, dickite, nacrite	$Al_2Si_2O_5(OH)_4$	Members are polymorphs (composing of the same formula and different structure.
2.	Smectite	Montmorillonite, pyrophyllite, talc, vermiculite, sauconite, saponite, nontronite	$(Ca, Na, H)\ (Al, Mg, Fe, Zn)_2\ (Si, Al)_4O_{10}(OH)_2 \cdot XH_2O$	"X" indicates varying level of water in mineral type.
3.	Illite	Illite	$(K, H)Al_2\ (Si, Al)_4\ O_{10}(OH)_2 \cdot XH_2O$	"X" indicates varying level of water in mineral type.
4.	Chlorite	**i.** Amesite, **ii.** Chamosite, **iii.** Cookeite, **iv.** Nimite, and so on	**i.** $(Mg, Fe)_4Al_4Si_2O_{10}(OH)_8$ **ii.** $(Fe, Mg)_3\ Fe_3\ AlSi_3O_{10}(OH)_8$ **iii.** $LiAl_5\ Si_3O_{10}\ (OH)_8$ **iv.** $(Ni, Mg, Fe, Al)_6\ AlSi_3O_{10}(OH)_8$	Each member mineral has a separate formula. This group has relatively larger member minerals and sometimes considered as separate group not as part of clays.

Table 1. Major groups of clay minerals [5].

S. no	Clay mineral group	Layer type	Layer charge
1.	Kaolinite	1:1	<0.01
2.	Montmorillonite or smectite	2:1	0.5–1.2
3.	Illite	2:1	1.4–2.0
4.	Vermiculite	2:1	1.2–1.8
5.	Chlorite	2:1:1	Variable

Table 2. Sheet structure for the layers of clay minerals [7].

layer; 2:1 clay mineral would contain two tetrahedral sheets and one octahedral sheet sandwiched between the two tetrahedral sheets (montmorillonite is an example of clay mineral having 2:1 sheet structure); and 2:1:1 clay minerals are composed of an octahedral sheet adjacent to a 2:1 layer [6]. The sheet structure for the layers of various clay minerals with the possible charge is shown in **Table 2** [7].

Natural reserves of montmorillonite are present in various parts of the world. An earliest discovery of montmorillonite was indicated in 1847 in Montmorillon in the Vienne prefecture of France. However, the use of montmorillonite for medicinal purposes may be in over 200 cultures including the ancient Egyptians, pre-Aztec Amargosians, natives of Mexico, South Americans, and North Americans [8].

The names used for montmorillonite are known in different languages, including montmorillonita (Portuguese, Catalan, and Spanish), montmorilloniet (Dutch), and montmorillonit (German, Hungarian, Slovak) [9].

The major montmorillonite deposits found at five places include Himalayas (China), Urals (Pakistan), Caucasians (Georgia, Russia), Andes (Peru, Ecuador), and Wasatch (UT, USA) [10].

2. Bentonite

Bentonite is an important rock of clay found in nature. It is an important source of montmorillonite in nature. It is a rock formed of highly colloidal and plastic clays mainly composed of montmorillonite [2]. In addition to montmorillonite, bentonite may contain some amount of crystalline quartz, cristobalite, and feldspar.

The variety of bentonite applications are the result of its useful and interesting chemical and physical properties. This range of properties include rheology, sorbent effects, plasticity and lubricity, high dry bonding strength, high shear and compressive strength, impermeability, and low compressibility [11].

Natural bentonite particles are indistinguishable from kaolin clay minerals viewed under scanning electron microscope; however, the main difference indicated was thickness. Sodium or potassium salts of bentonite exfoliate into thin plates that could be of 1 nm in thickness theoretically [12].

In general, the clay minerals based on bentonite may exhibit the properties of thixotropic gel formation with water, high water absorption, and high cation exchange capacity (CEC). These properties could be varied in clay minerals depending upon the nature of interstitial water and exchangeable cations in the interlayer space.

Bentonite, which mainly contained montmorillonite, was discovered in about 1890 in USA, and the name "bentonite" is associated with the name of an American geologist for the one time Fort Benton in the eastern Wyoming Rock Creek area, USA [2].

Montmorillonite derived from bentonite may contain sodium or calcium. Sodium montmorillonite is the main fraction in bentonite found in combination with 10–20% of various minerals including feldspar, calcite, silica, and gypsum [10].

3. Montmorillonite structure

The physical structure of montmorillonite particle is generally perceivable in sheets and layers. Each layer is composed of two types of structural sheets: octahedral and tetrahedral. The tetrahedral sheet is composed of silicon-oxygen tetrahedra linked to neighboring tetrahedra by sharing three corners resulting in a hexagonal network. The remaining fourth corner of each tetrahedron forms a part to adjacent octahedral sheet. The octahedral sheet is usually composed of aluminum or magnesium in sixfold coordination with oxygen from the tetrahedral sheet and with hydroxyl. The two sheets together form a layer. Several layers may be joined in a clay crystallite by interlayer cations, by Van der Waals force, by electrostatic force, or by hydrogen bonding.

Theoretical formula and structure is indicated in **Figure 1** [13]. The important natural physical properties of montmorillonite are given in **Table 3**. The best field indicators are softness, color, water, soapy feel, and expansion with water absorption.

The variation in the chemical formula of montmorillonite is possible resulting from the modifiable structure. The cation substitution introduces charge imbalance. Therefore, the chemical composition can vary. The exact theoretical formula is never seen in nature [13]. However, the structure in nature in any form consists of water molecules.

The chemical formula for montmorillonite discovered at Montmorillon, France, is $(Ca_{0.14}\ Na_{0.02})_{\sum = 0.16}\ (Al_{1.66}\ Mg_{0.36}\ Fe_{0.04})_{\sum = 2.08}\ (Si_{3.90}\ Al_{0.10})_{\sum = 4.00} O_{10}\ (OH)_2\ 1.02H_2O$.

The oxide composition comprises silicon and aluminum oxides; however, it was predominantly calcium montmorillonite discovered at Montmorillon. The dominant fractions were SiO_2 and Al_2O_3, where SiO_2 was slightly more than the 50% of total oxides.

The elementary molecular structure is based on units comprising silica tetrahedron and aluminum octahedral. The cation Si^{+4} is fourfold and possesses tetrahedral coordination with oxygen, while the cation Al^{+3} occurs in sixfold or octahedral coordination.

A layered structure is influenced by the presence of charge in tetrahedral and octahedral sheets. Isomorphous substitution in clay mineral mainly produces charge. Isomorphous

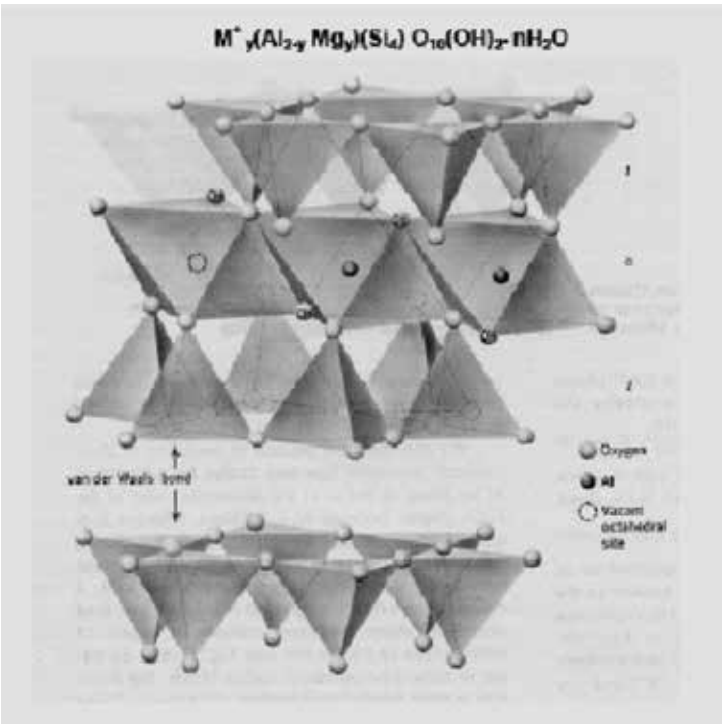

Figure 1. Theoretical formula and structure of montmorillonite (source: Nanocor Inc., IL (USA) [13]).

S. no	Property name	Description
1.	Density	2–3 g/cm^3 (measured)
2.	Crystal system	Monoclinic
3.	Hardness	1–2 on Mohs scale, soft, possess fine-grained occurrence
4.	Fracture	Irregular, uneven
5.	Cleavage	Perfect
6.	Luster	Earthy, dull
7.	Transparency	Translucent
8.	Color	White, buff, yellow, green, rarely pale pink to red (presence of high valance Mn produces pink to red coloration)

Table 3. Important natural physical properties of montmorillonite [9].

substitution is the replacement of an element with another element in mineral crystal without modifying its chemical structure. For example, Al^{3+} can replace Si^{+4} in tetrahedral coordination and replacement of Al^{3+} is possible by Mg^{2+}, Fe^{2+}, Fe^{3+} in octahedral coordination.

The sheets present in montmorillonite are composed of 2:1 structure. The sheets in the crystal plane have a negative charge and hydroxyl groups linked to aluminum or magnesium. The electrostatic force is primarily the force of attraction between the sheets; however, it is fragile.

Chemical composition, ionic substitution, layer structure, and particle size of natural clay minerals have important role in creating a variety of minerals with specific characteristics. However, sheet structure was used to classify the clay minerals, and chemical composition was used for nomenclature.

4. Montmorillonite in nanoclay

Montmorillonite is the basic raw material used in producing nanoclay. Chemically, it can be described as hydrated sodium calcium aluminum magnesium silicate hydroxide, $(Na, Ca)_{0.33}$ $(Al\ Mg)_2$ (Si_4O_{10}) $(OH)_2$ nH_2O [8]. The interaction between nanoclay particles and polymer matrix significantly depends upon the hydroxyl groups and charges present in the nanoclays particle.

In clay-polymer system, the clay nanoparticle can be intercalated or exfoliated. Where clay crystal is used as nanoparticle, it can be referred as intercalated clay (in this case, the polymer chains are between the clay platelets), and when the single particle of clay is the constituent unit, it is referred as exfoliated (i.e., clay platelets are isotropically dispersed in polymer). The important required characteristics include are particle size, surface area, and aspect ratio.

The length and breadth of the particles can range from 1.5 μm down to few tenths of a micron [14]. The third dimension of particle, in the study, is described as thickness, width, or diameter; however, diameter may be used. The diameter of the particle is exceptionally smaller relative

to its length, measuring to only one-billionth part of a meter (=1 nm). Therefore, an extremely high average length-to-diameter ratio (called aspect ratio) of 200–500 is achievable.

An increased aspect ratio produces a higher surface area. A smaller mass of nanoclay shows a high surface area, for example, typically 1 g of a nanoclay product is known to have a surface area in excess of 750 m^2 [15]: that is an equivalent area to nine soccer fields [16].

Nanoclays are available containing over 98% montmorillonite. The variable colors are the result of substitution of interlayer-cations by iron, titanium, and manganese within the lattice structure and depend upon the level of substitution and valence state of cations [13].

Montmorillonite is required to be surface modified to become organophilic and easy to disperse in polymers. Organophilic montmorillonite is produced using organic cation substitution.

The progress in the study to modify the structural composition of montmorillonite, its processing, and surface treatment may be indicated by the achievement of 40 patents issued to one commercial organization [17]. Montmorillonite nanoclay has experienced a variety of utilizations.

Montmorillonite nanoclay is indicated as a drug carrier system and as an additive. Montmorillonite composite for application in drug system can be produced through the utilization of anionic, cationic, and nonionic surfactants to enhance basal spacing resulting in organoclay to be used in drug loading and drug release. Important aspects in a drug carrier system including drug entrapment, molecular level interactions, analysis for a sustained drug release, and targeted drug release are reviewed [18].

This review discussed various aspects of montmorillonite nanoclay such as structure, properties, multifarious applications, and the results of biocompatibility studies.

Significantly rich intercalation chemistry at a reduced cost is an important reason in producing montmorillonite-polymer nanocomposites. Such hybrid materials, also termed as polymeric nanocomposites (PNC), received extensive interest in research and industry. PNC materials on the nanoscale level exhibit advantageous effects in mechanical properties, heat distortion temperatures, thermal stability, flame retardancy, and enhanced barrier properties.

Commercially, several desired effects obtained in PNC are resulting in an increasing consumption of montmorillonite. The combination of improved properties, including the weight reduction and low cost in the final product, resulted in important commercial applications in automotive and packaging, and so on. The significant findings in the montmorillonite- polymer nanocomposites are reviewed for material types: elastomers, thermosets, and polymers from natural resources or biopolymers [19].

The volume of recent research literature clearly indicates the interest and growing consumption of clay minerals particularly montmorillonite. In addition to natural montmorillonite applications, the studies are concentrating in the development of montmorillonite as nanoclay/organophilic clay through modifications in its physical and chemical structures. The utilization of nanoclay is discussed in the following sections where performance effects of montmorillonite are described.

5. Functional properties

5.1. Cation exchange property

Cation exchange capacity is a property of soil introduced by clay and organic matters. It is the capacity of soil to hold cations (generally Al^{3+}, Ca^{2+}, Mg^{2+}, Mn^{2+}, Zn^{2+}, Cu^{2+}, Fe^{2+}, Na^{+}, K^{+}, H^{+}) [20] and described as the quantity of positively charged ions held by the negatively charged surface of clay minerals. It may also be termed as cation exchange capacity (CEC) that may be measured as a centimol positive charge per kg of soil or milli-equivalent (meq) of positive charge per 100 g of soil.

Fine-grained particles of clay result in an increased surface area per unit mass. Smaller particle size (0.002–0.001 mm in diameter) results in a significantly higher surface area, where a large number of cations can be adsorbed. Theses adsorbed cations impart significant level of electrical conductivity in clay [21].

Ionic substitution in the sheet structure produces useful modifications. Ions like Fe^{3+} and Al^{3+} are small enough to enter the tetrahedral coordination with oxygen and substitute Si^{4+}. Similarly, cations like Mg^{2+}, Fe^{2+}, Fe^{3+}, Li^{1+}, Ni^{2+}, and Cu^{2+} can substitute Al^{3+} in the octahedral sheet [22]. Large-sized cations such as K^{+}, Na^{+}, and Cs^{+} are located between the layers and referred as interlayer cations.

5.2. Electrical conductivity

Clay particles are the porous materials. The pore fluid influences the electrical conductivity. The electrical conductivity (mS/m) of a porous material is the combination of electrical conductivities of the matrix material and the pore fluid [23].

Air, water, or saline water may be present in the pore. When the pore fluid is of low conductivity, for example, air or water, the bulk conductivity of clay mineral is contributed by the matrix material. Pore fluid having a higher electrical conductivity significantly enhances the total electrical conductivity of clay, for example, clay particles with a significant porosity level (40–50%), and saline water present in the pore; then the bulk conductivity is mainly the contribution of pore fluid. In this case, there would be negligible difference in the conductivities of sand and clay.

A higher content of clay particles with 2:1 structure present in montmorillonite sample produces an increased bulk electrical conductivity for non-saline soils [24]. This effect was attributed to the exchangeable cations or to proton transfer from the dissociation of interlayer water content. A reduced level of interlayer water contents in K-saturated clays resulted in the lowest electrical conductivity.

Since the clay content, pore fluid, clay type, saline water, and water saturation influence the soil conductivity, the assessment of electrical conductivity of reservoir rock may be used to estimate these factors [25]. However, the variation in the distribution of liquid and solid phases introduces the variation and complication in the electrical conductivity of heterogeneous porous medium.

The distribution of electrical ions around clay pores is called membrane polarization. In membrane polarization, the negative ions are oriented to one end of the pore under the influence of DC potential across the clay pore, and this polarization resists the current flow.

In the study of soil, the clay content in soil can be determined using electrical conductivity and membrane polarization as the function of clay content.

5.3. Heat resistance

Montmorillonite is a good heat insulator, and heat-resistant effects are obtainable using it as an additive in any substance. This is an area of significant research to produce thermal barrier effects in composite material structure.

Thermal barrier properties of clay minerals had been used in heat-resistant and flame-retardant applications. Nanoclay is currently used extensively and investigated in polymer composite to obtain an increased thermal stability and flame retardancy.

The variation in the expansion, under heat effects, for metals, polymers, and ceramics had been noted. Generally, the order of thermal expansion magnitude in polymer, metal, and ceramic may be indicated as follows:

$$\text{Polymer} > \text{metal} > \text{ceramic}.$$

This relative order is based on the values of linear thermal expansion coefficient which are in the range of 20–100, 3–20, and 3–5 ppm/°C for polymers, metals, and ceramics, respectively [26].

Therefore, an increased thermal stability of montmorillonite introduces its use as a filler in producing polymers to impart a low thermal expansion. However, enhancement in polymer thermal stability requires an increasing aspect ratio, and an aspect ratio of greater than 100 is useful.

5.4. Water sorption

Water sorption is an important characteristic of natural clay particles. Clay particles can absorb or lose water in response to changes in humidity content in the ambient environment; when water is absorbed, it fills the spaces between the stacked silicate layers [27].

Montmorillonite typically exhibits a gradual dehydration and phase change to a stronger nonexpendable clay. The specific gravity of any type of clay is variable resulting from loss or gain of water. Most of the known clay types are available in nature as a mixture containing several varieties including carbonates, feldspars, micas, and quartz.

Several studies addressed the swelling behavior of montmorillonite. The interaction of montmorillonite with water introduces useful effects. Water molecules cause swelling in montmorillonite. This swelling is a result of complex montmorillonite-water interactions between particles and within the particle itself.

Water molecule adsorption and swelling of montmorillonite introduce hydrated states and hysteresis. The migration of counter-ion, initially bound to montmorillonite surface to the central interlayer plane, leads to swelling in montmorillonite. Therefore, charge locus in montmorillonite has a strong influence on swelling dynamics [28].

An important concern in clay mineral study is how the monovalent and divalent cations affect the swelling pattern of K^+-, Na^+-, and Ca^{2+}-montmorillonites.

Montmorillonite is a 2:1 clay mineral; that is, two tetrahedral sheets separated by one octahedral sheet. The montmorillonite platelets can be negatively charged when

i. tetrahedral substitution of Si by Al in two tetrahedral sheets, or

ii. octahedral substitution of Al by Mg in central octahedral sheet.

In any of the above two (i and ii) cases, negative charge produced is compensated by interlayer ions. The hydration of interlayer cations produces swelling [29].

The small platelet size and stacking structure are indicated as complicated to accurately characterize through experiment. Therefore, molecular dynamic simulation (MDS) is a useful way of understanding the atomic level structure. MDS is useful to study montmorillonite structure including swelling and hydration of interlayer cations. MDS was performed for K^+-, Na^+-, and Ca^{2+}-montmorillonites with varying level of water content.

The valence of the cations showed a significant influence on montmorillonite-water system. Simulations indicate that the cation K^+ shows a strong interaction with dehydrated montmorillonite sheets; however, in case of hydrated montmorillonite sheets, cation Ca^+ interacts strongly. Therefore, the layer spacing of simulated K^+-, Na^+-, and Ca^{2+}-montmorillonites was obvious.

The simultaneous measurement of swelling and swelling pressure was done using a researcher- developed cell [30]. Undisturbed clay samples at a defined swelling (0–75%) were removed from the cell and analyzed using SEM, FTIR, and ATR (micro- attenuated total reflectance) spectroscopy. Silicate (Si-O)-stretching region (1150–950 cm^{-1}) showed significant changes with variation in swelling and orientation. It was found that the reduced particle size with increased swelling was related to increased misorientation of the clay platelets. The rearrangement of clay platelets was observed as a direct result of the breakdown of the clay particles with increased hydration.

6. Functional utilization

The addition of montmorillonite in material, polymer, and products may result in significant enhancement in the required performance. Interestingly, there is a great variety of montmorillonite utilization as an additive in composite or as a functional filler in polymers. The results obtained indicated useful effects. Examples included the applications as food additive for health and stamina, for antibacterial activity, as sorbent for nonionic, anionic, and cationic dyes, and as catalyst in organic synthesis, and so on.

The variety of montmorillonite utilization in material and product performance is significant in recent literature. The following sections describe the important useful effects that are obtainable using the selected type of montmorillonite.

6.1. Resistant to nausea and diarrhea

Dietary toxins, bacterial toxins, and metabolic toxins can be absorbed by clay to resist nausea, vomiting, and diarrhea. Montmorillonite-based product is indicated to work immediately on the digestive channel and bind the toxic substances resulting in their removal from the body through the stool [31].

The effects of montmorillonite-zinc oxide hybrid on diarrhea, intestinal permeability, and morphology were investigated on a total of 180 piglets. Piglets were divided in five groups and studied for 2 weeks using dietary treatment with montmorillonite and montmorillonite-ZnO in diet. Importantly, results obtained indicated that the dietary addition of 500 mg/kg of Zn from MMT-ZnO was similar to 2000 mg/kg of Zn from ZnO, and more effective relative to montmorillonite alone or 500 mg/kg of Zn, from ZnO, for the growth enhancement of piglets, alleviating diarrhea, improving intestinal microflora, mucosal barrier integrity, and morphology of weaned pigs [32].

6.2. Supportive to health and growth

The use of calcium montmorillonite (Nova Sil clay type) in human diet can diminish health-harming effects of aflatoxin-contaminated food. The study was based on a clinical trial of selected volunteers in the age range of 20–45 years. It included 23 males and 27 females. The volunteers received calcium montmorillonite low dose (1.5 g/day) and high dose (3 g/day) for weeks. The compliance to study trial by the volunteers was indicated as 99.1%.

Laboratory analysis of blood and urine samples was performed prior and after trial. Hematology, liver and kidney function, electrolytes, vitamins A and E, and minerals were not significantly changed in any study group. The study indicated the protection of participant from adverse effects of aflatoxins [33].

Montmorillonite can be the source of mineral for bacterial nutrition and found to maintain the pH levels required for a sustained growth [34]. Several bacterial species differing in morphology, motility, and Gram reaction were assisted in respiration by montmorillonite. The research results obtained show the relationship between clay minerals (montmorillonite and kaolinite), and population growth and ecology of microorganism in natural habitat.

6.3. Resistance to tooth decay

Another important obtainable effect is the resistance to tooth decay. Tooth decay can be resisted by filling micro-pore using a fluid resin which polymerizes *in situ* and creates a micromechanical interlock in the tooth structure. This bonding process is a selective substitution for tooth minerals. The use of montmorillonite as a reinforcing filler for dental adhesives (typically methacrylate monomers with solvent and a photo initiator) may be possible.

Results obtained for flexural strength, elasticity modulus, tensile strength, and thermal resistance on the applied dental adhesive, using montmorillonite as an additive, were encouraging. Adhesive produced with dimethacrylate copolymer and montmorillonite (0.2% concentration) showed significant performance as a dental adhesive. Improved performance obtained using 0.2% concentration of montmorillonite, indicated by X-ray diffraction (XRD) test results, was attributed to its exfoliated morphology. The resulting dental adhesive reduces the weakening of tooth structure. However, the highest concentration of 1.5% produced agglomerated clay and no significant performance enhancement [35].

The use of montmorillonite as a filler may be possible in any of the following morphologies:

i. Agglomerated particle comprising the particle with a joined layer structure. The surface particle interacts with a polymer or a substrate.

ii. Intercalated form, where a polymer or a substrate molecule can be between platelets.

iii. Exfoliated form where platelets are isotropically dispersed in polymer or substrate molecules.

6.4. Drug delivery system

Adsorption and swelling characteristics of montmorillonite are useful in drug delivery systems. An increased adsorption capacity provides improved drug entrapment and sustained release of pharmaceutical drugs. Solubility, dissolution rate, adsorption, and bioavailability of hydrophobic drugs are enhanced by montmorillonite. The effects of montmorillonite in improving the drug delivery system were reviewed [36].

6.5. Adsorption of dyestuff

Effluent loading, from dyeing industries and textile-processing units, to natural environment is a serious concern. Technological solution is required to remove residual dye content from the used water. The application of montmorillonite as an adsorbent for cationic dye is an important effect. The removal of cationic dye, methylene blue, from water is achievable through adsorption process. Montmorillonite concentration used for the removal of cationic dye depends upon the initial dye concentration, contact time, solution pH, and temperature. Results obtained on dye adsorption demonstrated the equilibrium data follow the Langmuir isotherm equation [37].

Thermodynamic study of methylene blue adsorption on montmorillonite indicates that the process is endothermic revealed by the determination of enthalpy, entropy, and Gibb's free energy. Importantly, the results support the possibility of using montmorillonite as low-cost adsorbent for wastewater treatment containing cationic dyestuff. There is a large number of textile dyeing industries, in India, Pakistan, and China, that release used dye bath water containing cationic dyestuff. Adsorption system developed using montmorillonite can be useful for water recycling in dyeing industries.

Possibly, montmorillonite can be used to influence the optical, chemical, and spectral characteristics of cationic dyes. The layer charge of montmorillonite can affect the cationic dye molecular aggregation. The subject was reviewed through the research literature discussing dye reaction with clay minerals [38].

6.6. Adsorption of toxic heavy metals

An important application of adsorption properties of montmorillonite is seen in the removal of toxic heavy metals from aqueous solution. The adsorption studies using montmorillonite and kaolinite for the removal of toxic metals including As, Cd, Cr, Co, Cu, Fe, Pb, Mn, Ni, and Zn were reviewed [39].

Montmorillonite and its modified forms exhibited a significantly increased metal adsorption capacity relative to kaolinite and modified kaolinite. The modified clay mineral form was produced by pillaring montmorillonite or kaolinite by using polyoxy cations including Zn^{4+}, Al^{3+}, Si^{4+}, Ti^{4+}, Fe^{3+}, Cr^{3+}, or Ga^{3+}. The modified form can also be produced using quaternary ammonium cations including tetramethylammonium-, tetramethylphosphonium-, and trimethylphosphonium-, N^{-}-didodecyl-N, N^{-}-tetramethylethanediammonium, etc.

Montmorillonite modified using sodium dodecylsulfate (SDS) can remove Cu^{2+} and Zn^{2+} by sorption from aqueous solutions. The study was conducted as a function of solution pH, solute concentration, and temperature (25–55°C). The thermodynamic parameters (ΔH^{o} and ΔS^{o}) for Cu^{2+} and Zn^{2+} sorption on modified montmorillonite were evaluated. The study finds out that the kinetics for the sorption of Cu^{2+} and Zn^{2+} was assessed and the pseudo-first-order rate constant was evaluated [40].

6.7. Montmorillonite in biopolymer

Biopolymer modification using montmorillonite as nanofiller is found to improve the thermomechanical properties. Biopolymer produced from chitosan/montmorillonite nanocomposite through diluted acetic acid used as solvent for dissolving and dispersing chitosan and montmorillonite.

Pure chitosan was compared with chitosan-montmorillonite nanocomposite with and without acetic acid in terms of morphological structure and selected properties. Results obtained in XRD and TEM indicated an intercalated and exfoliated nanostructure at a reduced montmorillonite loading and an intercalated and flocculated nanostructure at an increased montmorillonite loading.

Thermal stability and mechanical properties were determined using TGA and nanoindentation. Thermal stability, hardness, and elastic modulus of nanocomposite matrix improve with the increasing loading of nano-dispersed montmorillonite. Crystallinity, thermal stability, and mechanical properties may be influenced by acetic acid residue in chitosan matrix [41].

The study of montmorillonite in potato starch showed the improvement in thermal and Young modulus properties. Nanocomposite films of glycerol-plasticized starch/ montmorillonite were produced. Three different loadings of montmorillonite aqueous suspension were applied to potato starch.

Dispersion of montmorillonite in starch was studied using X-ray diffraction (XRD). Results indicated that the nanomontmorillonite formed an intercalated structure and complete exfoliation was not observed under the experimental conditions used. Thermogravimetric analysis indicated the enhancement in the thermal resistance with the increased loading of montmorillonite; however, the water absorption by the starch-montmorillonite nanocomposite, at 75%

constant relative humidity, was reduced. The result of micro-tensile test of nanocomposite film showed that Young modulus improved up to 500% at 5 wt.% of montmorillonite [42].

6.8. Effects in fiber-forming polymer

Important properties of fiber-forming polymers may be improved using montmorillonite as a filler [43]. In general, clay mineral (nm) showed flame–retardant effects as assessed by a reduction in the peak heat release rate for various thermoplastic polymers including polystyrene, polyamide-6, polypropylene, polyamide-12, poly(methyl methacrylate), polyethylene, and ethylene vinyl acetate (EVA).

Montmorillonite-nylon-6 (nm) composite was produced through melt bending or compounding technique followed by injection molding using percent loading of organo-montmorillonite (nm) composites ranging 0–5 wt.% content. The desired properties of tensile and flexural properties were indicated optimum at 5 wt.% loading. Other improvement observed includes storage modulus, stiffness, and heat distortion temperature, and the reduction in water absorption relative to virgin nylon-6.

Nanometer-sized particles of montmorillonite may be introduced in polymers/fibers, resulting in an increased resistance to electricity, chemicals, heat and flaming, and enhanced ability to block UV light.

Montmorillonite may be incorporated in fiber-forming polymer through electrospinning/melt spinning. Electrospinning is the technique successfully used for the production of a variety of polymer nanofibers.

The properties of polymer nanofiber produced through electrospinning are influenced by melt viscosity, surface tension, dielectric permeability, electric field strength, solvent properties to evaporate, polymer molecular weight, and concentration.

6.9. Flame-retardant finishing of cotton fiber

Interest in using the clay was observed to obtain the flame-retardant properties in cotton fiber [44]. The two types of local clay samples study to evaluate the flame-retardant effects on bleached cotton fabric.

Aqueous water dispersion was applied to bleached cotton fabric. The finished fabric was assessed using vertical flame-retardant test BS EN ISO 6940 2004. Flame retardancy was improved as indicated by the ease of ignition and the char length of burnt cotton fabric.

6.10. Geological repository for spent nuclear fuel

The growing variety of montmorillonite utilization is perhaps indicated by the use of bentonite in the study to form a part of deep geological repository for spent nuclear fuel. Pure homo ionic Ca-montmorillonite may be considered bentonite-similar system to obtain information on natural bentonite behavior. Water-saturated structure and porosity of Ca-montmorillonite were studied using X-ray diffraction, small angle X-ray scattering, nuclear magnetic resonance, transmission electron microscopy, and ion exclusion. The obtained results indicate multiple porosity for the bentonite structure [45].

Multiple porosity model supports two different groups of water present in bentonite: one present in the interlamellar space and the other found in the volume between clay stacks.

6.11. Bronsted acidity

Synthetic mica-montmorillonite (SMM) shows Bronsted acidity. SMM studied, for Bronsted acidity, was based on

i. isomorphous substitution of Si^{4+} by Al^{3+} in the tetrahedral layer, and additional NiF doping,

ii. the effects on platelets, and

iii. the edge termination of clay platelets.

The evaluation of SMM for adsorption energies using ammonia and pyridine showed the acid strength. The composition of SMM platelets influences the acidity [46]. Interesting results were obtained in the study explaining the Bronsted acidity in relation to the platelet structure.

The strongest acidity was demonstrated by SMM structure where octahedral $[AlO]^+$ was replaced adjacent to tetrahedral [Si-(OH)-Al] moieties in the tetrahedral layer.

Bronsted and Lewis acid catalytic sites in montmorillonite provided the useful applications [47]. The exchangeability of interlayer cations, through ion exchange, helps in altering the acidic nature. Modified montmorillonite types known as montmorillonite-K-10 (produced by the calcinations of montmorillonite) were found as efficient catalysts. Cation exchange produces more effective montmorillonite types including Fe^+ montmorillonite and clayfen.

Sodium montmorillonite (NaMMT) is indicated to accelerate the curing of urea-formaldehyde resin. In acid-curing conditions, urea-formaldehyde resin was used as adhesive for plywood and wood particleboard. Cross-linking of urea-formaldehyde in the presence of NaMMT produces plywood with improved water resistance. An accelerating effect on urea-formaldehyde curing was observed in differential scanning calorimetry results. Dry internal bond strength of wood particleboard increases with small additions of NaMMT [48].

Organic reagents synthesized using montmorillonite types (cation substituted) used as catalyst include α- aryl β-hydroxycyclic amines, silanols, and methyl cinamates, and the production of multi-substituted imidazopyridines, imidazopyrazines, and imidazopyrimidines.

7. Environment concern

Green chemistry is a demanding approach in organic synthesis, where the release of hazardous gases and liquids is undesired. Environment damage and ecological balance are required to be least affected. Montmorillonite is a solid acid used in organic synthesis. It has the potential to replace liquid acid catalyst with greener effects (**Figure 2**).

Natural and modified clays, including montmorillonite, received significant interest as catalyst (Section 7.8). The use of montmorillonite as a greener catalyst in organic synthesis is reviewed [49]. Several clay-based or montmorillonite-based catalysts are available in market including claycop TM, clayfen TM, clayzinc TM, envirocat TM, and so on.

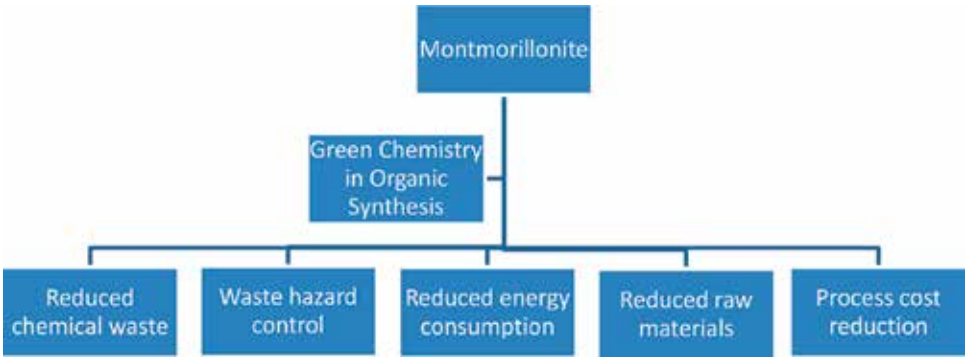

Figure 2. Green chemistry effects in organic synthesis using montmorillonite as catalyst.

Good mining practices have shown bentonite as environmentally not hazardous provided dust abatement mask used. Bentonites demonstrate good performance as sealant and absorbent and used as barrier for landfill and toxic waste repository.

Environmental concern in the extraction, use, and application of clay can range over the environmental characteristics of clay type and its minerals (=minerals present in clay sample). Montmorillonite particles, depending upon the size range, may come in contact with living species. The health and safety concern related to montmorillonite particles received interest for study.

The nature and distribution of inorganic contaminants, such as metals and metalloids like arsenic, iron, and lead, in clay-bearing rocks, may introduce the environmental concerns. These environmental factors may influence the use of clays in natural and industrial applications [50].

Information obtained on environmental effects for industrial minerals, including various clay types, sand, gravel, and crushed stone may not be applicable to montmorillonite composition, and studies will be more useful that is clearly based on any montmorillonite structure.

Information on occupational exposure to bentonite dust in mines, processing plants, and user safety is limited [5]. Varying amount of silica is present in bentonite and kaolin clays; however, there are no reported cases of marked diffuse/nodular pulmonary tissue fibrotic reaction to montmorillonite containing no free silica. Bentonite comprising montmorillonite as major fraction, and kaoline have not shown local or systematic adverse effects in cosmetics. However, these were indicated to cause reduced toxicity toward aquatic organisms.

Particle size and the chemical structure of montmorillonite are two obviously different aspects. The increased concerns in the toxicity of airborne fine (0.1–2.5 μm) and ultrafine (<0.1 μm) particles received research interest. Epidemiological studies indicated an increase in morbidity, and mortality was associated with the rise in airborne particles, particularly in ultrafine size range. The decreasing potencies of quartz, kaolinite, and montmorillonite to introduce lung damage were related to their known relative active surface areas and surface chemistry. Therefore, handling of ultrafine particles requires more vigilant control to abate health effects.

Natural clay particles are smaller than 0.004 mm in diameter; however, manufactured nanoclay particles are in ultrafine size range and have shown toxic properties [1]. These nanoparticles

can enter human body, reaching vital organs through blood circulation. The possibility is therefore indicated for tissue damage. Nanosized particles coming in contact with the tissue may introduce toxicity and health concerns; however, particles incorporated in the bulk materials or polymer products will not be exhibiting such effects.

Therefore, there is clear partition line in risk assessment for two types of particle composition: ultrafine, and agglomerated and bulk material. The properties of nanosized particles are different from the bulk material of the same composition.

Beneficial effects of montmorillonite are known in the form of a voluminous product used effectively and discussed in Section 7. Calcium montmorillonite is also known as "living clay" being containing minerals capable to improve enzyme production in living organisms [51, 52].

It is important that there are several standards practiced, mainly in industrialized regions, addressing the health and safety risks at work places. Therefore, it is unlikely that the future would eliminate montmorillonite uses.

8. Conclusion

Clay minerals have long been benefiting the human and society. Montmorillonite, an important clay type, has received growing interest in utilization as an additive in polymer and products for enhanced effects. Bentonite is an important source of montmorillonite in nature.

The basic molecular structure comprises silica tetrahedron and aluminum octahedral. The cation Si^{+4} is fourfold and possesses tetrahedral coordination with oxygen, while the cation Al^{+3} occurs in sixfold or octahedral coordination. Chemical composition, ionic substitution, layer structure, and particle size of natural clay minerals are important to introduce the functional properties and effects in the application of montmorillonite. Sheet structure was used to classify the clay minerals, and chemical composition was used for nomenclature.

Important applications of montmorillonite include uses additive for food, health, and stamina, for antibacterial activity, improved polymer performance; as sorbent for nonionic, anionic, and cationic dyes; and as green chemistry catalyst in organic synthesis, and so on.

Conflict of interest

The author declares no conflict of interest in publishing this chapter.

Author details

Faheem Uddin

Address all correspondence to: dfudfuca@yahoo.ca

Dadabhoy Institute of Higher Education, Karachi, Pakistan

References

[1] Lauterwarrer C, editor. Opportunities and risks of nanotechnologies. Allianz Report in Cooperation with the OECD International Future Program. June 2005;**4**:10

[2] EHC 231. Bentonite, Kaloline and Selected Clay Minerals. 2005. Available from: www.inchem.org [Accessed: July 9, 2007]

[3] Clay. Columbia Encyclopedia Article About Clay. 2007. Available from: www.Columbia.thefreedictionary.com [Accessed: July 10, 2007]

[4] Sherman LM. Nanocomposites, Plastic Technology. 2007. Available from: www.ptonline.com/articles/200705fa.html [Accessed: July 9, 2007]

[5] Uddin F. Clay, nanoclay and montmorillonite minerals. Metallurgical and Materials Transactions A. December 2008;**39**(**12**):2804-2814

[6] Dennis D. Eberi. Clay Minerals. Available from: htp://www.accessscience.com [Accessed July 09, 2007]. DOI: 10.1036/1097-8542.139900

[7] Anonymous. Clay Minerals. Available from: http://Jan.ucc.nau.edu [Accessed: January 31, 2008]

[8] Anonymous. Montmorillonite. Available from: www.en.wikipedia.org [Accessed: July 9, 2007]

[9] Mindat.org. An Outreach Project of Hudson Institute of Mineralogy. Available from: Mindat.org [Accessed: January 25, 2018]

[10] Anonymous. Montmorillonite Clay. Available from: www.symmetry4u.com [Accessed: July 9, 2007]

[11] Murray H. Report No. 64: Industrial clay case study, International Institute for Environment and Development (IIED). World Business Council for Sustainable Development (WBCSD); March 2002. pp. 6-7

[12] Mini-Encyclopedia of Papermaking, Wet-End Chemistry. Available from: www4.ncsu.edu [Accessed: July 16, 2007]

[13] Nanocor. Technical Data, Polymer Grade Montmorillonite. 2006; Lit. G-10 5 (Revised: 05/05/06). IL, USA: Nanocor Inc

[14] Nanocor. Technical Data, General Information about Nanocore Nanoclay. 2014; G-100 (12/04). IL, USA: Nanocor Inc

[15] Anonymous, Closite^{R}. Additives Nano-Scale Additives for Reinforced Plastics. USA: Southern Clay Products, Inc

[16] Uddin F. Advancement in nanotechnology of polymers and fibers. International Dyer. March 2008:33-35

[17] Nanocor. Technical, FAQ, 3. 2008. IL, USA: Nanocor Inc

[18] Jayrajsinh S, Gauri Shankar D, Agrawal YK, Lateef Bakre D. Montmorillonite nanoclay as a multifaceted drug-delivery carrier: A review. Journal of Drug Delivery Science and Technology. June 2017;**39**:200-209

[19] Bitinis N, Hernandez M, Verdejo R, Kenny JM, Lopez-Manchado MA. Recent advances in clay/polymer nanocomposites. Advanced Materials. November 23, 2011;**23**(44):5229-5236. DOI: 10.1002/adma.201101948

[20] Anonymous. Agronomy Fact Sheet Series (Fact Sheet 22), Cation Exchange Capacity, Cornell University Cooperative Extension. Available from: http://www.css.cornell.edu [Accessed: January 31, 2008]

[21] Anonymous. Estimating Clay Content, US Department of Transportation, Federal Highway Program. Available from: www.cflhd.gov [Accessed: January 29, 2008]

[22] Anonymous. Sci-tech Encyclopedia. McGraw Hill. Available from: www.answers.com [Accessed: July 9, 2007]

[23] Anonymous. Cation Exchange Capacity. Available from: http://en.wikipedia.org [Accessed: January 29, 2008]

[24] Hunt AG, Logsdon SD, Laird DA. Soil Science Society of America Journal. 2006;**70**:15

[25] Niwas S, Gupta PK, de Lima OAL. Current Science. March 2007;**92**(5):612

[26] Rao Y, Blanton TN. Macromolecules. 2008;**41**:935-941

[27] Anonymous. The Clay Mineral Group. Copyright ©1995-2014 by Amethyst Galleries, Inc. Available from: www.mineral.galleries.com [Accessed: August 09, 2007]. pp. 1-2

[28] Emiel JM, Hensen SB. Why clay swell. The Journal of Physical Chemistry B. 2002;**106**(49): 12664-12667

[29] Tao L, Feng TX, Zhao Y, Tao G. Swelling of K^+-, Na^+-, and Ca^{2+}-montmorillonites and hydration of interlayer cations: A molecular dynamics simulation. Chinese Physics B. 2010;**19**(10):109101

[30] Kati K, Kati D. Effect of Clay-Water Interactions on Swelling in Montmorillonite Clay. Available from: www.ce.washington.edu [Accessed: July 9, 2007]

[31] PR Web. Available from: www.prweb.com [Accessed: July 9, 2007]

[32] Hu CH, Gu LY, Luan ZS, Song J, Zhu K. Effects of montmorillonite-zinc oxide hybrid on performance, diarrhea, intestinal permeability and morphology of weanling pigs. Animal Feed Science and Technology. October 11, 2012;**177**(1-2):108-115

[33] Wang JS, Luo H, Billam M, Wang Z, Guan H, Tang L, Goldston T, Afriyie-Gyawu E, Lovett C, Griswold J, Brattin B, Taylor RJ, Huebner HJ, Philips TD. Short-term safety evaluation of processed calcium montmorillonite clay (Noval Sil) in humans. Food Additives & Contaminants. March 2005;**22**(3):270-279

[34] Stotzky G, Rem LT. Influence of clay minerals on microorganisms: I. Montmorillonite and kaolinite on bacteria. Canadian Journal of Microbiology. 1966;**12**(3):547-563

[35] de Menezes LR, da Silva EO. The use of montrmorillonite clays as reinforcing fillers for dental adhesive. Materials Research. 2016;**19**(1):236-242

[36] Park J-H, Shin H-J, Kim MH, Ji-Su K, Kang N, Lee J-Y, Kim K-T, Lee JI, Kim D-D. Application of montmorillonite in bentonite as a pharmaceutical excipient in drug delivery systems. Journal of Pharmaceutical Investigation. July 2016;**46**(4):363-375

[37] Almeida CAP, Debacher NA, Downs AJ, Cottet L, Mello CAD. Removal of methylene blue from colored effluent by adsorption on montmorillonite clay. Journal of Colloid and Interface Science. April 2009;**332**(1):46-53

[38] Bujdak J. Effect of layer charge of clay minerals on optical properties of organic dyes: A review. Applied Clay Science. October 2006;**34**(1-4):58-73

[39] Bhattacharyya KG, Gupta SS. Adsorption of few heavy metals on natural and modified kaolinite and montmorillonite: A review. Advances in Colloid and Interface Science. August 5, 2008;**140**(2):114-131

[40] Lin S-H, Juang R-S. Heavy metal removal from water by sorption using surfactant-modified montmorillonite. Journal of Hazardous Materials. June 2002;**92**(3):315-326. DOI: 10.1016/S0304-3894(02)00026-2

[41] Wang SF, Shen L, Tong YJ, Chen L, Phang IY, Lim PQ, Liu TX. Biopolymer chitosan/montmorillonite nanocomposites: Preparation and characterization. Polymer Degradation and Stability. October 2005;**90**(1):123-131. DOI: 10.1016/j.polymdegradstab. 2005.03.001

[42] Cyras VP, Manfredi LB, Ton-That M-T, Vázquez A. Physical and mechanical properties of thermoplastic starch/montmorillonite nanocomposite films. Carbohydrate Polymers. July 4, 2008;**73**(1):55-63. DOI: 10.1016/j.carbpol.2007.11.014

[43] Uddin F. Studies in Finishing Effects of Clay Mineral in Polymers and Synthetic Fibers. Advances in Materials Science and Engineering. 2013. p. 13. Article ID: 243515. DOI: https://doi.org/10.1155/2013/243515

[44] Uddin F. Local clay mineral in flame retardant finishing of cotton fabric. Chemical and Material Engineering. 2015;**3**(1):6-15. DOI: 10.13189/cme.2015.030102

[45] Matsuewicz PK, Liljestrom V, Root SJP, Muurinen A, Serimaa R, Olin M, Adams J. Microstructural investigation of calcium montmorillonite. Clay Minerals. 2013;**48**(2):267-276

[46] Liu C, Pidko EA, Hensen EJM. Origin of enhanced Brosted acidity of NiF- modified synthetic mica-montmorillonite clay. Catalysis Science & Technology. 2018;**8**:244-251

[47] Nasreen A. Montmorillonite. Synlett. 2001;**8**:1341-1342

[48] Lei H, Du G, Pizzi A, Celzard A. Influence of nanoclay on urea-formaldehyde resins for wood adhesives and its model. Journal of Applied Polymer Science. August 15, 2008;**109**(4):2442-2451. DOI: 10.1002/app.28359

[49] Kaur N, Kishore D. Montmorillonite: An efficient, heterogeneous and greener catalyst for organic synthesis. Journal of Chemical and Pharmaceutical Research. 2012;**4**(2):991-1015

[50] Foley NK. Environmental Characteristics of Clays and Clay Mineral Deposits, U.S. Geological Survey, Reston, VA. 1999. Available from: https://pubs.usgs.gov/info/clays/ [Accessed: February 18, 2018]

[51] Anonymous. Terramin Clay-A California Living Clay. Available from: www.rawfood-info.com [Accessed: July 9, 2007]

[52] SAN MATEO. Cavities and Gum Diseases in Americans Increase at an Alarming Rate. February 20, 2007. Available from: http://www.prweb.com/releases/2007/02/prweb505336.htm [Accessed: May 29, 2018]

Chapter 2

Recycling of Steelmaking Plant Wastes in Clay Bricks

Carlos Maurício F. Vieira, Lucas Fonseca Amaral and Sergio N. Monteiro

Additional information is available at the end of the chapter

http://dx.doi.org/10.5772/intechopen.74431

Abstract

The steelmaking industrial sector generates a wide variety of solid wastes, predominantly composed of slag, dust, sludge, and scrap. The need to find a correct environmental alternative to recycle steelmaking wastes, as well as the possibility to bring some technical advantageous to clay bricks for civil construction, makes this industrial segment present itself as an excellent alternative for the reuse of these residues. In this way, some studies were presented in this chapter that evaluated the effect of incorporation of different steelmaking plant wastes such as blast furnace sludge, sludge, and slag from oxygen steel-refining process in the physical and mechanical properties of clay bricks for civil construction. As final considerations, the most investigated wastes present a particle size distribution compatible to clay brick processing. Although the wastes display different chemical and mineralogical composition, low amounts are well tolerated by the ceramic, not impairing the physical and mechanical properties. Furthermore, the presence of determined constituent, as, for example, fine coke in blast furnace sludge, can contribute significantly to save energy during the firing stage.

Keywords: residue, ceramic, incorporation, environmental

1. Introduction

The steelmaking industry plays an important role in economy and in a modern society development. As a provider of employment and essential materials, this sector is connected to a huge variety of industrial productive chains. However, a clearer related view on how to manage this key industry with greater sustainability could positively impact the economy and the environment globally. To provide a more sustainable productive chain, besides avoiding

generating residue, the solid residues may be managed through a more noble and environmentally correct destination.

There are basically two main routes for steel production; they are the integrated route and the semi-integrated route. At the first route, the reduction of ore, including iron ore, coal or charcoal, and fluxing agents, occurs in the blast furnace to generate pig iron, in which it is then refined to produce steel, while in the second route the steel is directly produced in electric arc furnace [1].

During the steelmaking at both routes and also at the reefing step, the main residues generated can be divided into categories such as slag, sludge, and dust [2]. The mineralogical and chemical compositions of each of these wastes vary according to the raw materials employed in the process and to what they have as common elements, mostly composed of iron, carbon, calcium, magnesium, silicon, and manganese and still containing smaller proportions of aluminum, zinc, alkaline earth metals, and traces of other elements [3].

It is preferable that the valorization of the solid wastes is carried out on the steelmaking route itself; however, if this practice is not possible, it is necessary to look for other productive processes capable of incorporating this waste as raw material. In association with this practice, it is desired that these wastes, when hazardous or not inert, are inertized in order to reduce their toxicity. In this sense, it is verified that much of this waste is still disposed in landfills or sent for incineration; even if this constitutes an environmentally correct practice, it is considered the least noble practice according to solid waste management [2].

The ceramic industry for civil construction has gained prominence in recent years due to its potential for incorporation of solid waste generated in the most diverse industrial activities. This potential is based primarily on the characteristics of the raw material and the high production volume in this industrial sector [4].

The basic raw material for the bricks and roofing tiles manufacturing is clay, and due to the nature of its formation, it has natural variability in its chemical and mineralogical composition. This variation, coupled with the low technical performance required for its products, allows residues of different compositions to be incorporated into the ceramic clayey body. In addition to direct environmental benefit, technical improvements in processing or product quality may occur, and even energy savings can be generated when certain wastes are incorporated with combustibility characteristics. Another notorious benefit is the possibility of inertization, in the ceramic matrix, toxic metals contained in these residues [5]. Dondi, Marsigli, and Fabbri [6] still emphasize the function of improving sustainable development by providing the economy of clay, which is a natural nonrenewable resource.

The purpose of this book chapter was to provide a summary based on existing scientific references on the environmental, technical, and economic benefits of using the waste generated in the steelmaking process as a raw material for the ceramic industry, seeking, whenever possible, to correlate the characteristics of the residues and their influence on the properties and microstructure of the ceramics.

2. Steelmaking plant wastes as raw materials for clay brick production

2.1. The ceramic industry as an active agent for the improvement of sustainable development

The industrial segment of red clay-based ceramics, also known as structural ceramics, is part of the nonmetallic mineral sector of the mineral processing industry, sharing the entire production chain of civil construction. The following products make up this segment, bricks, roofing tiles, blocks, and paving ceramic floors, among others.

Several researches have reported on the state of the art of using various wastes to red clay-based ceramic products, such as red mud of Bayer process [7], fluorescent lamp glass waste [8], granite waste [9], effluent sludge from paper industry [10], blast furnace sludge [11], and sugarcane bagasse ash [12], among others. This potential is based on basically two particularities of this industrial sector, the characteristics of the raw material and the high production volume [4].

Dondi, Marsigli, and Fabbri [6] elaborated a classification in order to organize different types of industrial solid wastes as to their main influence when incorporated to the clayey bodies for ceramic production. Through extensive bibliographical research, these authors categorized the residues into combustible residues, fly ash, flux residues, and plasticity-modifying residues.

More recently, Vieira and Monteiro [13] presented a new classification for industrial solid waste aiming its application as raw material for ceramic production for civil construction. In this classification, the authors propose only three categories, being combustible residues, flux residues, and property-modifying residues. Thus, fly ash was excluded from the old classification and should now be classified as combustible waste, and the category of plasticity-modifying waste was renamed as property-modifying waste, since not only plasticity but also other properties could be altered by waste that did not fit the other categories of classification.

2.2. Characteristics of steelmaking wastes and their influence on clay brick properties

The steel industry generates a huge variety of wastes in the course of its process, mainly in the case of integrated mills. In relation to the solid wastes generated, the transformation of iron ore into steel can be classified into slags, sludges, and dusts, which together represent between 2 and 4 tons per ton of steel produced. The composition of these wastes varies according to the source of generation but usually contains iron, carbon, calcium, magnesium, silicon, manganese, zinc, and lead. Besides that, some slag and sludge contain a notable amount of heavy metals, and their improper deposition can negatively impact the environment [3, 14–19].

So, the disposals of these wastes in landfills are becoming less attractive which not only occupy plenty of land but also increase the costs. Therefore, it is desirable to identify productive cycles capable of using the steelmaking wastes as raw material. In this way, this will lead to a better evolution of sustainable development. The following will be analyzed as to how the

incorporation of these wastes in clayey bodies for production of ceramics for civil construction affects the properties and microstructure of these products.

2.2.1. Slag

The slag originated at the steelmaking refining process, denoted as steel slag (SS), may vary in chemical composition as a function of the raw materials used and the technology and equipments employed. Currently, this residue is recycled in cement production as well as a base for pavements and composition for aggregates.

The difficulty of using the steel slag as raw material for construction products is its capability to enlarge. This is a consequence of the presence of free CaO and MgO as well as the polymorphism of the dicalcium silicate combined with the oxidation and corrosion of the metallic iron [20].

In relation to the characterization of this waste, the particle sizes with no crush processing present a wide distribution range varying from 20 to 30 × 10^3 μm and mean particle sizes of 7.860 μm. This is an undesirable feature for traditional ceramic production, in which it typically uses raw material with particles having sizes lower than 2.000 μm. Aiming its application in an industrial way, it would be necessary to comminute this residue before it is added to the ceramic clayey body [14].

Table 1 presents the chemical composition and the loss on ignition (LoI) of the steel slag, which is predominantly composed of Ca, Fe, Mg, and Si. Ca is present in the form of silicates as well as carbonate. Mg occurs mainly as free oxide and Fe as reduced oxides such as wustite and magnetite. Si occurs as silica and also as complex silicates. The loss on ignition may be attributed to carbonate decomposition and also to the dehydration of hydroxides such as brucite ($Mg(OH)_2$). The chemical composition results also in identified traces of K, V, Ni, Cu, Zn, Nb, Rh, and I.

The incorporations of 0 (C0SS), 5 (C5SS), 10 (C10SS), 20 (C20SS), and 30 (C30SS) wt.% of SS into clayey body, sieved at 20 mesh (0.840 μm), were evaluated by `Vieira and Monteiro (2010) [14]. The specimens were sintered at 700, 900, and 1000°C at heating rate of 3°C/min.

The extrusion prognostic is an important parameter to production of ceramics for civil construction, since this property is related to the workability and productivity of the pieces. In **Figure 1**, it can be observed that the clayey body without waste incorporation is located within the limits of the acceptable and non-recommended regions, and in practice, the results indicate that the incorporation of SS did not practically present significant variation at the workability of the clay.

CaO	Fe_{total}	SiO_2	MnO	SO_3	TiO_2	Al_2O_3	P_2O_5	MgO	LoI*
45.10	23.62	10.29	5.40	0.54	0.34	2.90	1.81	10.33	12.96

*Loss on ignition.

Table 1. Chemical composition of the SS (wt.%) and loss on ignition (LoI) [14].

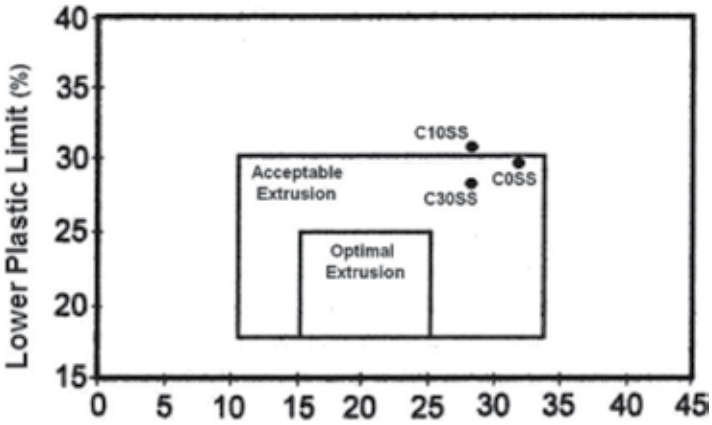

Figure 1. Extrusion prognostic through Atterberg limits [14].

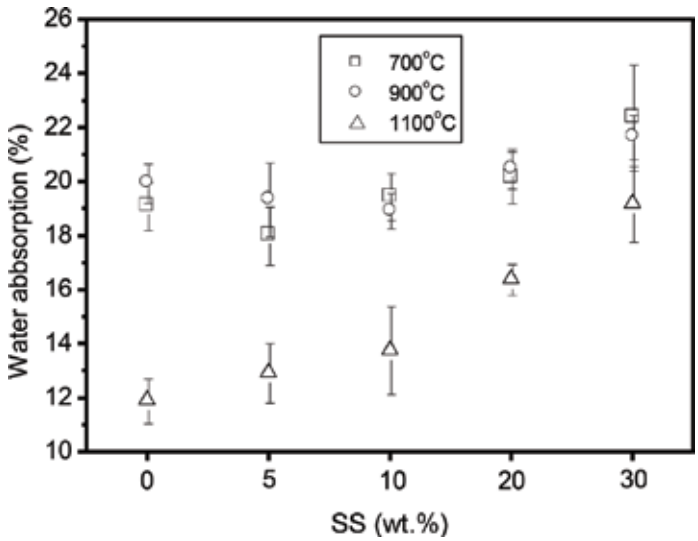

Figure 2. Water absorption of the clay as a function the amount of the SS incorporated [14].

The results of the technological properties evaluated are represented in **Figures 2–4**. In relation to the influence of the steel slag incorporation, the incorporation of higher up to 10 wt.% impairs the water absorption (**Figure 2**), while adding up to 5% has improved this property. This slight improvement in water absorption may be due to the better packaging provided by the addition of the residue. It may be noted that the temperature elevation of 700–900°C increased the water absorption; this can be explained by the combustion of coke fines at temperatures close to 800°C. The linear shrinkage (**Figure 3**) almost does not change with SS incorporation at sintering temperatures of 700 and 900°C. From another point of view, at temperature of 1100°C, the linear shrinkage significantly decreases with the SS incorporation. The flexural rupture strength is represented in **Figure 4**, and the results suggest that the incorporation

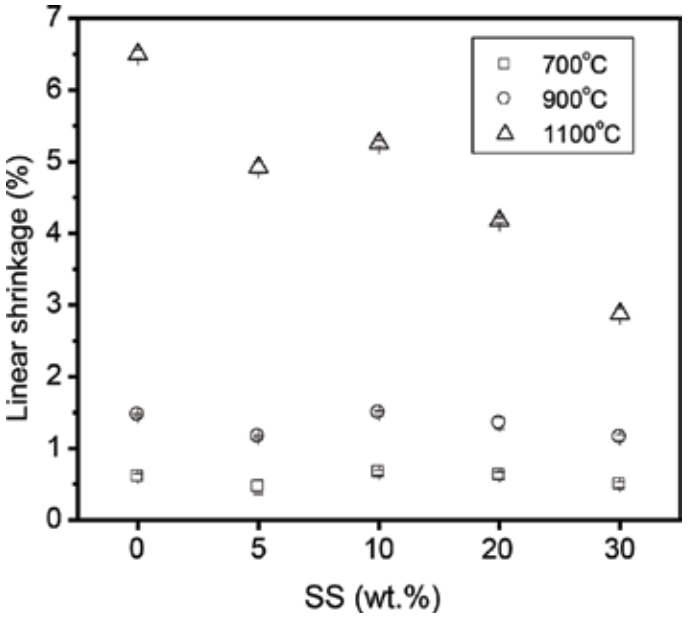

Figure 3. Linear shrinkage of the clay as a function the amount of the SS incorporated [14].

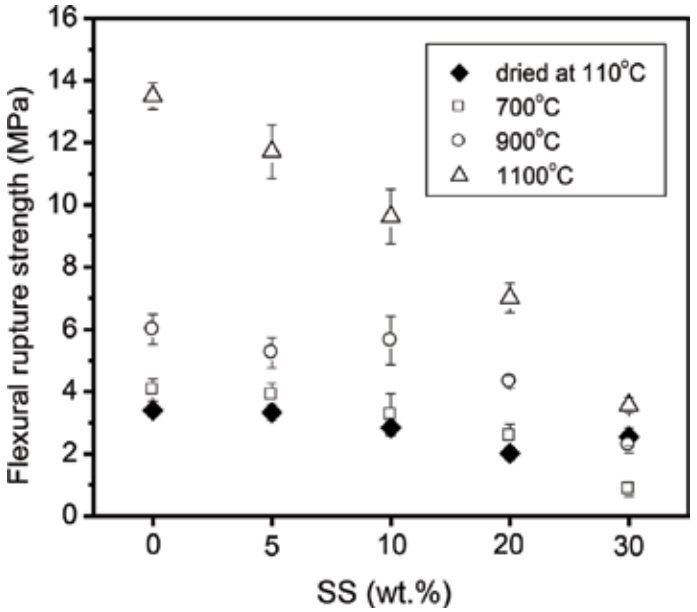

Figure 4. Flexural rupture strength of the clay as a function the amount of the SS incorporated [14].

of 10% SS (C0SS) sintered at 900°C is feasible for the reddish ceramic production since the values for this property are compatible with the products containing 0% of residue. At the lower temperatures investigated, 700 and 900°C, the clayey body (with no SS incorporation) supports SS addition up to 10 wt.% without significant changes on its properties.

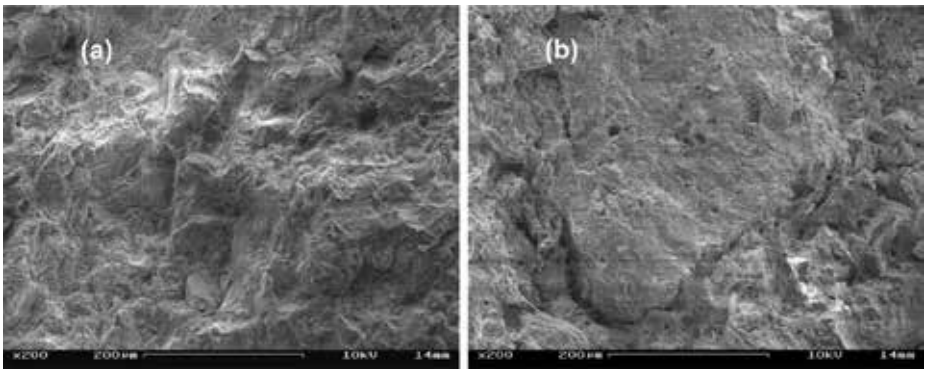

Figure 5. SEM micrographs of the fractured region of the clay (a) fired at 700°C; (b) fired at 1100°C [14].

At temperature of 1.100°C, the mechanical strength suddenly decreases with the amount of SS incorporation. At this temperature, the sintering mechanisms are highly intensified; in this sense, the clay minerals are extremely reactive during the sintering stages in temperatures higher than 950°C due to their morphology, constitution, and particle size [17], promoting both solid-state and liquid-state sintering. Thus, the reduction in the content of clay minerals due to the incorporation of residue reduces the reactivity of the ceramic clayey body; therefore, there will be fewer points of contact formed during the sintering, and as a consequence, the mechanical strength of the product will be impaired. For this reason, the deleterious effect of the SS addition on the open porosity and mechanical strength of the clay is more pronounced.

The microstructure of the fracture region of the ceramics containing 0 and 30% of residue is shown in **Figures 5** and **6**, respectively. At these micrographs, it may be noted that the two ceramics presented rougher texture. As expected, the ceramics sintered at higher temperatures produced samples with finer texture, but the cracks and voids are still present. It can be noted that the C30SS ceramic has typical regions in which the materials were plucked out at the moment of the mechanical resistance tests.

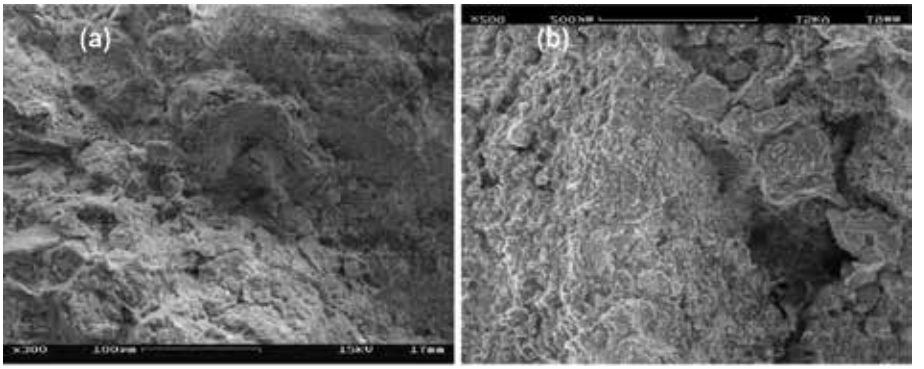

Figure 6. SEM micrographs of the fractured region of the clay with 30% of SS incorporated (a) fired at 700°C; (b) fired at 1100°C [14].

In this context, it is possible to predict that the SS particles do not react with the clay compounds. The insufficient level of chemical bonding leads the SS particles to stay loose from matrix and therefore generates defects such as voids and cracks in the product.

2.2.2. Sludge

As a result of the gas treatment, sludge from wet dedusting systems, which have a high iron content with the order of 75 to 80%, is obtained from the implantation of the dedusting systems in the steelworks. Companies that have not developed ways to recycle this waste end up destining them to the landfills, excessively increasing the cost of production, since its volume generation is considerable, reaching values of the order of 36 $kg.t^{-1}$ of steel produced. One of the main problems for the recycling of steel slurry in the steelmaking process itself is its high moisture content [3].

According to **Figure 7**, the steel sludge has a particle size distribution that the equivalent spherical diameter varies from 1 to 800 μm and mean particle sizes with 35.6 μm. For reddish ceramic production, this is an appropriate characteristic, in which these industries use materials with particles having sizes lower than 2000 μm.

In relation to the chemical composition (**Table 2**), the steel sludge is composed mainly by Fe, with 74.03%. The CaO comes from calcite introduced in the process to convert pig iron into steel. The small MgO content is associated with the desulfurizing agent also used in the steel process, which also contributes with CaO. The content of SiO_2 can be derived from the oxidation of silicon present in pig iron, while the ZnO content is associated with the use of galvanized scrap.

The influence of steel sludge incorporation into clayey ceramic products was evaluated by Vieira et al. (2007) [16]. In this paper, the authors evaluated the influence of incorporation of

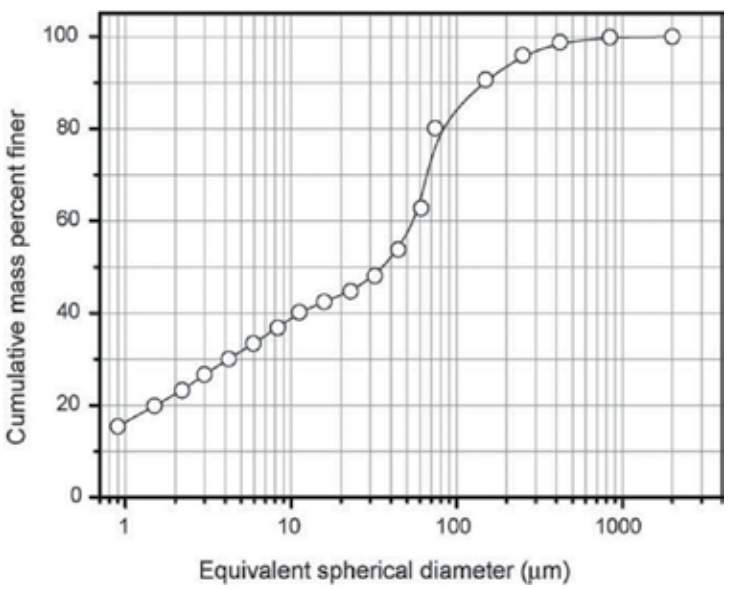

Figure 7. Steel sludge particle size distribution [15].

SiO_2	Al_2O_3	Fe_{total}	TiO_2	CaO	MgO	K_2O	Na_2O	ZnO	LoI*
1.86	0.12	74.03	0.90	16.50	3.42	0.16	0.33	2.78	—

*Loss on ignition.

Table 2. Steel sludge chemical composition (wt.%) [15].

up to 20 wt.% of fine steel sludge generated at an integrated siderurgic plant on the properties of a kaolinitic clay-based ceramic used to the produce bricks and tiles. Other authors [17] also focused on evaluating the microstructure and the inertization of potentially toxic elements through ceramic matrix by performing solution and leaching test in the ceramics with residue incorporation sintered at 900°C.

Figure 8 shows the fracture surface micrographs of the ceramic with 5% of waste incorporated. A very rough microstructure is observed with the presence of well-distributed porous particles. These particles are associated with fine steel sludge and are not adhered to the ceramic matrix. This may lead to a reduction in the mechanical strength of products incorporating higher residue content.

Figure 9 shows the fracture surface micrographs of the clay with 20% of waste incorporated. It is possible to observe that the steel sludge is relatively well distributed in the clay matrix. However, with the increase of its quantity, more regions appear with fails. In addition, increasing the waste amount, which exhibits an inert behavior during firing, reduces the amount of clay, the main material responsible for the consolidation of the ceramic particles.

In **Table 3** the leaching and solubilization results are presented, indicating the values obtained and the acceptable limit, according to the Brazilian legislation of potentially toxic metals of the formulation containing 5% of steel sludge. It is possible to observe that in the leached standard parameters, Ba, Cd, Cr, and Pb are present in quantities well below the limit values. Already solubilized, Al is present in a quantity nine times higher than the limit acceptable by norm. Al present in clay is one of its natural constituents and therefore apparently lies in equilibrium in nature. In this way its content above the stipulated limit by norm is questionable from the point of view of environmental problems. Other elements such as Cd, Cu, Fe, Mn, and Pb are in very small concentrations, being below the detection limit of the equipment.

To evaluate the effect of steel sludge incorporation on the properties of ceramics for civil construction, Vieira et al. [15] prepared specimens with additions of 0, 5, 10, and 20 wt.% of fine steel sludge into a kaolinitic clay from Brazil.

It can be seen in **Figure 10** the dried bulk density and the sintered bulk density of the formulations. One should notice that steel sludge waste (SSW) additions tend to increase the dried bulk density, mainly for the 20 wt.% addition. This behavior is probably due to the higher real density of the SSW particles compared with the clay particles and also the coarser particles of the SSW as compared with the clay, which may favor the packaging.

In **Figure 11**, the results of the analyzed properties of the sintered ceramics as function of residue incorporation are represented. An interesting result can be noted for water absorption;

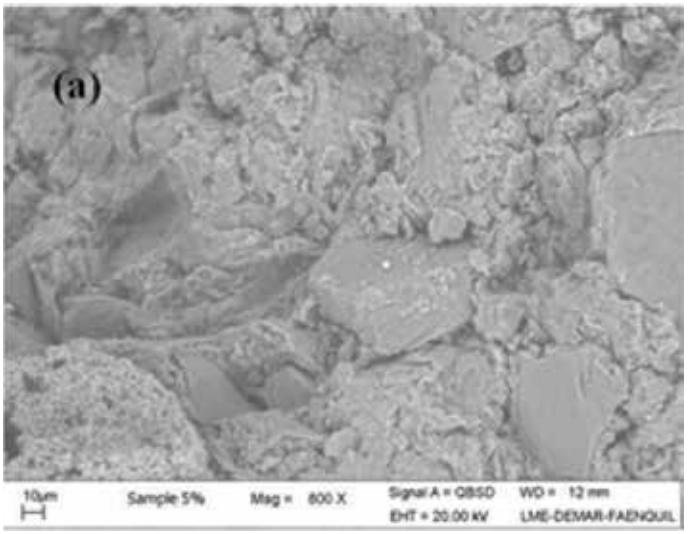

Figure 8. Micrograph obtained by SEM of the ceramic incorporated with 5% of steel sludge and sintered at 900° C in magnification of 800× [17].

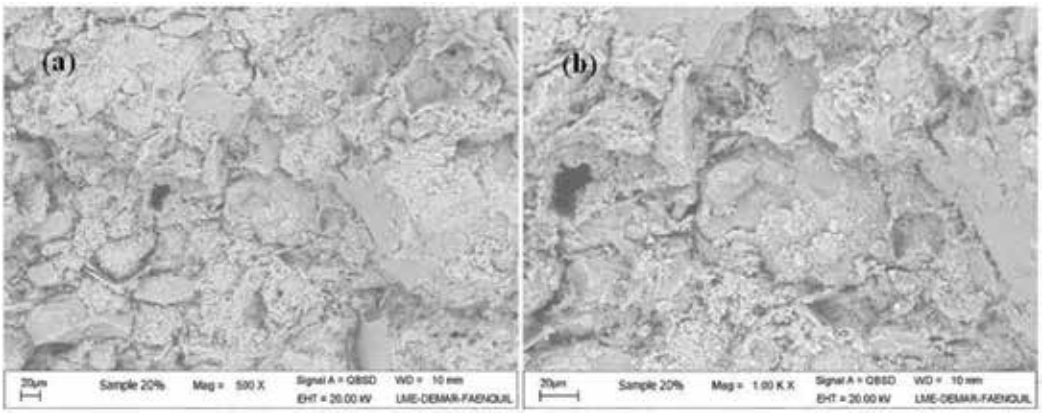

Figure 9. Micrograph obtained by SEM of the ceramic incorporated with 20% of steel sludge and sintered at 900° C in magnification of 500× (a) and 1000× (b) [17].

considering the error bars, this property is little affected by the residue amount increasing. Therefore, as the open porosity of the ceramics containing residue is practically unchanged, it is correct to affirm that the partial substitution of the clay by the residue aided in the reduction of the loss on ignition. It is known that the loss on fire caused by clay is due to dehydroxylation of kaolinite to form metakaolinite; in this way, this mechanism is responsible for leaving porosity in the ceramic. When the clay is replaced by the residue, although it is reducing the content of clay minerals which are the most reactive particles and contribute most to the consolidation mechanisms during the sintering, it is also reducing the loss to fire; for this reason, this property is little changed.

Element	Solubilized (mg/L)	Limits (mg/L)	Leached (mg/L)	Limits (mg/L)
Al	1.8	0.2	19	Not required
Ba	0.06	0.7	0.7	7.0
Cd	<0.003	0.005	0.04	0.5
Cr (total)	<0.02	0.05	<0.05	5.0
Cu	0.004	2.0	0.13	Not required
Fe	0.02	0.3	0.22	Not required
Mn	0.02	0.1	0.9	Not required
Na	10	200	—	Not required
Pb	<0.06	0.1	0.14	1.0
Zn	0.02	5.0	1.3	Not required

Table 3. Potentially toxic metals in the leaching and solubilization extracts of the ceramic with 5% of incorporated steel sludge [17].

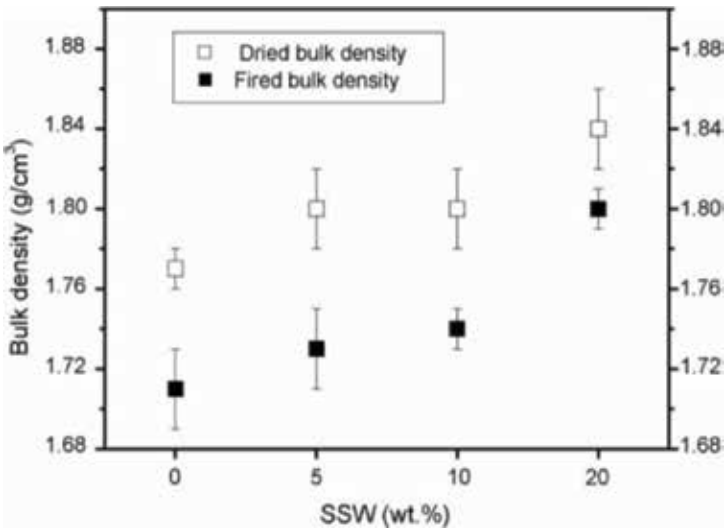

Figure 10. Dried and sintered bulk density of formulations containing steel sludge waste [15].

This same explanation helps in the understanding of the linear shrinkage behavior. The loss on fire reduction with the SSW incorporation consequently causes the reduction of the firing linear shrinkage. This behavior assists in the ceramic production favoring the better control of the dimensions of the products, besides, of course, to avoid defects during the drying and sintering stages.

The flexural rupture strength is also represented in **Figure 11**. Although the residue incorporation does not greatly affect the open porosity of the sintered ceramics, the mechanical

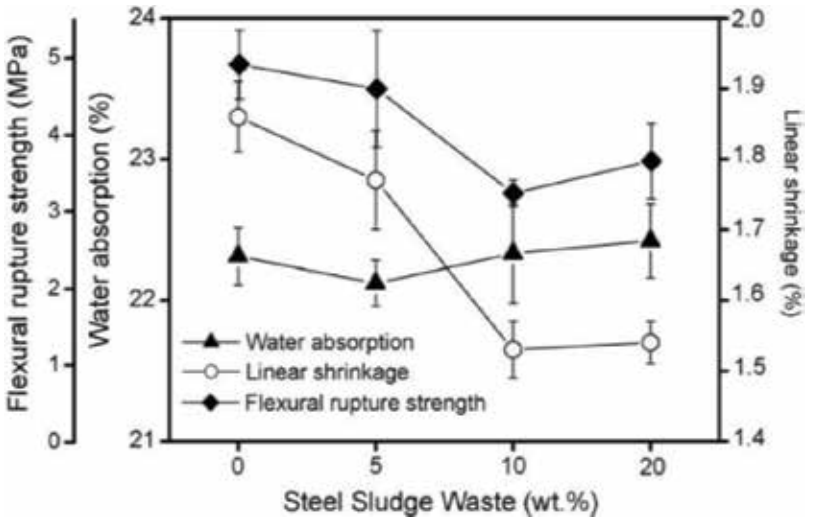

Figure 11. Sintered technical properties of formulations containing steel sludge waste [15].

strength is a property that is highly dependent on the particle consolidation during the sintering step. As seen, the mineralogical composition of this residue does not favor the sintering mechanism in these temperatures evaluated. In this way, additions of up to 5% by weight of waste are acceptable so that there is no too much reduction at the product resistance.

2.2.3. Dust

Dusts are obtained in the dry cleaning systems of process gases from the sintering stage of an integrated steelmaking plant, here denoted as PMW (particulate material waste). **Table 4** shows the chemical composition of the PMW, which is predominantly formed by iron compounds such as hematite and magnetite. CaO and SiO_2 also present relatively high amounts. The loss on ignition is predominantly associated with the combustion of coke fines and the decomposition of both calcite and dolomite. The amount of 2.28% of SO_3 suggests the presence of sulfates, possible of Ca, such as gypsum.

In **Figure 12**, the particle size distributions of the PMW with no crush processing are represented. It should be emphasized that this particle size distribution prevents its reuse in the process to which it originated. However, for reddish ceramic industry, this characteristic is ideal, since this residue can be used directly without undergoing any other crush processing.

Figures 13–15 show the graphs corresponding to the results of the technological properties after firing. A remarkable behavior can be noted with the water absorption (**Figure 13**) reduction due

Fe_{total}	SiO_2	MnO	SO_3	Al_2O_3	K_2O	MgO	CaO	ZnO	C	LoI*
70.70	6.82	0.82	2.28	1.20	1.81	10.33	9.70	0.72	3.30	10.70

*Loss on ignition.

Table 4. Chemical composition of the particulate material waste (wt.%) [18].

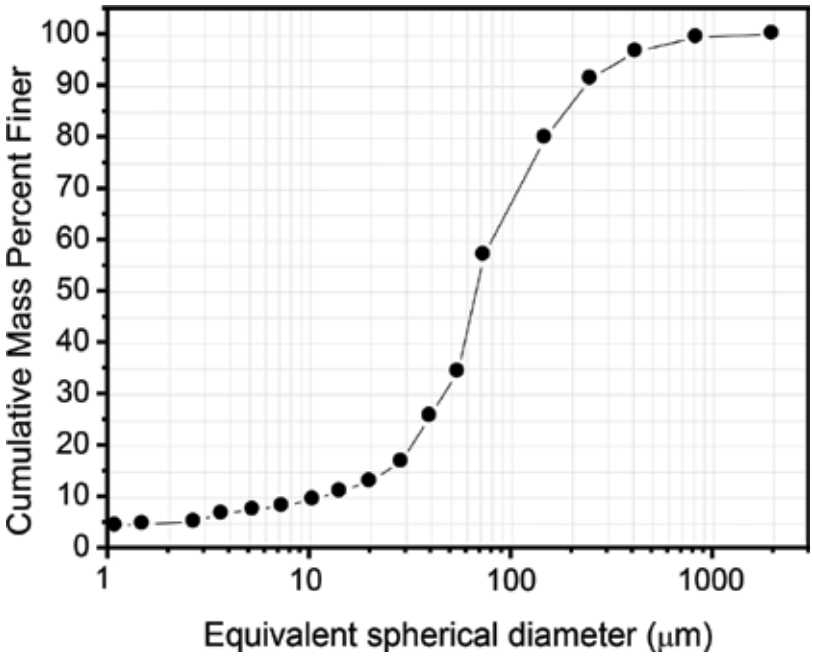

Figure 12. Particle size distribution of the PMW [19].

to the residue content increasing, principally at 1050°C. Although the ceramic clayey body was composed of highly refractory clay, the incorporation of 20% of the residue allowed the brick production at sintering temperature of 750°C and tiles at 900°C.

The firing linear shrinkage, represented at **Figure 14**, shows that the PMW addition doesn't contribute to the increasing of this property; it is therefore a residue capable of assisting in the dimensional control of the products.

In **Figure 15**, the mechanical resistance of the ceramics with PMW addition is represented. This residue with content lower than 20% was able to improve this property at all sintering temperatures investigated.

The mineralogical constitution of the PMW, which contains high amount of iron compounds, suggests an inert behavior during the sintering stage of red clay-based ceramics. Therefore, the explanation of how the residue may have acted to improve the properties may be based on dry bulk density. Probably the combination of these two raw materials helps in the better packaging at conformation stage favoring greater points of contact between the grains. Thus, there will be less void spaces which are responsible for the water absorption reduction and mechanical resistance increasing.

Figure 16 represents the SEM micrograph of ceramic with 0% of residue content and fired at 1050°C. The points located at this figure are derived from EDS analysis. The micrograph shows the intrinsic porosity probably related with void spaces left after the conformation step and consolidated as pores after sintering. The presence of pores can be associated with the dehydroxylation of some hydroxides and clay minerals and also with the different expansion

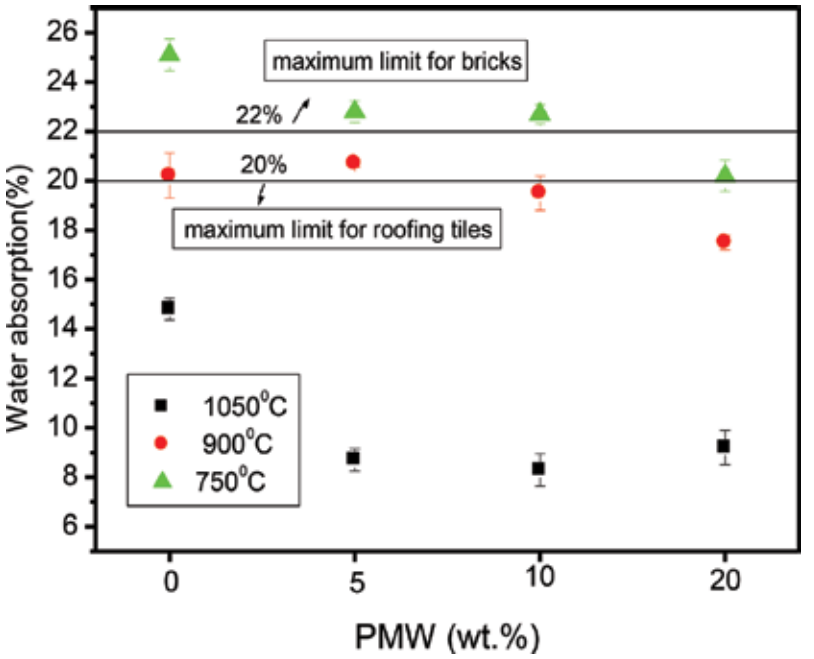

Figure 13. Water absorption of the clayey body as a function the amount of the PMW incorporated [19].

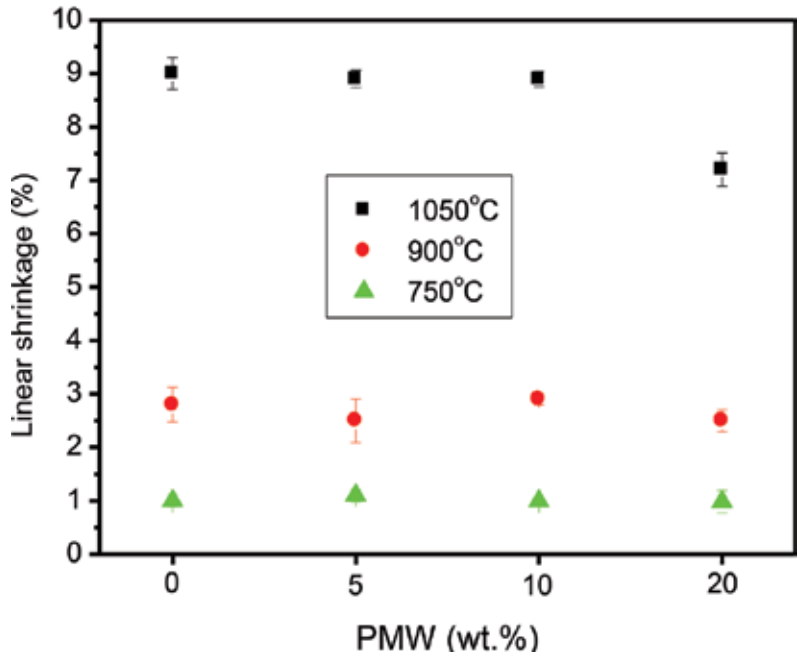

Figure 14. Linear shrinkage of the clayey body as a function the amount of the PMW incorporated [19].

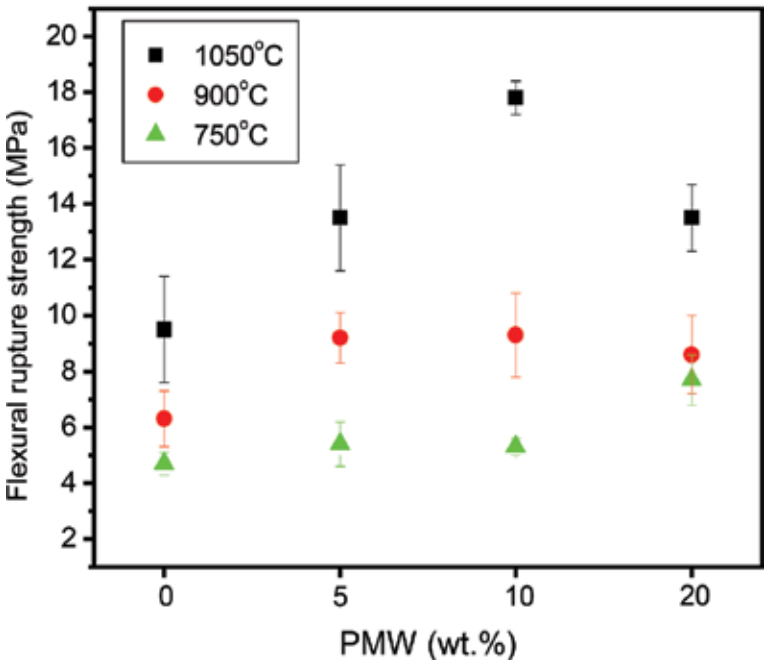

Figure 15. Flexural rupture strength of the clayey body as a function the amount of the PMW incorporated [19].

coefficients among the ceramic phases during the sintering stage. Due to the refractory nature of this clay, the sintering is impaired as well as the reduction of pores, event at temperatures around 1050°C.

The EDS spectrum of point 1 indicates the existence of Zr and Si that can correspond to zircon silicate. Punctual regions 2 and 3 are basically composed of Si, Al, and Fe, i.e., the basic constituents

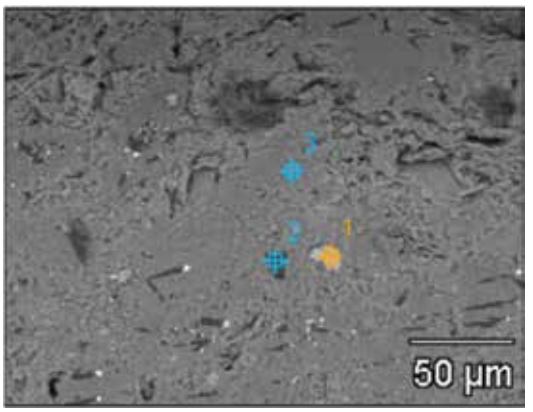

Figure 16. SEM micrograph of ceramic with 0 wt.% of steel dust incorporated and sintered at 1050°C, including EDS spectra of selected points [18].

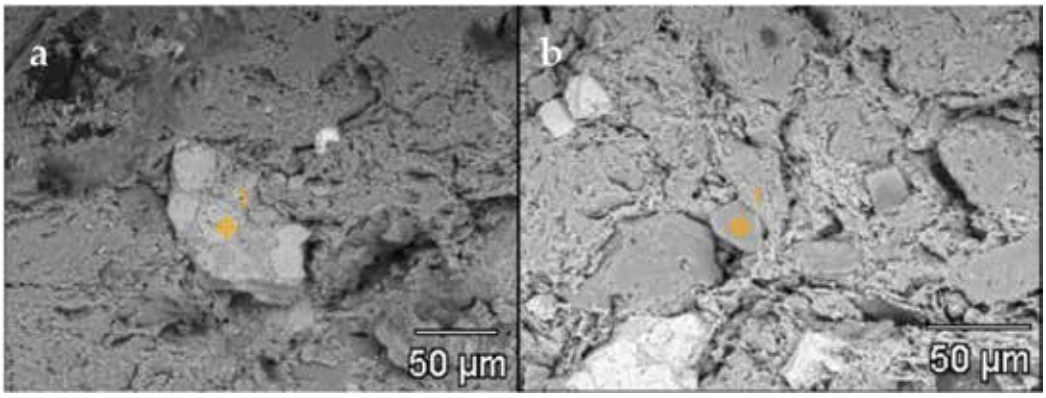

Figure 17. SEM micrographs of ceramic with 20 wt.% of steel dust incorporated and sintered at 1050°C, including EDS spectra of selected points [18].

of a kaolinitic clay. In this case, the Si and al predominantly constitute the aluminosilicate amorphous clayey matrix.

Figure 17 shows two SEM micrographs of ceramic specimen with 20 wt.% of dust steel waste incorporated, sintered at 1050°C. In this figure selected punctual regions, marked in the micrographs, were analyzed by EDS. In both micrographs of **Figure 17**, defects associated with microcracks and pores can be observed.

As already mentioned for the microstructure of ceramics with no dust waste addition (**Figure 16**), these defects are associated with the conformation step and further consolidation on sintering. It is important to notice in relation to **Figure 17** that the main microstructural distinction between the ceramics with residue addition and those with no waste (**Figure 16**) is the relatively larger particles apparently belonging to the waste. In fact, the EDS spectrum of the large particle in **Figure 17** (a) indicates the presence of Ca and Fe that are, as listed in **Table 4**, characteristics of the PMW. Moreover, the microcracks that surround the particles indicate that this residue can lead to occasional defects in ceramics.

It is correct mentioning that, in spite of the defects observed, this waste acts as an inert material and assists on the plasticity control of the clayey body. Despite the inert character of the residue particles, the observed microcracks (**Figure 16(a)**) may be associated due their different expansion coefficient at sintering stage, more pronounced at 1050°C. The particle analyzed in **Figure 16(b)** is relatively small and by its EDS spectrum, with Si and O, corresponds to a quartz particle, which already exists in the natural clay.

3. Final considerations

At this sense, it is technically possible to recycle steel slag by incorporating into clayey ceramic. However, the incorporation of this waste into clayey ceramics must be done in amounts of up to 10 wt.%. An elevated amount of steel slag can increase the porosity of the fired ceramic and decrease its mechanical strength due to its inert action and elevated weight loss.

It can be concluded by the influence investigation of the steel sludge as raw material for ceramic production in that its incorporation is technically feasible. The porous agglomerate constituents of the steel sludge do not adhere to the clayey matrix, creating regions of failure that contribute to the reduction of the mechanical strength of the final products with incorporations of residue above 5% by weight. The environmental evaluation shows excess of Al in the solubilization extract, coming from the clay. The other evaluated elements are within the limits required for both the solubilization tests and the leaching test. The fine steel sludge is a waste predominantly composed of Fe metallic, Fe oxides (magnetite and wustite), and calcium carbonate (calcite). This waste shows a fine particle size, average of 35.6 μm that is appropriate for red clay-based ceramic production. This waste contributes to increase the dried bulk density of the ceramic. Incorporations of 5 wt.% of the waste are beneficial to the ceramic since it decreased the fired linear shrinkage and does not increase the water absorption. And also, the mechanical strength does not decrease which is also a convenient result for this level of incorporation.

The incorporation of a particulate, PMW, waste generated in the sintering stage of an integrated steelmaking plant, caused significant changes in a kaolinitic clay-based ceramic sintered at 1050°C. Relatively large dark phases associated with Fe and Ca compounds in the waste were formed in the clayey ceramic matrix. These phases showed evidences of microcracks- and pores-induced defects. The PMW incorporation results not only in an increased amount of porosity but also pores with relatively larger sizes. It is suggested that the inert nature of the waste, as well as its different coefficient of thermal expansion with respect to the aluminum silicate matrix, is responsible for the additional defects produced in the clayey ceramic. It was found that the particulate material waste from the sintering stage of an integrated steelmaking plant has an elevated amount of Fe and Ca compounds. The incorporation of this waste, in amounts of up to 20 wt.%, into a clayey body did not change its workability and enhanced the evaluated physical and mechanical properties such as water absorption and flexural rupture strength. The results indicated that this type of waste has a potential to be used into red ceramics with real benefits both in the processing and in the quality of the products.

Acknowledgements

The financial support provided by the Brazilian agencies, FAPERJ and CNPq, is gratefully acknowledged.

Author details

Carlos Maurício F. Vieira[1]*, Lucas Fonseca Amaral[1] and Sergio N. Monteiro[2]

*Address all correspondence to: vieira@uenf.br

1 Advanced Materials Laboratory, LAMAV, State University of the Northern Rio de Janeiro, UENF, Campos dos Goytacazes, RJ, Brazil

2 Department of Materials Science, Military Institute of Engineering, IME, Rio de Janeiro, RJ, Brazil

References

[1] Fruehan RJ. The Making, Shaping and Treating of Steel. 11th ed. Pittsburgh: The AISE Steel Foundation; 1998. p. 767

[2] Lobato NCC, Villegas EA, Mansur MB. Management of solid wastes from steelmaking and galvanizing process: A brief review. Resources, Conservation and Recycling. 2015;**102**:49-57. DOI: https://doi.org/10.1016/j.resconrec.2015.05.025

[3] Das B, Prakash S, Reddy PSR, Misra VN. An overview of utilization of slag and sludge from steel industries. Resources, Conservation and Recycling. 2007;**50**:40-57. DOI: https://doi.org/10.1016/j.resconrec.2006.05.008

[4] Naga SM, El-Maghraby A. Industrial waste as raw materials for tile making. Silicates Industriels. 2003;**68**:89-92. DOI: 10.4028/www.scientific.net/KEM.206-213.1787

[5] Santos PS. Science and Technology of Clays (in Port.). 2nd ed. São Paulo: Edgard Blücher; 1989. pp. 408-491

[6] Dondi M, Masigli M, Fabbri B. Recycling of industrial and urban wastes in brick production – A review. Tile and Brick International. 1997;**13**:218-225

[7] Ribeiro LS, Babisk MP, Prado US, Monteiro SN, Vieira CMF. Incorporation of in natura and calcined red muds into clay ceramic. Materials Research (São Carlos. On-line). 2015;**18**:279-282. DOI: http://dx.doi.org/10.1590/1516-1439.372014

[8] Morais ASC, Vieira CMF, Sánchez RJ, Monteiro SN, Candido VS, Ferreira CL. Fluorescent lamp glass waste incorporation into clay ceramic: A perfect solution. JOM (Warrendale). 2016;**68**:2214-2225. DOI: 10.1007/s11837-016-1985-z

[9] Vieira CMF, Soares TM, Sánchez R, Monteiro SN. Incorporation of granite waste in red ceramics. Materials Science and Engineering. 2004;**373**:115-121. DOI: https://doi.org/10.1016/j.msea.2003.12.038

[10] Vieira CMF, Pinheiro RM, Sánchez RJ, Candido VS, Monteiro SN. Clay bricks added with effluent sludge from paper industry: Technical, economical and environmental benefits. Applied Clay Science (Print). 2016;**132-133**:753-759

[11] Riter AV, Vieira CMF, Candido VS, Monteiro SN. Microstructural analysis of clay ceramic added with blast furnace sludge. Materials Science Forum. 2014;**775-776**:718-723. DOI: 10.4028/www.scientific.net/MSF.775-776.718

[12] Faria KCP, Holanda JNF. Incorporation of sugarcane bagasse ash waste as an alternative raw material for red ceramic. Cerâmica. 2013;**59**:473-480. DOI: http://dx.doi.org/10.1590/S0366-69132013000300019

[13] Vieira CMF, Monteiro SN. Incorporation of solid wastes in red ceramics – An update review. Revista Matéria. 2009;**14**:881-905. DOI: http://dx.doi.org/10.1590/S1517-70762009000300002

[14] Vieira CMF, Monteiro SN. Use of steel slag into clayey ceramics. Materials Science Forum. 2010;**660-661**:686-691. DOI: 10.4028/www.scientific.net/MSF.660-661.686

[15] Vieira CMF, Andrade PM, Maciel GS, Vernilli F, Monteiro SN. Incorporation of fine steel sludge waste into red ceramic. Materials Science and Engineering. 2006;**427**:142-147. DOI: https://doi.org/10.1016/j.msea.2006.04.040

[16] Andrade PM, Vieira CMF, Monteiro SN, Vernilli F. Recycling of steel sludge into red ceramic. Materials Science Forum. 2006;**530-531**:544-549. DOI: 10.4028/www.scientific.net/MSF.530-531.544

[17] Vieira CMF, Intorne SC, Vernilli F, Monteiro SN. Red clayey based ceramic incorporated with fine steel sludge (in port.). Revista Matéria. 2007;**12**:269-275. DOI: http://dx.doi.org/10.1590/S1517-70762007000200004

[18] Vieira CMF, Ribeiro MM, Monteiro SN. Microstructural evaluation of clayey ceramic incorporated with powder waste from the sintering plant of a steel-making industry. Materials Science Forum. 2012;**727-728**:951-956. DOI: 10.4028/www.scientific.net/MSF.727-728.951

[19] Ribeiro MM, Monteiro SN, Vieira CMF. Clayey ceramic incorporated with powder from the sintering plant of a steel-making industry. In: TMS 2011 – 140th Annual Meeting & Exhibition. EPD Congress 2011. Vol. 1; San Diego; 2011. pp. 1061-1068. DOI: 10.1002/9781118495285.ch118

[20] Goldring DC, Juckes LM. Petrology and stability of steel slags. Iron making and Steelmaking. 1997;**24**:447-456

Chapter 3

Mineralogical and Chemical Characteristics of Raw and Modified Clays and Their Application in Arsenic and Fluoride Removal: Review

Mugera W. Gitari and Rabelani Mudzielwana

Additional information is available at the end of the chapter

http://dx.doi.org/10.5772/intechopen.74474

Abstract

Clay and clay minerals have always been used since the ancient times for making ceramic materials and also as a building material. Over the past decades, there has been a growing trend in their applicability in different areas such as industries, environmental remediation and water treatment sectors. The growing trend is mainly associated with the fact that they are chemically and mechanically stable, have higher specific surface area and cation exchange capacity. Furthermore, clays can be modified to improve their functionalities in different sectors. In this chapter, we present a review of the structural, mineralogical and chemical properties of clay and the effect of surface modification in their structures. We further looked at their applicability in arsenic and fluoride removal in their raw and also in their modified form. Although the literature showed that modified clay minerals yields higher adsorption capacity as compared to raw clays little nothing has been reported yet in relation to the cost of modifying clays with chemical species. As such new studies should also elaborate on the cost effectiveness of modifying clay minerals with chemical species.

Keywords: clay minerals, physicochemical properties, mineralogy, surface modification, adsorption

1. Introduction

Clay and clay minerals have attracted wide interest for application in various sectors including process industries, agricultural sectors, engineering and construction sectors, environmental remediation and water treatment [1]. This is not only due to their abundance and inexpensiveness but also because of their physicochemical properties such as chemical and

mechanical stability, larger specific surface area, higher charge density, layered structure, higher cation exchange capacity [2].

By definition clays are naturally occurring alumino-silicate materials composed mainly of fine grained materials with colloid fraction of soils, rocks, sediments and water [3–5]. Clay minerals are composed of groups of small crystalline particles of one or more members of a group of minerals. These minerals originate from weathering of silicate minerals [6, 7]. Common minerals that constitute clay minerals are kaolinite, illite, mica, vermiculite and montmorillonite or smectite. This chapter presents a review on mineralogical and chemical properties of clay minerals, their surface modification and their application in arsenic and fluoride removal potential from water.

2. Structure, mineralogical and physicochemical composition of clay

The structure of the clay consists of phyllosilicate sheets that are arranged properly to form structural layers. Individual layer is made by a stack of tetrahedral and octahedral sheets that shape the frame of all the clay mineral [8, 9]. The tetrahedral (T) sheet consist of cations coordinated to four oxygen atoms and linked to adjacent tetrahedral by sharing three corners to form two dimensional hexagonal mesh [10]. The most common tetrahedral cations are Si^{4+}, Al^{3+} and Fe^{3+}.

The second sheet is called octahedral sheet (O), which is comprised of six oxygen atoms which are closely parked together and hydroxyl ions in which cations are arranged to form octahedral coordination and linked to neighboring octahedral by sharing edge. The edge of shared octahedral forms sheet of hexagonal or pseudo hexagonal symmetry and shows different topologies depending on octahedral hydroxyl position [8]. Cations in octahedral sheet are usually Al^{3+}, Fe^{3+}, Mg^{2+} or Fe^{2+}. When cation with positive valence of three (Al^{3+} or Fe^{3+}) is present in the octahedral sheet, only two-thirds of the possible positions are filled in order to balance the charges and the mineral is therefore termed dioctahedral. Conversely, when cation with positive charge of two (e.g. Mg^{2+} and Fe^{2+}) is present, all three positions are filled to balance the structure and the mineral is termed trioctahedral. The phyllosilicate sheets are joined together by sharing the apical oxygen atom or hydroxyls to form hexagonal network with each sheet in a fundamental structure. **Figure 1** depicts structures of octahedron sheets and tetrahedron sheets proposed by Grim [11]. Based on the number and ratio of the sheets in the fundamental structural units, the existing cations substitutions in the octahedrons and tetrahedrons caused for resulting charge of the layers which can be descended into two main groups of clay mineral namely 1:1 (kaoline) and 2:1 (smectite and illite) [12, 13].

2.1. Type 1:1

This group of mineral is also called kaolin minerals, which is the basic mineral for kaolinite, dickite and hallocite [14]. They consist of single tetrahedral sheet of SiO_4 and an octahedral sheet with Al^{3+} as octahedral cation. Both sheets combine to form a common a unit in such that the tip of silica tetrahedral points toward the octahedral sheet [3]. The layer of the tetrahedral sheet is invented over the octahedral sheet with oxygen atoms and hydroxyls ions present to balance the charges being shared by the silica in the tetrahedral sheet and the aluminum in

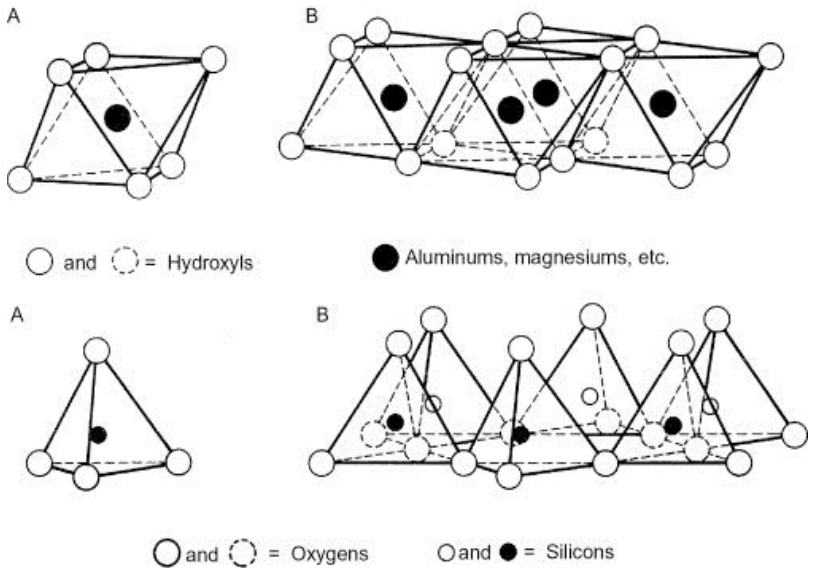

Figure 1. Schematic diagrams of octahedron and tetrahedron sheets. Top: (A) an alumina octahedron in which the central aluminum ion is coordinated to six hydroxyls; (B) an alumina octahedral sheet formed by linking octahedra through edge-sharing. Bottom: (A) a silica tetrahedron in which the central silicon ion is coordinated to four oxygens; (B) a tetrahedral sheet formed by linking silica tetrahedra through corner-sharing [11].

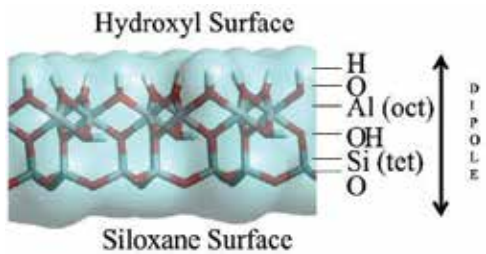

Figure 2. Typical structure of Kaoline mineral [15].

the octahedral sheet. With the layer charges close to zero, the kaolin mineral has essentially no interlayers and does not show interlayer expansion in the water because the contiguous layers within particles are strongly held together by Al-OH and O-Si-OH bonding supplemented by dipole–dipole and van der Waal interaction. **Figure 2** represents the typical structure of kaoline mineral [15].

2.2. Type 2:1

Clay mineral groups such as smectite and vermiculite are part of 2:1 type and it constitutes minerals such as montmorillonite, saponite, nontronite and beidellite. The 2:1 minerals are composed of one octahedral sheet between two tetrahedral sheets. For which the interlayer thickness is 1 nm when the sheet is closed [16]. Generally in this group of clay minerals

isomorphic substitutions are observed, for example, possible substitutions of Si^{4+} in tetrahedron by Al^{3+} or those of Al^{3+} in octahedron by Fe^{2+} [17]. Such substitution leads to permanent negative surface charge at the sheet by the presence of exchangeable cations [18]. The most common exchangeable cations in the interlayers are K^+, Na^+, Ca^{2+}, Mg^{2+} and H^+. The 2:1 group minerals have higher charge density, higher surface area and higher swelling capacity [3]. The swelling capacity of these type of clay arise from their structural features that enables water to overcome the electrostatic and van der Waals interactions keeping the layers together and penetrate into surface interlayers leading to hydrolization of Al and Si atoms to aluminol (AlOH) and silanol (SiOH) resulting in expansion. **Figure 3** presents the schematic diagram of 2:1 clay minerals.

2.3. Cation exchange capacity

One of the important properties of the clay minerals is that contains cations that can be exchanged for any guest species of anion or cation by treating clay mineral with such clay mineral. The exchangeable cations are held on the outside of silica-alumina clay mineral structural units and the exchange does not affect the layout of the silica-alumina units [11]. The ion exchange capacity phenomenon is measured in terms of milli-equivalents per gram or per 100 g. The commonly used cations used to evaluate the cation exchange capacity of the clay mineral includes; Mg^{2+}, Ca^{2+}, K^+, Na^+, H^+ and NH_4^+ [16].

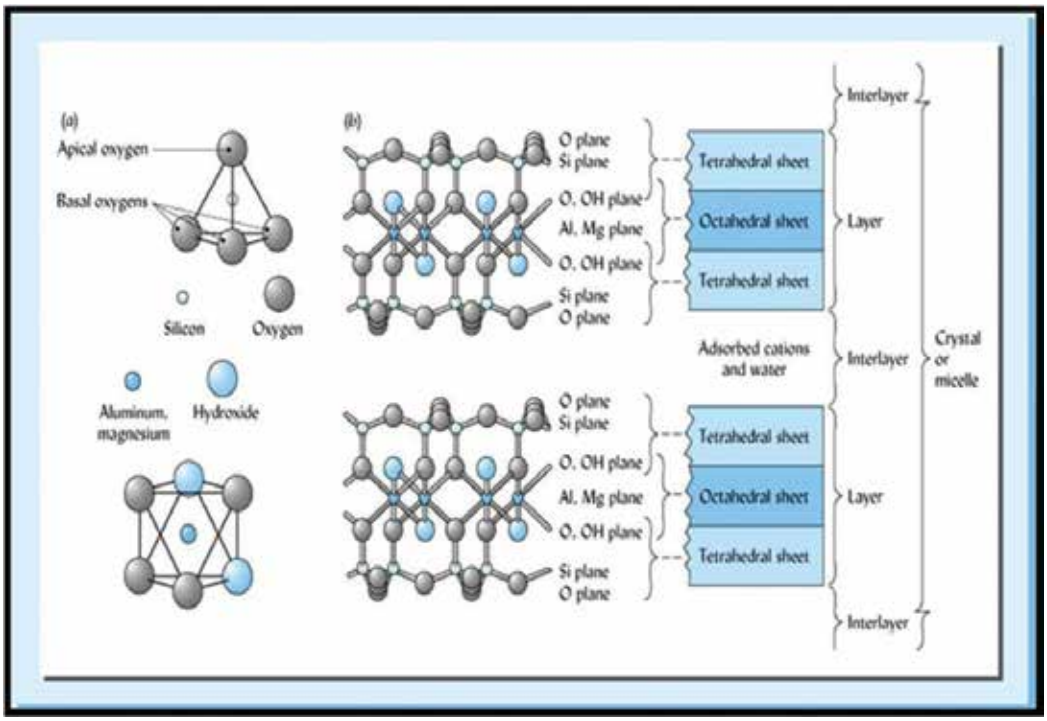

Figure 3. Typical structure of 2:1 clay [19].

Different clay minerals portray different cation capacity depending on the substitution within the lattice structure [11]. Type 1:1 clay minerals such as kaolinite have limited substitution between their lattice structure compared to type 2:1 clay minerals such as smectite, vermiculite and sepiolite and consequently they have lower cation exchange capacity [10]. Several studies have indicated that cation exchange capacity of the clay mineral decreases after modification by inorganic species [2, 20, 21]. This is because modification involves the ion exchange reaction between the exchangeable cations in the clay interlayer and the guest species. Low CEC of modified clays suggests the irreversibility of cationic exchange and thus intercalated metallic polycations are hardly exchanged [21]. **Table 1** summarizes the cation exchange capacity of different raw and modified clay minerals.

2.4. Specific surface area

One of the essential properties of clay minerals is their larger surface area. This characteristic allows clay minerals to adsorb water and other environmental contaminants [26]. Type 2:1 clay minerals such as smectite and vermiculite possess higher specific surface area as compared type 1:1 clay minerals such as kaolinite and halloysite because of their ability to swell [10]. The total specific surface area of the clay is denoted by the sum of external surface area and the internal surface area corresponding to the interlayer spaces [8].

Several authors have indicated that total specific area of the clay mineral can be increased through modification to increase their functionality in different areas of application. Hua [27] reported an increase in surface area of Na-bentonite from 34.1 to 77.2 m^2/g after modification with Mn oxides. Bentonite modified with the combination of Mn oxides and poly(diallyldimethylammonium chloride) showed a sharp increase in surface area to 128.9 m^2/g. The increase in total specific

Clay mineral	CEC (meq/100 g)	Ref
Unmodified smectite	118.5	[2]
Fe-exchanged smectite	115.75	[2]
Ti-Pillared smectite	105.75	[2]
Raw bentonite	265.5	[20]
Fe3+ modified bentonite	188.9	[20]
Na-montmorillonite	78	[21]
Fe(OH)-montmorillonite	12	[21]
Al(OH)-montmorillonite	14	[21]
Al3+ modified bentonite	183.3	[22]
Mukondeni smectite rich clay soils	79.93	[23]
Mixed mukondeni clay soils	137.7	[24]
Montmorillonite	91.61	[25]

Table 1. Cation exchange capacity of raw and modified clay minerals.

area could be attributed to swelling of bentonite clay during modification. Mishra and Paride [28] also reported increased specific surface area for bentonite pillared with manganese oxides at temperature of 500°C. This was attributed to decomposition of the complex with increasing temperature to form the oxide pillar which generated the void micropores inside the clay layers. This phenomenon was also emphasized by Bertella and Pergher [29] who also observed an increased in specific surface area of bentonite clay after pillaring using Al and Co from 58 to 304 m^2/g.

3. Application of clay in arsenic and fluoride removal

The presence of arsenic and fluoride has attracted worldwide attention due to their toxicity in human health after a prolonged period of exposure [30]. Excessive intake of fluoride can lead to dental and skeletal fluorosis while the intake of arsenic can lead to various types of cancer. The World Health Organization (WHO) has set the standard of fluoride and arsenic in water for human consumption at 1.5 and 0.01 mg/L, respectively [31]. Recently much attention is being driven into developing a technique that can be used to remove excess of fluoride and arsenic in drinking water to acceptable levels. Adsorption using clay mineral has emerged to be the promising technique and several studies pertaining to removal of fluoride and arsenic using clay minerals has been reported in the literature. This is because clay minerals are abundantly available in nature at little or no cost. Furthermore clay minerals are more chemical and mechanical stable, poses larger specific surface are and higher cation exchange capacity making them good adsorbents.

3.1. Arsenic removal

Mohapatra et al. [32] reported the adsorption of arsenic from water by Kaolinite, Montmorillonite and illite and its dependence on solution pH and temperature. The results indicated that As(V) adsorption is dependent on pH and optimum adsorption capacities of 0.86, 0.64 and 0.52 mg/g were achieved at pH 5 for kaolinite, montmorillonite and illite, respectively. Furthermore, it was found that increasing temperature decreases the adsorption efficiency indicating that the interaction between As(V) was exothermic. This was observed in both evaluated clay soils. When evaluating the mechanistic aspect for As(V) adsorption onto kaolinite, montmorillonite and illite, authors ascribed it to inner sphere surface complexion and strong specific ion adsorption.

The adsorptive properties of five different clay minerals namely, R-clay, Y-clay, E-clay, A-clay and Rhassoul-clay found in Morocco for As(V) removal has been evaluated by Bentahar et al. [33]. The results showed that As(V) adsorption was more favorable at acidic pH and clays containing higher iron oxide content had higher arsenic binding affinity. The maximum adsorption capacity observed was 1.076 mg/g.

3.2. Fluoride removal

The effectiveness of raw clay minerals in fluoride removal has been reported by several authors. Kau et al. [34] evaluated the fluoride retention by kaolin clay. It was observed that the degree of fluoride sorption by kaolin is dependent on solution pH and available fluoride

concentration. It was further believed that adsorption of fluoride by kaolinite clay is accompanied by slight expansion in the kaolin sheet lattice. After this study, Tor [35] evaluated the efficiency of montmorillonite clay mineral in adsorption of fluoride removal from groundwater. A maximum fluoride adsorption capacity of 0.263 mg/g was reported at initial pH of 6.

Mudzielwana et al. [23] reported the efficiency of Mukondeni smectite rich clay in fluoride removal. They observed that percentage fluoride removal decreases with increasing pH of the solution with about 92% fluoride removal noted at acidic pH of 2. Ngulube et al. [24] also observed the same trend in the adsorption of fluoride by mixed Mukondeni clays. The decrease in percentage of fluoride with increasing pH during adsorption by raw clay minerals is often attributed to abundance of OH^- at alkaline pH.

The fluoride adsorption capacity of selected South African clay soils was reported by Coetzee et al. [36]. They observed that kaolinite type clay has the lowest adsorption capacity while the gibbsite clay has the highest adsorption capacity toward fluoride ions. The adsorption capacity of South African clays can be summarized in the following increasing order: kaolinite> smectite> palygorskite> goethite> gibbsite. This was attributed to the structure of the clay, surface charges and also the chemical composition of the clay [36].

4. Modification of clays and application in arsenic and fluoride removal

It has been observed that raw clays exhibit low adsorption capacities toward arsenic and fluoride adsorption from solutions. This is attributed to the permanent negative charges on the edges of clay sheets [37]. As such clay modification by higher density charge species and organic cationic surfactant is essential to improve their binding affinity. Common techniques that have are used for modification of clays for arsenic and fluoride removal includes intercalation, coating and pillaring. Intercalation includes insertion of guest species in the interlayers of the clay mineral with preservation of the clay layered structure [38]. Guest species may be the inorganic cations such as Mn^{2+}, Fe^{3+} and Al^{3+} or organic cationic surfactants such as HDTMA and CTAB. Gitari et al. [20] intercalated Fe^{3+} ions onto South African bentonite clay, their results showed that the process involved the cation exchange between main exchangeable cations such as Mg^{2+}, Na^+, Ca^{2+} and K^+. This was confirmed by the subsequent decrease of the content of these chemical species in the Fe^{3+} modified bentonite. Mudzielwana et al. [39] and Masindi et al. [22] intercalated Mn^{2+} and Al^{3+} onto the interlayers of bentonite respectively, and also observed decrease in the content of Mg, Na Ca and K oxides. These results confirm that during intercalation basic exchangeable cations in the interlayers are exchanged for guest species.

Pillaring is the most commonly used procedure to transform phyllosillicate materials into microporous and mesoporous materials. It involves the formation, intercalation and subsequent fixation of polynuclear cations between the clay interlayers [29]. Thus the lamellar spacing and specific area increases, making these materials attractive adsorbents for adsorption of various inorganic contaminants. **Figure 4** presents a schematic diagram of a pillared clay [40].

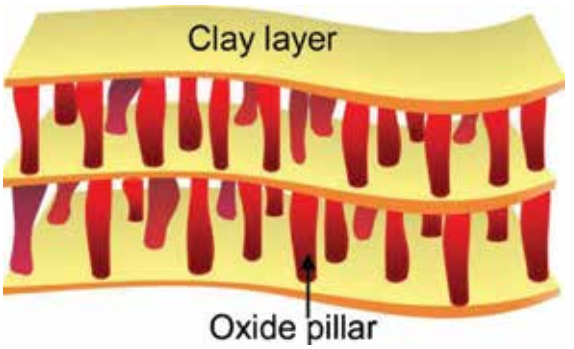

Figure 4. Schematic diagram of a pillared clay [40].

Lenoble et al. [21] pillared montmorillonite clay using titanium, iron and aluminum as pillaring solution. Their results confirmed that pillaring increases the basal spacing and the specific surface area by many folds. These results were confirmed by Mishra and Mahato [40] who also observed increased in both specific surface area for Mn and Fe pillared bentonite clay. Beside the side the change in basal spacing and chemical oxide content in the pillared clays, the whole process of pillaring does not change the mineralogical composition of the clay.

4.1. Arsenic removal using modified clay minerals

Mishra and Mahato [40] evaluated the effectiveness of Fe and Mn pillared bentonite clay in As(V) and As(III) removal from groundwater. Maximum As(III) and As(V) adsorption capacities of 17.57 and 25.77 μg/g were observed for Fe pillared bentonite while adsorption capacities of 25.77 and 26.17 μg/g were observed for Mn pillared bentonite clay. This was higher by many folds compared to 4.31 and 4.33 μg/g for raw bentonite clay. This was attributed to increased surface area in the pillared bentonite and also increased charge density in the pillared clay.

Ren et al. [25] intercalated Fe polycations and cetyltrimethylammonium bromide (CTMAB) onto montmorillonite clay mineral and test it for arsenic removal. The results showed that CTMAB had diffused into the interlayers of the montmorillonite minerals while Fe polycations were adsorbed on the outer surface and had formed flocculent particles. When tested for arsenic removal, CTMAB-Fe montmorillonite and Fe montmorillonite showed a maximum adsorption capacities of 8.85 and 15.15 mg/g for As(V), respectively, and 13.89 and 16.13 mg/g for As(III). Furthermore, the optimum adsorption capacities were observed at wide range of pH of 4–10.

4.2. Fluoride removal using modified clay minerals

Several studies have been reported concerning the adsorption of fluoride using chemically modified clay minerals and the results showed improved adsorption efficiency as compared to unmodified clay soils. Kamble et al. [41] reported better sorption capacity for La, Mn and Mg oxides incorporated bentonite clay compared to bare bentonite. Efficiency of magnesium incorporated bentonite in adsorption of fluoride has also been evaluated by Thakre et al. [42] and maximum adsorption capacity of 2.26 mg/g was achieved over a wide range of pH which

Adsorbent	CEC (meq/100 g)	Surface area (m^2/g)	Adsorbate	pH	Adsorbent dosage (g/L)	Adsorption capacity (mg/g)	Ref
Kaolinite	—	33	As(V)	5	40	0.86	[32]
Montmorillonite	—	58	As(V)	5	40	0.68	[32]
Illite	—	28	As(V)	5	40	0.54	[32]
Moroccan clays	35	22.5	As(V)	7	25	1.07	[33]
Smectite rich clay	79.9	20.35	F^-	2	8	0.21	[23]
Montmorillonite	—	18.5	F^-	6.0	8	0.26	[35]
Mixed Mukondeni clay	137.7	35.46	F^-	2	150	0.08	[24]
CTAMB-Fe montmorillonite	—	—	As(V)	4–10	4	8.85	[25]
Fe-montmorillonite	—	—	As(V)	4–10	4	15.15	[25]
Mg^{2+} bentonite	—	—	F^-	3–10	3	2.26	[41]
Fe^{3+} bentonite	188.9	49.95	F^-	2–10	20	2.29	[20]
Al^{3+} bentonite	183.3	33.1	F^-	2–12	10	5.7	[22]

NB: (–) = not reported.

Table 2. Comparison of the adsorption capacity between raw and modified clay toward arsenic and fluoride.

was better than the capacity achieved with unmodified bentonite. Gitari et al. [20] reported maximum adsorption capacity of 2.91 mg/g for the Fe^{3+} modified bentonite clay which was also better than the unmodified bentonite. The main factor which was leading to improved sorption fluoride capacity was the increased surface area that corresponds to availability of more active sites for fluoride ion adsorption. Furthermore, modification of clay mineral my high density charges polycations increases the amount of positive charges in the surface of adsorbent leading to increased sorption capacity of anions.

Table 2 summarizes the comparison between raw and modified clay soils toward fluoride and arsenic adsorption from water. It is observed that the adsorption of fluoride and arsenic increases by many fold after clay modification.

5. Mechanisms for arsenic and fluoride removal using clay soils

General mechanism involved for arsenic and fluoride removal using clay mineral can be summarized by the following three main steps: (i) Mass transfer of ions to the external of the adsorbent, (ii) adsorption of ions on the external particle surface and (iii) Intra-particle diffusion of ions from the exterior surface and the exterior surface and possible exchange with elements on the pore surface inside particles [30, 43]. These major three steps were observed during the adsorption of fluoride onto MnO_2 coated bentonite by Mudzielwana et al., [44]. Besides these

three steps, there are two adsorption processes that take place during the transfer of adsorbate ions into the adsorbent, namely, physisorption and chemisorption. Physisorption occurs when the ions are adsorbed to the surface through the weak intermolecular interactions such as Van der Waal forces, hydrogen bonding and dipole–dipole interactions [45]. Conversely, chemisorption occurs when adsorbate ions forms chemical bond through electron exchange. Lee et al. [46] evaluated the adsorption of As(III) and As(V) onto HDTMA modified clays and they concluded that the adsorption of As(III) was via physisorption while the adsorption of As(V) was via chemisorption. They further indicated that the adsorption of As(III) occurred on the outer layer of the adsorbent while the adsorption of As(V) occurred in the inner layer of the adsorbent.

Solution pH is the main factor that influences the adsorption of arsenic and fluoride onto clay minerals since it determines the surface charges [37, 47]. Several authors observed that adsorption of fluoride and arsenic by clay minerals is low at alkaline pH values due to the abundance of OH^- ions on the adsorbent surfaces that causes electrostatic repulsion. Furthermore, the adsorption of arsenic and fluoride has been observed to be favored by low pH values. This is mainly attributed to the fact that at low pH the clay surfaces are positively charges and as such ions will be removed easily through electrostatic attraction. Thakre et al. [42] used the Eqs. 1 and 2 to hypothesize the adsorption of fluoride onto magnesium incorporated bentonite under different pH conditions.

Acidic pH:

$$MOH + H^+ + F^- \leftrightarrow MF + H_2O \tag{1}$$

Alkaline pH:

$$M(OH)_2 + 2F^- \leftrightarrow MF_2 + 2OH^- \tag{2}$$

where M represents metals.

According to Ren et al. [5] the adsorption of As(V) and As(III) onto modified clay minerals at acidic and alkaline may be elucidated by Eq. 3–6:

Acidic:

$$FeOH + H_3AsO_4 \leftrightarrow FeH_2AsO_4 + H_2O \tag{3}$$

$$FeOH + H_3AsO_3 \leftrightarrow FeH_2AsO_3 + H_2O \tag{4}$$

Alkaline:

$$FeOH + H_3AsO_2 \leftrightarrow FeAsO_4^{2-} + H_2O + 2H^+ \tag{5}$$

$$FeOH + H_3AsO_3 \leftrightarrow FeHAsO_3 + H_2O + 2H^+ \tag{6}$$

6. Conclusion

This chapter presented a summary of mineralogical and chemical composition of raw and surface modified clay minerals and their application in arsenic and fluoride removal from drinking water. From the review, it is noted that properties of the clay minerals such as higher cation exchange capacity and specific surface areas as well as the chemical composition of clay minerals enables them to be used as arsenic and fluoride adsorbents. Furthermore, these physicochemical properties can be improved through intercalation and pillaring which consequently improves their applicability in arsenic and fluoride removal. Modification of clay minerals does not alter their phyllosilicate structure. However, it improves the basal spacing and specific surface areas of the clay minerals. The modification is mainly through ion exchange between the basic exchangeable cations such Na^+, K^+, Mg^{2+} and Ca^+ with the guest species. The effectiveness of the clay minerals in adsorption of arsenic and fluoride is mainly influenced by the surface charges which are determined by the solution pH. At acidic pH the sorption is higher due to the fact that the surface is positively charged which influences the sorption of anions through electrostatic attraction. Conversely, at alkaline pH the sorption is low due to electrostatic repulsion. Recently, the attention is mainly on modification of clay minerals to enhance their application in various fields. However, little has been done on evaluating the chemical stability and the cost effectiveness of modifying clay minerals. As such future studies should be directed toward evaluating the chemical stability of modified clay minerals especially those applied for drinking water treatment. Also, studies should elaborate the cost effectiveness for modifying clay minerals with chemical species.

Acknowledgements

Authors would like to acknowledge the financial assistance from the University of Venda research and publication committee (RPC).

Author details

Mugera W. Gitari* and Rabelani Mudzielwana

*Address all correspondence to: mugera.gitari@univen.ac.za

Environmental Remediation and Water Pollution Chemistry Research Group, Department of Ecology and Resources Management, School of Environmental Sciences, University of Venda, Thohoyandou, Limpopo, South Africa

References

[1] Suryadi I, Felycia ES, Aning A. Clay Materials for Environmental Remediation. New York: Springer; 2015. p. 5. DOI: 10.1007/978-3-319-16712-1

[2] Mukhopadhyay R, Manjaiah KM, Datta SC, Yadav RK, Sarkar B. Inorganically modified clay minerals: Preparation, characterization, and arsenic adsorption in contaminated water and soil. Applied Clay Sciences. 2017;**147**:1-10. http://dx.doi.org/10.1016/j.clay.2017.07.017

[3] Bhattracharyya KG, Gupta SS. Adsorption of few heavy metals on natural and modified kaolinite and montmorillonite: A review. Advances in Colloid and Interface. 2008; **140**:114-131. DOI: 10.1016/j.cis.2007.12.008

[4] Chatel G, Novikova L, Petit S. How efficiently combine sonochemistry and clay science? Applied Clay Science. 2016;**119**:193-201

[5] Fouodjou M, Fotouo-Nkaffo H, Laminsi S, Cassin AF, Brito-Benetoli LO, Debacher NA. Adsorption of copper (II) onto cameroonian clay modified by non-thermal plasma: Characterization, chemical equilibrium and thermodynamic studies. Applied Clay Sciences. 2016;**142**:136-144. http://dx.doi.org/10.1016/j.clay.2016.09.028

[6] Murray HH. Applied clay mineralogy today and tomorrow. Clay Minerals. 1999;**34**:39-49

[7] Shaik SMR, Nesser MS, Hussein I, Benamor A, Onaizi SA, Qiblawey H. Influence of polyelectrolytes and other polymer complexes on the flocculation and rheological behaviors of clay minerals: A comprehensive review. Separation and Purification Technology. 2017;**187**:137-161. http://dx.doi.org/10.1016/j.seppur.2017.06.050

[8] Jlassi K, Krupa I, Chehimi MM. Overview: Clay preparation, properties, modification. In: Jlassi K, Chehim MM, Thomas S, editors. Clay-Polymer Nanocomposites. Amsterdam: Elsevier Inc; 2017. p. 1-28. https://doi.org/10.1016/B978-0-323-46153-5.00001-X

[9] Lee SM, Tiwari D. Organo and inorgano-organo-modified clays in the remediation of aqueous solutions: An overview. Applied Clay Science. 2012;**59-60**:84-102

[10] Murray HH. Applied Clay Mineralogy: Occurrence, Processing and Application of Kaolins, Bentonites, Palygoroskite-sepiolite, and Common Clays. Amsterdam: Elsevier; 2007. 8

[11] Grim RE. Clay Mineralogy. 2nd ed. New York: McGraw-Hill; 1968. 384 p

[12] Tournassat C, Bourg IC, Steefel CI, Bergaya F. Surface properties of clay minerals. In: Tournassat C, Steefel CI, Bourg IC, Bergaya F, editors. Natural and Engineered Clay Barriers. Developments in Clay Science. vol. 6. Amsterdam: Elsevier; 2015. p. 5-31

[13] Moraes JDD, Bertolino SRA, Cuffini SL, Ducart DF, Bretzke PE, Leonardi GR. Clay minerals: Properties and applications to dermocosmetic products and perspectives of natural raw materials for therapeutic purposes–A review. International Journal of Pharmaceutics. 2017;**534**:213-2017. http://dx.doi.org/10.1016/j.ijpharm.2017.10.031

[14] Brigatti MF, Galan E, Theng BKG. Structure and mineralogy of clay minerals. In: Bergaya F, Lagaly G. Handbook of Clay Science. Development in Clay Sciences. 2013;**5**:21-81. https://doi.org/10.1016/B978-0-08-098258-8.00002-X

[15] Schoonheydt RA. Functional hybrid clay mineral films. Applied clay Sciences. 2014; **96**:9-21

[16] Odom IE. Smectite clay minerals: Properties and uses. Philosophical Transactions of the Royal Society of London. Series A, Mathematical and Physical Sciences. 1984;**311**(1517):391-409

[17] Ummartyoti S, Bunnak N, Manuspiya H. A comprehensive review on modified clay based composite for energy based materials. Renewable Energy and Sustainable Energy Reviews. 2016;**16**:466-472. http://dx.doi.org/10.1016/j.rser.2016.04.022

[18] Rouguerol J, Llewellyn P, Sing K. Adsorption by clays, pillared clays, zeolites and aluminophosphates. In: Rouguerol F, Rouguerol J, Sing KSW, Llewellyn P, Maurin, editors. Adsorption by Powders and Porous Solids. 2nd ed. Amsterdam: Academic Press; 2014:467-527. https://doi.org/10.1016/B978-0-08-097035-6.00012-7

[19] Ngulube T, Gumbo JR, Masindi V, Maity A. An update on synthetic dyes adsorption onto clay based minerals: A state of art review. Journal of Environmental Management. 2017;**191**:35-57

[20] Gitari WM, Ngulube T, Masins V, Gumbo JR. Defluoridation of groundwater using Fe^{3+} modified bentonite clay: Optimization of adsorption conditions. Desalination and Water Treatment. **53**:1578-1590. DOI: 10.1080/19443994.2013.855669

[21] Lenoble V, Bouras O, Deluchat V, Serpaud B, Bollinger J. Arsenic adsorption onto pillared clays and iron oxide. Journal of Colloid and Interface Science. 2002;**255**:52-58. DOI: 10.1006/jcis.2002.8646

[22] Masindi V, Gitari WM, Ngulube T. Defluoridation of drinking water using Al^{3+} modified bentonite clay: Optimization of fluoride adsorption conditions. Toxicology and Environmental Chemistry. 2014;**96**:1-16. DOI: 10.1080/02772248.2014.977289

[23] Mudzielwana R, Gitari MW, Msagati TAM. Characterization of smectite rich clay soil: Implication for groundwater defluoridation. South African Journal of Chemistry. 2016; **112**(11/12):1-8. http://dx.doi.org/10.17159/sajs.2016/20150442

[24] Ngulube T, Gitari MW, Tutu H. Defluoridation of groundwater using mixed Mukondeni clay soils. Water Science and Technology. 2017;**17**(2):480. DOI: 10.2166/ws.2016.157

[25] Ren X, Zhang Z, Lou H, Hu B, Dang Z, Yang C, Li L. Adsorption of arsenic on modified montmorillonite. Applied Clay Sciences. 2014;**97**(98):17-23

[26] Mucht F, Eusterhues k PGJ, Totsche KU. Specific surface area of clay minerals: Comparison between atomic force microscopy measurements and bulk-gas (N_2) and -liquid (EGME) adsorption methods. Applied Clay Science. 2011;**53**:20-26. DOI: 10.1016/j.clay.2011.04.006

[27] Hua J. Synthesis and characterization of bentonite based inorgano-inorgano-composite and their performances for removal of arsenic from water. Applied Clay Science. 2014; **114**:239-246. http://dx.doi.org/10.1016/j.clay.2015.06.005

[28] Mishra T, Parida K. A comparative study of textural and acidic properties of manganese (III) pillared montmorillonite and pillared acid-activated montmorillonite. Journal of Materials Chemistry. 1997;**7**(1):147-152

[29] Bertella F, Pergher SBC. Pillaring of bentonite clay with Al and Co. Micorporous and Mesoporous Materials. 2015;**201**:116-123. http://dx.doi.org/10.1016/j.micromeso.2014.09.013

[30] Alarcon-Herrera MT, Bundschuh J, Nath B, Nicolli HB, Gutierraz M, Reyes-Gomez VM, Nunez D, Martin-Dominguez IR, Sracek O. Co-occurrence of arsenic and fluoride in groundwater of semi-arid regions in Latin America: Genesis, mobility and remediation. Journal of Hazardous Materials. 2013;**262**:960-969. http://dx.doi.org/10.1016/j.jhazmat.2012.08.005

[31] World Health Organization. Guidelines for Drinking-water Quality, 4th ed. Geneva: Switzerland; 2011

[32] Mohapatra D, Mishra D, Chaudhury GR, Das RP. Arsenic adsorption mechanism on clay minerals and its dependence on temperature. Korean Journal of Chemical Engineering. 2007;**24**(3):426-430

[33] Bentahar Y, Hurel C, Draoui K, Khairoun S, Marmier N. Adsorptive properties of moroccan clays for the removal of arsenic(V) from aqueous solution. Applied Clay Science. 2016;**119**:385-392. http://dx.doi.org/10.1016/j.clay.2015.11.008

[34] Kau PMH, Smith DW, Binning DWS. Fluoride retention by Kaolin clay. Journal of Contaminant Hydrology. 1997;**28**:267-288

[35] Tor A. Removal of fluoride from aqueous solution by using montmorillonite. Desalination. 2006;**201**:267-276

[36] Coetzee PP, Puka R, Mubeng S. Characterization of selected South African clays for defluoridation of natural waters. Water SA. 2003;**29**(3):331-338

[37] Ma J, Qi J, Yao C, Cui B, Zhang T, Li D. A novel bentonite-based adsorbent for anionic pollutant removal from water. Chemical Engineering Journal. 2012;**200**(202):97-103. http://dx.doi.org/10.1016/j.cej.2012.06.014

[38] Schoonheydt RA, Pinnavala T, Lagaly G, Gangas N. Pillared clays and pillared layer solids. Pure Applied Chemistry. 1999;**71**(12):2367-2371

[39] Mudzielwana R, Gitari WM, Akinyemi SA, Msagati TAM. Synthesis, characterization, and potential application of Mn^{2+} intercalated bentonite in fluoride removal: Adsorption modeling and mechanism evaluation. Applied Water Science. 2017;**7**(8):4549-4561. DOI: 10.1007/s13201-017-0608-3

[40] Mishra T, Mahato DK. A comparative study on enhanced arsenic(V) and arsenic(III) removal by iron oxide and manganese oxide pillared clays from ground water. Journal of Environmental Chemical Engineering. 2016;**4**:1224-1230. http://dx.doi.org/10.1016/j.jece.2016.01.022

[41] Kamble SP, Dixit P, Rayalu SS, Labhsetwar. Defluoridation of drinking water using chemically modified bentonite clay. Desalination. 2009;**249**:687-693. DOI:10.1016/j.desal.2009.01.031

[42] Thakre D, Rayalu S, Kawade R, Meshram S, Subrt J, Labhsetwar N. Magnesium incorporated bentonite clay for defluoridation of drinking water. Journal of Hazardous Materials. 2010;**180**:122-130. DOI: 10.1016/j.jhazmat.2010.04.001

[43] Gupta SS, Bhattacharyya KC. Kinetics of adsorption of metal ions on inorganic material: A review. Advances in Colloid and Interface Science. 2011;**162**:39-58. DOI: 10.1016/j.cis.2010.12.004

[44] Mudzielwana R, Gitari WM, Akinyemi SA, Msagati TAM. Synthesis and physicochemical characterization of MnO_2 coated Na-bentonite for groundwater defluoridation: Adsorption modeling and mechanistic aspect. Applied Surface Sciences. 2017;**422**:745-753. http://dx.doi.org/10.1016/j.apsusc.2017.05.194

[45] Dawood S, Sen T. Review on dye removal from its aqueous solution into alternative cost effective and non-conventional adsorbents. Journal of Chemical Processing Engineering. 2014;**1**(104):1-7

[46] Lee SM, Laihmunsiama T, Tiwari D. Porous hybrid materials in the remediation of water contaminated with As(III) and As(V). Chemical Engineering Journal. 2015;**270**:496-507. http://dx.doi.org/10.1016/j.cej.2015.02.053

[47] Tiwari D, Lee MK. Novel hybrid materials in the remediation of ground waters contaminated with As(III) and As(V). Chemical Engineering Journal. 2012;**204**(206):23-21. http://dx.doi.org/10.1016/j.cej.2012.07.086

Chapter 4

Polymer-Clay Nanocomposites for Corrosion Protection

Abdullah Al-Shahrani, Ihsan Taie, Aziz Fihri and Gasan Alabedi

Additional information is available at the end of the chapter

http://dx.doi.org/10.5772/intechopen.74154

Abstract

Nanoclays have evoked a great deal of attention lately for the preparation of novel nanocomposite materials for several applications. This is attributed to their lamellar structures, which are distinguished by having high in-plane strength and stiffness, as well as a high aspect ratio. Nanocomposites have exhibited an advanced gas and water barrier properties compared to the pristine polymers. Such advancement plays a major role in enhancing the coating industry, specifically for corrosion protection. One main factor attributing to coating failure is its inability to maintain low water and oxygen permeability thought its service life. The penetration of these elements through the coating leads to corrosion initiation under the coating. The addition of clay to polymeric coatings has great potential to improve the corrosion protection performance of the coatings. This chapter will present the recent advancement in the preparation and utilization of clay nanocomposites as enhanced coatings for corrosion protection.

Keywords: clay, nanocomposite, organic coating, corrosion protection

1. Introduction

The function of a good coating on the metallic surface is to provide a physical barrier, preventing the metal to be in direct contact with the environment. Generally, the main principle to prevent corrosion is to eliminate one of the four main components causing the corrosion process (anodic reaction, cathodic reaction, electrolyte, and electrical connection between the cathode and the anode) [1]. Until about 1950, coatings were believed to act as a barrier, preventing water and oxygen to reach the metal. These two species are needed to drive the

oxygen reduction reaction (cathodic reaction) that initiates the corrosion process. In 1952, Mayne found that the diffusion rate of water and oxygen in an unpigmented coating is too high. Consequently, he suggested that the amount of water and oxygen arriving at the metal/coating interface is greater than the one required for corrosion to precede [2–4]. His hypothesis was based on the fact that the barrier action could not explain the effectiveness of the coating, while the conductivity of the coating is the main factor controlling the corrosion protection degree offered by the coating [2, 5, 6]. Mayne also reported that when the coating is immersed in a solution, it will gain a certain charge, negative or positive, depending on the nature of the coating. In this case, the coating will allow the opposite charge species to pass through. He believed that the permeation of these species will be through the bulk of the matrix. Corti attributed that the permeation of such species is affected by the presence of pores or imperfections in the coating. Based on that, he concluded the permeation to be through the pores and voids in the coating [2, 3]. Funke has a different understanding to the way the coating works to protect the steel. He believed that the protection degree that the coating offers depends on the degree of adhesion. The permeation of water through the coating will result in a water accumulation between the substrate and the coating, leading to coating blistering or coating delamination as a result of generating hydroxyl ions as products of the corrosion process. Such ions are believed to break the bond between the coating and the metal surface, and consequently, the coating adhesion will be significantly degraded [2, 7, 8]. Considering all the above approaches, loss of adhesion, the diffusion of water and oxygen, and the transport of the charged species can potentially result in poor corrosion protection performance. In general, mass transfer (diffusion) of a material in a specific environment is a result of a natural process tending to reach equality in concentration between two points. In the case of gases, the diffusion process will be mainly based on the difference in partial pressure, which is the driving force pushing the gasses from one side to another.

In case of polymeric coatings, the diffusion process will mainly depend on three factors: the nature of the polymeric coating, the magnitude of the driving force, and the nature of the diffusing species. The general mechanism of the permeability through the coating will follow three main steps: solution of small molecules in polymer, migrating through the polymer, and emergence of that molecule at the outer surface. Accordingly, the permeability can be presented mathematically as the product of solubility and diffusion as shown in Eq. (1) [9, 10]:

$$\text{Permeability} = \text{Solubility} \times \text{Diffusion (Henry's Law)} \tag{1}$$

When a coating is exposed to an electrolyte, the diffusion of the electrolyte follows two processes, which can be classified as fast and slow diffusion [11]. The fast process can occur within a few minutes of exposure, while the slow step can take weeks or months. According to Scantlebury, during the fast process, the electrolyte can reach the surface of the metal, but its electrical properties do not support the corrosion process, while the amount of electrolyte can reduce the adhesion strength of the coating [3].

There are many factors affecting the diffusion of the electrolyte and the corrosive species, namely water and oxygen. Considering the fact that the permeability of a coating depends on the amount of defect present, it can be concluded that the diffusion will be through areas of imperfection. These areas can be considered as free volume including pores and area of

weak cross-linking density. The free volume concentration increases, as the temperature goes above the glass transition temperature (Tg) of the coating. Tg is known as the temperature at which the coating state changes from glassy or solid state to a rubbery state. Above the Tg, the energy of the coating molecules increases, leading to an increase in the movement of these molecules. As a result of this, the free volume can increase, providing more areas for the diffusing species to transport through the coating. Based on that, it is highly recommended to select a coating having Tg higher than the temperature of the process [2, 10]. Film thickness has a great effect on the permeability of the coating. As the film thickness increases, the penetration of the corrosive species through the coating can be delayed. Increasing the film thickness above a critical thickness can increase the probability of having cracks in the coating [2]. Certain pigments have a significant effect on the permeability of coating. It is believed that water and oxygen cannot pass through pigment particles; therefore, the permeability can be reduced with increasing the pigment volume concentration (PVC). The PVC value should not exceed the critical pigment volume concentration (CPVC). Above the value of CPVC, the pigments will introduce voids and gaps inside the coating. These defects can provide an easy way for water and oxygen to go through [2]. It was reported that the pigmentation of inert particles such as nanoclays inside the coating can act as a barrier to reduce the diffusion rate of water and the oxygen through the polymer-clay nanocomposite coatings.

The nanoclays have evoked a great deal of attention lately for the preparation of novel nanocomposite materials for several applications [12]. The uniform dispersion of the layered silicates into polymers matrix leads to the preparation of nanocomposites with improved mechanical properties, thermal stability, and low flammability [13, 14]. This is attributed to their lamellar structures, which are distinguished by having high in-plane strength and stiffness, as well as a high aspect ratio [15]. Additionally, the clays possess excellent stability and low toxicity, and they are cheaper and widely available compared to other nonorganic fillers. Such advancement plays a major role in enhancing the coating industry, specifically for corrosion protection [16, 17]. One main factor attributing to coating failure is its inability to maintain low water and oxygen permeability throughout its service life. The penetration of these elements through the coating leads to corrosion initiation under the coating. The addition of clay to polymeric coatings has great potential to improve the corrosion protection performance of the coatings. This chapter will present the recent advancement in the preparation and utilization of polymer-clay nanocomposites as enhanced coatings for corrosion protection.

2. Structure of layered silicates

The most commonly used layered silicates to produce the polymer-clay nanocomposites belong to a group of clays classified as 2:1 layered or phyllosilicates [18]. This structural family includes natural clays, such as montmorillonite, hectorite, and saponite. Their crystal structure consists of two-dimensional layers made up of two tetrahedral silicon sheets fused to octahedral sheet of alumina or magnesia by the tip so that the oxygen ions of the octahedral sheet also belong to the tetrahedral sheets. The layer thickness of a sheet is of the order of 1 nm, and the lateral dimensions vary from 300 Å to several microns depending on the

specificity of the silicate. The relatively weak Van der Waals force ensures the stacking of the sheets between them and each layer called interlayer [19–21]. Stacking of the layers leads to a regular gap between each adjacent silicate layers called the interlayer or gallery. A negative surface charge is present on the layers due to the isomorphic substitution of tetrahedral silicon or aluminum and octahedral magnesium. The charge deficit is counterbalanced by alkali and alkaline earth cations situated inside the galleries [22].

The most used layered silicates are montmorillonite, hectorite, and saponite [23]. Their chemical formulae are illustrated in the **Table 1** [24]. All these layered silicates are characterized by a high surface area (700–800 m^2/g in the case of montmorillonite) and a moderate cation-exchange capacity (CEC) generally expressed in milliequivalents per 100 g (mequiv. per 100 g). The charge indicated by the chemical formula is an average over the whole crystal because the charge varies from layer to layer. Only a small proportion of the charges are located at the surface of the crystal, the majority being mainly in the interlayer spaces [22]. These cations are then exchangeable in solution.

To produce the nanocomposite with the required properties, the silicate layers should be exfoliated before being dispersed inside the polymer. Indeed, the hydrophilic characteristic of the clay does not allow it to be dispersed in the polymer matrix, which is generally organophilic. To render the mixture compatible, it is necessary to modify the clay before it is dispersed. For this reason, a pretreatment process should take place to weaken the forces holding the structure [24–27]. The main goal of this process is to render the surface of the layered silicate more organophilic. This improves the dispersion process of the layers inside the polymer under well-defined experimental conditions [28]. Given the structure and properties of clay, there are several modification techniques. However, the most commonly used technique for organophilic modification of clay is the ion-exchange reactions with cationic surfactants, including primary, secondary, tertiary, and quaternary alkylammonium cations to replace the hydrated cations with the protonated amine with long-chain alkylammonium cations. Alkylammonium cations in the treated clay decrease the surface energy of the inorganic host and increase interlayer spacing, rendering the modified organoclay is more compatible with organic polymer [29–33]. The above treatment process is basically an intercalating process to increase the spacing and decrease the adhesion forces between the silicate layers. The amine has the ability to achieve such target by acting as an intercalating agent. The efficiency of the intercalating agent is mainly influenced by the agent properties such as its hydrocarbon chain length [1]. It is very important to stress that there are also other original and interesting methods for modifying 2:1 phyllosilicates, such as the use of ionomers or block copolymers, and

Silicate	Chemical formula	Location of isomorphic substitutions	CEC (mequiv./100 g)
Hectorite	$M_x(Mg_{6-x}Li_x)Si_8O_{20}(OH)_4$[a]	Octahedral	120
Saponite	$M_xMg_6(Si_{8-x}Al_x)Si_8O_{20}(OH)_4$[a]	Tetrahedral	86.6
Montmorrillonite	$M_x(Al_{4-x}Mg_x)Si_8O_{20}(OH)_4$[a]	Octahedral	110

[a]M = monovalent cation; x = degree of isomorphous substitution (between 0.5 and 1.3).

Table 1. General formula and characteristic parameters of phyllosilicates 2:1.

the grafting of organic substances, such as organosilanes. In the clay, the hydroxyl functional groups are located on the surface of the layers and their edges, and so the silane agents possess the ability to form strong covalently bonds with inorganic clays.

3. Nanocomposite structures

Variations in the strength of interfacial interactions between the polymer matrix and layered silicates result in the formation of three main kinds of nanocomposites as described below [34].

- **Intercalated nanocomposites**: When the polymer is not able to intercalate between the silicate layers, a biphasic composite is obtained, whose properties remain in the same range as the conventional microcomposites structure, in which the clay sheets are not swollen by the polymer and are in the form of clumps or agglomerates in the matrix.
- **Flocculated nanocomposites**: Conceptually, this is similar as intercalated nanocomposites. More polymer molecules are getting inside the layers structure to give more spacing between the silicate layers.
- **Exfoliated nanocomposites**: In this type of nanocomposite, the individual clay layers are separated in a continuous polymer matrix. Usually, the clay content of an exfoliated nanocomposite is much lower than that of an intercalated nanocomposite. The **Figure 1** shows illustrations of the three types of polymer-clay nanocomposites.

Despite the impressive progress that has been reported during the last few years regarding the use of polymer-clay nanocomposites for corrosion protection, its effect on the corrosion performance has rarely been investigated. Although most organo-modified clay nanocomposites

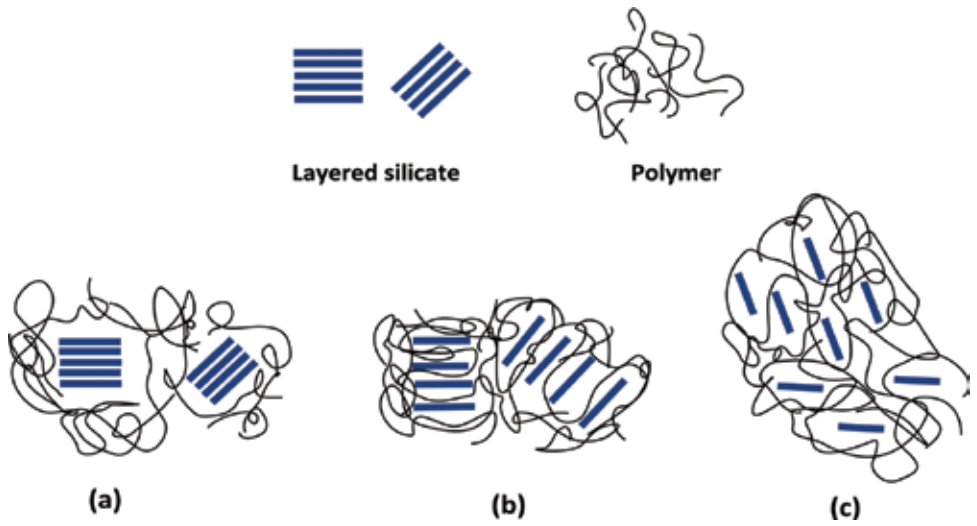

Figure 1. The main types of nanocomposite. (a) Intercalated, (b) flocculated, and (c) exfoliated.

reported so far are intercalated, exfoliated structures are more desirable in property improvement of the polymeric materials. In this context, Chen and co-workers described the processing of epoxy-layered silicate nanocomposites with different properties as corrosion resistant coatings on aluminum surfaces [35]. Based on their studies, they concluded that there is a slight enhancement in anticorrosion properties for the exfoliated nanocomposites coatings and no enhancement for the intercalated nanocomposites. Finding shows that these criteria are related to the better dispersion of silicate nanosheet in some epoxy matrix than the other grades of resin matrix. However, these findings were not very conclusive, and it appears that an epoxy with a lower barrier resistance or higher permeability will help in discriminating the corrosion behavior through the introduction of clay into the matrix. Similarly, Sakai and co-workers found that the exfoliated clay structures were more fixed in polymeric matrix compared to intercalated and conventional clay structures [36]. Additionally, exfoliated clay structures exhibited better corrosion performance compared to intercalated coatings nanocomposites. This is mainly attributed to the larger clay interlayer distance, smaller clay aggregate, and uniform homogeneity of exfoliated clay structures inside the epoxy matrix. In some case, a mixture of intercalated and exfoliated nanocomposites was obtained, and it was difficult to evaluate the effect of nanocomposite structures on the corrosion performance of the prepared nanocomposites [37].

4. Methods used for the synthesis of nanocomposites

Several methods were reported to prepare clay-based polymer nanocomposites. These include in-situ polymerization, melt intercalation, and solution casting, according to the starting materials and processing techniques:

1. **Intercalation of polymer from solution.** This is based on a solvent system, in which the polymer is soluble and the silicate layers are swellable. The layered silicate is first swollen in a solvent, such as water, chloroform, or toluene. When the polymer and layered silicate solutions are mixed, the polymer chains intercalate and displace the solvent within the interlayer of the silicate. Upon solvent removal, the intercalated structure remains, resulting in nanocomposite [38, 39].

2. **In-situ intercalative polymerization.** In this method, the layered silicate is swollen within the liquid monomers or a monomer solution so that the polymer formation can occur between the intercalated sheets. Polymerization can be initiated either by heat or radiation [40, 41]. This method technique was used to prepare nanocomposites based on polyamide, poly(e-caprolactone), polystyrene, polyolefien, and polyethylene terephthalate [41].

3. **Melt intercalation.** The melt intercalation involves annealing, statically or under shear, a mixture of the polymer and modified clays. This method has great advantages over either in-situ intercalative polymerization or polymer solution intercalation. Firstly, this method is environmentally benign due to the absence of organic solvents. Secondly, it is compatible with current industrial process [42, 43]. This process is widely used to design nanocomposites based on polyamide, such as polyethylene terephthalate and nylon 6 [12]. **Table 2** shows the advantages and the limitations of different methods used to prepare the polymer-clay nanocomposites.

Processing methods	Advantages	Limitations
Intercalation of polymer from solution	• More suitable at laboratory scale • Uniform dispersion of the clay particles inside the polymer • Preparation of intercalated nanocomposites based on polymers with low polarity	• Environmentally unfriendly due to the use of large amounts of solvents • Limited to certain polymer/solvent pairs, in which the polymer is soluble and the silicate layers are swellable
In-situ intercalative polymerization	• Easy method, based on the dispersion of the filler in the liquid monomer	• Monomer and clay must have similar hydrophobicity to mix • Limited applications • Suitable monomer is not always available • Difficult control of intragallery polymerization
Melt intercalation	• Environmentally benign • Compatible with industrial polymer process • Use of polymers not suited for other methods	• Limited applications to polyolefins • Organo-modified clay must be thermally stable at the softening point of the polymer

Table 2. Summary of different methods used for the synthesis of nanocomposites.

Concerning the characterization of polymer-clay nanocomposites, the small-angle X-ray scattering (SAXS), transmission electron microscopy (TEM), and scanning electron microscopy (SEM) are the main techniques used to identify the structure of nanocomposites. Indeed, the SAXS allows to monitor the position, shape, and the intensity of the peak, while TEM provides information on the spatial disposition of the internal structure and the spatial distribution of the various phases. SEM is employed to identify the response of the clays to the cationic exchange reaction.

5. Corrosion and organic coatings

Corrosion is defined as the gradual oxidation of metallic materials by converting them to their original state of oxide, sulfide, carbonate, or other stable salts in the ambient environment. Corrosion results from a combination of reactions occurring at the metal-solution interface by involving electrons and the chemical species. More specifically, the oxidation of the metallic material naturally occurs at the metal-environment interface and constitutes the anodic reaction, whereas the reduction of oxygen typically takes place in solution and often constitutes the cathodic reaction [44]. The cathodic and anodic reactions form an electrical circuit, which is completed by conduction of electrons in the metal and by ionic conduction through the electrolyte. There are various forms of corrosion that can take place depending on the surrounding environment and the design of the equipment that suffers corrosion. The galvanic, pitting, intergranular, crevice, and uniform corrosions are the most investigated corrosion

in the literature [45, 46]. In general, the corrosion protection methods commonly used are mainly organic and metallic coatings, inhibitors, cathodic, and anodic protection. This latter is relatively new, and it was first demonstrated and tested by Edeleanu 1954 [47].

The use of organic coatings on metal is usually an effective way to protect metal surfaces from corrosion while still preserving the desirable physical and mechanical properties of the metal [47, 48]. Corrosion on a bare metal surface is very complex process in itself, as the morphology of the corrosion layers formed on the surface and corrosion rate depends on several factors [49]. To evaluate the performance of any organic coatings, several parameters must be taken into consideration such as the permeability to water and oxygen, adhesion performance to the metal, coating thickness, ionic conductivity, as well as pore size distribution [50]. Commonly, the corrosion mechanism of an organic coating to protect the metal against corrosion can be divided into three groups: the electrochemical effect, the physicochemical effect, and the adhesion to the substrate [8]. The organic coating is a complex formulation of variety of materials each having a specific function. Examples of those materials include, but not limited to the following: polymeric materials, solvents, pigments, and various additives. Organic coating simply acts as a barrier between the metal surface and the surrounding environment. The barrier ability of such coating might be attributed to its structure or due to some additives or pigments implemented inside the coating. For this reason, understanding the nature and the constituents of the coating to be applied is essential to predict the performance of this coating as a corrosion protective technique. There are several reasons that can lead to failures in the coating applied, and the most common failures and the reasons leading to such failures are the permeability of the coating, adhesion, blistering, and cathodic delamination. Importantly, it was reported that a poor coating applied to a well-prepared surface is better than a good coating applied to a poorly prepared surface [51]. Contaminations on the surface of the metal can cause a direct failure to the applied coating. These contaminations can be the reason for a poor coating adhesion, which is one of the most critical factors controlling the quality of the coating. It is also well known and documented that no matter how good the coating is, the corrosion still can take place under the coating if the surface is contaminated.

6. Anticorrosive properties of layered silicate nanocomposites

It is well known that polymeric coatings are not permanently impenetrable, as the presence of defects in the coatings will lead to the formation of the pathways for the corrosive species to reach and attack the metallic surface, and a localized corrosion will be initiated. Various fillers such clays as were incorporated into the polymeric coatings to improve their barrier properties by reducing their permeability and increase the length of the diffusion pathways for oxygen and water species [52]. Indeed, the addition of clay as filler creates a maze that impedes the diffusion of corrosive molecules as illustrated in **Figure 2**. The use of clay as pigments appears to be one of the promising solutions to enhance the corrosion performance of nanocomposites. This section presents an overview on the recent advances of using of polymer-clay nanocomposites for corrosion protection.

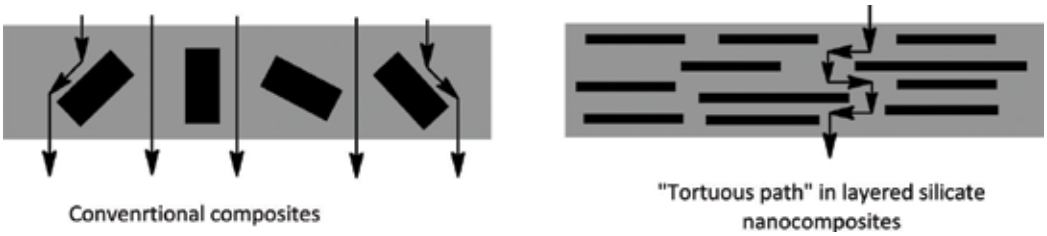

Figure 2. The difference between conventional composite and nanocomposites.

Different kinds of polymers were used to prepare nanocomposites coatings such as conjugated polymers and thermoplastic polymers [53]. Using the in-situ thermal polymerization, Yeh and colleagues prepared a series of polymer-clay nanocomposite by dispersing layered montmorillonite (MMT) clay into an organic poly(methyl methacrylate) matrix [54]. Firstly, methyl methacrylate monomers were intercalated into the montmorillonite that was exfoliated by cation-exchange reaction with quaternary alkylammonium cations or alkylphosphonium cations followed by a typical free-radical polymerization. The as-synthesized polymer-clay nanocomposites exhibited enhanced Tg compared to pure polymer. TEM analysis revealed that after the dispersion of the clay, the prepared nanocomposite displayed a mixed nanomorphology with well-exfoliated silicate layers into the polymer matrix. The electrochemical measurements using polarization resistance, corrosion current, and impedance spectroscopy revealed that nanocomposites coatings with the low clay loadings (e.g., 1 wt%) exhibited better anticorrosion protection for steel compared to the pure poly(methyl methacrylate). In an independent study, the same group has also designed several nanocomposite materials containing polyaniline (PANI) and layered montmorillonite clay and investigated their corrosion performance for cold-rolled steel [55]. Firstly, the organophilic montmorillonite was prepared via cation-exchange reaction with cocamide-propylhydroxysultaine before being mixed with aniline monomers in diluted hydrochloric acid followed by one-step oxidative polymerization. TEM analysis of as-synthesized nanocomposite revealed that the prepared materials possessed mixed nanomorphology, and the silicate layers were found to be well dispersed in the polyaniline matrix. The electrochemical measurements of potentiodynamic (e.g., Tafel plots) of a series of polyaniline nanocomposites with varying clay loadings at room temperature are illustrated in **Table 3**. Electrochemical corrosion current values of polyaniline nanocomposites were found to be decreasing progressively with further increment in clay loading. Importantly, visual inspection of the corrosion products revealed the presence of grayish oxide layer formed over polyaniline nanocomposites, showing better corrosion performance. It is very important to stress that the incorporation of the montmorillonite in polyaniline matrix resulted in a decrease in mechanical strength and in thermal decomposition temperature. This could be attributed to the significantly decreased molecular weight of polyanilines formed in the montmorillonite. Same research group evaluated the effect of adding organo-modified clay on the corrosion protection performance of conducting polymer/layered silicate, such as poly(o-methoxyaniline) and poly(3-hexylthiophene) [56]. The experimental findings revealed that the conducting polymer/layered silicate nanocomposites with low clay loading (3 wt.%) were found exhibiting better anticorrosion properties compared to the pure conducting polymer.

Compound code	Feed composition (wt.%)		Inorganic content found in the product (wt%)[a]	Electrochemical corrosion measurements[b]			
	PANI	MMT		E_{corr} (v)	R_p (KΩ cm²)	$I_{corr \times 10^{-6}}$ (A/cm²)	R_{corr} (mm/year)
Bare	—	—	—	−0.641	0.8	44.4	86.1
PANI	100	0	0	−0.590	3.4	12.0	23.3
CLAN0.25	99.75	0.25	0.70	−0.581	13.7	2.9	5.6
CLAN0.5	99.25	0.50	1.50	−0.568	15.4	2.7	5.2
CLAN0.75	99.00	0.75	3.80	−0.555	20.0	2.4	4.5
CLAN1	99.00	1.00	4.70	−0.551	36.2	1.1	2.1
CLAN3	97.00	3.00	7.10	−0.543	57.9	0.5	1.0

[a]As determined by thermogravimetric analysis.
[b]Saturated calomel electrode was employed as reference electrode.

Table 3. Relations of the composition of polyaniline (PANI)-MMT clay nanocomposite materials with the E_{corr}, R_p, I_{corr}, and R_{corr} measured from electrochemical methods[a].

In a subsequent study, the same research group investigated the corrosion properties of polyaniline/clay nanocomposites prepared from Na^+-montmorillonite or organo-modified montmorillonite with dodecylbenzene sulfonic acid using in-situ emulsion polymerization in the presence of aniline monomer [57]. The authors conducted a series of electrochemical measurements and concluded that the polyaniline nanocomposites coatings modified with low loading of Na^+-montmorillonite exhibited better anticorrosion performance compared to conventional polyaniline on cold-rolled steel. This was attributed to the co-existence of the redox catalytic properties of polyaniline and the barrier effect of montmorillonite dispersed in the nanocomposites. Yeh and colleagues were also reported the anticorrosive properties of thermosetting polymer-layered silicate nanocomposites, such as polyimide and epoxy nanocomposites, prepared by solution dispersion procedure and thermal ring opening polymerization [58, 59]. The standard electrochemical measurements such as impedance spectroscopy, corrosion potential, and corrosion current revealed that the prepared thermosetting polymer/layered silicate nanocomposites exhibited enhanced protection against the corrosion on cold-rolled steel compared to bulk polymers. Danaee and co-workers investigated the effect of adding nanoclay on corrosion protection of zinc-rich epoxy coatings on steel [60]. The TEM findings revealed that the clay nanolayers were effectively dispersed and successfully separated between zinc particles in coating. The electrochemical measurements revealed that the incorporation of 1 wt.% clay enhanced the cathodic protection duration and sacrificial properties of the coatings. These findings clearly demonstrate that the incorporation of clay into the coating decreased the electrical contact between the zinc particles without affecting the zinc sacrificial properties. The authors indicated that high clay loadings lead to the increment of the porosity in coatings and the decrease in the intercalation of clay which could decrease the long-term protective performance of the coating. Spathis and co-workers investigated the performance of epoxy-clay nanocomposite coatings for steel protection [61].

The montmorillonite clay was firstly modified with quaternary or primary octadecylammonium cations before being mixed with the epoxy resin. The experimental findings revealed that the mechanical and thermomechanical of all epoxy-organoclay nanocomposites were enhanced compared to those of the pure epoxy polymer. The electrochemical impedance measurements indicated that the epoxy-montmorillonite clay modified with primary octadecylammonium cations exhibited better protection performance compared to those modified with quaternary octadecylammonium cations. Indeed, the total resistance value, R_{tot}, after 4 days exposure in the corrosive environment, improved from 1.03×10^2 of bare steel, to 5.34×10^3 in the case of pure epoxy resin, to 7.40×10^3 in the case of epoxy-loaded with clay modified with quaternary octadecylammonium ions, and to 2.96×10^4 (Ωcm^2) in the case of nanocomposite made from modified clay with primary octadecylammonium ions. Importantly, the total resistance values decrease continuously in case of bare steel, with exposure time and the relation between these two factors were observed to be linear, indicating a constant corrosion rate. Importantly, the protective corrosion protection performance of the nanocomposite coatings was found to depend on the clay loading up to the saturation level. The excellent mechanical properties and thermal stability, as well as the high corrosion protection of these epoxy-clay nanocomposites, make them attractive candidates for various demanding coating applications. Al-Shahrani and colleagues demonstrated that the incorporation of modified bentonite with intercalating agents in the epoxy-based coatings resulted in the development of epoxy-bentonite nanocomposites with intercalated structures as shown in the **Figure 3** [62]. The presence of the silicate layers was evident in the TEM images with different degree of intercalation. The corrosion resistance abilities of a series of epoxy-bentonite nanocomposites, as coatings on carbon steel, were evaluated by electrochemical impedance spectroscopy, in 3.5% NaCl solution, at room temperature and compared to unpigmented epoxy. The experimental findings indicated that the presence of nanolayers has successfully improved the corrosion protection of epoxy resin as shown in **Table 4**. Furthermore, the amount of bentonite has an influence of the performance of the coating as the epoxy modified with 3% of bentonite led to

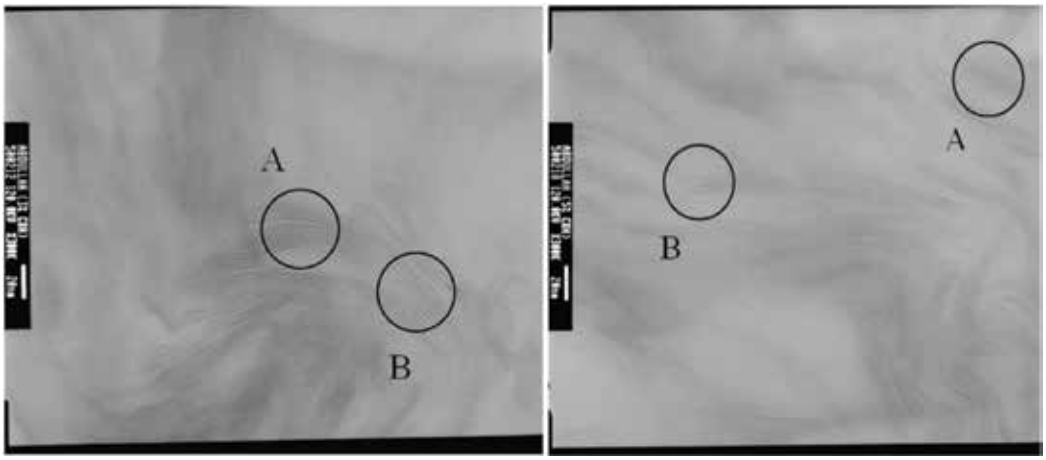

Figure 3. TEM micrographs of epoxy/bentonite nanocomposites: 3% (left) and 5% (right).

Coatings systems	Resistance (KΩ.cm^2)	Capacitance (F)
Neat epoxy	5.60	4.00E-04
Epoxy and 1 wt.% clay nanocomposites	4.5E + 05	1.04E-10
Epoxy and 3 wt.% clay nanocomposites	5.60E + 05	9.65E-11
Epoxy and 5 wt.% clay nanocomposites	1.60E + 05	5.00E-10

Table 4. The resistance and capacitance of coated samples from electrochemical impedance spectroscopy calculations after 40 days of immersion.

a high protection level. 5 wt% clay loading showed the lowest performance, indicating that it exceeded the saturation level of clay into the epoxy and consequently generated areas of agglomeration that can be identified as weaknesses in the coating. Such findings suggest that there is a critical loading value above which the coating might be affected [63, 64].

Navarchian and co-workers prepared polyaniline and polyaniline/montmorillonite nanocomposites via in-situ oxidative polymerization, and the resulted nanoparticles were incorporated into the epoxy resins and coated on steel substrates [65]. The anticorrosion performance of prepared epoxy-based coatings was conducted through electrochemical Tafel and electrochemical impedance spectroscopy tests. It was reported that the epoxy coating modified by polyaniline/montmorillonite nanocomposite particles exhibited improved corrosion protection compared to unpigmented epoxy and epoxy/polyaniline coatings as it can be seen in **Table 5**. Furthermore, these findings indicated also that the incorporation of polyaniline and organo montmorillonite (OMMT) into epoxy coating improves its anticorrosion performance compared to polyaniline/montmorillonite and neat polyaniline. Similar findings were reported by Kalaivasan and Shafi using polyaniline/montmorillonite clay nanocomposites prepared by mechanochemical intercalation method [66].

It is worth noting that the effect of clay in the polymer/layered silicate nanocomposites coatings was commonly evaluated at room temperature, and the investigation of the corrosion performance of these materials at higher temperature has attracted little attention. Do the coatings operated at high temperatures still maintain their good corrosion efficiency as even compared to that of electrode coated with neat polymer at room temperature? In this context, Yeh and colleagues performed the electrochemical corrosion parameter measurements of water-based conducting polyaniline/montmorillonite nanocomposites of polyaniline with

Sample code	$I_{corr} \times 10^6$ (A/cm^2)	$E_{corr} \times 10^3$(v)	R_p (KΩ cm^2)	R_{corr} (mm/year)
Epoxy	1.170	−483	11.35	0.013
Epoxy/PANI	0.798	−463	17.24	0.009
Epoxy/PANI/MMT	0.651	−459	19.97	0.007
Epoxy/PANI/OMMT	0.467	−418	28.51	0.005

Table 5. The Tafel plot data for steel panels coated with neat and modified epoxy in NaCl (3.5 wt. %) solution.

Compound code	Feed composition (wt.%)		Inorganic content found in the product (wt.%)[a]	Electrochemical corrosion measurements[b]			
	PMBS	MMT		E_{corr} (v)	R_p (KΩ cm²)	$I_{corr} \times 10^{-6}$ (A/cm²)	R_{corr} (mm/year)
Bare	—	—	—	−0.670	1.91	80.00	37.24
PMBS	100	0	4.56	−0.644	13.87	31.40	14.62
CLMA1	99.00	1.00	6.13	−0.568	20.86	11.60	5.40
CLMA3	97.00	3.00	7.05	−0.528	67.36	10.20	4.75
CLMA3 (M)	97.00	3.00	7.28	−0.575	50.33	15.20	7.08

[a]As determined by thermogravimetric analysis.
[b]Saturated calomel electrode was employed as reference electrode.

Table 6. Relations of the composition of polyacrylate-latex clay nanocomposite materials with the E_{corr}, R_p, I_{corr}, and R_{corr} measured by electrochemical methods.

raw Na^+-montmorillonite clay [67]. In this study and based on the electrochemical tests such as corrosion potential, polarization resistance, corrosion current corrosion rate, and electrochemical impedance spectroscopy, the nanocomposite coating containing 1 wt% of clay exhibited an noticeable improved corrosion efficiency on cold-rolled steel electrode at high temperature of 50°C and was found even much better than that of no coated and electrode coated with unpigmented polyaniline at room temperature. Indeed, the Ecorr of polyaniline nanocomposites measured at 50°C (E_{corr} = −572.5 mV) was lower than that of uncoated (E_{corr} = −664.1 mV) and polyaniline-coated electrode measured at room temperature.

Yeh and colleagues recently reported the anticorrosive properties of water-based polyacrylate/layered silicate nanocomposites [68]. Raw Na^+-montmorillonite clay and organo montmorillonite clay were used for the preparation of nanocomposites. The anticorrosion performance of cold-rolled steel coupons coated with as-prepared unpigmented polyacrylate (denoted PMBS) and a series of nanocomposite latexes were evaluated by operating sequential electrochemical corrosion parameters, such as corrosion potential, polarization resistance, corrosion current, and corrosion rate as illustrated in **Table 6**. It should be noted that nanocomposite latexes with Na^+-MMT clay exhibit better corrosion protection efficiency on cold-rolled steel coupons than that of with organo-MMT clay based on the studies of E_{corr}, R_p, I_{corr}, $R_{corr,}$ and R_{ct}.

7. Concluding remarks

In conclusion, an impressive progress has been reported during the last few years regarding the preparation and the use of polymer-clay nanocomposites for corrosion protection. These materials offer a number of advantages, such as excellent mechanical and thermal stability, improved anticorrosion protection, and wide accessibility of clay. The corrosion protection properties of these materials were found influenced by the type of the clay and curing agents

used to process the nanocomposites. Despite the significant progress of research efforts, a number of challenges remain untapped to understand the complex structure in clay-based nanocomposites. For example, exfoliation of clay layers into polymers matrix is still ambiguous to understand. This is very critical to prepare new nanocomposite with enhanced corrosion properties. A highly exfoliation of the clay inside the polymer matrix is usually difficult to attain. In addition, the most of works reported in the literature revealed the absence of direct relationship between the nanocomposite structures and their final anticorrosive properties most probably, thanks to negligence of the interface properties in determination of final anticorrosion performance. An in-depth understanding of the effect of morphology of clays on the corrosion performance of nanocomposites is necessary to design an ideal coating. With these present challenges combined with emergent interest in the use of polymer-clay nanocomposites for corrosion protection, it is certain that this field will continue to be a fast-moving research topic for the next several years.

Acknowledgements

We thank Philip J. Embleton from our Internal Relations Unit and Corporate Relations Division for his careful and critical reading of this manuscript.

Author details

Abdullah Al-Shahrani*, Ihsan Taie, Aziz Fihri and Gasan Alabedi

*Address all correspondence to: abdullah.shahrani.13@aramco.com

Oil and Gas Network Integrity Division, Research and Development Center, Saudi Aramco, Dhahran, Saudi Arabia

References

[1] Jones DA. Principles and Prevention of Corrosion. 2nd ed. New Jersey: Prentice Hall; 1996

[2] Wicks ZW Jr, Jones FN, Pappas SP, Wicks DA, editors. Organic Coating: Science and Technology. 3rd ed. Hoboken, NJ, USA: John Wiley and Sons; 2007

[3] Greenfield D, Scantlebury JD. The protective action of organic coatings on steel. Journal of Corrosion Science and Engineering. 2000:3, paper 5

[4] Sykes JM, Whyte EP. Behaviour of zinc-iron bimetallic couple coated with poly-vinyl butyral lacquer during intermittent exposure to salt solution. Corrosion Science. 2007;**49**: 3361-3380

[5] Mayne JE, Mills DJ. The effect of the substrate on the electrical resistance of polymer film. Oil and Petroleum - American Chemical Society. 1975;**58**:155-159

[6] Mayne JEO, Scantlebury JD. Ionic conduction in polymer films: II. In homogeneous structure of varnish films. British Polymer Journal. 1970;**2**:240-243

[7] Funke W, Arslanov V. The effect of water on the adhesion of organic coating on aluminium. Progress in Organic Coating. 1988;**15**:355-363

[8] Funke W. Problems and progress in organic coatings science and technology. Progress in Organic Coating. 1997;**31**:5-9

[9] Barrer RM. Diffusion in and Through Solids. Cambridge: Cambridge University Press; 1951

[10] Brydson JA. Plastics Materials. Butterworth Scientific, London: 4th; 1982

[11] Wong F, Buchheit RG. Utilizing the structural memory effect of layered double hydroxides for sensing water uptake in organic coatings. Progress in Organic Coating. 2004;**51**: 91-102

[12] Zabihi O, Ahmadi M, Nikafshar S, Preyeswary KC, Naebe M. A technical review on epoxy-clay nanocomposites: Structure, properties, and their applications in fiber reinforced composites. Composites Part B Engineering. 2018;**135**:1-24

[13] Burnside SD, Giannelis EP. Synthesis and properties of new poly(dimethylsiloxane) nanocomposites. Chemistry of Materials. 1995;**7**:1597-1600

[14] Gilman JW. Flammability and thermal stability studies of polymer layered-silicate-clay/nanocomposites. Applied Clay Science. 1999;**15**:31-49

[15] Park JH, Jana SC. Mechanism of exfoliation of nanoclay particles in epoxy-clay nanocomposites. Macromolecules. 2003;**36**:2758-2768

[16] Bagherzadeh MR, Mahdavi F. Preparation of epoxy-clay nanocomposite and investigation on its anti-corrosive behavior in epoxy coating. Progress in Organic Coating. 2007;**60**: 117-120

[17] Pinnavaia TG, Beall GW. Polymer-Clay Nanocomposites. Oxford, UK: Wiley Series in Polymer Science; John Wiley & Sons; 2000

[18] Xie W, Gao Z, Pan W-P, Hunter D, Singh A, Vaia R. Thermal degradation chemistry of alkyl quaternary ammonium montmorillonite. Chemistry of Materials. 2001;**13**:2979-2990

[19] Theng BKG. The Chemistry of Clay-Organic Reactions. New York: Wiley; 1974

[20] Giannelis EP, Krishnamoorti R, Manias E. Model systems for confined polymers and polymer brushes. Advances in Polymer Science. 1999;**118**:108-114

[21] Sinha-Ray S, Okamoto M. Structure-property relationship in biodegradable poly(butylene succinate)/layered silicate nanocomposites. Macromolecules. 2003;**36**:2355-2367

[22] Shipp DA. In: Andrews DL, Scholes GD, Wiederrecht GP, editors. Comprehensive Nanoscience and Technology. Academic Press; 2011. pp. 265-276

[23] Giannilis EP, Krishnamoorti R, Manias E. Polymer-silicate nanocomposites: Model systems for confined polymers and polymer brushes. Advances in Polymer Science. 1999;**138**:108-147

[24] Le Pluart L, Duchet J, Sautereau H, Gerard JF. Surface modifications of montmorillonite for tailored interfaces in nanocomposites. The Journal of Adhesion. 2002;**78**:645-662

[25] Zhao Z, Tang T, Qin Y, Huang B. Relationship between the continually expanded interlayer distance of layered silicates and excess intercalation of cationic surfactants. Langmuir. 2003;**19**:9260-9265

[26] Li Z, Jiang W-T, Chen C-J, Hong H. Influence of chain lengths and loading levels on interlayer configurations of intercalated alkylammonium and their transitions in rectorite. Langmuir. 2010;**26**:8289-8294

[27] Ca Pazos M, Castro MA, Mar Orta M, Pavón E, Rios JSV, Alba MD. Synthetic high-charge organomica: Effect of the layer charge and alkyl chain length on the structure of the adsorbed surfactants. Langmuir. 2012;**28**:7325-7332

[28] Khayankarn O, Magaraphan R, Schwank JW. Adhesion and permeability of polyimide-clay nanocomposite films for protective coatings. Applied Polymer Science. 2003;**89**: 2875-2881

[29] Yu YH et al. Preparation and properties of polyimide-clay nanocomposite materials for anticorrosion application. Applied Polymer Science. 2004;**92**:3573-3582

[30] Yeh JM, Chin CP, Chang S. Enhanced corrosion protection coatings prepared from soluble electronically conductive polypyrole-clay nanocomposite materials. Applied Polymer Science. 2003;**88**:3264-3272

[31] Yeh J-M, Liou S-J, Lai C-Y, Wu P-C. Enhancement of corrosion protection effect in polyaniline via the formation of polyaniline-clay nanocomposite materials. Chemistry of Materials. 2001;**13**:1131-1136

[32] Lepoittevin B, Pantoustier N, Devalckenaere M, Alexandre M, Calberg C, Jérôme R, Henrist C, Rulmont A, Dubois P. Polymer/layered silicate nanocomposites by combined intercalative polymerization and melt intercalation: a master batch process. Polymer. 2003;**44**:2033-2040

[33] Chena C, Khobaib M, Curliss D. Epoxy layered-silicate nanocomposites. Progress in Organic Coating. 2003;**47**:376-383

[34] Pavlidou S, Papaspyrides CD. A review on polymerelayered silicate nanocomposites. Progress in Polymer Science;**33**(122008):1119-1198

[35] Chen C, Khobaib M, Curliss D. Epoxy layered-silicate nanocomposites. Progress in Organic Coating. 2003;**47**:376-383

[36] Keyoonwong W, Guo Y, Kubouchi M, Aoki S, Sakai T. Corrosion behavior of three nanoclay dispersion methods of epoxy/organoclay nanocomposites. International Journal of Corrosion. 2012, Article ID 924283:10

[37] Chang K-C, Chen S-T, Lin H-F, Lin C-Y, Huang H-H, Yeh J-M, Yu Y-H. Effect of clay on the corrosion protection efficiency of PMMA/Na^+-MMT clay nanocomposite coatings evaluated by electrochemical measurements. European Polymer Journal. 2008;**44**: 13-23

[38] Xu R, Manias E, Snyder AJ, Runt J. New biomedical poly(urethane urea)-layered silicate nanocomposites. Macromolecules. 2001;**34**:337-339

[39] Yano K, Usuki A, Okada A, Kurauchi T, Kamigaito O. Synthesis and properties of polyimide-clay hybrid. Journal of Polymer Science, Part A: Polymer Chemistry. 1993;**31**: 2493-2498

[40] Biswas M, Sinha-Ray S. Recent progress in synthesis and evaluation of polymer-montmorillonite nanocomposites. Advances in Polymer Science. 2001;**155**:167-221

[41] Azeez AA, Rhee KY, Park SJ, Hui D. Epoxy clay nanocomposites-processing, properties and applications: A review. Composites: Part B. 2013;**45**:308-320

[42] Vaia RA, Giannelis EP. Lattice model of polymer melt intercalation in organically-modified layered silicates. Macromolecules. 1997;**30**:7990-7999

[43] Vaia RA, Giannelis EP. Polymer melt intercalation in organically-modified layered Silicates: model predictions and experiment. Macromolecules. 1997;**30**:8000-8009

[44] Dickie Ray A, Floyd FL. Polymeric materials for corrosion control: An overview. In: Polymeric Materials for Corrosion control, ACS Symposium Series. American Chemical Society; 1986

[45] Bryant WMD. Free energies of formation of fluorocarbons and their radicals. Thermodynamics of formation and depolymerization of polytetrafluoroethylene. Journal of Polymer Science. 1962;**56**:277-296

[46] Hines RA, Bryant WMD, Larchar AW, Pease DC. Synthesis of linear polyethylene by a free radical route at very high pressures. Industrial and Engineering Chemistry. 1957;**49**: 1071-1074

[47] Edeleanu C. Method for the study of corrosion phenomena. Meta. 1954;**50**:113-116

[48] Grundmeier G, Schmidt W, Stratmann M. Corrosion protection by organic coatings: Electrochemical mechanism and novel methods of investigation. Electrochimica Acta. 2000;**45**:2515-2533

[49] Schmidt DP, Shaw BA, Sikora E, Shaw WW. Corrosion protection assessment of barrier properties of several zinc-containing coating systems on steel in artificial seawater. Corrosion. 2006;**62**:323-339

[50] Mansfeld F. Electrochemical impedance spectroscopy (EIS) as a new tool for investigating methods of corrosion protection. Electrochimica Acta. 1990;**35**:1533-1544

[51] Jones DA. Principles and Prevention of Corrosion, New Jersey. 2nd ed. USA: Prentice-Hall Inc.; 1996

[52] Keyoonwong W, Guo Y, Kubouchi M, Aoki S, Sakai T. Corrosion behavior of three nanoclay dispersion methods of epoxy/organoclay nanocomposites. International Journal of Corrosion. 2012;**2012**, Article ID 924283:10

[53] Dhirde PG, Chada VGR, Mallik BP, Moitra N. Alkyd-clay nanocomposites for improved anticorrosion and mechanical performance of coating. 2017. DOI: 10.1002/pc.24291

[54] Yeh JM, Liou SJ, Lin CY, Cheng CY, Chang YW, Lee KR. Anticorrosively enhanced PMMA-Clay nanocomposite materials with quaternary alkylphosphonium salt as an intercalating agent. Chemistry of Materials. 2002;**14**:154-161

[55] Yeh JM, Liou SJ, Lai CY, Wu PC, Tsai TY. Enhancement of corrosion protection effect in polyaniline via the formation of polyaniline-clay nanocomposite. Materials Chemistry of Materials. 2001;**13**:1131-1136

[56] Yeh JM, Chin CP. Structure and properties of poly(o-methoxyaniline)-clay nanocomposite materials. Journal of Applied Polymer Science. 2003;**88**:1072-1080

[57] Chang KC, Lai MC, Peng CW, Chen YT, Yeh JM, Lin CL, Yang JC. Comparative studies on the corrosion protection effect of DBSA-doped polyaniline prepared from in situ emulsion polymerization in the presence of hydrophilic Na^+-MMT and organophilic organo-MMT clay platelets. Electrochimica Acta. 2006;**51**:5645-5653

[58] Yu YH, Yeh JM, Liou SJ, Chang YP. Organo-soluble polyimide (TBAPP–OPDA)/clay nanocomposite materials with advanced anticorrosive properties prepared from solution dispersion technique. Acta Materialia. 2004;**52**:475-486

[59] Yeh JM, Huang HY, Chen CL, Su WF, Yu YH. Siloxane-modified epoxy resin-clay nanocomposite coatings with advanced anticorrosive properties prepared by a solution dispersion approach. Surface and Coating Technology. 2006;**200**:2753-2763

[60] Shirehjini FT, Danaee I, Eskandari H, Zarei D. Effect of nano clay on corrosion protection of zinc-rich epoxy coatings on steel 37. Journal of Materials Science and Technology. 2016;**32**:1152-1160

[61] Merachtsaki D, Xidas P, Giannakoudakis P, Triantafyllidis K, Spathis P. Corrosion protection of steel by epoxy-organoclay nanocomposite coatings. Coatings. 2017;**84**:2-19

[62] Al-Shahrani A et al . to be published

[63] Huttunen-Saarivirta E, Vaganov GV, Yudin VE, Vuorinen J. Characterization and corrosion protection properties of epoxy powder coatings containing nanoclays. Progress in Organic Coatings. 2013;**76**:757-767

[64] Tomić MD, Dunjić B, Likić V, Bajat J, Rogan J, Djonlagić J. The use of nanoclay in preparation of epoxy anticorrosive coatings. Progress in Organic Coating. 2014;**76**:757-767

[65] Navarchian AH, Joulazadeh M, Karimi F. Investigation of corrosion protection performance of epoxy coatings modified by polyaniline/clay nanocomposites on steel surfaces. Progress in Organic Coating. 2014;**77**:347-353

[66] Kalaivasan N, Shafi SS. Enhancement of corrosion protection effect in mechanochemically synthesized Polyaniline/MMTclay nanocomposites. Arabian Journal of Chemistry. 2017;**10**:S127-S133

[67] Chang KC, Jang GW, Peng CW, Lin CY, Shieh JC, Yeh JM, Yang JC, Li WT. Comparatively electrochemical studies at different operational temperatures for the effect of nanoclay platelets on the anticorrosion efficiency of DBSA-doped polyaniline/Na^+–MMT clay nanocomposite coatings. Electrochimica Acta. 2007;**52**:5191-5200

[68] Lai MC, Chang K-C, Yeh J-M, Liou SJ, Hsieh M-F, Chang H-S. Advanced environmentally friendly anticorrosive materials prepared from water-based polyacrylate/Na+–MMT clay nanocomposite latexes. European Polymer Journal. 2007;**43**:4219-4228

Section 2

Clay in Civil Engineering

Chapter 5

The Importance of Clay in Geotechnical Engineering

Nazile Ural

Additional information is available at the end of the chapter

http://dx.doi.org/10.5772/intechopen.75817

Abstract

Clay is a very important material in geotechnical engineering, because it is often observed in geotechnical engineering practice. Generally, this soil type has numerous problems due to its low strength, high compressibility and high level of volumetric changes. Clay needs to be improved before it can be used in road construction, dams, slurry walls, airports and waste landfills. Improved gradation, a reduction in plasticity and swelling potential, as well as an increase in strength and workability, generally improve the stability of clay. Clay is a fine-grained soil, but not all fine-grained soils are clay. Clay minerals are very electrochemically active; thus, they affect soil microstructures. Due to these characteristics, many important soil problems related to clay have been observed in the past, the importance of which is understood. In this chapter, the properties of clay, as well as the use of clay in geotechnical engineering and geotechnical studies on clay, are examined.

Keywords: clay, soils, geotechnical properties, soil problems, microstructure

1. Introduction

Geotechnical engineering is a broad discipline consisting of soil mechanics and foundation engineering. Geotechnical engineering is also called geotechnique engineering or geomechanics. Geotechnical engineering addresses the application of engineering mechanics to soil and rock problems. The properties, behavior and performance of soils are addressed by engineering mechanics. Subsequently, the obtained data are processed and interpreted [1]. Geotechnical engineers consider landslides and earthquakes when planning and designing structures for buildings, roads, embankments and landfills. Geotechnical engineers also examine billions of years of geological history through soils. Therefore, examinations of the heterogeneous nature of soils require the resolution of complex problems. All types of

engineering structures such as residential buildings, service buildings, bridges, dams, roads and airports are located on or in the ground. As Richard said in 1995, "is supported by almost every construction ground or rocks. Unsupported are either fly or float or fall" [2]. Even when they are well designed, the safety of an engineering structure cannot be ensured when there is inadequate bearing capacity, high swelling/shrinking potential and settlement (compression) of the soil. For this reason, geotechnical applications in soils have become obligatory. Many studies were carried out in the 1910s due to the large number of landslides and docks that occurred in Sweden. The recommendations that resulted from these studies are now being applied as a landslide analysis method known as the Swedish slice method. With an increasing number of wall demolitions, Skempton presented calculations in 1979 [2]. Today, the latest technologies used in geotechnical soil applications are problematic for transportation power with the increase in industrialization and different kinds of construction.

Looking at the history of geotechnical engineering, Turkey is an important place. Karl von Terzaghi, who is the founder of geotechnical engineering or the father of soil mechanics, investigated Haliç clay in Turkey and laid the foundation of geotechnical science. In his investigations of a clay-rich ground, which is abundant today, Terzaghi managed to obtain clay samples from the Black Sea coast (Kilyos) with the assistance of two brave students who endured many difficulties, including bandits, and being 20 km from the nearest motorway. The clays in Terzaghi's study in 1925 are numbered II and IV in the book, which is entitled "Erdbau Mechanic." This book is accepted as the foundational document of modern soil mechanics. The mathematical formulation of clay consolidation under constant pressure over time was investigated in this book, and it was discovered that there may be an analogy between heat conduction and the damping of additional void water pressure. Thus, the "clay consolidation problem" has been solved in all its aspects. In 1925, the results of Terzaghi's research in Turkey were published in the book "Soil Physics Fundamentals of Soil Mechanics" by the Franz Deutick Publishing House in Vienna. This book is recognized by the World Society of Civil Engineers as the foundational document for modern ground engineering [3].

The first building which comes to mind regarding soil problems is the Pisa Tower. Its construction began in 1173 and took approximately 200 intermittent years to complete. The tower began to lean during construction and the leaning has continued after the construction was completed. In 1982, the hill was 58.4 m long and deviated by 5.6 m from the plumb (**Figure 1**). This soil problem is explained by clay soil settlement of up to 11 m from the surface [2]. The soils of interest in geotechnical engineering are formed from rock degradation. This process consists of physical and chemical weathering. Clay is largely composed of chemically altered and different materials of bedrock. The change in contents and structures due to physical, chemical and biological processes that occur in rocks is called weathering. Physical weathering is the mechanical disintegration of rocks by heat exchange and the effects from glaciers, waves and wind. Biological weathering results from the activities of plants and animals within a rock. Chemical weathering is caused by the effects of oxidation, reduction, hydrolysis, carbonation and organic acids in rocks. As a result of weathering, all kinds of soils are formed. In physical weathering, blocks of rock, gravel, sand and silt materials are formed, whereas clay minerals are formed by chemical weathering [4]. In geotechnical engineering practices, clay is generally seen as a problematic soil. When these soils are seen during the construction of road

Figure 1. Pisa tower [2].

dams, slurry walls, airports and waste landfills, it becomes even more important to address. Clays generally have low strength, high compressibility and high volumetric changes. Because of clay's high plasticity, permeability, bearing capacity and settlement characteristics, it is a material that has been studied and is still being studied in geotechnical engineering. In this study, the characteristics of clay are discussed and its importance in geotechnical engineering practices is noted. This chapter is composed of five main sections. In the first section, the importance of clay in geotechnical engineering is presented. In Section 2, clay is defined and its properties are discussed. Section 3 presents the use of clay in geotechnical engineering practices. In Section 4, previous, related studies are summarized. Finally, in Section 5, the subject of clay is summarized and conclusions from this chapter are provided.

2. Clay definition and properties

2.1. Clay definition

Clay minerals are called secondary silicates, because they are formed from the weathering of primary rock-forming minerals. Clay minerals occur in small particle sizes (<0.002 mm) and are very fine grained and flake shaped; they are separated from sand, gravel and silt due to the negative electrical load on the crystal edges and positive electrical load on the face. Clay

minerals consist of two basic structures. First, silica oxygen is formed through the bonding of silicon ions to the oxygen atoms on all four sides (tetrahedron). Second, an octagon forms with aluminum and magnesium ions coordinated on eight-sides with oxygen and hydroxyl ions (octahedron). All clay minerals are formed from octahedral and tetrahedral sheets with certain types of cations, which are in various forms and connected to each other in a certain system. Changes in the structures of the octahedral and tetrahedral sheets result in the formation of different clay minerals [4]. More common clay mineral groups include kaolinite, illite and smectite (montmorillonite). Kaolinite consists of silica and alumina plates, and these plates are connected very strongly, because kaolin clay is very stable (**Figure 2a**). Illite has layers made from two silica plates and one alumina plate (**Figure 2b**). However, illite contains potassium ions between each layer; this characteristic makes the structure of the clay stronger than smectite. Smectite has layers made from two silica plates and one alumina plate. Because there is a very weak bond between the layers, large quantities of water can easily enter the structure (**Figure 2c**). This event causes the swelling of such clay [5].

2.2. Clay properties

Certain features of the clay affect the structure of the soil, which determines its properties such as strength, hydraulic conduction, settlement and swelling. These features include isomorph substitution and surface anion and cation exchange capacity. This event is called isomorphic substitution if the octahedral or tetrahedral sites are replaced by a different atom normally found elsewhere. The specific surface area is the property of solids, which is defined as the total surface area of a material per unit of mass. With the separation of hydroxyl ions from the clay surface, which results in crystal deficiency at the crystal head, anions subsequently attach to the surface and organic molecule content causes an electrical load imbalance. This imbalance results in clay's extreme affinity to water and cations in the environment (**Figure 3**). Water is a dipolar molecule, namely, it has one positive and one negative charge. The surface of the clay crystal is electrostatically held to the water molecule. In addition, water is held to the clay crystal by hydrogen bonding. Also, negatively charged clay surfaces attract cations in

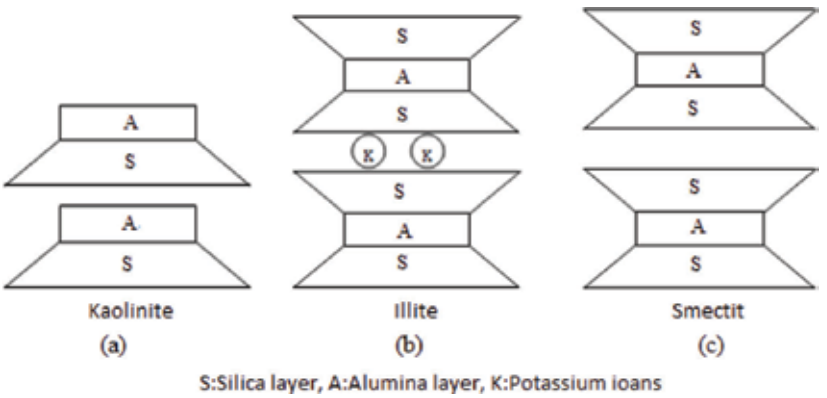

Figure 2. Display of structure of common clay minerals.

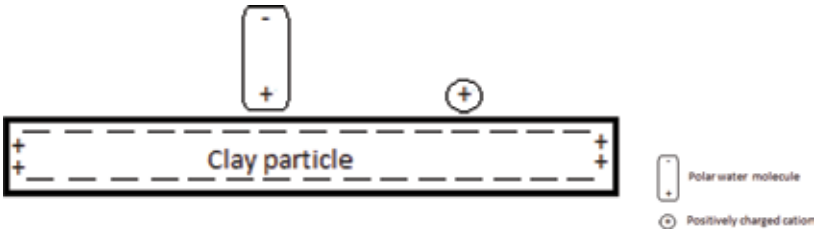

Figure 3. Clay particle and surface charge display.

the water. The cation/anion changes in the clay minerals are different between clay minerals. Therefore, it is expected that the clay that attracts more water molecules to the surface will have more plasticity, more swelling/shrinkage and more volume change, depending on the load on it. Thus, water influences clay minerals. For example, the water content changes consistency limits and this affects the ground plasticity. Ultimately the change in clay plasticity directly affects the mechanical behavior of the soil. Studies generally accept clays as fully saturated in geotechnical engineering. Therefore, the behavior of clays is affected by the individual clay particle arrangements and pore water content. The surfaces of clays are negatively charged, and so they tend to adsorb the positively charged cations in pore water. In this way, the cations on the surface of a clay particle that are entering the water spread into the liquid. This spreading is called the double layer. Briefly, the cations are distributed around the negatively charged surface of the clay particles, with the greatest density near the surface and decreased density with increasing distance from the surface. The cations form a positively charged layer and the double layer is created with a negatively charged surface of the clay particles. The double layer affects the arrangements of the clay particles, and hence, the physical and mechanical properties of the soil are also affected [6]. The interaction of these forces controls the engineering behavior of soils to a great extent. At the same time, this interaction leads to the formation of different compositions and settlements in the soil planes, which are defined as structures in clay soils [4]. Environmental temperature, precipitation, groundwater level and pH and salinity all play roles in clay properties, as well as in the conversion of rock into clay. Clay derived from the same rock can be different under different environmental conditions.

2.3. Structure of clay and physico-chemical properties

Around the clay that is faced with a liquid, there are distance-varying push-pull curves. If there is a force lifting the two clay minerals, the particles clump together. This is called flocculation. If the net force is thrust, the particles are separated from each other; this is called dispersion. Particle orientations of soils vary between flocculated and dispersed (**Figure 4**). Forces between the particles are important for clay, because the behavior of clay depends on the geological history and structure. This difference in the orientation of fine-grained soils affects the engineering behavior of the soil. The geological process in the formation of soils in nature constitutes the arrangement of soils. For this reason, geotechnical engineering studies are interested in the physical and mechanical behavior of soils-bearing structures, as well as the strength between the structure, texture and performance of soils. There are many studies

on the soil-orientation effects on the soil properties such as strength, hydraulic conductivity and the swelling-shrinkage relative to each particle [7–12]. Ingles [7] examined soil fabric during consolidation. Due to an increase in the degree of particle orientation, the total volume of the voids was reduced.

Flocculation increases depending on the electrolyte concentration, ion valence, temperature, decreasing dielectric constant, hydrated ion diameter, pH value and surface absorbed ions. Soil engineering properties depend on the size, shape, a high amount of surface area and a negative surface charge of clay particles. In 1925, Terzaghi proposed the concept of clay arrangement. He said that clay minerals stick to each other at the points of contact, with forces sufficiently strong to construct a honeycomb structure. In 1932, it was shown by Casagrande that this honeycomb shape is a special structure in clay-containing soils and this structure can vary depending on many characteristics of the environment [4]. **Figure 5** shows further compression with progress of soil sedimentation. Later, other researchers also proposed fabric models [13–17].

Collins and McGown [17] defined the elementary particle arrangement, particle assemblages and pore spaces in the fabric model. Researchers provided an elementary particle arrangement,

Figure 4. Clay particle orientations.

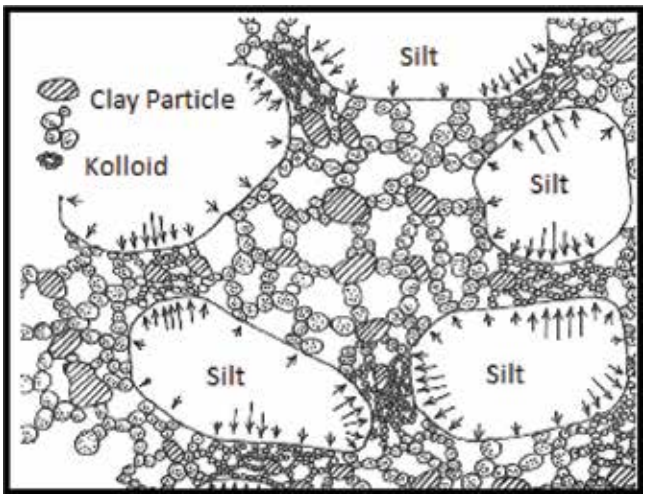

Figure 5. Casagrande's fabric model (1932) [4].

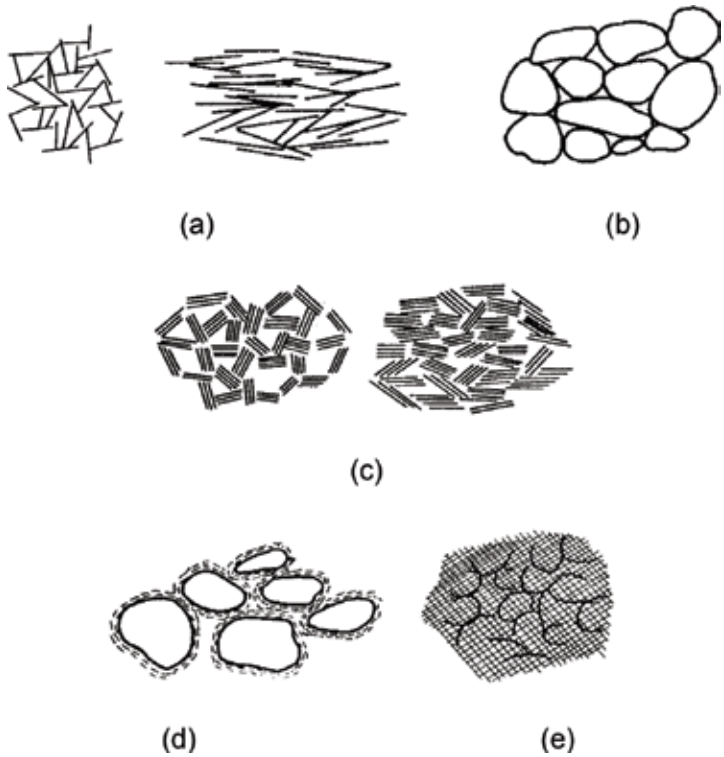

Figure 6. Arrangement of clay particles [11]. (a) Elementary particle arrangements of clay; (b) elementary particle arrangements of sand and silt; (c) clay assemblages; (d) clay coated silt and sand arrangement; (e) not fully defined arrangement.

a single clay, silt or sand, which is shown in **Figure 6a** and **b**; the group effect of clay plates is shown in **Figure 6c**, and the interaction between silt and sand is shown in **Figure 6d**. Particle assemblages contain one or more elementary particle arrangements or small particle clusters. Pore spaces are defined with spacing between elementary particle arrangements and particle assemblages. Bennet and Hulbert [18] suggested that the fabric of soils is mostly determined by the physical arrangement of particles, which is gained at the time of sediment deposition by the physical–chemical conditions of the depositional environment. The fabrics of soils describe clusters, clusters are formed by other clusters and space between the clusters and structure of the soils describes the fabric, mineral content and decontamination forces. Also, the fabrics of soils can sometimes be visualized under a microscope. The structure of soils can be examined more extensively by an X-ray diffractometer (XRD) and a scanning electron microscope (SEM).

3. Role of clay in geotechnical engineering

Studies on soil behavior that do not consider the physico-chemical and microstructural properties of clay soils may be missing important information regarding the soil's physical and mechanical

properties. This is because most physical and mechanical behaviors can be explained by the soil's physico-chemical and microstructural properties. In general, clay is an unwanted material because it creates significant engineering problems. Unlike other minerals of the same size, clay forms mud when mixed with water. Clay has plasticity and can be shaped into dough, and when cooked it turns into a solid with great strength increments. Clay generally shows a volume increase when wet, and when it is dried, its volume decreases, which creates many cracks.

3.1. Physical and mechanical behavior of clay

In geotechnical engineering, it is important to identify a clay type, as the type directly affects the important properties of clay, such as Atterberg's limits, hydraulic conductivity, swelling-shrinkage, settlement (compression) and shear resistance. Atterberg's limits, known as consistency limits, define the relationship between ground particles and water and the state of the soil relative to varying water contents. With increasing moisture content, clay changes from solid state, to semisolid state, to plastic state and to liquid state, which is given in **Figure 7**. In **Figure 7**, the clay-water mixture shows a total volume reduction, which is equivalent to the volume of water lost around the liquid and plastic limits, as the clay transitions from liquid to dry, and if the decrease in water content continues, no reduction in volume is observed. This limit value is called the shrinkage limit. Therefore, the shrinkage limit is the moisture content at which the soil volume will not reduce further if the moisture content is reduced. The plastic limit is the moisture content at which the soil changes from a semisolid to a plastic (flexible) state. The liquid limit is the moisture content at which the soil changes from a plastic to a viscous fluid state [19]. In geotechnical engineering, the liquid and plastic limits are commonly used. These limits are used to classify a fine-grained soil, according to the Unified Soil Classification system, AASHTO system or TS1500 (Turkey).

3.1.1. Hydraulic conductivity properties of clay

Water is a problem in geotechnical engineering, such as water in voids in the ground mass, flowing in pores, or in the pressure or stress that water creates in the pores. Clay plays an important role in the emergence of water problems, especially on fine soils, and these

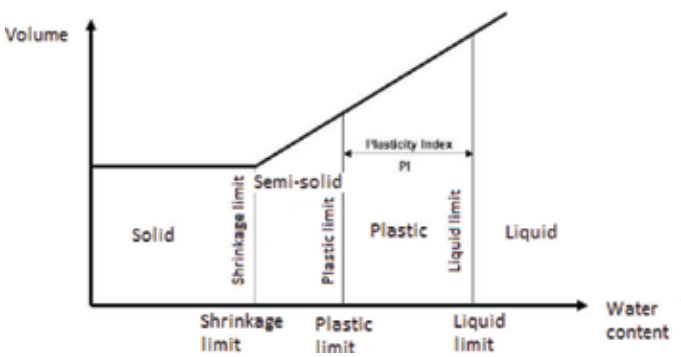

Figure 7. Water content-volume relationship of soils.

problems include permeability, shear resistance, setting and swelling problems. In addition, capillarity, freezing and infiltration can be additional issues. Structures built on clay and slope stability are particularly problematic when affected by water. Dams and dikes also cause the destruction of structures without leakage and piping [4]. Therefore, it is necessary to estimate the quantity of underground seepage under various hydraulic conditions to investigate problems that involve pumping water for underground construction and for stability analyses of earthen dams and earth-retaining structures that are subject to seepage forces [19].

The hydraulic conductivity coefficient commonly used in geotechnical engineering is also used for permeability. Hydraulic conductivity is a property that expresses how water flows in the soil. Soils are permeable due to the existence of interconnected voids, through which water can flow from the points of high energy to the points of low energy [4]. Fluid viscosity, pore-size distribution, grain-size distribution, void ratio, roughness of particles and the degree of soil saturation affect the hydraulic conductivity of soils. Clay soil has electrical ions, so the hydraulic conductivity of clays affects the ionic concentration and thickness of water layers held to the clay particles. **Table 1** provides the typical values for soils. The hydraulic conductivity value of soils determines the constant head test (for coarse soils) and the falling head test (for fine-grained soils) [19].

3.1.2. Swelling-shrinkage behavior of clay

The effect of swelling-shrinkage on fine-grained soils is often seen as a problem in geotechnical engineering applications. Shrinkage behavior in clay soils is effective in reducing the strength in a slope and a foundation's bearing capacity. Shrinkage is usually visible from evaporation in dry climates, reduction of groundwater and sudden arid periods. Swelling can be seen due to rising water. These volume changes are harmful to heavy construction and road coverings. Swelling occurs when the inflation pressure is greater than the pressure from the covering or structure. The material damage from the swelling-shrinkage of soils is more likely to occur in the United States due to greater water pressure, floods, typhoons and earthquakes [4].

Jones and Holtz [20] estimated that shrinking and swelling soils cause approximately $2.3 billion in damage annually to small buildings and road surfaces in the United States. This amount of damage is twice the amount of damage incurred from floods, earthquakes and hurricanes. Krohn and Slosson [21] estimated that swelling soils cause approximately $7 billion in damage each year. According to Holts and Hart [22] 60% of 250,000 newly constructed

Soil type	k (cm/s)
Clean gravel	100–1.0
Coarse sand	1.0–0.01
Fine sand	0.01–0.001
Silty clay	0.001–0.00001
Clay	<0.000001

Table 1. Hydraulic conductivity of soils [19].

homes incur minor expansive soil damages and 10% incur significant expansive soil damage each year in the United States. Coduto [2] noted that expansive soils caused $490,000 in damage to a building over a 6-year period. The estimated annual cost due to significant structural damages, such as cracked driveways, sidewalks and basement floors, heaving of roads and highway structures, condemnation of buildings; and disruption to pipelines and other utilities in Colorado, is $16 billion, according to AMEC [23].

Swelling pressure depends on the type of clay mineral, soil structure and fabric, cation exchange capacity, pH, cementation and organic matter. Any cohesive soil can involve clay minerals, but montmorillonite or bentonite clay minerals are more active regarding swelling-shrinkage. Swelling is calculated by swelling experiments with chemical and mineralogical analysis, soil indices and some empirical formulas from soil classifications. The shrinkage limit is determined from a laboratory test or approximate calculation recommended by Casagrande. Properties of clay improve with chemical additives such as cement, lime, lime-fly ash, cement-fly ash, calcium chloride and so on. [24].

Structures transfer loads to the subsoil through their foundations. The imposed stress from the structure compresses the subsoil. This compression of soil mass leads to a decrease in the volume of the mass, which results in the settlement of the structure, and this should be kept within tolerable limits. Therefore, settlement (compression) should be estimated before construction. The settlement is defined as the compression of a soil layer due to the construction of foundations or other loads. The compression is seen in deformation, relocation of soil particles and expulsion of water or air from void spaces. In general, the soil settlement under load falls into three categories: immediate or elastic settlement, which is caused by the elastic deformation of dry soil or moist and saturated soils without change in the moisture content; primary consolidation settlement, which is the result of a volume change in saturated cohesive soils because of the expulsion of water occupying void spaces; and secondary consolidation settlement is the volume change under a constant effective stress due to the plastic adjustment of soil fabrics [19]. The consolidation settlement is seen when a structure is built on saturated clay or the water level is permanently lowered. Simultaneously, consolidation settlement is seen under its own weight or the weight of soils that exists above the clay. The consolidation settlement of clay takes a long time, and the reason for this is the low hydraulic conductivity and slow drainage of clay. Settlement of the soil is determined by one-dimensional consolidation (odometer) and hydraulic consolidation (Rowe). In experiments, the vertical loads and void ratios are recorded. Afterwards, the relationship between the pressure and void ratio is determined from the measured data. These data are also useful in determining the consolidation coefficient. The consolidation coefficient is determined by the root of time method and the log-t method. **Figure 8** shows the relationship between the void ratio and stress for a typical odometer test for consolidation.

3.1.3. Shear strength behavior of clay

The shear strength of soils is one of the most important aspects of geotechnical engineering. The strength of the soil provides safety for geotechnical structures. The bearing strength, slope stability and bearing wall of the bases are influenced by the shear strength of the soils. Failure in the soils occurs in the form of shear. If the stresses in the soil exceed the shear strength, failure occurs. The shear failure of the soil depends on the interactions between the

soil particles. These interactions are divided into friction strength and cohesion strength [2]. When the clay soils are subjected to shear, the volume change in the drainage shear depends on the environmental pressure, as well as the stress history of the soil. In addition, loading on clay soils does not allow water to escape from the pores, and thus, this creates excess water pressure. If the loading does not cause failure, the excess water pressure is dampened, consolidation occurs and volume change is observed. The long process of this volume change in the clays is due to very low hydraulic conductivity. Determination of the shear strength of the clay is performed by a direct shear test, triaxial compression test, vane test and standard penetration tests [4]. **Figure 9** presents the relationship between the shear stress and normal stress for a typical shear strength test and triaxial compression test. After the failure envelope is drawn, the cohesion (c) and internal friction angle (f) are obtained.

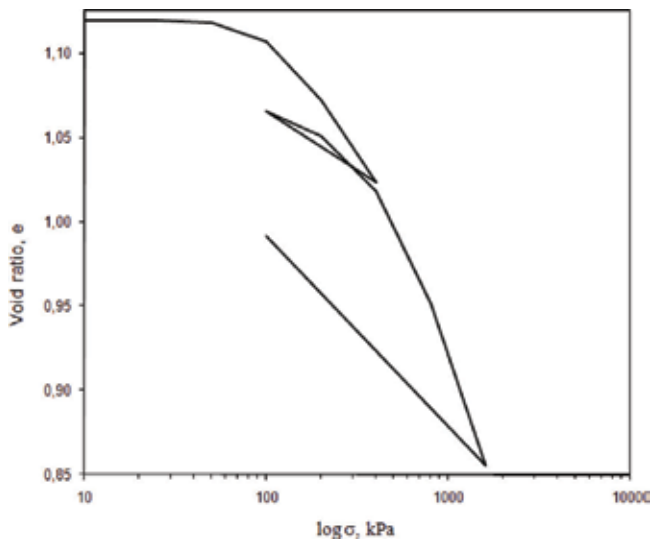

Figure 8. The graph of a typical test for consolidation test by oedometer.

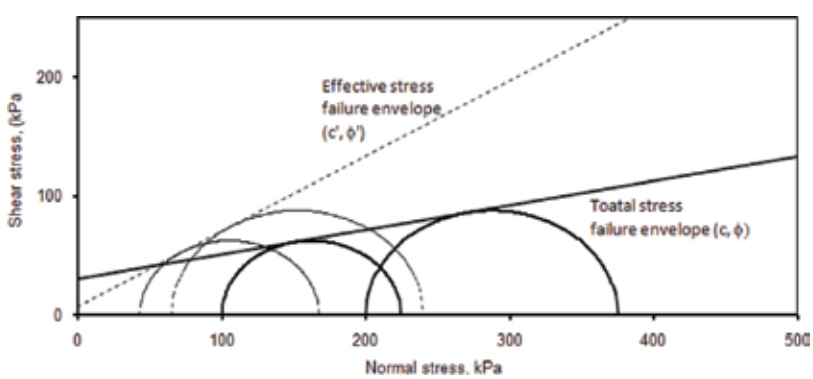

Figure 9. The graph of a typical test for shear strength test by triaxial compression test.

3.2. Physico-chemical and microstructure behavior of clay

For the determination of the physico-chemical and microstructural properties of clay soils, X-ray diffractometer (XRD) and scanning electron microscope (SEM) are commonly conducted. In addition, to determine the physico-chemical properties and structure of the soils, a pH test, electrical conductivity, cation exchange capacity, helium pycnometer, mercury intrusion porosimetry (MIP), surface area analysis (SSA), Brunauer-Emmett-Teller (BET) method or likewise, zeta potential and wavelength dispersive X-ray fluorescence test and Differential Thermal Analysis (DTA) are conducted. The pH value indicates the degree of H+ or OH− ions present. The change in pH affects the soil-water relations. Low pH indicates flocculation, and high pH indicates dispersion. The electrical conductivity of clay is defined by its ion number and type. Cation exchange capacity is a measure of isomorph displacement capacity. Isomorph displacement is when other ions of equal or different valence to those of the ions are left. This change emerges from the unbalanced electrical charge for every change. To prevent this imbalance, the cations in the environment enter the edges of the clays and between the blocks.

X-ray diffractometer (XRD) analyses: The mineralogical composition of soils is critical due to its significant influence on soil behavior; the soils are affected at first degree, especially by physical, chemical and mechanical properties of clay and by the mineral content. In geotechnics, it is important to find the type of minerals present in clay, as well as their proportions to understand the mechanical behavior. The XRD curve for typical clay is displayed in **Figure 10**. The X-ray diffraction patterns of clay show a mineralogical composition of montmorillonite, anorthite, quartz, calcite and silica.

Mercury intrusion porosimetry (MIP) analyses: In geotechnical engineering, the pore-size distributions for clay significantly influence the geotechnical behavior of soil. The pore-size distributions for typical clay from the MIP tests are displayed in **Figure 11**. This figure shows the relationship between incremental intrusion and pore-size diameter.

Scanning electron microscope (SEM): The microstructure of soils, especially clays, is observed using a versatile, analytical and ultrahigh-resolution field-emission SEM. An SEM provides

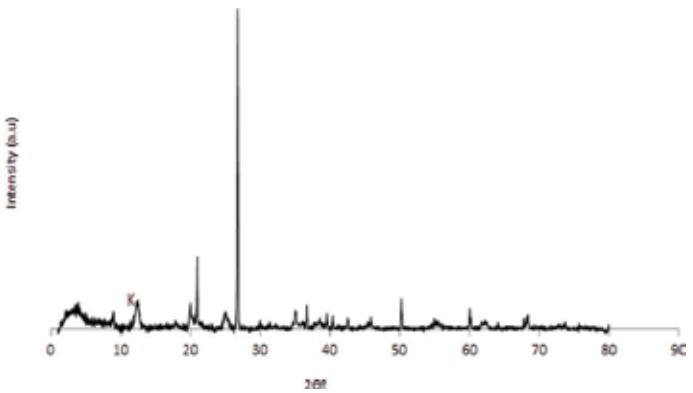

Figure 10. The XRD curve for typical clay.

a high level of magnification. Soil specimens that are magnified up to 1,000,000 times enable the evaluation of differences in the surface by imaging the surface structures. The changes in the microstructural development of soils play a significant role in the behavior of soils. In particular, these parameters could lead to a better understanding of the engineering properties of compacted soils. The SEM images of typical clays are present in **Figure 12**. Thus, flocculated and dispersed structures are observed in the soil samples.

Surface area analysis (SSA): The specific surface area is affected by grain-size distribution and the types and amounts of different clay minerals. Specific surface area is affected by the physical and chemical properties of soils.

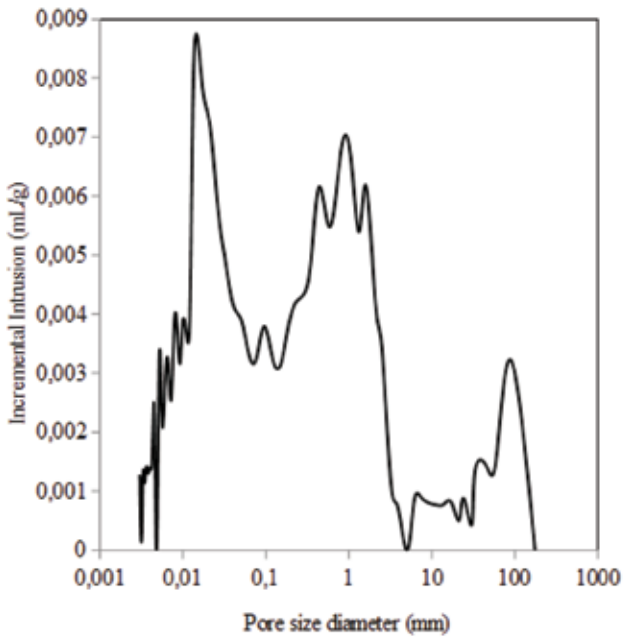

Figure 11. The pore size distributions for typical clay from the MIP tests.

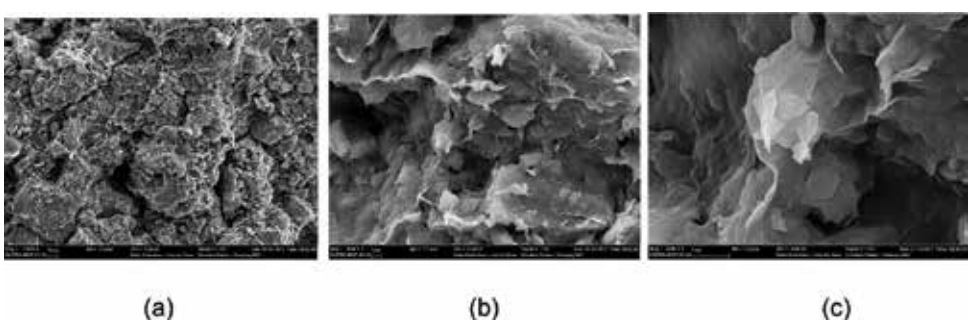

Figure 12. The SEM images of typical clay for different magnification (a. 1000×, b. 10,000×, c. 35,000×).

4. Previous related studies

Clay soils are important in the construction of buildings, dams, roads, airports, pavements and highways [25–34]. Soil problems encountered in geotechnical engineering need to be solved. Because of its double layer, clay can absorb water 10–500 times its own weight. In addition, it is considered to be a problematic soil that can show settlement under loading, with swelling or compression when it receives water. Karmi et al. [26] investigated two case studies of embankment dams in Iran. Researchers indicated that for large dams, the internal friction angle plays a more critical role in stability analyses than the cohesion parameter. Çabalar [28] investigated various fine contents and their effects on the triaxial behavior of coarse sand. Consequently, the high compressibility and other clay-like behaviors of mixtures were attributed to the particle characteristics (size and shape). Shanyoug et al. [31] investigated the effects of fine contents on the mechanical behavior of completely decomposed granite during dynamic compaction grouting. Consequently, researchers indicated that the compaction efficiency increases with the increasing fine content.

Naik et al. [32] investigated the settlement of an institutional building located in South Goa, India. This building developed cracks when the construction reached the beam level. Some foundations were located in unconsolidated filled ground, according the standard penetration test, and thus, differential settlement was observed in the foundations. Dafalla [34] investigated the cohesion and angle of internal friction for granular soils using the direct shear test for different clay contents and different moisture contents. Consequently, researchers observed a steep drop in both cohesion and angle of internal friction in a moist, clay-sand mixture when the clay content was high. In addition, many researchers have studied the geotechnical engineering behavior of clays and their microstructure [35–39]. Rajasekaran et al. [35] investigated the influence of lime and sodium hydroxide on the microchanges in two marine clays using scanning electron microscopy (SEM). These researchers suggested that the addition of lime and sodium hydroxide created an optimal pozzolanic reaction.

Horpibulsuk et al. [36] investigated the strength development and microstructural changes of stabilized, silty clay. SEM, mercury intrusion and thermal gravity analyses for qualitative and quantitative analyses of the sample microstructures were conducted in this research. Researchers suggested that the volume of large pores increased due to the presence of coarser particles in a short period, whereas the volume of small pores decreased due to the solidification of the hydrated cement. Some studies indicated that Atterberg's limits and grain-size distribution are indicators of the soil mineralogy and for the determination of many fine-grained soil properties [37–38]. Simultaneously, Atterberg's limits affect grain-size distribution and mineral composition. For example, an increase in the surface area is observed with increased liquid limits [37, 40–43]. Grabowska-Olszewska [44] investigated the relationship between the colloidal activity and the specific surface area of model soils of kaolinite and bentonite mixtures. Researchers observed that when the clay fraction increases, the total surface area also increases. Rahardjo et al. [45] investigated the index property and engineering property tests on residual soils from two major geological formations in Singapore. These researchers suggested that that the variations in the index and engineering properties of the residual soils

at different depths were largely influenced by the pore-size distributions, which vary in accordance with the degree of weathering.

Dananaj et al. [46] investigated the microstructural formation and geotechnical properties of Ca-bentonite and Na-bentonite by XRD, chemical analysis and scanning electron microscopy (SEM). Researchers suggested that the differences in bentonite quality and smectite quantity influence the permeability. Dimitrova and Yanful [47] examined the factors affecting the shear strength of mine tailings. These researchers suggested that adding clay to mine tailings would cause a decrease in the frictional strength, but the magnitude of this decrease was greater when the clay was bentonite and lower when it was kaolinite. The stabilization of clays generally requires sand, lime, cement and fly ash as additive materials. Soil stabilization using additives comprises the oldest and most common method of soil improvement. Known applications date as far back as ancient Greek, Egyptian and Roman times [48]. In clayey soils, sand is preferred due to its ease of application and economy. Some researchers have observed clays with sand stabilization to investigate the mechanical and microstructural changes of the soils [49–56]. Other researchers have used chemical additives (lime, cement, fly ash and bitumen) in the stabilization of clayey soils [57–62]. Chemical stabilization may be the most economical and practical method of soil stabilization techniques, as well as for problematic soils under existing structures.

Al-Mukhtar et al. [61] examined the effect of the lime stabilizers on the geotechnical properties of highly plastic clay using microscopic data. These researchers suggested that the treatment of the expansive soil behavior in the geotechnical properties was primarily due to pozzolanic reaction. Al-Mukhtar et al. [62] examined lime consumption by 10% lime improvement, kaolinite, illite, smectite-kaolinite, smectite-illite and smectite, using X-ray diffraction and thermogravimetric tests. These researchers suggested that the amount of lime consumed during the short-term reaction varies from nothing for kaolinite to the maximum with sodium-smectite. Khemissa and Mahamedi [63] examined improvement with a mixture of various ratios of cement and lime on expansive over-consolidated clay. These researchers observed an increase in soil strength and durability due to the reaction between the soil and additive materials. In chemical stabilization, cation exchanges, flocculation and agglomeration, carbonation reactions and pozzolanic reactions occur. The soil workability affects the cation exchange, flocculation and agglomeration mechanisms, and in addition, the bearing strength affects the carbonation reactions and pozzolanic reactions [64].

Also, clay is desirable in many cases due to its properties, which may be used to benefit a geotechnical engineer's design. Clay provides impermeability in fill dams, and waste landfill clay provides effective support in the form of gellable slurry for the untreated soils when excavated for pond water retention. Clay also becomes a binding material when it joins a certain ratio to coarse-grained soils.

5. Conclusions

Geotechnical engineering is one of the most important parts of any kind of construction. No matter how well the superstructure is projected, there is no sense in beginning construction

if the ground materials are not considered. As Karl Terzaghi said in 1939, *"…In engineering practice, difficulties with soils are almost exclusively due not to soils themselves but to water contained in their voids. On a planet without any water there would have been no need for Soil Mechanics ."* It is not adequate to only see the soil from the surface, also it must be determined whether the soil classes and groundwater are changing. Clay has a great influence on the engineering behavior of soils. Clay soils are found in nature. Deposition, weathering and stresses during geological processes ensure that the natural structure is different. In geotechnical engineering, besides determining the settlement, swelling and strength properties, mineral properties of the soil, particle structure and strength must be known when clay is encountered. In this chapter, the properties of clay, the role of clay in geotechnical engineering and geotechnical studies on clay were reviewed. In this chapter, the importance and benefits of determining clay properties before building construction were determined. Consequently, clay is shown to have different properties, and it is understood that some soils behave differently. This chapter contains material drawn from different sources, as well as a literature review, and will provide available information to civil and geotechnical engineers regarding clay.

Author details

Nazile Ural

Address all correspondence to: nazile.ural@bilecik.edu.tr

Department of Civil Engineering, Engineering Faculty, Bilecik Şeyh Edebali University, Bilecik, Turkey

References

[1] Budhu M. Soil Mechanics and Foundations. 2nd ed. Hoboken, NJ: Wiley; 2007. 656 p

[2] Coduto DP. Geotechnical Engineering Principles and Practices. Upper Saddle River, NJ, USA: Prentice Hall; 1988. 759 p

[3] Özüdoğru K. Establishment of modern soil mechanics. Karl Terzaghi and Turkey. İstanbul Technical University Journal/d Engineering. 2003;**2**(5):3-11

[4] Holtz RD, Kovacs WD. An Introduction to Geotechnical Engineering. New Jersey: Prentice-Hall; 1981. 733 p

[5] Al-Khafaji AW, Andersland OB. Geotechnical Engineering & Soil Testing. United states of America: Sounders College Publishing; 1992. 714 p

[6] Dunn IS, Anderson LR, Kiefer FW. Fundamentals of Geotechnical Analysis. New York, United states of America: John Wiley & Sons; 1980. 414 p

[7] Ingles OG. Soil chemistry relevant to the engineering behavior of soils. In: Lee IK, editor. Soil Mechanics—Selected Topics. New York: Elsevier; 1968. pp. 1-57

[8] Diamond S. Microstructure and pore structure of impact-compacted clays. Clays and Clay Minerals. 1971;**19**:239-249

[9] Rahman M, Sıddıque A, Uddin K. Microstructure and chemical properties of cement treated soft Bangladesh clays. Soils and Foundations. 2010;**50**:1-7

[10] Vichan S, Rachan R, Horpibulsuk S. Strength and microstructure development in Bangkok clay stabilized with calcium carbide residue and biomass ash. Science Asia. 2013;**39**:186-193

[11] Kiki YT, Saiyouri N, Gbaguidi V, Anguy Y, Gaborieau C, Fabre R. Microstructural, chemical and mineralogical analyses for understanding the geotechnical properties of clayey soils. Journal of Minerals and Materials Characterization and Engineering. 2016;**4**:305-319

[12] Norsyahariati NDN, Hui KR, Juliana AGA. The effect of soil particle arrangement on shear strength behavior of Silty sand. MATEC Web of Conferences. 2016;**47**:03022

[13] Lambe TW. The structure of inorganic soil. Proceedings of the American Society of Civil Engineers. 1953;**79**(10):1-49

[14] Tan TK. Structure Mechanics of Clays. Vol. 8/1. Harbin, China: Academia Sinica; 1957. pp. 83-87

[15] Push R. Influence of salinity and organic matter on the formation of clay microstructure. Proceedings of the International Symposium on Soil Structure. Gothenburg, Sweden: Swedish Geotechnical Society. 1973. pp. 161-166

[16] Yong RN, Sheeran DE. Fabric unit interaction and soil behavior. Proceedings of the International Symposium on Soil Structure. 1973. p. 176-183

[17] Collins K, McGown A. The form and function of microfabric features in a variety of natural soils. Géotech-nique. 1974;**24**(2):223-254

[18] Bennet RH, Hulbert MH. Clay Microstructure. Boston: International Human Resources Development Corperation Press, Prentice Hall; 1986. p. 161

[19] Das BM. Principles of Foundation Engineering. 6th ed. New York, USA: Thomson; 2007. 480 p

[20] Jones DE, Holtz WG. Expansive soils-the hidden disaster. Civil Engineering ASCE. 1973;**43**:87-89

[21] Krohn JP, Slosson JE. Assessment of expansive soils in the United States. Proceedings of the 4th International Conference on Expansive. Denver, CO; 1980. pp. 596-608

[22] Holtz WG, Hart SS. Home construction on shrinking and swelling soils. Colorado Geological Survey Publication SP-11. Denver. 1978. 18 p.

[23] AMEC Earth and Environmental. Boulder County Multi-Hazard Mitigation Plan. CO Hazard Mitigation and Emergency Management Programs. Denver. 2008

[24] Bowles JE. Foundation Analysis and Design. New York, United states of America: McGraw-Hill International Book Company; 1996. 478 p

[25] Prakash S, Jain PK. Engineering Soil Testing. Roorkee: Nem Chand & Bros; 2002. 88 p

[26] Karmi MV, Mehrdad MA, Eslami A. Simultaneous effect of height of shear strength parameters on optimization of embankment dams-two case studies. In: Berga et al., editors. Dams and Reservoirs, Societies and Environment in the 21st Century. London: Taylor & Francis Group; 2006. pp. 945-951

[27] Prashant A, Penumadu D. Effect of microfabric on mechanical behavior of kaolin clay using cubical true triaxial testing. Journal of Geotechnical And Geoenvironmental Engineering ASCE. 2007;**133**(4):433-444

[28] Çabalar A F. Effect of fines content on the behavior of mixed samples of a sand. Electronic Journal of Geotechnical Engineering. 2008;**13**:Bundle D

[29] Langroudi A, Yasrobi S. A micro-mechanical approach to swelling behavior of unsaturated expansive clays under controlled drainage conditions. Applied Clay Sciences. 2009;**45**:8-19

[30] Ferber V, Auriol JC, Cui YJ, Magnan JP. On the swelling potential of compacted high plasticity clays. Engineering Geology. 2009;**104**(3-4):200-210

[31] Shanyoug W, Chan D, Lam KC. Experimental study of the fines content on dynamic compaction grouting in completely decomposed granite of Hong Kong. Construction and Building Materials. 2009;**23**:1249-1264

[32] Naik S, Naik NP, Kandolkar SS, Mandrekar RL. Settlement structure—A case study. Proceedings of the Indian Geotechnical Conference, Kochi. 2011. pp. 1031-1034

[33] Jahangir E, Deck O, Masrouri F. An analytical model of soil-structure interaction with swelling soils during droughts. Computers and Geotechnics. 2013;**54**:16-32

[34] Dafalla MA. Effects of clay and moisture content on direct shear tests for clay-sand mixtures. Advances in Materials Science and Engineering. 2013;**2013**:1-8

[35] Rajasekaran G, Murali K, Srinivasaraghavan R. Fabric and mineralogical studies on lime treated marine clays. Ocean Engineering. 1995;**24**(3):227-234

[36] Horpibulsuk S, Rachan R, Chinkulkijniwat A, Raksachon Y, Suddeepong A. Analysis of strength development in cement-stabilized silty clay from microstructural considerations. Construction and Building Materials. 2010;**24**(24):2011-2021

[37] Mitchell JK. Fundamentals of Soil Behavior. New York: John Wiley & Sons; 1993. 437 p

[38] Mcbride RA. Atterberg limits. In: Dane JH, Topp GC, editors. Methods of Soil Analysis Part 4: Physical Methods. Madison, WI, USA: Soil Science Society of America Inc. publishing; 2002. pp. 389-398

[39] Robinson RG, Allam MM. Effect of clay mineralogy on coefficient of consolidation. Clays and Clay Minerals. 1998;**46**(5):596-600

[40] Farrar D, Coleman J. The correlation of surface area with other properties of nineteen British clay soils. Journal of Soil Science. 1967;**18**:118-124

[41] Kuzukami H, Ozaki E, Nakaya M. Relationships between specific surface and liquid limit. Transactions of the Japanese Society of Irrigation, Drainage and Reclamation Engineering. 1971;**37**:61-67

[42] Wetzel A. Interrelationships between porosity and other geotechnical properties of slowly deposited, fine-grained marine surface sediments. Marine Geology. 1990;**92**:105-111

[43] Dolinar B, Misic M, Trauner L. Correlation between surface area and atterberg limits of fine-grained soils. Clays and Clay Minerals. 2007;**55**:519-523

[44] Grabowska-Olszewska B. Physical properties of clay soils as a function of their specific surface. Proceedings of the 1st International Congress of the International Association of Engineering Geology. 1970;**1**:405-410

[45] Rahardjo H, Aung KK, Leong EC, Rezaur RB. Effects of pore-size distribution on engineering properties of residual soils. Geotechnical Engineering & Transportation. Proceedings of the Second World Engineering Congress. Sarawak, Malaysia. 2002. pp. 70-76

[46] Dananaj I, Frankovska J, Janotk I. The influence of smectite content on microstructure and geotechnical properties of calcium and sodium bentonites. Applied Clay Science. 2005;**28**:223-232

[47] Dimitrova RS, Yanful EK. Factors affecting the shear strength of mine tailings/clay mixtures with varying clay content and clay mineralogy. Engineering Geology. 2012;**125**: 11-25

[48] Fang HY. Foundation Engineering Handbook. 2nd ed. New York: Van Nostrand Reinhold; 1990. 905 p

[49] Mollins LH, Stewart DI, Cousens TW. Predicting the properties of bentonite-sand mixtures. Clay Minerals. 1996;**1**:243-252

[50] Studds PG, Stewart DI, Cousens TW. The effects of salt solutions on the properties of bentonite-sand mixtures. Clay Minerals. 1998;**33**:651-660

[51] Rao MK, Giribabu G, Rani SC. Influence of coarse fraction on swelling characteristics. Electronic Journal of Geotechnical Engineering. 2006;**0627**

[52] Hydma N, Avar BB. Changes in swell behavior of expansive clay soils from dilution with sand. Environmental and Engineering Geoscience. 2006;**12**(2):137-145

[53] ElKholy SM. Improving the characteristics of expansive soil using coarse-grained soil. Journal of Engineering and Computer Sciences. Qassim University. 2008;**1**(2):71-81

[54] Kalkan E. Impact of wetting–drying cycles on swelling behavior of clayey soils modified by silica fume. Applied Clay Science. 2011;**52**:345-352

[55] Louafi B, Bahar R. Sand: An additive for stabilization of swelling clay soils. International Journal of Geosciences. 2012;**3**:719-725

[56] Muhmed A, Wanatowski D. Effect of lime stabilisation on the strength and microstructure of clay. IOSR Journal of Mechanical and Civil Engineering (IOSR-JMCE). 2013;**6**(3):87-94

[57] Komine H, Ogata N. Experimental study on swelling characteristics of compacted bentonite. Canadian Geotechnical Journal. 1994;**31**:478-490

[58] Prusinski JR, Bhattacharya S. Effectiveness of Portland cement and lime in stabilizing clay soils. Transportation Research Board. 1999;**1652**(2):198-206

[59] Galvão TCB, Elsharief A, Simões GF. Effects of lime on permeability and compressibility of two tropical residual soils. Journal of Environmental Engineering. 2004;**130**(8):881-885

[60] Gharib M, Saba H, Barazesh A. The effect of additives on clay soil properties using cement and lime. International Journal of Basic Sciences & Applied Research. 2012;**1**(3):66-78

[61] Al-Mukhtar M, Khattab S, Alcover JF. Microstructure and geotechnical properties of lime-treated expansive clayey soil. Engineering Geology. 2012;**139-140**:17-27

[62] Al-Mukhtar M, Lasledj A, Alcover JF. Lime consumption of different clayey soils. Applied Clay Science. 2014;**95**:133-145

[63] Khemissa M, Mahamedi A. Cement and lime mixture stabilization of an expansive overconsolidated clay. Applied Clay Science. 2014;**95**:104-110

[64] Mitchell JK. The properties of cement-stabilized soils. Proceedings of Residential Workshop on Materials and Methods for Low Cost Road. Rail, and Reclamation Works. 1976. pp. 365-404

Chapter 6

Clay Grouting Mechanisms and Applications

Wen-Chieh Cheng

Additional information is available at the end of the chapter

http://dx.doi.org/10.5772/intechopen.74091

Abstract

Grouting in clay soils could easily lead to a poor grouting efficiency because of a lack of good understanding of the fundamental clay grouting mechanisms and grout rheological characteristics and grout hose system. Additionally, for the purpose of lifting tilted building and/or structure in clay soils, the dissipation of the excess porewater pressure generated during grout injection is likely to lead a negative final compensation efficiency. To address the said key engineering issues, a comprehensive study on the properties of grouts and effective grout injection is deemed to be necessary for the success of the project. Since grouting in clay soils rules out any other ground improvement methods other than fracturing grouting, the chapter presented herein would introduce not only previous studies for a better understanding of the grout properties but also two case histories for demonstrating how the final compensation efficiency can be improved by introducing the proposed simultaneous and multiple grouting technique.

Keywords: soft clay, fracturing grouting, ground improvement, compensation efficiency, rheological characteristics

1. Introduction

Foundation soil bearing capacity for Taipei basin is usually inadequate, where a 40–55-m-thick alluvial formation (the Sungshan formation) of alternating soft clay and silty sand layers is deposited, followed by a gravel formation (the Chingmei gravel formation) [1, 2]. The shear strength of the soft soil deposits due to the water contents close to their liquid limits is very low, leading to an inability of supporting upper buildings and/or structures [3–7]. To tackle this key engineering issue, grouting technologies have been widely adopted to improve the mechanical properties of the soft soil deposits [8–23]. Notwithstanding that, the effectiveness of grouting in such geological conditions can be significantly affected by the configuration of

grouting programme. The differential settlement or tilting of building, for instance, can be contributed not only by the soil right below the building foundation but by the successive soils. Thus, a grouting programme aimed to first stabilise the successive soils by 'stabilisation' grouting and then to lift the tilted building by 'jacking-up' grouting in the foundation soil is proved to be effective [24]. In the event that the grouting programme is designed to improve the properties of the foundation soil only, the jacking of the tilted building would not be effectively implemented due to a lack of the sufficient reaction forces given by the successive soils. Additionally, the intrusion of grouts may swell the cohesive soil and generate the positive excess porewater pressure. As long as the porewater pressure dissipates along with time, the associated settlement could override the heave generated during grout intrusion and thus result in a negative final compensation efficiency which is defined as a ratio of the total heaved volume to the injected volume of grouts [25–29]. Since the fracturing grouting due to easy travelling of the low viscosity grouts could generate higher porewater pressure than compaction grouting, regrouting at the same injection point is deemed to be necessary in order to change the stress state of cohesive soil to the overconsolidated state from its ordinary state [24, 30]. Any further grouting activity would only generate negative excess porewater pressure, and resettlement would not be occurred, thereby improving the final compensation efficiency. If both closer spacing between grout injection points and simultaneous injection are introduced, the final compensation efficiency can be further improved [27]. The above indicates that configuration and design parameters of the grouting programme play a leading role in the success of project.

The objectives of this study are (i) to present the results of an application of this proposed simultaneous and multiple grouting technique for levelling two tilted buildings seated on soft soil deposits in Taipei basin, (ii) to verify the effectiveness of introducing a grouting programme consisting of the stabilisation grouting of first stage and jacking-up grouting of the second stage by analysing the elevated and settled efficiencies and (iii) to outline the lessons learnt from the case studies.

2. Grouting mechanisms

Hydrofracturing of soil occurs in many important geotechnical engineering issues. It corresponds to the process of initiation and propagation of a crack by injecting water and air as well as chemicals into soils. As the pressure of the fluid injected surpasses a certain threshold value, the hydrofracturing of soil is thus triggered. A typical application of hydrofracturing is fracturing grouting. The fracturing grouting that involves the intentional hydrofracturing of soil with a low viscosity grout to generate a network of interconnected grout lenses has been extensively used to create surface heave and compensate settlements as well as strengthen the soil. To implement an effective field application of the fracturing grouting, a good understanding of its fundamental mechanism is deemed to be necessary. Wong Ron and Alfaro Marolo carried out a field mapping of sand-propped hydraulic fractures at a contamination remedial site where the ground is primarily consisted of silt and clay. The fractures

were found to be nearly horizontal, indicating that the ground is overconsolidated, with a K_0 value greater than unity [31]. The sand proppant was thicker at locations where soils were relatively weak, but there was no strong evidence that soil stratigraphy at this worksite controlled the orientation of the fractures. Murdoch and Slack reported similar results in sand-propped hydraulic fractures [32]. Additionally, the horizontal fractures imply that the shallow soil strata should be overconsolidated. Moreover, the elevated volume would be considerably smaller than the injected volume in the event the hydraulic fractures vented to the ground surface. Liu and Yuan established an in situ slurry fracturing apparatus to analyse the slurry fracturing and fracture propagation phenomena [33]. It was observed that the fracturing pressure was highly related to the soil and slurry properties and that slurry with large bulk density and high viscosity was beneficial in preventing slurry fracture propagation. Conducting grouting in clay due to its low permeability rules out any other grouting techniques other than fracturing grouting. The excess porewater pressure generated during grout injection is greater than the in situ effective stress, leading to fractures in the surrounding clay. Existence of fractures accelerates the consolidation process and shortens the strength increase time due to consolidation. During injection, the fractures provide a channel for exchangeable cations, which make the strength increase due to chemical reactions much more quickly than anticipated. Additionally, the compensation efficiency may not be governed by clay type but by the setting time of grout, soil stress history, injection volume of grout and so on. However, the high mobility and low viscosity of the grout can lead to an inability of limiting the travel of grout, thereby resulting in a lower soil-heaved volume to injected volume of grout ratio also known as the grouting efficiency. The grouting efficiency is generally smaller than 1 due to the loss of fluid, resulting from the bleeding effect of grout and escape of the grout from the designated area by migration along fractures, and the ground settlement caused by the dissipation of excess porewater pressure generated in injection [31]. Marchi et al. carried out a comprehensive case study in Venice where a rather unique soil fracturing intervention was implemented to improve the mechanical properties of the soft silty clay underlying the ancient Frari bell tower [34]. For soils with negative values of liquidity index, the gradients from the plots of fracturing pressure against initial confining pressure are approximately 2, which indicated the fracture initiated by tensile failure in these cases, while for soils with positive values of liquidity index, the gradients are approximately 1, indicating that the fracture was triggered by shear failure. Komiya et al. conducted a field trial of shield tunnelling in a deep soft clay deposit to investigate the long-term consolidation effect on grouting efficiency [25]. The grouting programme was consisted of the tail void grouting and grout jacking. In both cases, the monitoring results indicate that the upward displacement owing to grout injection was negated by the consolidation settlement resulting in a net settlement. The considerable consolidation of clay after grout injection due to the dissipation of the excess porewater pressure generated as the grout intruded the sensitive and compressible clay contributed to this phenomenon. This also indicates that the grouting efficiency in soft clay may be negative.

It is reported by Au et al. that for normally consolidated or slightly overconsolidated clays, the significant decrease in the grouting efficiency with time was due to the dissipation of

the positive excess porewater pressure generated during grout injection [26]. However, for heavily overconsolidated clays, the excess porewater pressure was positive at the injection boundary, but it was negative at the outer boundary due to dilative behaviour of the clay. The compression around the injection point induced by the dissipation of the positive excess porewater pressure and swelling some distance away from the injection point caused by the dissipation of the negative excess porewater pressure led to a negligible consolidation effect. As discussed, the bleeding effect of grout has been deemed to be one of the factors affecting the grouting efficiency. Au et al. conducted additional injection tests with grouts that were prepared with the water-to-cement (w/c) ratios of 0.5, 1 and 3, respectively, using the 50-mm diameter oedometer [26]. The final grouting efficiency was reduced from about 20% for the grout with the w/c ratio of 0.5 to around −30% for the grout with the w/c ratio of 3. The higher the solid content of grout, the lesser the bleeding effect of grout, and the higher the final grouting efficiency. The effect of boundary condition was also examined by injecting 5 ml of grout into the modified oedometers with the diameters of 50 mm and 100 mm, respectively [26]. The results show that the reduction in the radial boundary size enabled the final grouting efficiency to be improved dramatically as the overconsolidation ratio was within a range of 1–2. In other words, the smaller the spacing of injection point, the smaller the magnitude and extent of excess porewater pressure, and the higher the final grouting efficiency. It is common practice to introduce the tube-a-manchette (TAM) while performing compensation grouting, which allows grout to be injected many times from the same injection port. In the case that a given volume of grout is injected over a fixed area, it is possible to either regrout many times at the same port with smaller injection volumes or, conversely, conduct a small number of regrouting but with larger injection volumes. A series of injection tests comprising the regrouting injection and single injection tests were undertaken in normally consolidated clay specimens to investigate the effect of waiting period on the long-term grouting efficiency after injection [26]. An injection of 5 ml for each injection was made four times for the regrouting injection tests. The test results were compared with the result of a single injection test which was undertaken by injecting 20 ml at once. The results show that in the stage of consolidation, more excess porewater pressure was generated in the subsequent injections for the regrouting injection test, thereby leading to a lower grouting efficiency than that from the single injection test. Additionally, the efficiency of compensation grouting defined as the ratio of building settled volume to total injected volume of grout may be further reduced as only the grout beneath the mat foundation can contribute to the effective lift of titled building. Moreover, injection of extra quick setting grout can only be achieved by introducing the two-shot grout hose system [35]. The shorter the grout gel time, the lesser the excess porewater pressure generated, and the higher the final compensation efficiency. To summarise, it is evident that there are many factors (soil stress state, boundary condition, bleeding of grout, regrouting, grout rheological characteristics, grout hose system and so on) affecting the final compensation efficiency. Lifting tilted building in soft clay deposit can be better achieved by introducing a grouting programme that at least takes the previously discussed factors into account. Also, the two-stage grouting consisting of the stabilisation grouting of first-stage and jacking-up grouting of second stage may be used to ensuring the final compensation efficiency.

3. Case descriptions

3.1. Engineering geology

Based upon the preliminary geological investigation [36], the ground for Case A is generally consisted of a 1.5-m-thick surface backfill, a 4.5-m-thick low plasticity clay, a 4-m-thick silty sand and a successive very soft silty clay, as shown in **Figure 1**. The blow count N value for the clays varies from 1 to 4, whereas for the sands it varies from 5 to 10. The groundwater level is close to the ground surface. The soft soil deposits can thus easily get softened once disturbed or even washed away as subjected to significant hydraulic gradients.

The geological profile at the worksite of Case B is consisted of a 4-m-thick alluvial loam, a 7-m-thick very soft silty clay and an underlying soft silty clay, as shown in **Figure 2**. The static groundwater level in the vicinity of the worksite is some 2 m below the surface. The N value varies from 1 to 2 for the very soft silty clay, whereas for the soft silty clay, it varies from 2 to 3. The soft clays thus can behave as a fluid once subjected to construction disturbances.

3.2. Grouting programme

In the Case A, the eight-storey reinforced concrete building with one-storey basement was seated on the silty sand. The nonuniform consolidation of the successive silty clay led to the tilting of the eight-storey building afterwards. Since the tilting of the eight-storey building was amplified along with time, jacking the tilted eight-storey building back to the acceptable range of tilting was urgently needed. After considering all the possible alternatives to level up the tilted eight-storey building, grouting method was chosen due to the two reasons, that

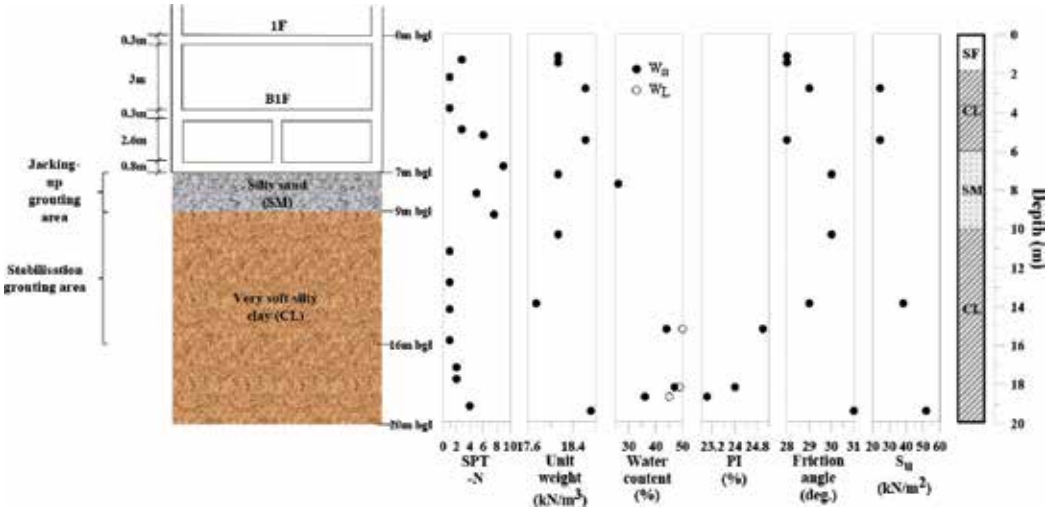

Figure 1. Geological profile of worksite and properties of soft soil deposits (Case A).

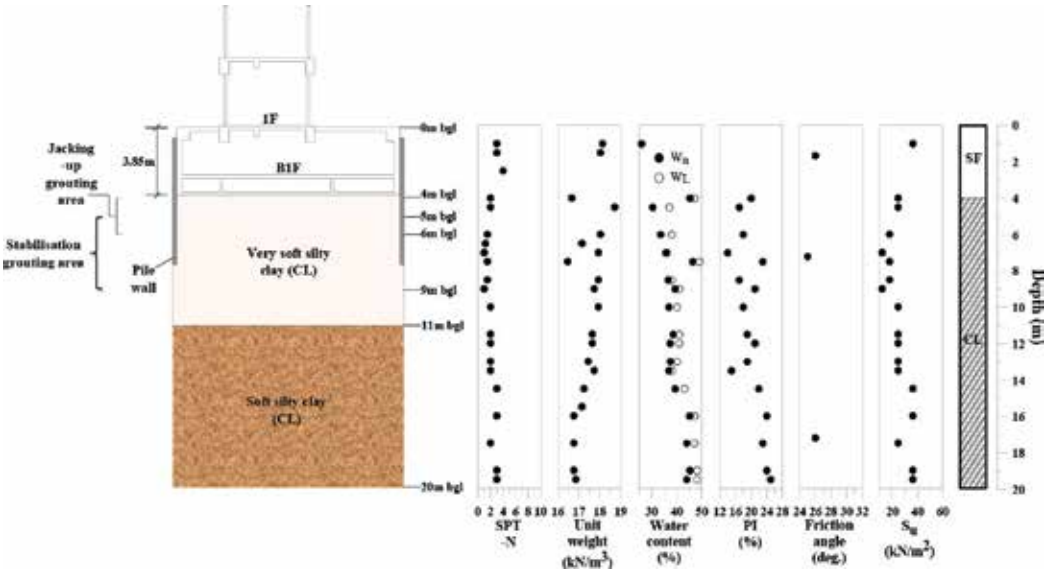

Figure 2. Geological profile of worksite and properties of soft soil deposits (Case B).

is, (1) the concentrated grouting pressure during injection was distributed over the rigid mat foundation and would not damage the integrity of the tilted building, and (2) the unoccupied basement provided free and easy access to install grouting pipes and associated grout injection facilities. A reaction block right below the foundation soil should be given prior to the implementation of the jacking-up grouting. In this regard, the first stage of sleeve grouting (the stabilisation grouting) with the mild setting grout was carried out at a depth range of 9–16 m below the ground surface using a series of sleeve pipes (known as TAM). The pipe spacing varied from 3 to 4 m, and the layout of the 35 sleeve pipes is shown in **Figure 3**. The grout began intruding the soils upwards from the bottom of each sleeve pipe through one rubber sleeve at a period of time for a total of 15 rubber sleeves. As the building tilted to the southwest, the grout intake per sleeve pipe for the three different grouted zones depicted in red, black and green in **Figure 3** was 16.8, 14.7 and 6.3 m^3, respectively, and was distributed evenly to 14 ports for 8 cycles of injection. The grout mix adopted in this stage is shown in **Table 1**.

Once the successive silty clay was strong enough to serve as a reaction block, the second stage of JOG grouting (the jacking-up grouting) was carried out where the quick setting grout was injected into the silty sand right below the mat foundation at a depth range of 7–9 m below the surface to level the tilted building. Each JOG grouting pipe was 20 cm offset from the sleeve pipe installed previously. To achieve the purpose of simultaneous injection, a multiple injection system involved with 18 JOG grouting pipes and a central controlling unit were introduced in grouting operations, as shown in **Figure 4**. The daily monitoring records from SB 1 to SB 7 were used for determining the grouting duration at each JOG grouting pipe and grouting order of each injection cycle. The injection of the extremely short setting grouts (**Table 2**) was achieved using the double tube, thereby preventing premature solidification and limiting the travel of grouts. Two types of grouts separately injected were mixed and solidified at the outlet of the

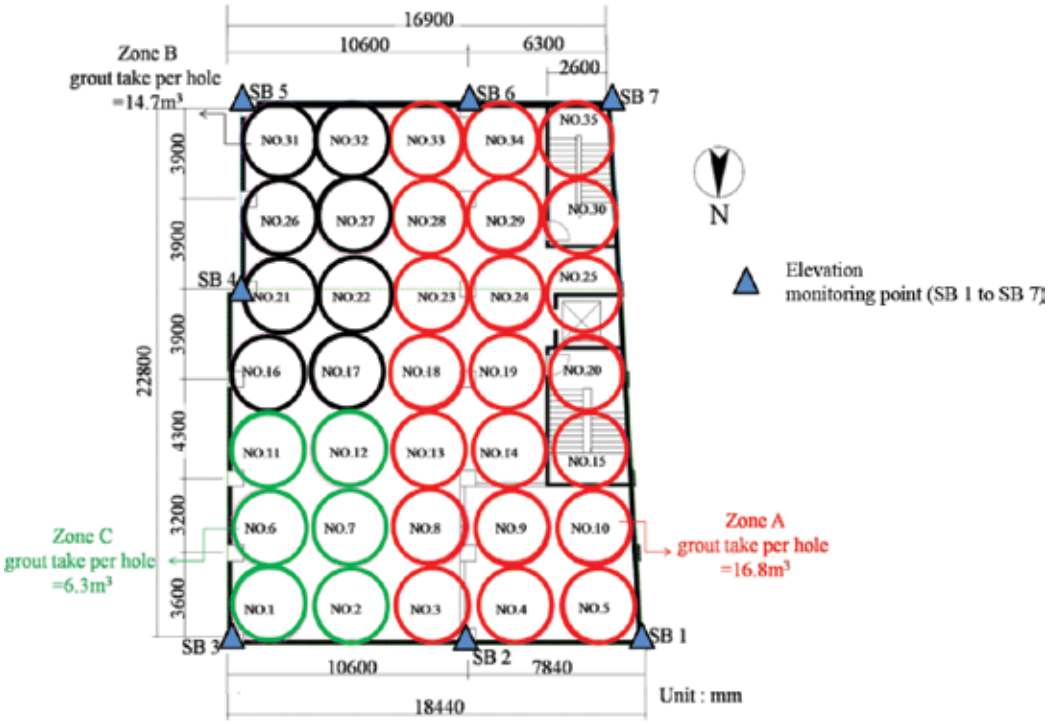

Figure 3. Layout of 35 sleeve pipes (Case A).

double tube. Thus, the grouting mode (penetration or fracturing) could be chosen by varying the cycle time which is defined by the summation of injection time for each grouting pipe in the simultaneous injection operations. The grout due to the cycle time shorter than the setting time would penetrate through the yet-to-be hardened zone from previous injection to create a reaction block. In the event that the cycle time is longer than the setting time, the grout was injected repeatedly into the region where the grout from previous injection had already been hardened to level tilted building. With this simultaneous injection system, the travel of grouts was effectively limited, and the heave of ground was successfully initiated, jacking up the tilted building.

Since performing injection in clay easily promotes hydrofracturing of soil due to its low permeability. During grouting works at the Case B, the soft clay deposits right below the mat foundation of this eight-storey building, thus ruled out any other ground improvement methods other than fracturing grouting. Because the final compensation efficiency could

	Cement	Calcium oxide	Water
Weight (kg)	400	20	866
Volume (L)	1000		

Table 1. Grout mixture for the stabilisation grouting (Case A).

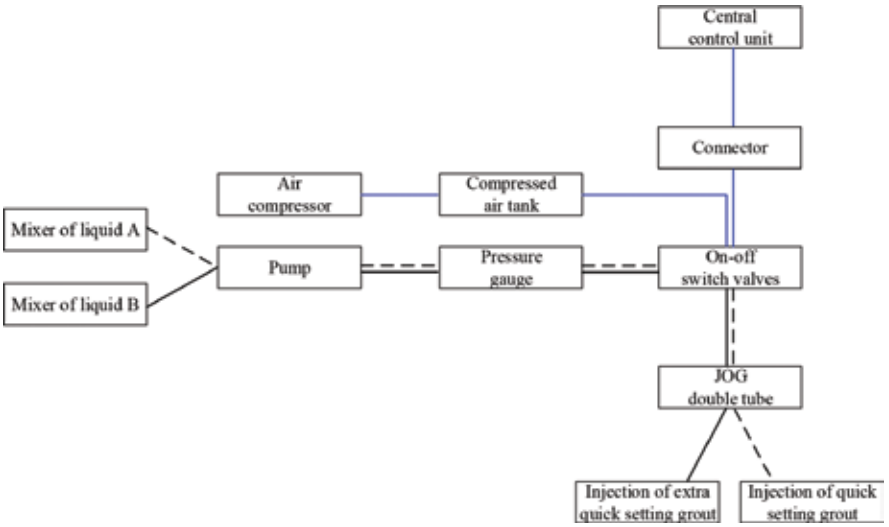

Figure 4. Illustration of the proposed multiple and simultaneous grouting system.

A liquid (200 L)				
	PR silica	**SG hardener**	**Water**	
Volume (L)	56.7	11	132.3	
B liquid (200 L)				
	Cement	**Permarock**	**PR actor**	**Water**
Weight (kg)	100 ± 25	12.5 ± 2.5	5 ± 2	160

Table 2. Grout mixture with 2-s setting time for the jacking-up grouting (Case A).

A liquid (500 L)				
	Cement	**Pulverised coal**	**CaO**	**Water**
Weight (kg)	400	300	90	250
B liquid (500 L)				
	Na_2O-3SiO_2		**Water**	
Volume (L)	150		350	

Table 3. Grout mixture with 25-s setting time for the stabilisation grouting (Case B).

be largely improved with the repetitive injection procedure, a total of 49 sleeve pipes were installed 5 m beyond the mat foundation. Their locations are depicted by solid grey circle in **Figures 7a** and **8a**. The spacing between the sleeve pipes was 2 m. The grout hose system of 1.5 shot with a quick setting grout (**Table 3**) was introduced to ensuring the compensation efficiency. Similarly, two stages of grouting were implemented; the first stage of sleeve

A liquid (500 L)				
	Cement	**Pulverised coal**	**CaO**	**Water**
Weight (kg)	400	300	90	325
B liquid (500 L)				
	Na_2O-3SiO_2		**Water**	
Volume (L)	250		250	

Table 4. Grout mixture with 20-s setting time for the jacking-up grouting (Case B).

grouting (the stabilisation grouting) with a maximum grouting pressure of 20 kg/cm^2 was to stabilise the soft clays in the depth range of 5–9 m to provide the reaction required in the next jacking-up stage, and the second stage of sleeve grouting (the jacking-up grouting) was to intrude the clays ranging from 4 to 6 m depth to level up the tilted building. The grout mixture used in the jacking-up grouting is shown in **Table 4**.

4. Analysis and discussions

4.1. Multiple and simultaneous grouting results

The effectiveness of the proposed multiple and simultaneous grouting programme for the Case A was demonstrated using the measured column elevations from SB 1 to SB 7. The column elevation before each day grouting and the change in the column elevation after grouting were measured. **Figure 5** shows the relationship between the grout take and the change in the column elevation for this simultaneous and multiple jacking-up grouting. Most of grouts were injected into the southwest corner (SB 7), and the associated change in the column elevation measured 15.6 cm at the end of the grouting, as shown in **Figure 5**. Only a few grouts were injected into the northeast corner (SB3) and resulted in a nearly unchanged column elevation. The elevation change contour lines of the mat foundation were also prepared based upon the monitoring results of the column elevation change. The volume between the mat foundation contour lines before grouting and those after grouting represented the elevated volume of tilted building at the end of each day. Additionally, the volume between the mat foundation contour lines after grouting and those before next day grouting corresponded to the overnight settled volume of tilted building caused by the dissipation of excess porewater pressure resulting from previous grouting. Thus, both the elevated efficiencies defined by the ratio of the elevated volume to the injected grout volume and the settled efficiency defined by the ratio of the settled volume to the injected grout volume can be derived.

Figure 6 shows the cumulative elevated, settled and injected grout volumes, respectively, against each grouting day of this jacking-up grouting. From day one, the elevated volumes were greater than the settled volumes for each grouting day, which indicated a benefit from the reaction block, resulting from the stabilisation grouting. In the event that the soils subjected to the stabilisation grouting are not satisfactorily strengthened and showed an inability of

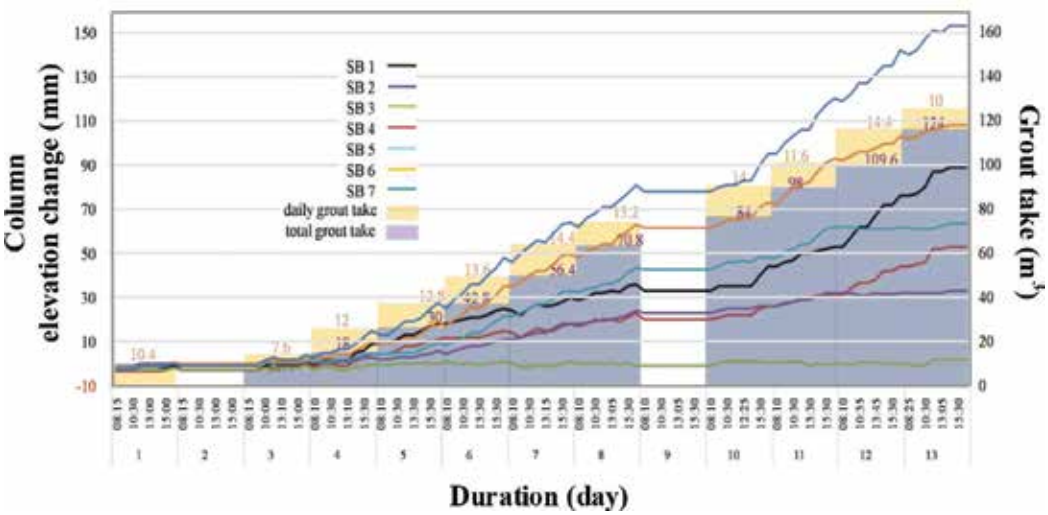

Figure 5. Relationship between the column elevation change and the grout take for the jacking-up grouting (Case A).

providing sufficient reaction force for levelling the tilted building, the final compensation efficiency may be negative as the resettlement overrides the ground heave. The results from the end of the jacking-up grouting showed that the elevated, settled and injected grout volumes measured 35.7, 3.9 and 134 m^3, respectively, corresponding to the final compensation efficiency of 23.7% which is derived by subtracting the settled efficiency of 2.9% from the elevated efficiency of 26.6%. Upon the completion of the jacking-up grouting, this building initially tilted to the southwest at an angle of 1/68 was restored to the near level at an angle of 1/328 in 11 days.

Figure 7 shows the elevated, settled and injected grout volumes, respectively, from day one of the jacking-up grouting for the Case B. The injected grout volume measured 8.7 m^3,

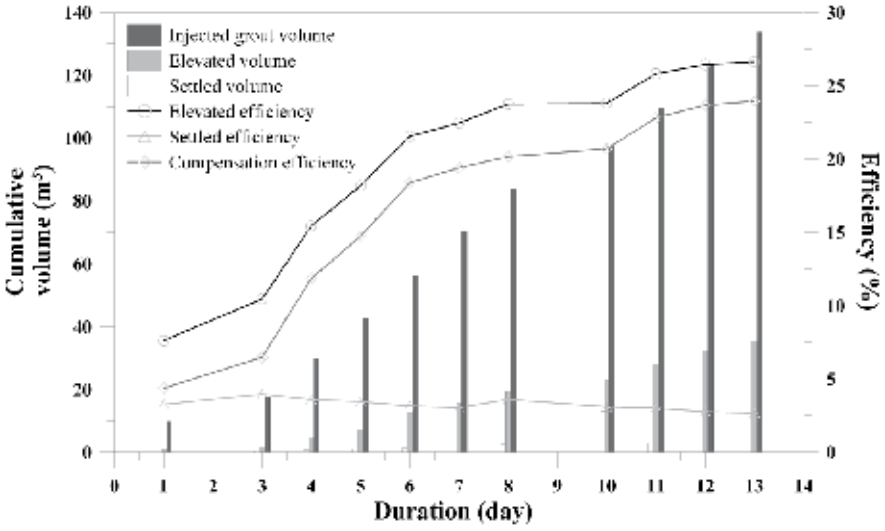

Figure 6. Variations of the elevated, settled and compensation efficiencies for the jacking-up grouting (Case A).

while the elevated volume measured 3.2 m^3, corresponding to the migrated volume being equal to 5.5 m^3. The overnight settled volume measured 3.9 m^3 however was greater than the elevated volume of 3.2 m^3, which indicated the compensation efficiency being negative.

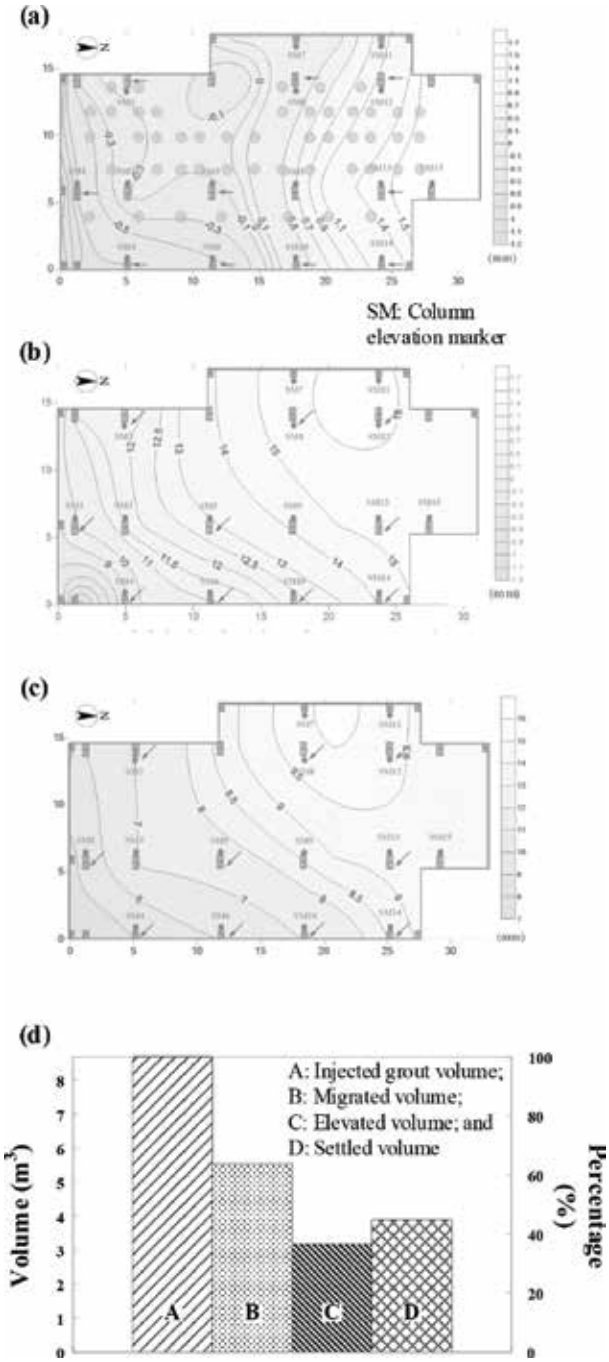

Figure 7. (a) Contour lines of mat foundation before grouting of day one, (b) contour lines after grouting of day one, (c) contour lines before grouting of day two and (d) compensation efficiency from day one (Case B).

Notwithstanding that, the normally consolidated clay owing to the repetitive injection procedure was likely to be changed to the slightly overconsolidated clay. This was verified through the positive compensation efficiency of 4.3% from day four where the elevated, overnight settled and injected grout volumes measured 7.5, 5.2 and 54.7 m^3, respectively, as shown in **Figure 8**. The injection was subsequently suspended for 7 days to investigate how long it takes for the excess porewater pressure to dissipate. The results showed that it took 5 days to reach the cumulative settlement of 3.82 m^3 being almost identical to the elevated volume of 3.9 m^3 at day four, as shown in **Figure 9**. **Figure 10** shows the cumulative elevated, overnight settled, migrated and injected grout volumes, respectively, against each grouting day of this jacking-up grouting. The cumulative elevated volume surpassed the cumulative settled volume at day four, and from day four on, the cumulative elevated volume was greater than the cumulative settled volume for each grouting day. It is due to the fact that the higher the overconsolidated ratio, the lesser the soil compressibility, and the higher the final compensation efficiency. It is inferred that a sand deposit due to its lesser compressibility would provide better compensation efficiency than a clay deposit in general. The final compensation efficiency of 11.1% was derived by subtracting the final settled efficiency of 6.0% from the final elevated efficiency of 17.1%, as shown in **Figure 10**. This eight-storey building originally tilted to the southwest at an angle of 1/190 was restored to near level at an angle of 1/707 in 18 days.

4.2. Lessons learnt

Both the presented grout injection cases adopted two-stage grouting, that is, stabilisation grouting and jacking-up grouting. The results from the Case A showed that from day one on, the elevated volume was greater than the overnight settled volume for each grouting day, leading to the final compensation efficiency being equal to 23.7%. This eight-storey building originally tilted to the southwest at an angle of 1/68 was restored to near level at an angle of 1/328 in 11 days.

Compared to the Case A, the overnight settled volume from day one of this jacking-up grouting for the Case B measured 3.9 m^3 was greater than the elevated volume of 3.2 m^3, leading to the compensation grouting being equal to −8.2%. The positive compensation grouting of 4.3% was first observed as the cumulative elevated volume of 7.5 m^3 from day four surpassed the cumulative overnight settled volume of 5.2 m^3. From day four on, the cumulative elevated volume was greater than the cumulative overnight settled volume for each grouting day. The final compensation efficiency measured 11.1% was lower than 23.7% from the Case A, which was most likely due to the inappropriate grout hose system and adopted grout mixture. The use of two-shot grout hose system is not only to minimise the generation of the excess porewater pressure during soil hydrofracturing process but to prevent the negative compensation efficiency from occurring at early stage. Additionally, the shorter the setting time of grout, the lesser the excess porewater pressure generated, and the higher the compensation efficiency. Two-shot grout hose system along with extra quick setting grout may provide an access of achieving a higher final compensation efficiency for lifting of tilted building.

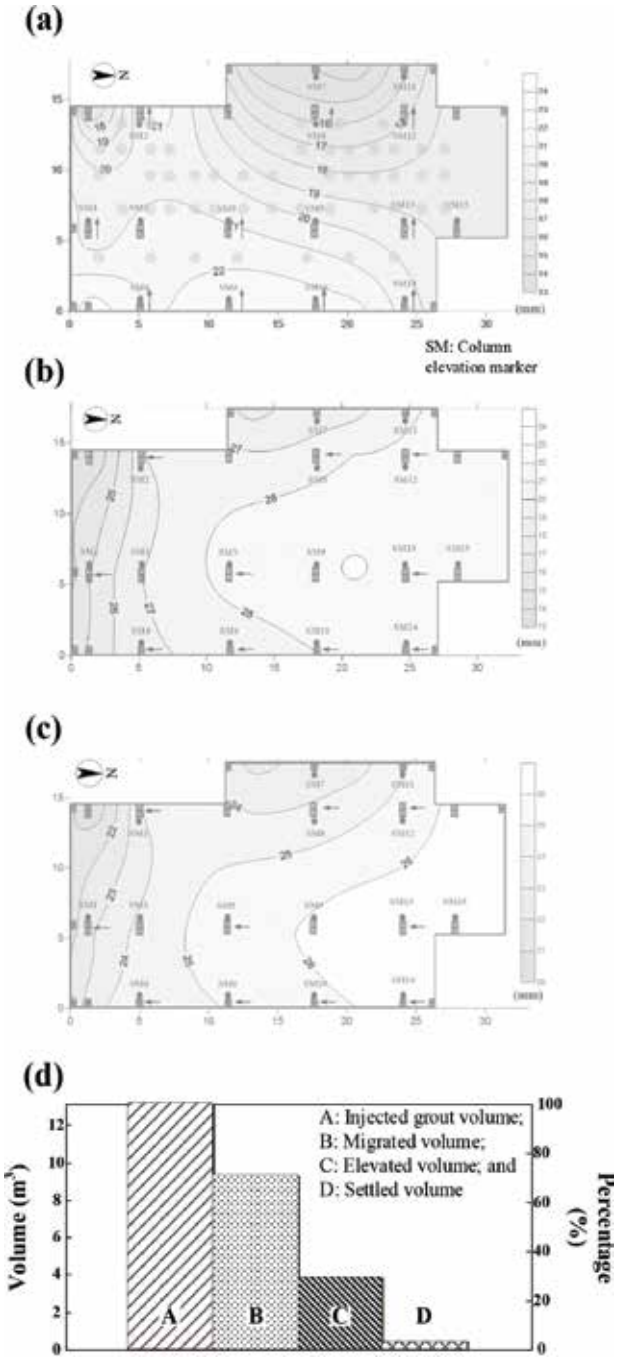

Figure 8. (a) Contour lines of mat foundation before grouting of day four, (b) contour lines after grouting of day four, (c) contour lines before grouting of day five and (d) compensation efficiency from day four (Case B).

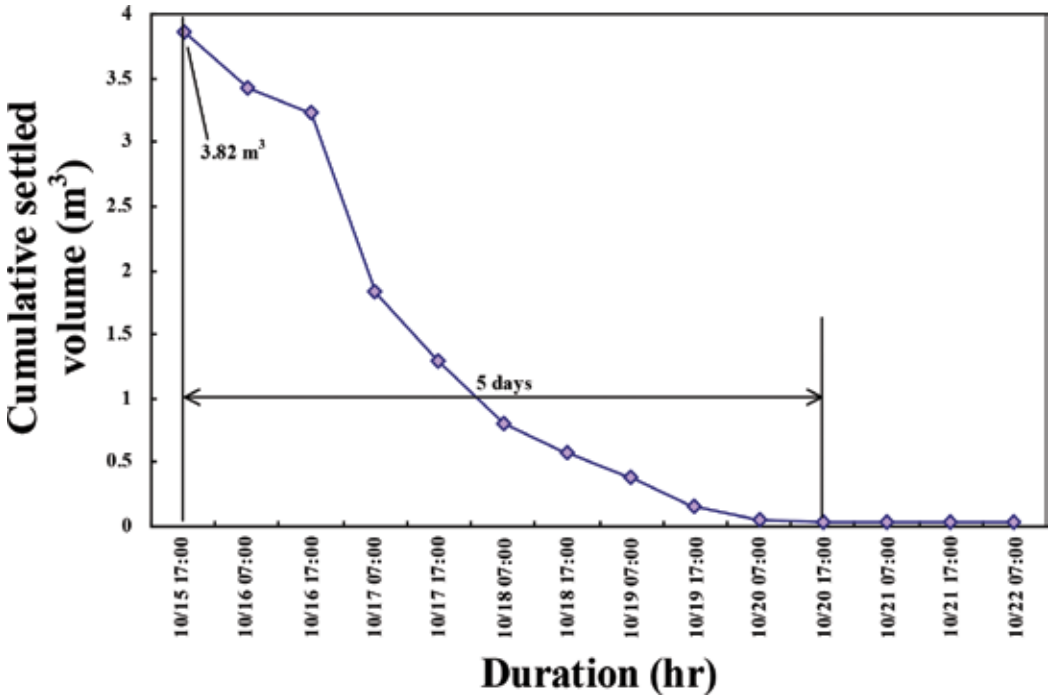

Figure 9. Excess porewater pressure dissipation with time after grouting of day four (Case B).

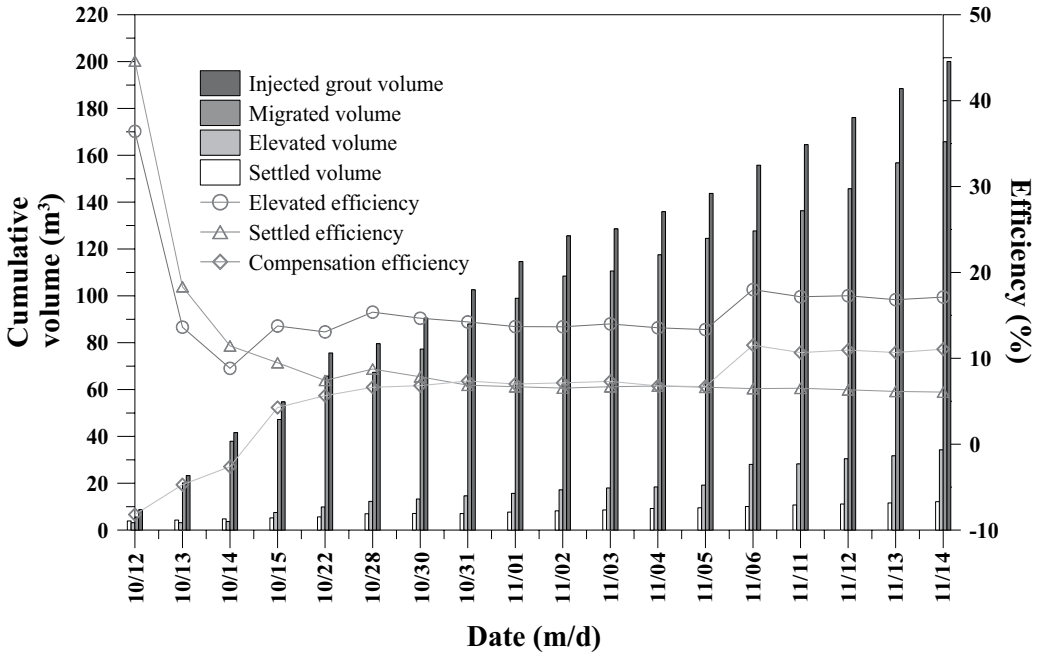

Figure 10. Variations of the elevated, settled and compensation efficiencies for the jacking-up grouting (Case B).

5. Conclusions

From the results of an application of the proposed multiple and simultaneous grouting programme for levelling up the two tilted buildings seated on the soft soil deposits in Taipei basin, the following conclusions can be drawn:

1. Two-stage grouting was deemed to be necessary; the reaction block created from the first stage of grouting (the stabilisation grouting) was to provide the reaction forces required in the second stage of grouting (the jacking-up grouting) to level up the tilted building.
2. Two-shot grout hose system along with extra quick setting grout might be used not only to mitigate the generation of the excess porewater pressure during soil hydrofracturing process but to prevent the negative compensation efficiency from occurring at early stage.
3. The proposed multiple and simultaneous grouting programme gave an effective access of jacking the two tilted buildings back to near level without damaging the structural integrity of their mat foundations.
4. The final compensation efficiency of 11.1% from Case B lower than that from Case A was most likely due to the inappropriate grout hose system and grout mixture. The use of two-shot grout hose system led to a reduced amount of the excess porewater pressure generated during injection, leading to a higher compensation efficiency. The shorter the setting time of grout, the lesser the shrinkage of grout, and the higher the compensation efficiency.

Acknowledgements

Discussions and opinions exchange with retired Professor James C. Ni at National Taipei University of Technology are much appreciated.

Conflict of interest

The author declares there is no conflict of interests regarding the publication of this article.

Author details

Wen-Chieh Cheng

Address all correspondence to: w-c.cheng@xauat.edu.cn

Institute of Tunnel and Underground Structure Engineering, School of Civil Engineering, Xi'an University of Architecture and Technology, Xi'an, China

References

[1] Ni JC, Cheng WC, Ge L. A case history of field pumping tests in a deep gravel formation in the Taipei Basin, Taiwan. Engineering Geology. 2011;**117**(1-2):17-28. DOI: 10.1016/j.enggeo.2010.10.001

[2] Ni JC, Cheng WC, Ge L. A simple data reduction method for pumping tests with tidal, partial penetration, and storage effects. Soils and Foundations. 2013;**53**(6):894-902. DOI: 10.1016/j.sandf.2013.10.008

[3] Tan Y, Li MW. Measured performance of a 26 m deep top-down excavation in downtown Shanghai. Canadian Geotechnical Journal. 2011;**48**(5):704-719. DOI: 10.1139/t10-100

[4] Ni JC, Cheng WC. Steering characteristics of microtunnelling in various soils. Tunnelling and Underground Space Technology. 2012;**28**:321-330. DOI: 10.1016/j.tust.2011.11.003

[5] Tan Y, Wei B. Observed behaviors of a long and deep excavation constructed by cut-and-cover technique in Shanghai soft clay. Journal of Geotechnical and Geoenvironmental Engineering. 2012;**138**(1):845-854. DOI: 10.1061/(ASCE)GT.1943-5606.0000553

[6] Cheng WC, Ni JC, Shen SL, Huang HW. Investigation into factors affecting jacking force: A case study. Geotechnical Engineering, ICE Proceedings. 2017;**170**(4):322-334. DOI: 10.1680/jgeen.16.00117

[7] Cheng WC, Ni JC, Shen SL. Experimental and analytical modeling of shield segment under cyclic loading. International Journal of Geomechanics. 2017;**17**(6):04016146. DOI: 10.1061/(ASCE)GM.1943-5622.0000810

[8] Poh TY, Wong IH. A field trial of jet-grouting in marine clay. Canadian Geotechnical Journal. 2001;**38**(2):338-348. DOI: 10.1139/t00-093

[9] Kim DS, Lee BC. Instrumentation and numerical analysis of cylindrical diaphragm wall movement during deep excavation at coastal area. Marine Georesources & Geotechnology. 2005;**23**(1-2):117-136. DOI: 10.1080/10641190590953728

[10] Modoni G, Croce P, Mongiovi L. Theoretical modelling of jet grouting. Geotechnique. 2006;**56**(5):335-347. DOI: 10.1680/geot.2006.56.5.335

[11] Gallagher PM, Pamuk A, Abdoun T. Stabilization of liquefiable soils using colloidal silica grout. Journal of Materials in Civil Engineering. 2007;**19**(1):33-40. DOI: 10.1061/(ASCE)0899-1561(2007)19:1(33)

[12] Díaz-Rodríguez JA, Antonio-lzarraras VM, Bandini P, López-Molina JA. Cyclic strength of a natural liquefiable sand stabilized with colloidal silica grout. Canadian Geotechnical Journal. 2008;**45**(10):1345-1355. DOI: 10.1139/T08-072

[13] Ni JC, Cheng WC. Shield machine disassembly in grouted soils outside the ventilation shaft: A case history in Taipei Rapid Transit System (TRTS). Tunnelling and Underground Space Technology. 2011;**26**(2):435-443. DOI: 10.1016/j.tust.2010.11.015

[14] Mollamahmutoglu M, Yilmaz Y. Engineering properties of median-to-fine sands injected with microfine cement grout. Marine Georesources & Geotechnology. 2011;**29**(2):95-109. DOI: 10.1080/1064119X.2010.517715

[15] Modoni G, Bzòwka J. Analysis of foundation reinforced with jet grouting. Journal of Geotechnical and Geoenvironmental Engineering. 2012;**138**(12):1442-1454. DOI: 10.1061/(ASCE)GT.1943-5606.0000718

[16] Shen SL, Wang ZF, Horpibulsuk S, Kim YH. Jet-grouting with a newly developed technology: Twin-jet method. Engineering Geology. 2013;**152**(1):87-95. DOI: 10.1016/j.enggeo.2012.10.018

[17] Shen SL, Wang ZF, Sun WJ, Wang LB, Horpibulsuk S. A field trial of horizontal jet grouting with composite-pipe method in soft deposit of shanghai. Tunnelling and Underground Space Technology. 2013;**35**(4):142-151. DOI: 10.1016/j.tust.2013.01.003

[18] Shen SL, Wang ZF, Yang J, Ho EC. Generalized approach for prediction of jet grout column diameter. Journal of Geotechnical and Geoenvironmental Engineering. 2013;**139**(12):2060-2069. DOI: 10.1061/(ASCE)GT.1943-5606.0000932

[19] Wang ZF, Shen SL, Ho CE, Xu YS. Jet grouting for mitigation of installation disturbance. Geotechnical Engineering, ICE Proceedings. 2014;**167**(6):526-536. DOI: 10.1680/geng.13.00103

[20] Modoni G, Flora A, Lirer S, Ochmański M, Croce P. Design of jet grouted excavation bottom plugs. Journal of Geotechnical and Geoenvironmental Engineering. 2016;**142**(7):04016018. DOI: 10.1061/(ASCE)GT.1943-5606.0001436

[21] Porcino D, Ghionna VN, Granata R, Marcianò V. Laboratory determination of mechanical and hydraulic properties of chemically grouted sands. Geomechanics and Geoengineering. 2016;**11**(2):164-175. DOI: 10.1080/17486025.2015.1057621

[22] Shen SL, Wang ZF, Cheng WC. Estimation of lateral displacement induced by jet grouting in clayey soils. Geotechnique. 2017;**67**(7):621-630. DOI: 10.1680/jgeot.16.P.159

[23] Atangana Njock PG, Shen JS, Modoni G, Arulrajah A. Recent advances in horizontal jet grouting (HJG): An overview. Arabian Journal for Science and Engineering. 2017. DOI: 10.1007/s13369-017-2752-3

[24] Ni JC, Cheng WC. Using fracture grouting to lift structure in clayey sand. Journal of Zhejiang University-SCIENCE A. 2010;**11**(11):879-886. DOI: 10.1631/jzus.A0900748

[25] Komiya K, Soga K, Akagi H, Jafari MR, Bolton MD. Soil consolidation associated with grouting during shield tunneling in soft clayey ground. Geotechnique. 2001;**51**(10):835-846. DOI: 10.1680/geot.2001.51.10.835

[26] Au SKA, Soga K, Jafari MR, Bolton MD, Komiya K. Factors affecting long-term efficiency of compensation grouting in clays. Journal of Geotechnical and Geoenvironmental Engineering. 2003;**129**(3):254-262. DOI: 10.1061/(ASCE)1090-0241(2003)129:3(254)

[27] Soga K, Au SKA, Jafari MR, Bolton MD. Laboratory investigation of multiple grout injections into clay. Geotechnique. 2004;**54**(2):81-90. DOI: 10.1680/geot.2004.54.2.81

[28] Wisser C, Augrade CE, Burd HJ. Numerical modelling of compensation grouting above shallow tunnels. International Journal for Numerical and Analytical Methods in Geomechanics. 2005;**29**(5):443-471. DOI: 10.1002/nag.421

[29] Contini A, Cividini A, Gioda G. Numerical evaluation of the surface displacements due to soil grouting and to tunnel excavation. International Journal of Geomechanics. 2007;**7**(3):217-226. DOI: 10.1061/(ASCE)1532-3641(2007)7:3(217)

[30] Suddeepong A, Chai JC, Shen SL, Carter JP. Deformation behaviour of clay under repeated one-dimensional unloading-reloading. Canadian Geotechnical Journal. 2015; **52**(8):1035-1044. DOI: 10.1139/cgj-2014-0216

[31] Wong Ron CK, Alfaro Marolo C. Fracturing in low-permeability soils for remediation of contaminated ground. Canadian Geotechnical Journal. 2001;**38**:316-327. DOI: 10.1139/cgj-38-2-316

[32] Murdoch LC, Slack WW. Forms of hydraulic fractures in shallow fine-grained formations. Journal of Geotechnical and Geoenvironmental Engineering. 2002;**128**(6):479-487. DOI: 10.1061/(ASCE)1090-0241(2002)128:6(479)

[33] Liu XY, Yuan DJ. An in-situ slurry fracturing test for slurry shield tunneling. Journal of Zhejiang University-Science A. 2014;**15**(7):465-481. DOI: 10.1631/jzus.A1400028

[34] Marchi M, Gottardi G, Soga K. Fracturing pressure in clay. Journal of Geotechnical and Geoenvironmental Engineering. 2014;**140**(2):04013008. DOI: 10.1061/(ASCE)GT.1943-5606.0001019

[35] Ni JC, Cheng WC. Monitoring and modeling grout efficiency of lifting structure in soft clay. International Journal of Geomechanics. 2010;**10**(6):223-229. DOI: 10.1061/(ASCE)GM.1943-5622.0000026

[36] Cheng WC, Ni JC, Arulrajah A, Huang HW. A simple approach for characterising tunnel bore conditions based upon pipe-jacking data. Tunnelling and Underground Space Technology. 2018;**71**:494-504. DOI: 10.1016/j.tust.2017.10.002

Section 3

Clay in Medical Applications

Chapter 7

Calcium Phosphate/Clay Nanotube Bone Cement with Enhanced Mechanical Properties and Sustained Drug Release

Udayabhanu Jammalamadaka, Karthik Tappa and David K. Mills

Additional information is available at the end of the chapter

http://dx.doi.org/10.5772/intechopen.74341

Abstract

Calcium phosphate cement (CPC) has limited use in bone repair due to their poor mechanical properties. Halloysite nanotubes (HNTs) are clay tubes with an aluminosilicate composition. The physicochemical properties, cytocompatibility, and cellular response to the CPC/HNT composites were assayed. Compression strength, FTIR analysis, protein synthesis, and mineralization were assessed. The cumulative data show that composites of tricalcium phosphate (TCP), anhydrous calcium diphosphate (DCPA) as the solid phase agent, and 10% chitosan lactate solution as the setting liquid produced cement with sustained release properties without loss of material strength. The composite also showed enhanced material properties (adhesiveness, surface roughness, and increased strength). Cellular assays confirm its osteoconductive and osteoinductive nature. CPCs, loaded with gentamicin- and neomycin-doped HNTs, showed sustained antibacterial release and marked zone of growth inhibition. CPCs fabricated with drug-doped HNTs offer a means for inducing bone growth at the site of implantation while controlling infection. This treatment modality should hasten patient healing time and enhance restoration of function. The increase in materials properties suggests that this CPC may be clinically applied to repair injuries in load-bearing bones.

Keywords: bone cement, bone repair, calcium phosphate, halloysite nanotubes, osteoblasts, sustained release, tissue engineering

1. Introduction

Polymethylmethacrylate (PMMA) is widely commercially used bone cement [1, 2]. The most common method of application is the dry mixing of drugs along with the bone cement and administering it into the body [3]. While long considering the 'gold' standard in local antibiotic therapy, it has many disadvantages. A radiolucent fibrous tissue is often observed at the bone/cement interface due to the release of toxic methylmethacrylate (MMA) monomers which damages surrounding tissue [3, 4]. These cements also exhibit a high exothermic setting temperature. Temperatures ranging from 70–120°C have been reported during setting of the PMMA bone cement during implantation [2, 5]. In an experiment conducted by Stańczyk and Rietbergen on bovine cancellous bone, the temperature exposure of 70°C by a fraction (10%) of the bone at the bone/cement interface was recorded [6]. The addition of antibiotics results in reduced mechanical properties in the cement [7]. Furthermore, the release of the antibiotic is short lived and results in less than maximal antibiotic release [7, 8]. Finally, PMMA cements lack elasticity and have dense structure which does not allow bone growth inside the cement [9].

Brown and Chow were the first to propose the use of calcium phosphate cement (CPC) in bone repair [10]. CPC was approved in 1996 by the Food and Drug Administration (FDA) for repairing craniofacial defects [11]. CPCs have many advantages over PMMA cement. Low shrinkage, durable, dense or porous (depending on the site of injury), and formability (ability to fill cavities of complex configurations) are additional positive qualities of CPCs [12–14]. Due to their similarity to apatite minerals in natural bone, calcium phosphate (CaP) bioceramics, such as hydroxyapatite (HA), are osteoconductive and osteoinductive [15–17]. CPCs implants provide an ideal environment for colonization by osteoblasts to form a functional interface [18, 19]. The end product is easily resorbed by osteoclast cells, leading to new natural bone formation at the bone-implant interface [21].

All CPCs are formulated by mixing a solid and a liquid component. The solid component consists of two or more calcium phosphate salts. The solid phase usually consists of a basic and an acidic salt, which reacts together in an aqueous medium and precipitates HA as a final product [19, 20]. The liquids used can be either water, alginates, chitosan, or sodium phosphates [20–22]. To obtain maximum biological use, these components are mixed in predetermined proportions that will lead to the formation of HA. Resorbability of the CPCs completely depends on its end product [22]. The physicochemical reactions that occur during mixing are complex, and cement setting time depends on factors such as solid-liquid composition, liquid-to-powder ratio, and particle size of the powder. Setting conditions also influence the mechanical properties of the cement [23]. However, due to its brittleness, CPCs are restricted to the reconstruction of non-loading bearing bone [24, 25]. Recently, absorbable fibers [23] and chitosan [26] were used to improve the load-bearing capability of CPC [27, 28]. Chitosan and its derivatives are natural biopolymers that are biocompatible, biodegradable, and osteoconductive [29]. CPCs can also be modified through additives (i.e., silicon, strontium, and zinc) and delivered as paste, putty or in an injectable form and set *in situ* to provide intimate adaptation to complex-shaped defects [23, 24]. Polymer materials added as an organic phase to the CPCs have been shown to improve the biological response, physicochemical, and mechanical properties, such as injectability, cohesion, resorption, and toughness [27, 28, 30].

Halloysite nanotubes (HNTs) are commercially inexpensive and two-layered aluminosilicate nanotubes are found naturally as raw mineral deposit. When dehydrated, 15–20 clay layers form a hollow tubule which is capable of carrying drugs [31, 32]. Inside of the lumen is positively charged and the external surface is negatively charged, permitting additional functional modifications of these surfaces. This charge on both outer and inner surfaces affects the efficiency of loading drugs and chemical agents [33, 34]. Substances with overall negative charge can be easily loaded into the lumen when compared to positively charged particles. The size of HNTs varies from 500 to 1000 nm with an inner diameter of 15–100 nm depending on the deposit [35]. Due to physical properties such as nanosized lumens, high L/D (length to diameter) ratio, low hydroxyl group density, low cost, and abundant natural deposits, HNTs have been intensely studied as a controlled or sustained release agent [31, 33, 34]. Loading HNTs with pharmaceuticals showed low initial release concentrations, preventing an initial outburst and uniform drug delivery (particularly with drugs, such as antibiotics, hormones, and growth factors) [35–37]. The drugs dexamethasone, furosemide, and nifedipine gave an extended 6–10 h release profile [29]. Under optimal conditions, a maximum loading of 12% volume (very close to theoretical capacity) was obtained [29]. When HNTs are added to polymeric materials, they improve material and mechanical performance and stability [34]. HNTs have been used to increase surface area, impart high surface reactivity, and improve mechanical strength with a relatively low cost [32, 34]. To achieve an increase in the toughness, mechanical strength, and thermal stability, HNTs have incorporated into a variety of polymers and examples include: poly(methyl-methacrylate) [35], poly(butylene succinate) [38], polyamide [12, 39], styrene-butadiene [40], epoxy [41], and chitosan [42]. In two previous studies using electrospinning, HNTs were used to enhance the polymer material properties including biological, chemical, mechanical, and thermal properties (see Kamble et al., (2012) for a more detailed review) [34].

Presently, the use of CPCs in regenerative medicine and orthopedic surgery is limited only to non-load bearing regions, that is, cranioplasty [43, 44]. There is a critical need for developing osteogenic and osteoconductive cement that can be used in load-bearing sites. The objective of this study is to improve the mechanical and anti-infective properties of CPCs. The common thread between these two objectives is the use of HNTs to provide a means for sustained release of anti-infective agents (gentamicin sulfate and neomycin sulfate) and to improve the material properties (tensile strength and adhesiveness) of the cement. The choice of CPC component materials was also a critical factor.

2. Materials and methods

2.1. Materials

Calcium phosphate dibasic anhydrous ($HCaO_4P$, DCPA), β-tri calcium phosphate ($Ca_3O_8P_2$, β-TCP), calcium phosphate monobasic monohydrate ($H_4\ CaO_8\ P_2\ H_20$, MCPM), chitosan oligosaccharide lactate ($(C_{12}H_{24}N_2O_9)_n$), chitosan (low molecular weight), dexamethasone, gentamicin, neomycin, calcium L-lactate ($C_6H_{10}CaO_6 \times H_2O$), and HNTs ($H_4Al_2O_9Si_2\ 2H_2O$) were purchased from Sigma-Aldrich, St. Louis, MO. Tetra calcium phosphate (Ca_4O_4P, TTCP) was ordered from CaP Biomaterials, E. Troy, WI. Cupric chloride ($CuCl_2$) and calcium carbonate ($CaCO_3$) were delivered

from Nasco, Fort Atkinson, WI. Sodium phosphate dibasic (Na_2HPO_4) was purchased from Fisher Scientific Company, Waltham, MA. Human osteoblast cells (C-12760) and osteoblast growth medium were purchased from PromoCell, Heidelberg, Germany. Mouse pre-osteoblast cell lines MC3T3-E1 (ATCC® CRL-2593™) and mouse bone marrow stromal cells (MSCs) CRL-12424 (ATCC® CRL-12424™) were obtained from ATCC (Manassas, VA.). Cell culture and lab plastics were obtained from MidScientific, St. Louis, Mo. Alpha minimal essential medium (α-MEM) and Dulbecco's DMEM were obtained from GIBCO Invitrogen, Grand Island, NY. Fetal bovine serum and penicillin-streptomycin were purchased from Phenix Research Products (Candler, NC). TryplE, an animal free trypsin substitute, and Trypan blue were obtained from GIBCO Invitrogen, (Grand Island, NY). Cell Titer Blue assay was purchased from Promega (Sunnyvale, CA). The Picrosirius red staining kit was obtained from Polysciences, Inc. (Warrington, PA.)

2.2. Sample preparation

Different types of calcium phosphate salts were mixed in different proportions using various chemicals as part of the liquid phase to identify the best composition with respect to their mechanical properties (**Table 1**). All samples were mixed using mortar and pestle under ambient conditions (room temperature and atmospheric pressure). The powder phase was mixed thoroughly until all the salts were uniformly dispersed. To this, the liquid phase was added in small quantities and triturated until the mixture became a thick, moldable paste.

The most suitable formulation was achieved when tetracalcium phosphate (TTCP provided by CaP Biomaterials) and dicalcium phosphate (DCPA provided by Sigma-Aldrich, St. Louis, MO.) were used as the solid phase and chitosan lactate (CL) was used as the setting liquid. An equimolar ratio of TTCP and DCPA was mixed and to this 10% w/v solution of CL was added. This mixture was thoroughly mixed using mortar and pestle to form a soft mass. The soft mass could then be set in different mold shapes depending on the assay or test being performed.

2.2.1. Sample preparation for SEM

Scanning electron microscopy (SEM) was used to analyze the surface of CPCs. Specimens fractured during compression test were taken for SEM imaging. S4800 Field Emission SEM, HITACHI was used for our research. Gold nanolayer (about 3 nm) was laid over specimens before analyzing using SEM.

Group	CPC Composition
Group 1	CPC powder without HNTs
Group 2	CPC powder with 5% wt. HNTs
Group 3	CPC powder with 10% wt. HNTs
Group 4	CPC powder with 15% wt. HNTs

Table 1. Control and experimental groups use in osteoconductive studies.

2.2.2. Compression strength testing

Compression test was performed on cylindrical shape specimens (12 mm length and 6 mm diameter). Compression test was performed on dry specimens and on specimens placed in simulated biological fluid (SBF) for 24 h before testing. Testing was done using an ADMET tensile tester with a load speed of 1 mm/min. FTIR spectroscopy was done to analyze the composition of CPCs after setting.

2.2.3. Flexural strength testing

Samples of dimensions 65 mm × 10 mm × 4 mm were prepared using paraffin wax in accordance with the ASTM F417-78 standards. Cement samples were put in these molds and used for flexural testing. The same compression machine was used at a cross-head speed of 1 mm/min. Three samples for each concentration of HNTs were used and an average was calculated.

2.3. FTIR analysis

Potassium bromide (KBr) pellet method was used for FTIR spectroscopy. Thin discs of KBr were prepared by placing a small amount of KBr into the die set and were subjected to a pressure of 8 tons. This pressure caused the KBr to re-crystallize to form thin transparent discs. These discs were used to obtain the background. A small amount of test sample powder was added to KBr and thin discs were prepared by a similar procedure.

2.4. Loading of the HNTs with dexamethasone (DEX)

HNTs were loaded using the vacuum loading technique. Saturated solution of Dex was made by dissolving 200 mg of Dex in 50 mL of ethanolic water (50%v/v). To this solution, 9 g of HNTs were added and subjected to vacuum cycles. The suspension of HNTs in Dex was kept in a vacuum for 20 min and at atmospheric pressure for 20 min, this was repeated thrice. This suspension was left under the vacuum overnight and centrifuged. The supernatant was discarded and HNTs were washed twice with deionized water to remove drug adsorbed on the HNT surface. Washed HNTs were dried in a vacuum and these were used in further experiments.

Drug release from HNTs was measured for a period of 96 h. Accurately measured quantity of 50 mg of Dex loaded HNTs was taken in a centrifuge tube and 1 mL of simulated biological fluid (SBF) was added and placed in a shaker. After specific time intervals, the tube was centrifuged to precipitate HNTs and the supernatant was collected. Equal volume of SBF was replaced every time supernatant was collected to maintain sink conditions. Collected supernatant was observed using a UV-visible spectrophotometer (NanoDrop) at a wavelength of 240 nm.

2.5. Cell culture, proliferation, and differentiation

Mouse pre-osteoblast cell lines MC3T3-E1 (ATCC® CRL-2593™) were obtained from ATCC (Manassas, VA.). Mouse pre-osteoblast (OB) was used for evaluating the osteoconductive potential CPC/HNT composites (details are provided below). OBs were maintained in a minimum essential medium, Eagle's α-modification (α-MEM), containing ribonucleosides,

deoxyribonucleosides, sodium bicarbonate, and supplemented with 2 mM L-glutamine, 1% antibiotics (100 U/mL penicillin and 100 U/mL streptomycin), and 10% fetal bovine serum (FBS) (complete α-MEM). Cells from passage 3 to 4 were used.

Mouse bone marrow stromal cells (MSCs) CRL-12424 (ATCC® CRL-12424™) were used for evaluating the osteoinductive potential CPC/HNT composites (details are provided below). MSCs were maintained in Dulbecco's Modified Eagles Medium (DMEM) with 10% FBS and 1% antibiotics (100 U/mL penicillin and 100 U/mL streptomycin (complete DMEM)). Cells from passage 3 to 4 were used.

Human osteoblast (HOB) cells were used to assess potential cytotoxicity issues. HOBs were cultured in osteoblast growth media according to the manufacturer's directions. Cells from passage 2 to 3 were used.

2.5.1. Cell proliferation

To check the cytocompatibility of the formulated scaffolds, XTT was performed on human osteoblast (HOB) cells C-12760 purchased from PromoCell, Heidelberg, Germany. XTT assay kit (X4751) with 1% PMS was ordered from Sigma-Aldrich. CPC discs of 5 mm × 1 mm dimensions were molded using different concentrations of HNTs (5, 10, and 15%). Control discs without any HNTs and blank cell lines were also cultured for comparative studies.

XTT or 2,3-bis-(2-methoxy-4-nitro-5-sulfophenyl)-2*H*-tetrazolium-5-carboxanilide is a sensitive and reliable quantitative assay. It is a colorless or slightly yellow color tetrazolium dye which gets converted into bright orange color formazan on reduction. When this dye is used in cell cultures, the dehydrogenase enzymes produced from mitochondrial cycle of actively respiring cells reduces the dye to orange color formazan. This assay is greatly improved by adding an electron accepting agent such as PMS (*N*-methyl dibenzopyrazine methyl sulfate). Unlike MTT, this assay does not require to go through laborious procedures such as solubilization prior to quantization, making this process quick and easy. Osteoblast cells, upon reaching to 90% confluency, were trypsinized and resuspended into culture media. In a 96 well plate, 100 μL of cell suspension was added in each well and incubated for 24 h. Activated XTT solution (20 μL) was then added to each well and incubated for 2 h and optical densities were measured using a Phenix LT-4000 absorbance microplate reader at 450 nm.

2.5.2. Assessment of CPC/HNT osteoconductive and osteoinductive potential

For seeding into CPC/DEX (+/−)/HNTs, OBs and MSCs were detached from the flasks by adding TryplE, an animal free trypsin substitute, and mixed with HBSS. Cells were then centrifuged and the cell pellets resuspended in either complete α-MEM or DEM. Setting liquid remained the same for all the formulations except for changes in solid components as described below.

For cell-culture techniques, disc-shaped specimens 10 × 2 mm were made using steel molds. The liquid phase used in this process was prepared from sterile deionized water. After setting, the samples were removed from the molds, dipped in alcohol, and dried under a class II hood.

Two different scaffold types were made for culturing cells (**Tables 1** and **2**). One set of scaffolds were made to evaluate the osteoconductive nature of CPCs while the other set was used to assess its osteoinductive potential. Osteoconductive scaffolds contained CPC powder with varied amounts of HNTs (**Table 1**). Four groups were prepared containing 0, 5, 10, and 15% wt. of HNTs to CPC powders. These HNTs were not loaded with DEX or any other growth factors. Mouse OBs were used for seeding on these scaffolds to evaluate the osteoconductive property of fabricated CPC. To evaluate the osteoinductive potential of our formulation with DEX-doped HNTs, four set of scaffolds were prepared (**Table 2**). Scaffolds in both groups were tested for cell viability, proliferation, ECM production, and alkaline phosphatase activity over a 14-day period. Standard histochemical staining techniques were used. We predicted that MSCs would differentiate into osteoblasts after the exposure to DEX-doped HNT/CPC composites.

2.6. Histochemical staining

As the CPC scaffolds were opaque, bright field microscopy or confocal microscopy images could not be taken. Accordingly, an indirect method of estimating the ECM deposition and amount was used. Collagen content was estimated using Picrosirius red (PS) staining and acidic mucopolysaccharides were estimated using Alcian blue (AB). To quantify staining, stained CP discs were destained measured for staining the dye concentration using UV-visible spectrophotometry. Indirect estimation was done using the destaining method. Glacial acetic acid 7% solution was used as destaining solution. After staining the hydrogel films, destaining solution was added to remove the dye that was fixed on the films. Destaining solution was then collected and measured for the concentration of staining the dye using UV spectrophotometry.

2.6.1. Picrosirius red staining

Picrosirius red is a specific collagen fiber stain and also is capable of detecting thin fibers. Media was removed from the wells and a wash was given with Dulbecco's phosphate buffered saline (DPBS) before fixing the cells using 95% ethanol. These fixed cells were stained with Picrosirius red for quantifying the amount of collagen secreted. The staining kit had three different solutions—A, B (Picrosirius stain), and C (hydrochloric acid—HCl). Solution A was added to the cells and removed after 5 min and solution B was added and was removed after an hour. A wash was given with solution C to remove excess staining. Glacial acetic acid 7% aqueous solution was used as de-staining solution. As the CPC scaffolds were too thick

Group	CPC composition
Group 1	CPC powder without HNTs
Group 2	CPC powder with 10% wt. HNTs
Group 3	CPC powder with 5% wt. DEX-doped HNTs and 5% wt. plain HNTs
Group 4	CPC powder with 10% wt. DEX-doped HNTs

Table 2. Control and experimental groups used in osteoinductive studies.

for light to penetrate, microscopic imaging and quantification were difficult to accomplish. To quantify staining, de-staining was used and measured for staining the dye concentration using UV-visible spectrophotometry.

2.6.2. Alcian blue staining

Alcian blue is used to stain sulfate glycosaminoglycans and proteoglycans in the extracellular matrix. The same procedure, as indicated above, was followed using Alcian blue solution as the dying reagent and destained samples were collected. These samples were later analyzed using a Thermo Scientific NanoDrop 2000c spectrophotometer.

2.6.3. Alkaline phosphatase (AP) assay

During *in vitro* bone formation, AP activity is greatly enhanced and hence used as a marker to evaluate the differentiation of MSCs towards osteoblastic lineage or maintenance of the osteoblast phenotype. It is easily detected using BCIP/NBT as a substrate, which stains cells blue-violet when AP is present. Alcohol fixed plates were washed with a buffer and carefully aspirated without disrupting the monolayer of cells. Enough BCIP/NBT substrate solution was added to just cover the monolayer and left in the dark for 5–10 min. It was then washed and destained using 7% glacial acetic acid for 5 min to quantify the AP activity. The solution was aspirated and analyzed using a NanoDrop 2000c spectrophotometer.

3. Results and discussion

3.1. SEM analysis

SEM was used to analyze the nature of the surface topography of CPCs. Surfaces in all formulations had granules of small and large size (**Figure 1**) No definitive difference could be observed visibility in these images between CPS with and without HNTS. Chitosan lactate was flakes or scales that were observed in thin layers around the particles of DCPA and TTCP (**Figures 1** and **2**). Granular particles of DCPA and TTCP are seen in a matrix of chitosan lactate. HNTs were also observed in few images distributed as clumps and as fine particles. As seen in **Figure 2**, aggregations of HNTs were observed distributed within the matrix of CPCs filling up the voids between the calcium and lactate particles. Cell viability and cell proliferation are largely dependent on the substrate surface, and cellular response to surface roughness is different depending on the cell type [32, 33]. Rough surfaces are preferred by many cell types for attachment and further functionality [33, 34]. Osteoblasts grown on surfaces with microtopography were stimulated towards differentiation as compared with a lack of specific bone marker expression when grown on smooth surfaces [35, 36]. SEM images of CPCs clearly indicate that all CPC formulations possess very rough surfaces and provide a conducive environment for cell attachment (**Figure 1**). This observation was confirmed by the cellular response of OBs and MSCs on the CPC surfaces.

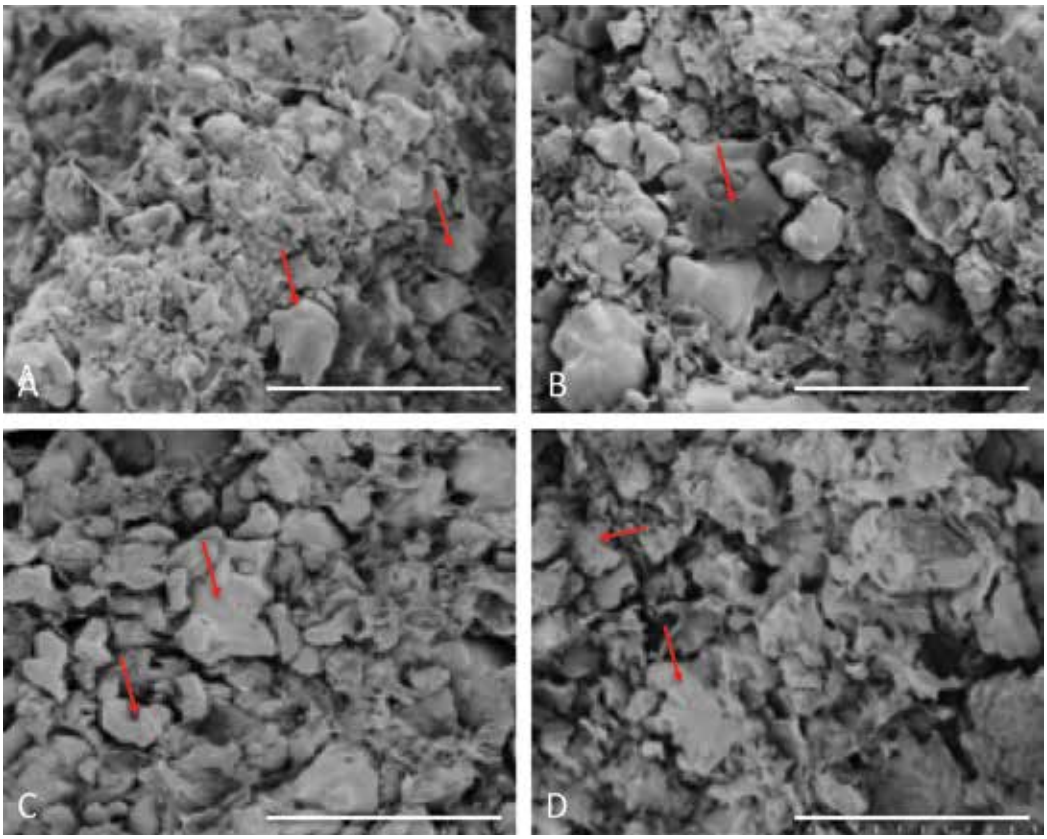

Figure 1. SEM images of CPCs with and without HNTs. (A) CPCs with 0% w/w HNTs (1200× magnification); (B) CPCs with 5% w/w HNTs (1200× magnification); (C) CPCs with 10% w/w HNTs (1500× magnification); and (D) CPCs with 15% w/w HNTs (1500× magnification). (A) and (B) scale bar = 40 microns; (C) and (D) scale bar = 30 microns. Red arrow = chitosan lactate.

3.2. Compression strength

Specimens made for the compression test were analyzed for maximum compressive strength and peak load taken before they were fractured. Of the various combinations of calcium salts and setting liquid salts tested, only those samples that had anti-washout property and good compressive strength were chosen. Most of the samples had decent compressive strength when dry, but upon placing them in an aqueous environment, they became soft and collapsed. Specimens made with TTCP and DCPA using chitosan as a setting liquid had good mechanical properties. As chitosan is soluble only in acidic solutions, aqueous solution of chitosan in acidic water was used. This resulted in elution of acid into SBF while testing for their anti-washout property. The pH of SBF was maintained at 7.40, but when these samples were immersed in SBF, the pH of the solution increased as high as pH 2.0. Hence, in-spite-of having good mechanical properties, these samples were not selected as it would create hostile microenvironment for cells. To prevent cytocompatibility issues, chitosan lactate was, accordingly, selected as the setting liquid as it was soluble in neutral water. When all samples were

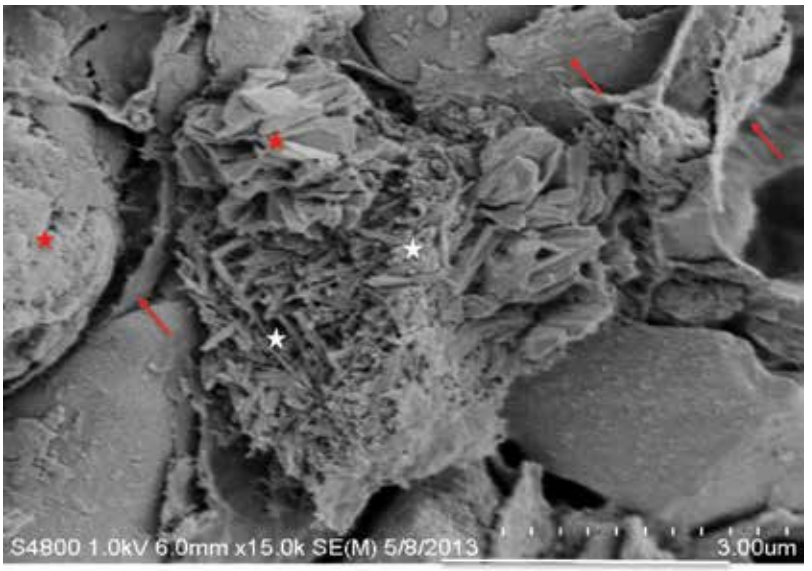

Figure 2. Scanning electron micrograph of CPC added with 5% wt. HNTs showing aggregation of HNTs. Red arrows = chitosan lactate flakes. Red star = calcium phosphate particles. White star = HNTs concentrations.

tested, the composition with the most desired properties was an equimolar mixture of TTCP and DCPA in the solid phase with chitosan lactate as the liquid phase.

Different concentrations of HNTs were added to this composition. These compositions were then tested for compression and flexural strengths. The addition of HNTs has an observable and significant change in the compressive strengths of CPCs (**Figure 3A**). Peak compressive strength was seen in groups that were added with 5% wt. HNTs. Peak compression pressure of 16.48 ± 0.95 MPa was observed for CPCs that were added with 5% wt. HNTs. CPCs that were not added with HNTs had a compressive strength of 11.65 ± 2.24 MPa. Compressive strength of CPCs is increased by 41.47% upon the addition of 5% of HNTs. At concentrations of 10 and 15% wt. HNTs, compressive strength of CPCs was recorded as 14.43 ± 1.64 MPa and 13.54 ± 1.67 MPa. Minimum of five samples in each group were tested and statistical analysis was performed on the data sets. One way ANOVA was done to analyze the statistical significance among the four groups. Results suggest that there is a significant difference in the means of all four groups at $\alpha = 0.05$. Post hoc analysis was done to identify the group with the highest mean compressive strength. Results from Tukey's HSD suggest that groups containing 5% wt. HNTs have the highest mean compressive strength.

Addition of nanoparticles in the matrix of CPCs improves the compression strength up to certain concentration and beyond this concentration no significant improvement was observed. The optimal concentration for this composition was observed to be at 5% wt. The particle size of TTCP contributes an important role in determining the compressive strength of CPCs. Smaller particles attribute for increased strength compared to larger particles. As shown in **Figure 3B**, at a particle size of 1.9 ± 0.31 μm, the compressive strength of CPCs was 23.49 ± 1.36 MPa. Larger particles with a diameter of 4.1 ± 1.15 μm had a peak compression strength of 8.25 ± 2.56 MPa. Particles with an average diameter of 2.4 ± 0.42 μm had a compression strength

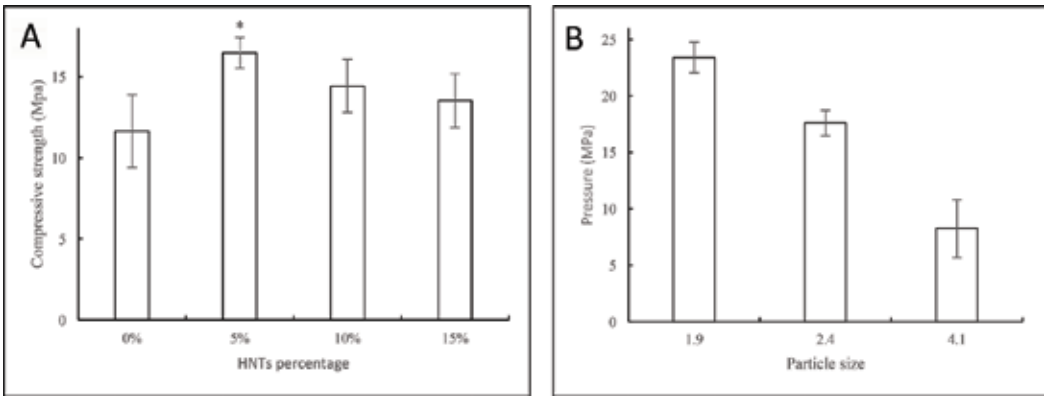

Figure 3. (A) Compressive strength of CPCs with varying amount of HNTs. (B) Compression strength as a function of particle size of TTCP. Error bars = standard deviation.

of 17.59 ± 1.13 MPa. It can be inferred that smaller particles may be arranged in a compact manner resulting in smaller voids between the particles and thus resulting in greater compression strengths of CPCs. This improvement in compression strength by the addition of HNTs can be useful in applications where primary forces acting on cements are compression. Bone cements used in vertebral augmentation are primarily subjected to compressive forces and the CPC/HNTs composite may be of use in this surgical procedure.

Much research was directed towards improvement of CPCs by introducing additives in solid and liquid phases. Improvements were observed in mechanical strengths, setting times, bioactivity, and degradability. Addition of gelatin and chitosan resulted in increased setting time, improved cell adhesion and ECM formation, and improved compressive strengths. Addition of other polymers including collagen, alginate, hyaluronate, cellulose, and synthetic polymers had various effects depending on the CPC composition and the amount of polymer [37, 38].

3.3. Flexural strength

Three-point bending test was performed to evaluate the flexural strength of CPCs (**Figure 4A**). Flexural strength of control group containing just DCPA, TTCP, and chitosan lactate was recorded as 13.86 ± 2.45 MPa. Addition of HNTs at 5% wt. improved the strength to 17.12 ± 2.49 MPa. This increase was not statistically significant at $\alpha = 0.05$. CPCs containing 10 and 15% wt. HNTs had flexural strengths of 15.38 ± 0.26 MPa and 17.41 ± 1.45 MPa, respectively. This trend of flexural strengths is graphically represented in **Figure 4B**. The standard deviation error bars in **Figures 3** and **4** may be attributed to air gaps formed while preparing the bone cement and loading them into the molds. Presence of air pockets can reduce the compression and flexural strength of cements. This may be avoided by using a vacuum chamber to mix and prepare the specimens.

The inability to provide significant resistance to applied mechanical loads has limited CPCs to non-load-bearing, mostly craniofacial applications [37–39]. Their toughness and fatigue resistance are much less than those of cortical bone. The incorporation of a polymer during the CPC liquid phase increases ductility, allowing for a higher deformation before breaking [39, 40]. Moreover, polymer fiber reinforcement has been extensively explored as a strategy to increase the toughness and strength of cements [41].

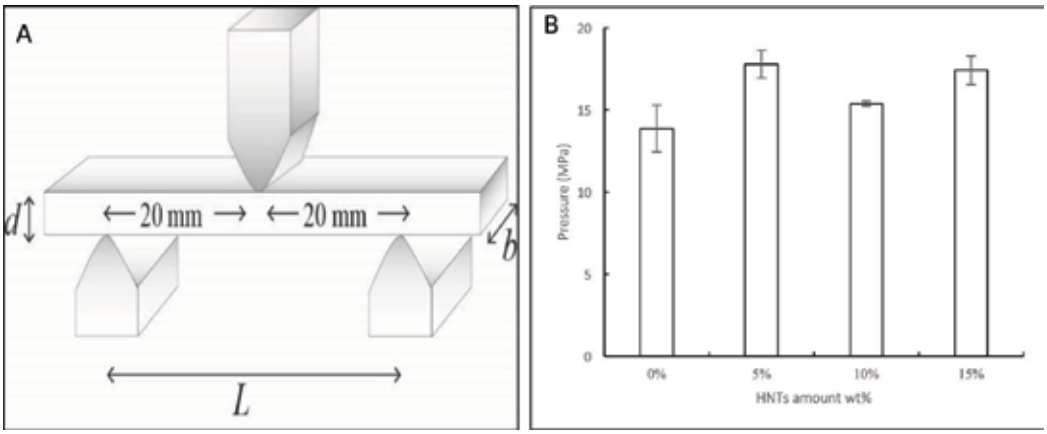

Figure 4. (A) Flexural test method. (B) Flexural strength of CPCs with varying amount of HNTs. Error bars = standard deviation.

One explanation for a portion of the gain in material strength could be HNT addition to the CPC cement. HNTs have been widely used as a nanofiller for the modification of nanocomposite materials [24, 25, 27]. HNTs have been used to increase surface area and impart high surface reactivity, improving mechanical and overall strength (see Zhang et al. for an excellent review [42]). To achieve the increase in mechanical strength, thermal stability, and toughness HNTs has been combined into a variety of polymers. Examples of polymer studied modification by HNTs include: poly(butylene succinate) [44], polyamide [12, 45], styrene-butadiene [46], epoxy [47], poly(methyl-methacrylate) [48], and chitosan [43]. In our case, we speculate that HNTs distribution the CPC cement fills voids resulting in the increase of mechanical strength by preventing crack propagation. HNTs have been suggested as mechanism nanoparticle deflect or absorb a propagating crack, thus preventing the formation of weak points and improving strengths. However, when the HNT concentration exceeds a certain value, the CPC deformability decreased sharply. This may be because of the pattern of HNT dispersion [47]. The interfacial binding between HNT/chitosan composites was proposed as resulting from hydrogen bonding and electrostatic interactions and a uniform dispersion results in a uniform interfacial-binding matrix and favorable to force conduction [43]. In contrast, too many HNTs and HNT clustering may inhibit the dispersion state and create interfacial gaps, which are easy to break.

3.4. FTIR analysis

The final setting product of apatite cements was hypothesized to be hydroxyapatite. To evaluate the end-product formation, FTIR analysis was used. A comparison of IR spectra of CPC control, CPCs (no HNTs added), CPCs with 5% HNTs, and hydroxyapatite is shown in **Figure 5**. Band of peaks seen at wavenumber 900–1200 cm^{-1} are due to PO + 4 groups present in all the test samples. Peaks at 1450 cm^{-1} are characteristic of the CO_3^{2-} group found in HA. Peaks at 3100–3700 cm^{-1} are due to the —OH groups of hydroxyapatite. Comparing peaks for the —OH group, we observe that CPCs with HNTs have stronger peak than control CPCs. This observation can be attributed to the presence of HNTs that acted as seeding/nucleating agents facilitating the precipitation of hydroxyapatite crystals.

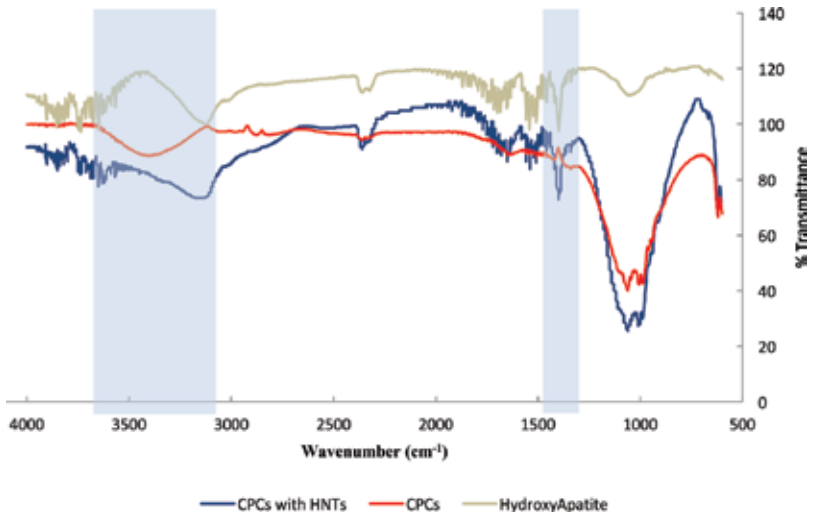

Figure 5. FTIR spectra of HA and CPCs with and with HNTs. Peaks at 1450 cm^{-1} and 3100–3700 cm^{-1} are characteristic of HA (CO_3^{2-} and —OH groups, respectively).

3.5. Dexamethasone elution profile

Drug elution was studied using 50 mg of DEX loaded HNTs (**Figure 6A**). It can be observed that there is an initial burst release from HNTs during the first 10 h of release and from then onwards it was sustained. This 50 mg elution form of HNTs is above the desired micro to nanomolar range to stimulate the differentiation of MSCs towards osteoblastic lineage. DEX release from scaffolds was also studied using scaffolds with only 5% of HNTs loaded with DEX. It can be observed that drug release was slow and the concentration of drug released from scaffolds is much lower compared to HNTs. **Figure 6B** shows the release of DEX from scaffolds. The drug release may be even more extended during scaffolds degradation exposing more HNTs to extracellular fluids (*in vivo*). Drug release from CPC scaffolds was less compared to HNTs. This may be attributed to the surface release and doped HNTs in the matrix did not have contributed to this release.

3.6. Cell proliferation

The viability of HOBs on the surface of the CPC scaffolds was analyzed at days 3, 7, and 14 (**Figure 7**). The absorbance values of the XTT assay reflects the mitochondrial activity of the live cells. The absorbance values across the 14-day period indicate that all samples showed no cytotoxic effects. The mean values of absorbance also varied strongly with the HNT concentration. On day 3, a 20.35% increase in absorbance values was observed for control CPC scaffolds when compared to wells containing only cells. On addition of 5% HNTs to the CPC scaffolds, 28.3% significant increase in the absorbance value was noticed. For 10 and 15% HNT absorbance was 9.8 and 12.8% larger, respectively. But, when compared with control CPC scaffold (no HNTs added), 8.7 and 6.1% decrease in the absorbance values for 10 and 15% CPC-HNT scaffolds were seen. By day 7, absorbance was larger for CPC scaffolds than for control wells. Wells containing 5% HNT samples showed 26.7% larger absorbance compared to CPC

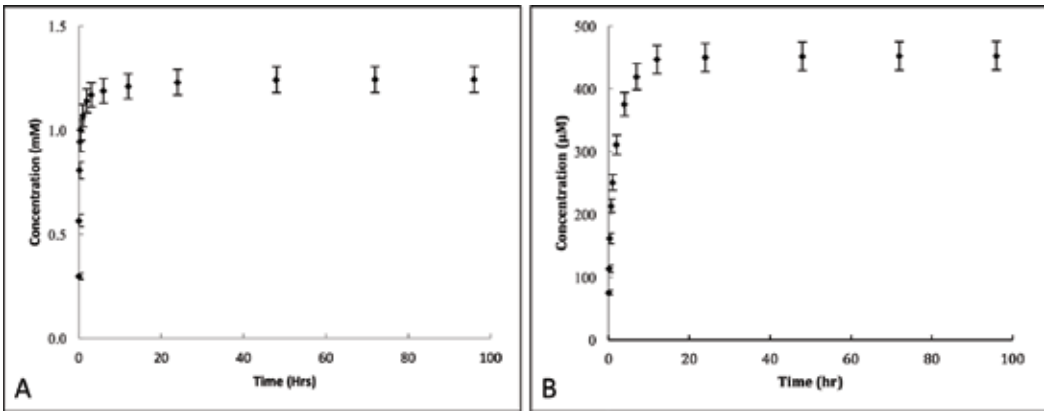

Figure 6. (A) Dexamethasone elution from loaded HNTs. (B) Dexamethasone release from CPC scaffolds loaded with DEX-doped HNTs.

samples without HNTs. CPCs with 10% HNTs had the highest absorbance value. Finally, at day 14, all wells containing CPC scaffolds showed higher absorbance values than control wells and it was the largest in scaffolds with 15% HNTs. The results further suggest that HNT/CPC composites are cytocompatible and enhance the osteoblast viability of the osteoblast cells. In addition, further increase in viability (cell growth) was seen with HNT addition.

3.7. Histochemical staining of HNT-doped CPC discs

As all CPC scaffolds were opaque, bright field microscopy or confocal microscopy micrographs were unable to be taken. An indirect method of estimating ECM production was

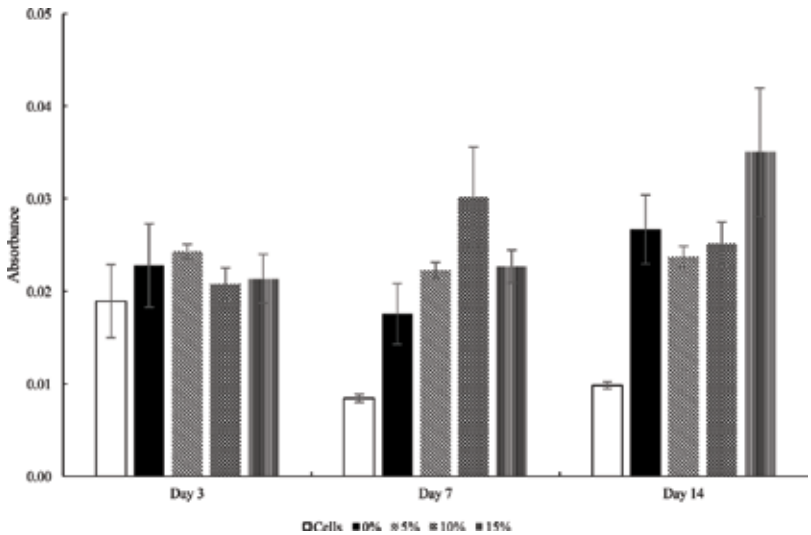

Figure 7. Cell viability assessed in human osteoblast culture on different CPC-HNT scaffolds (mean ± SD; n = 6).

employed using a staining and destaining method. Collagen content was estimated using the Picrosirius red stain, the presence of acidic mucopolysaccharides using an Alcian blue stain, and alkaline phosphatase activity was examined to confirm the osteoblastic phenotype of cells cultured of HNT/CPC discs.

3.7.1. Picrosirius red staining (PSR)

Graphical representation of PSR stain absorbance is shown in **Figure 8**. Higher absorbance indicates greater collagen content secreted by osteoblasts on the scaffolds. All test groups supported collagen production and throughout the length of the experimental period. On average, a higher amount of collagen synthesis was observed on day 14 stain as compared to day 7. However, there was no significant difference in the amount of collagen synthesized among all the groups on given day.

3.7.2. Alcian blue staining

Alcian blue staining was used to determine the acidic mucopolysaccharides synthesis. **Figure 9** is graphical representation of Alcian blue staining for all scaffolds over the testing period. Higher absorbance indicates higher acidic mucopolysaccharides synthesis. On day 7, acidic mucopolysaccharides synthesis was almost same across all CPC scaffold groups. Day 14 staining showed an improvement in mucopolysaccharide synthesis with an increase in the HNT concentration. CPC scaffolds with 15% HNTs showed the highest level of Alcian

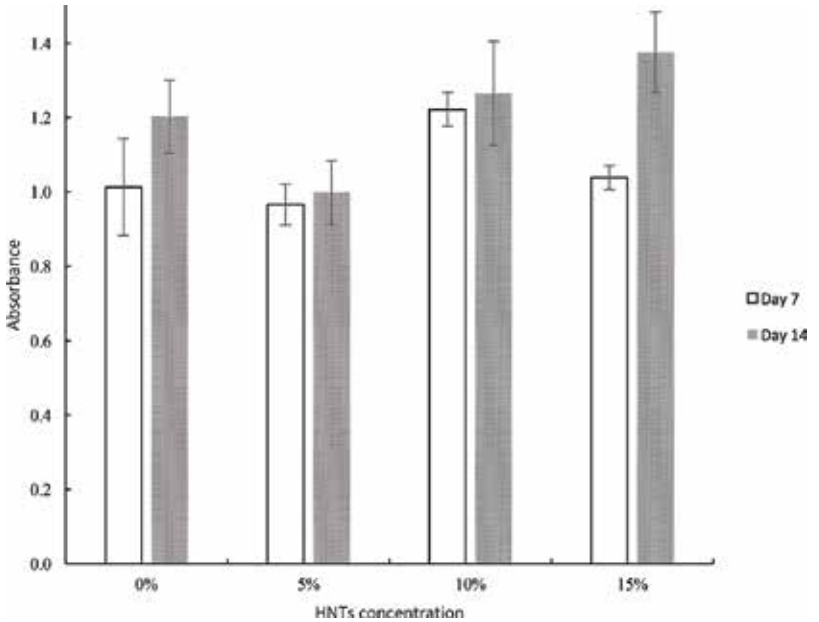

Figure 8. Destained well-plates showing red color, due to Picrosirius red, staining on and around osteoblast seeded CPC scaffolds indicating the presence of collagen. A = 7 days in culture and B = 14 days in culture. (C) Absorbance values for different HNT concentrations at day 7 and 14.

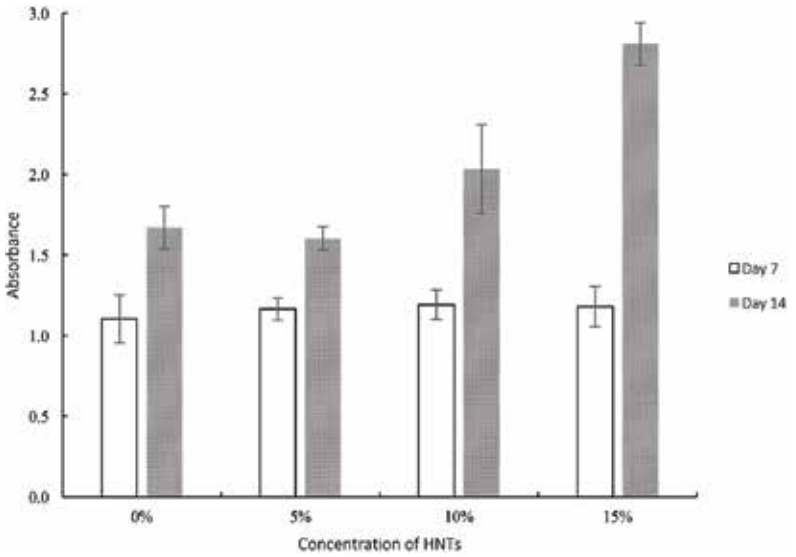

Figure 9. Destained well-plates showing blue color, due to Alcian blue dye, on and around CPC scaffolds indicating the presence of acid mucosubstances. A = 7 days in culture and B = 14 days in culture. (C) Absorbance values for different HNT concentrations at day 7 and day 14.

blue staining indicating the higher acidic mucopolysaccharides synthesis. However, there was no significant difference in the amount of collagen synthesized among all the groups on given day.

The Picrosirius red and Alcian blue staining results suggest that CPC surfaces are conducive for osteogenesis and cell viability. Production of ECM molecules is a critical factor during bone tissue regeneration.

3.7.3. Alkaline phosphatase activity (ALP)

Preservation of the osteoblastic phenotype in OB cells was assayed using ALPase activity. It was observed that all CPC groups had a strong ALPase activity showing the preservation of the osteoblast phenotype (**Figure 10**). From the graph, it can be inferred that the cells had enhanced ALPase activity on day 14 compared to day 7. A pronounced increase in ALPase activity was seen in CPC discs without HNTs and CPCs with 10% wt. HNTs. There was, however, no statistical difference among groups on a given day of assay. All histochemical staining results suggest that CPC surfaces are conducive for osteoblast attachment, proliferation, and synthesis of an organic matrix that was subsequently mineralized. Osteogenesis and cell viability are the critical requirements for bone tissue regeneration.

3.8. Histochemical staining of DEX-doped HNT/CPC discs

As with the HNT/CPC discs, an indirect method of estimating ECM production was employed using the same staining methods and destaining protocols.

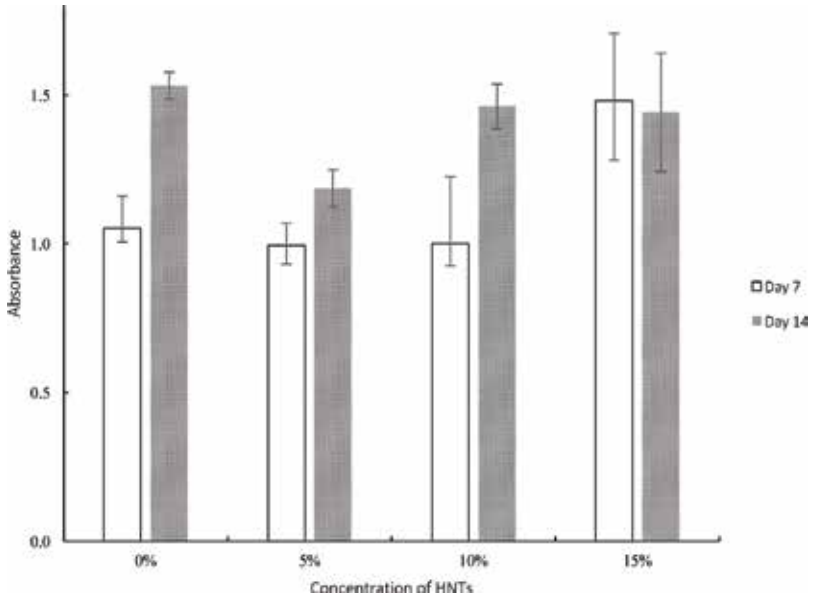

Figure 10. Comparison of absorbance values for samples collected at different concentrations of HNTs at day 7 and day 14 for ALPase activity.

3.8.1. Picrosirius red staining (PSR)

MSC collagen production was observed across all the test groups and throughout the length of the experimental period (**Figure 11**). Collagen synthesis remained almost same for any given group on all the days except for Group 3. By day 7 and 14, these scaffolds were stained equally compared to the rest other scaffold groups. By the end of day 14, all the scaffolds were equally stained with PSR stain referring to similar amount of collagen production by cells on all the scaffolds. However, no significant difference in the amount of collagen is synthesized among all the groups on given day. In comparing OB and MSC collagen synthesis on CPC/HNT discs, the pattern observed was similar for Group 1 (CPCs no HNTs) and OB Group #3/MSC Group #2 (CPCs with 10% HNTs).

3.8.2. Alcian blue staining

Each group of scaffolds followed a different trend for each day of experiment in terms of acidic mucopolysaccharide synthesis (**Figure 12**). Group 1 scaffolds had an increase in staining for day 3 and slight decrease on the following days 7 and 14. Staining on Group 2 scaffolds had deep staining on day 7, while on rest other days, similar amount of staining was observed. Group 3 scaffolds showed a similar staining for all the test days, in contrast, Group 4 scaffolds were deeply stained on day 14 compared to other days (**Figure 12**). Results from Picrosirius red and Alcian blue stains suggest cytocompatibility of these scaffolds with bone marrow stromal cells. The presence of dexamethasone does not appear to enhance or decrease the ECM synthesis as revealed by histochemical staining.

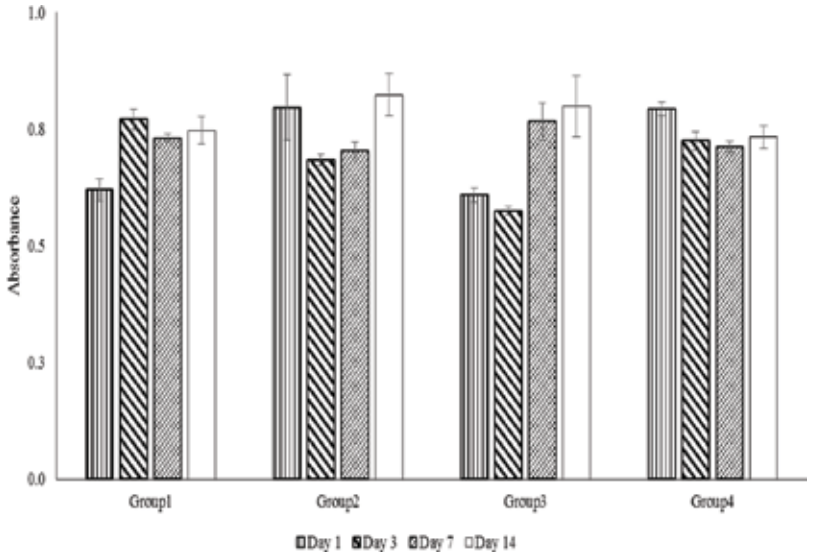

Figure 11. Picrosirius red staining. Collagen synthesis was consistent and steady across all study groups.

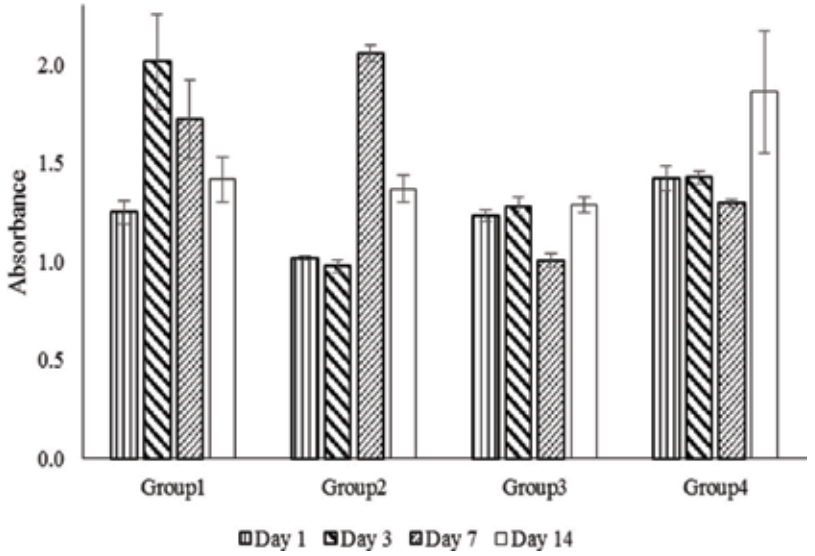

Figure 12. Alcian blue staining for osteoinductive scaffolds. A different trend was observed in terms of acidic mucopolysaccharide synthesis for all four groups.

3.8.3. Alkaline phosphatase activity

According to the hypothesis, scaffold Groups 3 and 4 would induce differentiation of BSCs towards osteoblastic lineage as they contained different concentrations of DEX- doped HNTs. Hence, more alkaline phosphatase activity was predicted in these groups. Staining results of

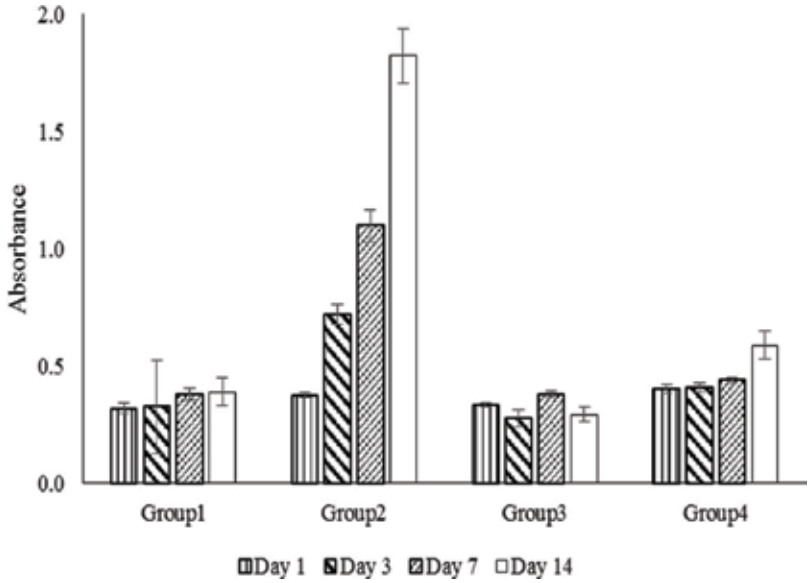

Figure 13. Alkaline phosphatase activity assay for osteoinductive scaffolds.

alkaline phosphatase assay are shown in **Figure 13**. Differentiation was more pronounced on Group 2 scaffolds that contained empty HNTs. Scaffolds of Groups 3 and 4, containing DEX loaded HNTs did not induce osteoblastic differentiation in the BSCs. Cell culture wells containing Group 2 scaffolds were deeply stained in purple while the rest other wells were stained slightly or none. Group 2 scaffolds' alkaline phosphatase activity was significantly higher on day 14 compared to other groups. Inability of Group 3 and 4 scaffolds to induce differentiation may be attributed to very high concentrations of DEX released. The optimum concentration of DEX needed to induce the osteogenic differentiation is 10–7 [49–51]. In the CPC discs doped with DEX, DEX may have been eluted in excess and thus had an inhibitory effect.

The ability of HNTs alone (no DEX) to induce osteogenic differentiation was previously reported using montmorillonite-doped biopolymers [52]. It may be inferred from this study and the study by Ambre et al. that many aluminosilicate clays may be inherently osteoinductive [53].

4. Conclusions and future work

We conclude that CPCs fabricated using TTCP and DCPA as the solid phase and 10% chitosan lactate solution as the setting liquid and doped with HNTs have an osteoconductive nature as evidenced by a production of an abundant ECM synthesis and alkaline phosphatase activity. Surface roughness was increased with HNT addition which favors cell attachment, proliferation, and ECM synthesis. Halloysite increased the compressive strength of CPCs. The composition of CPCs after setting was analyzed using FTIR which reveals that the addition of HNTs increased HA production by acting as seeding agents for the precipitation of

HA. CPC with DEX-doped HNTs showed an extended release of DEX from CPC scaffolds. DEX-loaded HNTs were used in varying concentrations in the fabrication of osteoinductive scaffolds. Osteoinductive scaffolds were seeded with MSCs to evaluate their osteoinductive nature. Our results suggest that HNTs with DEX loaded in the scaffolds started inducing differentiation in MSCs after 14 days while scaffolds with empty HNTs started inducing differentiation towards osteoblastic lineage after 3 days. At the end of 14th day, scaffolds containing non-loaded HNTs had the highest amount of alkaline phosphatase activity suggesting maximum differentiation of BSCs to osteoblastic phenotype. HNTs promoting differentiation of BSCs to osteoblastic phenotype can be explored further using different compositions. HNTs loaded with different drugs, antibiotics, growth factors, and chemotherapeutic agents can be used in fabricating CPCs. Addition of other polymers can also be considered to enhance the CPC mechanical properties further. *In vivo* experiments are being conducted in small animals to evaluate the tissue formation properties effectiveness of the CPCs fabricated.

Acknowledgements

The authors would like to acknowledge the Louisiana's Governor's Biotechnology Initiative, LASPACE and the Louisiana Board of Regents OPT-IN program for their funding support (awarded to Dr. David K. Mills).

Conflicts of interest

The authors declare that they have no conflicts of interest.

Author details

Udayabhanu Jammalamadaka[1], Karthik Tappa[1] and David K. Mills[2]*

*Address all correspondence to: dkmills@latech.edu

1 Center for Biomedical Engineering and Rehabilitation Science, Louisiana Tech University, Ruston, LA, USA

2 Center for Biomedical Engineering and Rehabilitation Science and the School of Biological Sciences, Louisiana Tech University, Ruston, LA, USA

References

[1] DiMaio FR. The science of bone cement: A historical review. Orthopedics. 2002;**25**(12): 1399-1407

[2] Webb JCJ, Spencer RF. The role of polymethylmethacrylate bone cement in modern orthopaedic surgery. Journal of Bone and Joint Surgery. British Volume (London). 2007;**89**(7):851-857

[3] Lidgren L, Robertson O. Acrylic bone cements: Clinical developments and current status. Scandinavia. The Orthopedic Clinics of North America. 2005;**36**(1):55-61

[4] Kühn K-D. Properties of bone cement: What is bone cement. In: Breusch S, Malchau H, editors. The Well-Cemented Total Hip Arthroplasty. Heidelberg: Springer Medizin Verlag; 2005. pp. 52-59

[5] Gough JE, Downes S. Osteoblast cell death on methacrylate polymers involves apoptosis. Journal of Biomedical Materials Research. 2001;**57**(4):497-505

[6] Stańczyk M, van Rietbergen B. Thermal analysis of bone cement polymerization at the cement-bone interface. Journal of Biomechanics. 2004;**37**(12):803-810

[7] Lautenschlager EP, Jacobs JJ, Marshall GW, Meyer PR. Mechanical properties of bone cements containing large doses of antibiotic powders. Journal of Biomedical Materials Research. 1976;**10**(6):929-938

[8] Vaishya R, Chauhan M, Vaish A. Bone cement. Journal of Clinical Orthopaedics and Trauma. 2013;**4**(4):157-163. http://doi.org/10.1016/j.jcot.2013.11.005

[9] Bistolfi A, Massazza B, Verné E, Massè E, Deledda DA, Ferraris S, Miola M, Galetto F, Crova M. Antibiotic-loaded cement in orthopedic surgery: A review. ISRN Orthopedics. 2011:1-8

[10] Brown WE, Chow LC. A new calcium phosphate setting cement. Journal of Dental Research. 1983;**62**:672-678

[11] Friedman CD, Costantino PD, Takagi S, et al. BoneSource hydroxyapatite cement: A novel biomaterial for craniofacial skeletal tissue engineering and reconstruction. Journal of Biomedical Materials Research Part B: Applied Biomaterials. 1998;**43**:428-432

[12] Komlev VS, Fadeeva IV, Gurin N, Shvorneva LI, Bakunova NV, Barinov SM. New calcium phosphate cements based on tricalcium phosphate. Doklady Chemistry. Apr. 2011;**437**(1):75-78

[13] Lee KY, Park M, Kim HM, Lim YJ, Chun HJ, Kim H, et al. Ceramic bioactivity: Progresses, challenges and perspectives. Biomedical Materials. 2006;**1**:R31-R37

[14] Dorozhkin SV, Epple M. Biological and medical significance of calcium phosphates. Angewandte Chemie, International Edition. 2002;**41**:3130-3146

[15] Kühn K-D. Properties of bone cement. In: Breusch S, editor. The Well-Cemented Total Hip Arthroplasty. Heidelberg: Springer MedizinVerlag; 2005. pp. 52-59

[16] Ducheyne P, Qiu Q. Bioactive ceramics: The effect of surface reactivity on bone formation and bone cell function. Biomaterials. 1999;**20**:2287-2303

[17] Radin S, Reilly G, Bhargave G, et al. Osteogenic effects of bioactive glass on bone marrow stromal cells. Journal of Biomedical Materials Research. Part A. 2005;**73**:21-29

[18] Albrektsson T, Johansson C. Osteoinduction, osteoconduction and osseointegration. European Spine Journal. 2001;**10**:S96-S101

[19] Barinov SM, Komlev VS. Calcium phosphate bone cements. Inorganic Materials. 2011; **47**(13):1470-1485

[20] Bohner M. Reactivity of calcium phosphate cements. Journal of Materials Chemistry. 2007;**17**(38):3980-3992

[21] Ginebra MP. Cements as bone repair materials. In: Planell JA, editor. Bone Repair Biomaterials. Cambridge, England: Woodhead Publishing Limited; 2009. pp. 271-308

[22] Shchukin DG, Sukhorukov GB, Price RR, Lvov YM. (2005) Halloysite nanotubes as biomimetic Nanoreactors. Small. 2005;**1**:510-513

[23] Abdullayev E, Lvov Y. Halloysite clay nanotubes for controlled release of protective agents. Journal of Nanoscience and Nanotechnology. 2011;**11**(11):10007-10026

[24] Du M, Guo B, Jia D. Newly emerging applications of halloysite nanotubes: A review. Polymer International. 2010;**59**(5):574-582

[25] Liu M, Wu C, Jiao Y, Xiong S, Zhou C. Chitosan/halloysite nanotubes bionanocomposites: Structure, mechanical properties and biocompatibility. International Journal of Biological Macromolecules. 2012;**5**:566-575

[26] Karnik S, Jammalaka U, Tappa K, Mills DK. Performance evaluation of nanoclay enriched anti-microbial hydrogels for biomedical applications. Heliyon. 2016;**2**(2):1-21

[27] Lee J-W, Park S-J, Kin TH. Improvement of interfacial adhesion of incorporated halloysite-nanotubes in fiber-reinforced epoxy-based composites. Applied Sciences. 2017;**7**:441. DOI: 10.3390/app7050441

[28] Lai X, Agarwal M, Lvov YM, Pachpande C, Varahramyan K, Witzmann FA. Proteomic profiling of halloysite clay nanotube exposure in intestinal cell coculture. Journal of Applied Toxicology. 2013;**33**:1316-1329

[29] Lovo Y, Aerov A, Fakhrulli R. Clay nanotube encapsulation for functional biocomposites. Advances in Colloid and Interface Science. 2014;**207**:189-198

[30] Bellani L, Giorgetti G, Riela S, Lazzara G, Scialabba A, Massaro M. Ecotoxicity of halloysite nanotube–supported palladium nanoparticles in Raphanus sativus L. Environmental Toxicology and Chemistry. 2016;**35**:2503-2510

[31] Wei W, Abdllayev E, Goeders A, Hollister A, Lvov L, Mills DK. Clay nanotube/poly(methyl methacrylate) bone cement composite with sustained antibiotic release. Macromolecular Materials and Engineering. 2012;**297**:645-653

[32] Khalili AA, Ahmad MR. A review of cell adhesion studies for biomedical and biological applications. International Journal of Molecular Sciences. 2015;**16**:18149-18184

[33] Chang H-I, Wang Y. Cell responses to surface and architecture of tissue engineering scaffolds, regenerative medicine and tissue engineering. In: Eberli D, editor. ISBN: 978-953-307-663-8Cells and Biomaterials. InTech; 2011

[34] Zan X, Sitasuwan P, Feng S, Wang Q. Effect of roughness on in situ biomineralized CaP-collagen coating on the osteogenesis of mesenchymal stem cells. Langmuir. 2016;**32**(7):1808-1817

[35] Hatano K, Inoue H, Kojo T, Tsujisawa T, Uchiyama C, Uchida Y. Effect of surface roughness on proliferation and alkaline phosphatase expression of rat calvarial cells cultured on polystyrene. Bone. 1999;**25**:439-445

[36] Lim JY, Hansen JC, Siedlecki CA, Runt J, Donahue HJ. Human foetal osteoblastic cell response to polymer-demixed nanotopographic interfaces. Journal of The Royal Society Interface. 2005;**2**:97-108

[37] Eliaz N, Noah Metoki N. Calcium phosphate bioceramics: A review of their history, structure, properties, coating technologies and biomedical applications. Materials. 2017;**10**(4):334. DOI: 10.3390/ma10040334

[38] Perez RA, Kim HW, Ginebra MP. Polymeric additives to enhance the functional properties of calcium phosphate cements. Journal of Tissue Engineering. 2012;**3**(1):1-20. DOI: 10.1177/2041731412439555

[39] Zhang JT, Tancret F, Bouler JM. Fabrication and mechanical properties of calcium phosphate cements (CPC) for bone substitution. Materials Science and Engineering: C. 2011;**31**(4):740-747. DOI: 10.1016/j.msec.2010.10.014

[40] Khashaba M, Moussa MM, Mettenburg DJ, Rueggeberg FA, Chutkan NB, Borke JL. Polymeric-calcium phosphate cement composites-material properties: In vitro and in vivo investigations. International Journal of Biomaterials. 2010;**2010**:223-239

[41] Ambard AJ, Mueninghoff L. Calcium phosphate cement: Review of mechanical and biological properties. Journal of Prosthodontics. 2006;**15**:321-328

[42] Zhang Y, Tang A, Yang H, Ouyang J. Applications and interfaces of halloysite nanocomposites. Applied Clay Science. 2016;**119**(1):8-17

[43] Liu M, Zhang Y, Wu C, Xiong S, Zhou C. Chitosan/halloysite nanotubes bionanocomposites: Structure, mechanical properties and biocompatibility. International Journal of Biological Macromolecules. 2012;**51**:566-575

[44] Wu W, Cao X, Luo J, He G, Zhang Y. Morphology, thermal, and mechanical properties of poly(butylene succinate) reinforced with halloysite nanotube. Polymer Composites. 2014;**35**:847-855

[45] Lecouvet B, Gutierrez J, Sclavons M, Bailly C. Structure property relationships in polyamide 12/halloysite nanotube nanocomposites. Polymer Degradation and Stability. 2011;**96**:226-235

[46] Guo B, Chen F, Lei Y, Liu X, Wan J, Jia D. Styrene-butadiene rubber/ halloysite nanotubes nanocomposites modified by sorbic acid. Applied Surface Science. 2009;**255**:7329-7336

[47] Deng S, Zhang J, Ye L. Halloysite–epoxy nanocomposites with improved particle dispersion through ball mill homogenization and chemical treatment. Composites Science and Technology. 2009;**69**:2497-2505

[48] Wei W, Abdllayev E, Goeders A, Hollister A, Lvov Y, Mills DK. Clay nanotube/ poly(methyl methacrylate) bone cement composite with sustained antibiotic release. Macromolecular Materials and Engineering. 2012;**297**:645-653

[49] Langenbach F, Handschel J. Effects of dexamethasone, ascorbic acid and β-glycerophosphate on the osteogenic differentiation of stem cells in vitro. Stem Cell Research & Therapy. 2013;**4**(5):117. http://doi.org/10.1186/scrt328

[50] Yuasa M, Yamada T, Taniyama T, Masaoka T, Xuetao W, Yoshii T, Sotome S. Dexamethasone enhances osteogenic differentiation of bone marrow- and muscle-derived stromal cells and augments ectopic bone formation induced by bone morphogenetic protein-2. PLoS One. 2015;**10**(2):e0116462 http://doi.org/10.1371/journal.pone.0116462

[51] Rimando MG, Wu H-H, Liu Y-A, Lee C-H, Kuo S-W, Lo Y-P, Tseng K-F, Liu Y-S, Lee OK. Glucocorticoid receptor and histone deacetylase 6 mediate the differential effect of dexamethasone during osteogenesis of mesenchymal stromal cells (MSCs). Science Reports. 2016;**30**(6):37371. DOI: 10.1038/srep37371

[52] Ambre AH, Katti DR, Katti KS. Nanoclays mediate stem cell differentiation and mineralized ECM formation on biopolymer scaffolds. Journal of Biomedical Materials Research. Part A. 2013;**101**(9):2644-2660

[53] Ambre AH, Katti DR, Katti KS. Biomineralized hydroxyapatite nanoclay composite scaffolds with polycaprolactone for stem cell-based bone tissue engineering. Journal of Biomedical Materials Research. Part A. 2015 Jun;**103**(6):2077-2101. DOI: 10.1002/ jbm.a.35342

Chapter 8

The Effect of Clay Type on the Physicochemical Properties of New Hydrogel Clay Nanocomposites

Tatiana Munteanu, Claudia Mihaela Ninciuleanu, Ioana Catalina Gifu, Bogdan Trica, Elvira Alexandrescu, Augusta Raluca Gabor, Silviu Preda, Cristian Petcu, Cristina Lavinia Nistor, Sabina Georgiana Nitu and Raluca Ianchis

Additional information is available at the end of the chapter

http://dx.doi.org/10.5772/intechopen.74478

Abstract

This study focuses on the investigation of clay type effect on the final properties of semi-interpenetrated Salecan/poly(methacrylic acid)/clay hydrogel nanocomposites. Previous studies have indicated that the presence of clay in polymer composites leads to better swelling capacity and mechanical properties as functions of clay type. On the other hand, Salecan, which is a water soluble extracellular polysaccharide, was proved to assure greater flexibility to hydrogels. These properties recommend clay and Salecan for semi-interpenetrated hydrogels preparation with specific application in biomedicine. The purpose was to determine the most suitable type of clay as well as Salecan influence for developing the desired water retention/delivery ability and mechanically enhanced semi-interpenetrating polymer network (SIPN) nanocomposites. For our investigations, we have chosen commercially available montmorillonite (ClNa) and different commercial organomodified clay (Cl30B, Cl20A and Cl15A). Several analyses results (FTIR, TGA, DMA, XRD, microscopy and swelling studies) demonstrated that not only the presence of Salecan but also the clay type influenced the structure and properties of the final nanocomposites.

Keywords: clay mineral, Salecan, poly(methacrylic acid), hydrogel, nanocomposites

1. Introduction

Hydrogels can be defined as three-dimensional cross-linked polymer networks that have the property of swallowing a substantial amount of water without dissolving as an effect of their physical and/or chemical cross-linking matrix architecture [1, 2]. Besides excellent swelling capacity, other features of hydrogels include an outstanding biocompatibility, high permeability for water-soluble agents and adjustable mechanical properties. Consequently, these materials have been studied extensively for medical application purposes such as tissue engineering, drug delivery systems and biosensor fields [3]. Lately, polysaccharide-constructed hydrogels have gained more attention. The main disadvantage of polysaccharide hydrogels is the lack of mechanical strength, and for this reason, the introduction of a rigid synthetic polymer in order to develop interpenetrating or semi-interpenetrating polymer network hydrogels (IPN/SIPN) with improved strength is being recently studied. IPN or SIPN differs from other multicomponent systems through the highly intimate contact between the polymers, though no chemical bond exists between them. The unique properties of the final nanomaterials are given by the entanglement between the polymer chains. Moreover, the porous morphology of the structure allows numerous applications in various fields. The challenge of synthesizing clay mineral-containing nanocomposite hydrogels in an effective way is still present. More attention is necessary to be paid for combining the strong aspects of layered clay minerals and those of the polymers where both can be modified and functionalized as function of the final materials desired to be manufactured.

Salecan is a polysaccharide that possesses a high number of hydroxyl groups on the main chain, allowing this way to be accordingly managed in SIPN architecture. Antioxidant and nontoxic character as well as biocompatibility and biodegradability make it highly suitable for drug delivery purposes. Poly(methacrylic acid) (PMAA) is a synthetic polymer often investigated for being a desirable component of a SIPN. Methacrylic acid (MAA) is a water-soluble monomer that has the ability of polymerizing via *free radical polymerization* under convenient condition. PMAA is a synthetic polyelectrolyte capable of donating or accepting protons upon pH changes, accompanying reversible conformational alterations between the collapse and extension state [3]. Nontoxicity and outstanding mechanical strength sustain its usage in pharmaceutical industry.

Regarding Salecan/PMMA semi-IPN, the study conducted by Qi et al. [3] showed, besides a successful incorporation of the components in a semi-IPN architecture, several features: (1) Salecan addition leads to a better thermal stability of the network; (2) an increment in the Salecan dose resulted in an increase in the average pore size, resulting in an enhanced hydrophilicity of the construction; at the same time, an increase in the cross-linker agent leads to a decrease in pore size as a consequence of a higher density of the network; (3) Salecan facilitates the penetration of water molecules into the network, thus higher equilibrium swelling ratio is obtained while the cross-linker has a completely opposite effect; (4) the pH effect of swelling is assigned to the protonation and ionization balance of the carboxyl acid groups appearing in the hydrogel chains, whose pKa value was approximately 5.5; and (5) at lower pH, the acid groups in the hydrogel cannot be easily ionized.

The hydrogen bonds between the hydroxyl groups in Salecan and the protonated acid groups in PMAA restrained the swelling of the hydrogel. When the pH is increased, the carboxyl groups of PMAA chains dissociated, undermining the H-bonds between the Salecan and PMAA chains.

On the other hand, clay nanocomposites have also attracted attention worldwide. The contact between the polymer and clay leads to better thermal and mechanical stability, durability or reduced permeability to small molecules and solvent uptake [4], thus being effectively used to modify drug delivery systems. As a hydrogel network component, clays have proven to act as a trap for the drug that would be released, preventing uncontrolled diffusion of the drug from the gel network and offering a better control of the release. In absence of clay, the drug-loaded hydrogels suffer a burst type of delivery [5]. Over the years, numerous studies demonstrated the outstanding properties of the clay-polymeric materials [6–8]. For instance, Pinnavaia et al. reported increased tensile strength, modulus and heat distortion temperature of polymer-clay nanocomposites compared to the simple polymer [6]. Park et al. showed great enhancement in the release rate of the drug for the inorganic–organic hybrid successfully realized by intercalating donepezil molecules into smectite clays [9]. The improvement achieved with the clay inclusion is better defined when the silicate lamellas tend to an intercalated to exfoliated structure.

All the aforementioned features and described techniques lead to the conclusion that on one hand, we have the semi-IPNs, in particular, Salecan/PMMA with outstanding potential for being designed as drug delivery systems, and on the other hand, there are clay-polymeric nanocomposites intended for various medical applications. Therefore, we considered the advantages of both systems and decided to develop a novel synergic system suitable for oral delivery of drugs, by combining the hydrophilic networks composed of poly(methacrylic acid) and Salecan with clay mineral nanoparticles. The designed polymer nanocomposite carriers would be able to provide cancer treatment by direct delivery of the medicine to the colon. More than that, we aimed to investigate the effect of the initial clay composition upon the final properties of Salecan/PMMA semi-IPN. In most of the cases, the developing of clay/polymer nanocomposites with sodium montmorillonite (ClNa) was envisaged.

Interesting investigations, in our opinion, would be regarding the structures obtained with ClNa but with hydrophobic montmorillonites as well. As the clays are basically hydrophilic compounds, the only way to turn them into a structure compatible with hydrophobic network is to functionalize them using ammonium salts [10] or by sol–gel process with various long alkyl chain silanes [11, 12]. The synthesis of various *in house* advanced modified Cloisites were previously reported starting from commercial clay by edge covalent bonding at the clay edges [13]. By measuring the static contact angle values for water, the modified clay minerals proved to have an enhanced hydrophobic behavior [12, 14]. But for this study, we have chosen the commercially available Cloisite Na and organomodified montmorillonite with different ammonium salts: (methyl, tallow, bis-2-hidroxyethyl)-Cloisite 30B, (dimethyl, dehydrogenated tallow)-Cloisite 20A and (dimethyl, dehydrogenated tallow)-Cloisite 15A.

These hydrophilic-hydrophobic complex systems are foreseen to find application in controlled drug release where *co*-delivery of polar-unpolar substances at the target site is mandatory.

2. Experimental

2.1. Materials

Commercial clays ClNa, Cl30B, Cl20A and Cl15A were kindly offered by Southern Clay Products Inc. PMAA (polymethacrylic acid, Janssen Chimica), Salecan (Souzhou Chemicals), N, N′-methylenebisacrylamide (Sigma Aldrich) and ammonium persulfate (Sigma Aldrich) were used as received.

2.2. Synthesis of PMAA/Salecan/clay nanocomposites

In order to obtain the proposed systems, two main types of hydrogels were manufactured: PMAA/clay hydrogel nanocomposites and PMAA/Salecan/clay hydrogels. The method used was adapted from the one found in the literature [3], as follows: primarily, a 0.2 g clay (ClNa, Cl30B, Cl20A and 15A) was dispersed in 14 ml of deionized water under magnetical stirring (around 800 rpm) and room temperature for 15 min. Thus, the clay dispersion was obtained and ultrasonicated for 5 min. When the hydrogels with Salecan were prepared, 0.16 g of Salecan powder was added, and the system was kept under mechanical stirring for another 15 min followed by 1 min ultrasonication.

For the PMAA/clay nanocomposites, this step was omitted. As the mass became homogenous and cooled, 2 ml MAA and 2 ml BIS (1%, w/v) were added under continuous stirring for 10 min followed by 10 min ultrasonication in an ice bath. Two milliliter APS (1.2%, w/v) was added, keeping the mass under magnetical stirring for another 5 min. The system was injected for polymerization into our own-designed glass mold. The mold was introduced into a thermostated water bath at 70°C (the desired temperature for the polymerization to occur) for 6 h.

The obtained hydrogels were cut into pieces and immersed into deionized water for 7 days. The water was changed two times a day in order to assure that the residual monomers were removed. As for analyses, the fabricated hydrogel nanocomposites were cut with an eyelet punch. One part of the cuts was deposed on polyethylene foils for water evaporation at ambient temperature for several days and the other part was freeze dried.

3. Characterization

3.1. Fourier transform infrared spectroscopy

The FTIR spectra were obtained by a Fourier transform infrared spectrophotometer BRUKER Tensor on ATR mode in the range of the scanning wave numbers 4000–400 cm^{-1} with a 40 scans per sample cycle and a resolution of 4 cm^{-1}. Milled samples were used for FTIR analyses.

3.2. X-ray diffraction

Powder X-ray diffraction was used for phase identification of the crystalline material and to determine the lattice parameters of the crystal structure. A multifunctional system powder X-ray diffractometer, Rigaku Ultima IV (Tokyo, Japan), was used to perform the measurements. The equipment conditions were as follows: X-ray generator was operated at 40 kV voltage and 30 mA current, using Cu target (CuKα radiation, $\lambda = 1.5406$ Å); the goniometer was set in parallel beam geometry system, with cross beam optics (CBO), θ-θ scanning mode and with a step width of 0.02°; a scintillation counter was used. For low angle measurements, the optics used were DS and SS (divergence and scattering slits) = 1°, RS (receiving slit) = 0.2° and receiving side Soller slit 0.5°, collecting data between $0.6 < 2\theta < 6°$ measuring range, with a scanning speed of 1°/min. For wide angle measurements, the optics used were DS (divergence slit) = 1°, SS and RS (scattering and receiving slits) = open and receiving side Soller slit 0.5°, collecting data between $3 < 2\theta < 50°$ measuring range, with a scanning speed of 2°/min. The measurements were performed in the continuous mode, at room temperature and atmospheric pressure.

3.3. Thermal gravimetric analysis

Thermogravimetric (TGA) measurements were performed with a TGA Q5000 instrument. The samples were heated, in nitrogen atmosphere 10 ml/min with a rate of 10°C/min.

The isotherms of equilibrium swollen hydrogel disks were carried at 37°C for 10 mL/min in nitrogen atmosphere. All experiments were realized in triplicate.

3.4. Swelling behavior measurements

Swelling studies of semi-IPNs were conducted by immersing the dried samples in deionized water at 37± 1°C. The samples were removed from the thermostatic bath at regular intervals of time, their surface was dried with filter paper and then weighed; afterward, they were immersed into the same recipient.

The swelling degree (*SD*) was calculated using Eq. (1):

$$SD = (Wh - Wi)/Wi \tag{1}$$

where *Wh* is the weight of swelled hydrogel at a certain time and *Wi* is the weight of initial dried hydrogel. All experiments were performed in triplicate.

3.5. Electron microscopy analyses: SEM and TEM

ESEM-FEI Quanta 200 (Eindhoven, Netherlands) instrument was used to record SEM images in low vacuum mode with GSED detector. Micrographs were taken in vacuum conditions, operating pressure of 2 torr, 25–30 KV accelerating voltage.

The morphologies of PMAA nanocomposites were obtained by transmission electron microscopy using TEM, Tecnai™ G2 F20 TWIN Cryo-TEM, FEI Company™, at 200 kV acceleration voltages. Powdered samples were deposited on carbon film grids.

3.6. Mechanical properties

Dynamic mechanical analysis (DMA) was performed using the DMA-Q 800 device (TA Instruments New Castle, DE, USA). Freeze-dried hydrogels were analyzed in "Temperature Ramp" mode and swollen hydrogels in DMA Multi-Frequency-Strain "Frequency sweep-isothermal." Dual cantilever-powder clamp was used for freeze-dried hydrogels and compression clamp was used for hydrogels. Hydrogels disk were cut with an eyelet (part of DMA-Q 800 Dynamic Analyzer compression set) before analyses, the dimensions of the analyzed specimens being about 12.5 mm diameter. Rectangles of 60 mm × 12.77 × 2–3 mm were used for lyophilized hydrogels. These were then measured with a caliper in order to enter the initial values. "Isothermal" mode was carried out at 30°C with 4 μm oscillation amplitude for 120 min from 0.1 to 10 Hz at 11 frequencies (frequency sweep segment repeat for 10 times). A 14.5 mm compression plate was used for all samples. A 0.01 N compressive static force was applied to the specimen to ensure that the upper compression plate did not lose contact with the sample. The measurements were repeated for three times.

For the "Temperature ramp" mode, the temperature ranged from 275 to 300°C/min, oscillation amplitude of 20 μm, 1 Hz frequency and 0.5 sampling.

DMA-Q 800 used Universal Analysis 2000 for calculating dynamic mechanical properties and exports the data for plotting the investigated properties as a function of time, temperature and frequencies.

4. Results and discussion

4.1. Fourier transform infrared spectroscopy

The presence of montmorillonite in the polymer matrix was checked by FTIR analysis (see **Figure 1**, only PMAA-ClNa and Cl15A data are presented here). FTIR spectra of Cloisites show the presence of clay characteristic peaks, confirmed also by the literature data [12, 15]. For all four types of montmorillonites, around 3633 cm^{-1} we noticed the OH stretching of latex water. The peak from 1011 cm^{-1} with a shoulder at 921 cm^{-1} was attributed to Si–O stretching vibration while the Si–O bending vibration was identified in the 400–600 cm^{-1} area, more exactly 518 cm^{-1} and 454 cm^{-1}. The difference between the ClNa and the modified clays (Cl30B, Cl15A and Cl20A) is given by the presence of additional peaks at 2926 cm^{-1} and 2852 cm^{-1}, specific for quaternary ammonium salts. As for the pure PMAA, its spectra reveal the characteristic peaks around 3000 cm^{-1} corresponding to the O–H stretching vibration and at 1737 cm^{-1} associated to CO group stretching vibration. At the wavelength of 2960–2875 cm^{-1}, the peaks for stretching vibration of methyl and methylene groups were found [16]. The absence of vinyl group stretching vibration at 1628–1692 cm^{-1} indicates that the polymerization occurred [15].

Referring to the spectra of Salecan, a broad peak was identified at 3329 cm^{-1}, being characteristic for O–H stretching vibration, as well as the intermolecular hydrogen bonding of the polysaccharide [17]. Peaks from the 800–1100 cm^{-1} area are assigned to polysaccharide structure and include C–OH stretching in the glucopyranose rings. More specifically, the band at

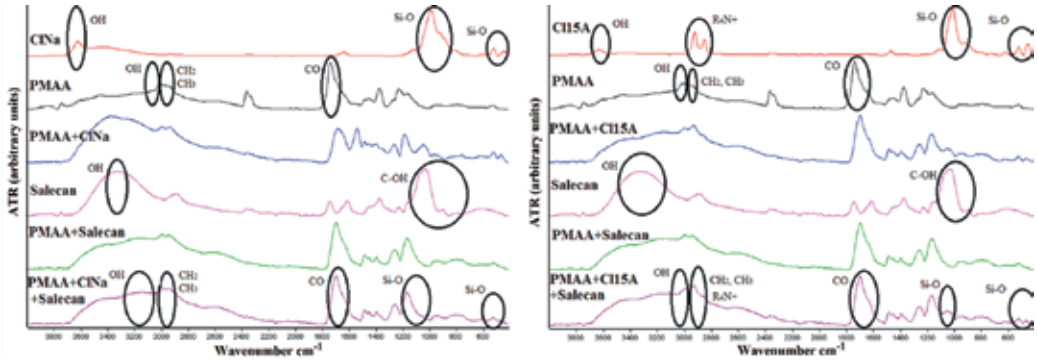

Figure 1. FT-IR spectra of the pristine clay/PMAA/PMAA-Cloisite/Salecan/PMAA-Salecan/PMAA-Salecan-Cloisite exemplified for ClNa and Cl15A.

1039 cm^{-1} was related to C–OH stretching in the glucopyranose ring, a broad, weak peak at 896 cm^{-1} suggested that D-glucopyranose had a β-configuration whereas the almost unidentifiable peak at 818 cm^{-1} confirmed the presence of small amounts of α-glucopyranose form.

Analyzing the spectra of the nanocomposites that have the modified montmorillonite as a component, alterations were noticed but also the preservation of some characteristic peaks. For instance, specific clay bands were observed. The Si–O–Si stretching vibration shifted from 1011 to 1050 cm^{-1} and the peaks from 400 to 600 cm^{-1} suffered a bathochromic shift. In the hydrogels, we found the Si–O bending and stretching vibration at 463 and 622 cm^{-1}, respectively.

For the composites prepared using modified montmorillonites, the bands at 2856 and 2925 cm^{-1} state that the quaternary ammonium salts are present in the network. At the same time, PMAA peaks were identified. Thus, we have C=O group stretching vibration, moved from 1737 to 1697 cm^{-1}(much lower intensity for 20A and 30B Cloisites), and the stretching vibration for methyl and methylene groups that slightly shifted to 2996–2925 cm^{-1} [18].

In a comparative analysis of PMAA and PMAA-Salecan bands, we noticed a change in the 2942 cm^{-1} peak. In the hydrogel structure, the peak broadens and suffers a decrease in sharpness, which can be explained by the formation of the intercalated structure between the polymer and the polysaccharide.

The fact that within the final structure, we find the skeleton of the compounds, we started with, serves as proof that the synthesis of semi-IPN hydrogels went successfully. The slight changes in wavelength and intensity could be explained by the interactions between the components of the hydrogels with the obtaining of a complex compact structure.

4.2. X-ray diffraction

XRD analysis was carried out in order to investigate the type of morphology of the clays, we study as well as the structure of final composites materials. According to the recorded data (**Figure 2**, I–IV), a broad peak centered at 2θ = 20° was observed in the XRD patterns of

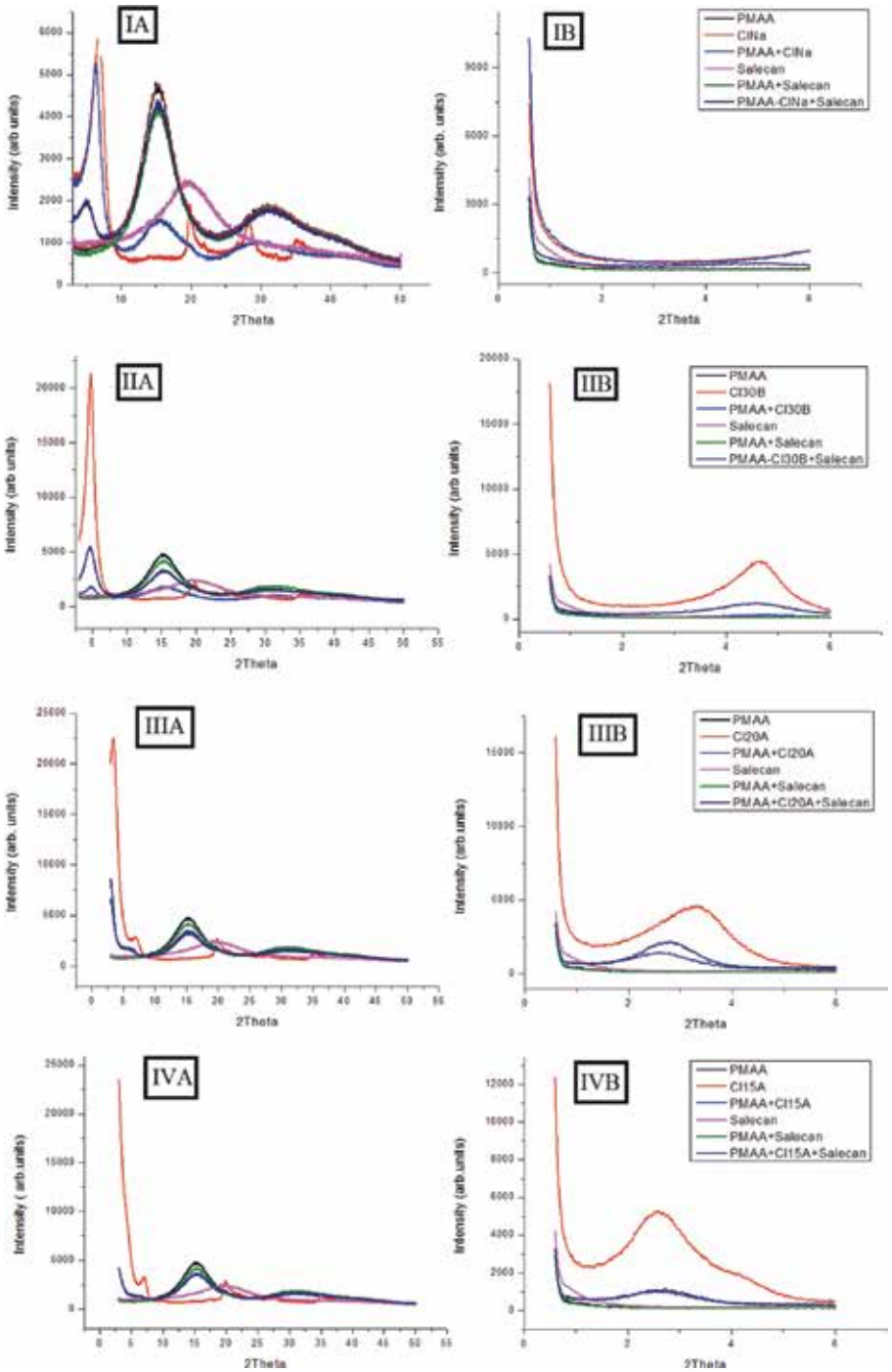

Figure 2. I. XRD results. I PMAA/ClNa/PMAA-ClNa/Salecan/PMAA-Salecan/PMAA-Salecan-ClNa; **II.** PMAA/Cl30B/PMAA-Cl30B/Salecan/ PMAA-Salecan/ PMAA-Salecan-Cl30B; **III.** PMAA/Cl20A/PMAA-Cl20A/Salecan/PMAA-Salecan/PMAA-Salecan-Cl20A; **IV.** PMAA/Cl15A/PMAA-Cl15A/Salecan/PMAA-Salecan/PMAA-Salecan-Cl15A; **A**: Wide angle; **B:** Low angle.

Salecan. These results along with the literature data [3] prove that the Salecan had an amorphous structure. From the spectrum of pure PMAA hydrogel, it could be seen that the PMAA showed prominent diffraction peak posited around 2θ = 15°, suggesting the high crystallinity. The peak form and angle value are later noticed in the composites containing PMAA, with a slight loose in intensity due to the presence of Salecan and/or unmodified/modified clay.

XRD data of ClNa show the characteristic peak at 2θ = 7.3°. This peak is preserved in PMAA-ClNa spectra with a slight displacement at a lower angle (2θ = 6.7°). In the case of PMAA-ClNa-Salecan, the peak registered a decrease in intensity and was shifted to 2θ = 5°. The narrow, intense peak of ClNa present in PMAA-ClNa structure stands for a microcomposite, tactoid structure, while the decrease in intensity and broadening of the same peak in the PMAA-Salecan-ClNa hydrogels proves a highly intercalated network. The XRD pattern of Cloisite 30B reveals the main diffraction peak at 2θ = 4.9°. The same angle value of this peak is noticed in the PMAA-Cl30B composite as well as in the spectra of the final PMAA-Cl30B-Salecan hydrogel. A decrease in diffraction intensity and sharpness of the Cloisite peak in the composites leads to the conclusion that the montmorillonite tends to spread into an intercalated structure.

As for Cl20A and Cl15A, the characteristic diffraction peaks were identified at 2θ = 3.5° and 2θ = 2.3°, respectively. This was in conformity with the literature data [19] and stands for well-defined crystalline nature of Cloisites. The Cloisites have a tendency of spreading leading to slight intercalated layered structures of the PMAA-Cloisites and PMAA-Cloisites-Salecan, more obviously for the Cl15A.

The conclusion was deducted from the examination of Cloisite peaks that suffered an enlargement and decrease in intensity. From the all abovementioned Cloisites, Cloisite Na and Cloisite 30B seemed to have the highest degree of intercalation, whereas Cloisite 20A and Cloisite 15A formed only microcomposites (tactoid structure). What is interesting to notice is that in case of ClNa, the tactoid structure was perfectly preserved when PMAA-ClNa composites were synthesized but spread and turned into an intercalated-exfoliated structure once Salecan was added. As for other Cloisites, we do not have the same observation, for all of them, a little more intercalated morphology is noticed rather for PMAA-Cloisite composites than for final PMAA-Salecan-Cloisite hydrogel.

4.3. Thermal-gravimetric analysis

The thermal stability of the synthesized PMAA/Salecan hydrogel and hydrogel nanocomposites (PMAA/Salecan/clay) were examined by TGA analyses. Three steps of weight loss were registered (see **Figure 3**) with two maximum decomposition temperatures. The first weight loss is a result of water volatilization and the degradation of organic compounds [20].

The second and third steps are assigned to PMAA decomposition as well as the degradation of the main skeleton of Salecan. At this point, the polymer backbone is destroyed. Regarding the samples of nanocomposites obtained in the presence of simple/modified montmorillonite, some changes of the thermal stability of final materials were registered. These modifications were due to the presence of quaternary ammonium salts [4], more evident in the case of Cl15A and 20A. It is worth to mention that when Salecan was added, semi-interpenetrated networks were obtained, and the systems behave as homogenous architectures. Thus, the

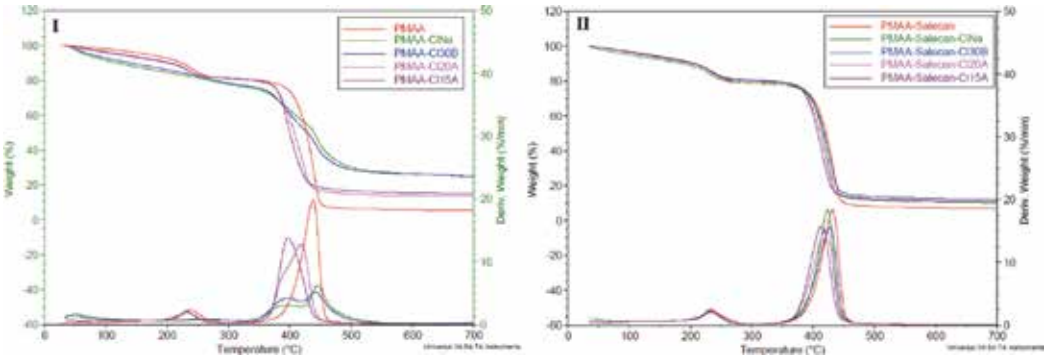

Figure 3. I. TGA results on samples without Salecan; **II.** TGA results on samples with Salecan.

energy consumed for nanocomposites thermal destruction is within the same range regardless of Cloisite type. The growing residue is related to the presence of inorganic filler and proves the inclusion of clay into hydrogels.

4.4. Swelling/deswelling behavior measurements

The data resulted from the swelling studies are shown in **Figure 4**. The swelling kinetics demonstrated that in all the cases, the capability to absorb water is much higher for nanocomposites than for PMAA/Salecan hydrogels. In the case of nanocomposite hydrogel based on ClNa, the swelling degree is about eight times higher than for pure hydrogel. Also, as can be noticed, the swelling degree (SD) decreases as we move from the hydrophilic ClNa to the most hydrophobic modified montmorillonite, Cl15A. Increasing the hydrophobicity of the clay, we designed a highly cross-linked hydrogel with intercalated/exfoliated silica lamellae, which lowers the freedom of polymeric chains and blocks the inflow of water to the network. This aspect should also be taken into consideration as the capability of hydrogels to absorb water is decisive for the drug loading and release as well as for the applications where superabsorbency is necessary.

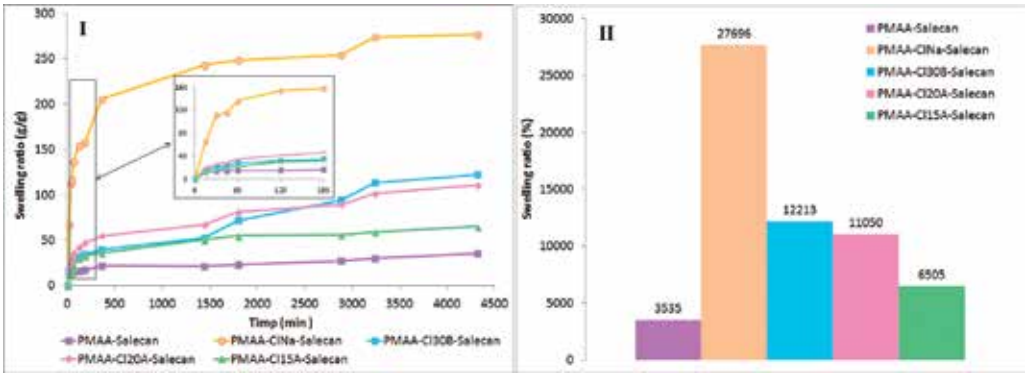

Figure 4. I. Time-dependent swelling profiles of the hydrogels; **II.** Representation of final degree ratio as a function of the clay type.

TGA/DTG analyses provide information about deswelling behavior of the equilibrium swollen hydrogel samples. **Table 1** summarizes the characteristic values calculated from isotherm and derivative curves of the obtained samples. Derivative curves (see **Figure 5**) discover a slower weight change over time (50–80 min interval) in the following order: PMAA-Salecan, PMAA-Salecan-Cl20A, PMAA-Salecan-Cl15A and PMAA-Salecan-Cl30B/PMAA-Salecan-ClNa. The samples with clay exhibit higher dehydration rate and released

Sample	Isotherm curves, 37°C		Derivative curves	
	Time (min)	Weight (%)	$t_{1/2}$ (min)	t_{end} (min)
PMAA-Salecan	74.92	91.43	72.27	79.22
PMAA-Salecan-Cl Na	134.81	98.83	134.10	138.82
PMAA-Salecan-Cl 30B	103.14	96.20	101.96	106.68
PMAA-Salecan-Cl 20A	93.69	97.53	92.03	96.05
PMAA-Salecan-Cl 15A	99.83	95.47	97.70	104.09

Table 1. TGA/DTG data for PMAA-Salecan and PMAA-Salecan-clay nanocomposites, respectively.

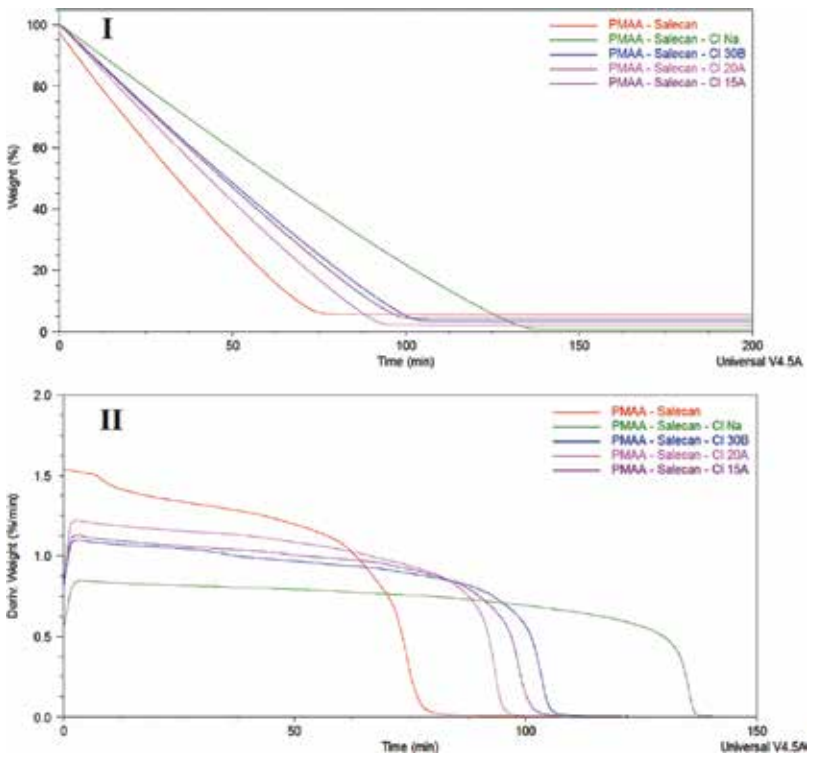

Figure 5. I. Weight loss as a function of time measured at constant temperature (37°C) of the equilibrium swollen hydrogel samples; **II**. Weight derivative as function of time for the equilibrium swollen hydrogel samples; PMAA-Salecan; PMAA-Salecan–ClNa; PMAA-Salecan–Cl30B; PMAA-Salecan–Cl20A; and PMAA-Salecan–Cl15A.

more water compared to the pure hydrogel are as follows: 91.43% water released versus 98.83% (ClNa sample), 96.2% (Cl30B sample), 97.53% (Cl20A sample) and 95.47% (Cl15A) at constant weight. We can notice that the samples with clay lost more water than PMAA-Salecan hydrogel, and PMAA-Salecan-ClNa lost the highest amount of water. This result is well correlated with swelling studies where the PMAA-Salecan-ClNa sample absorbed the largest amount of water. It was previously proved that clay affects the swelling by cross-linking the polymer chains which restricts the mobility of the hydrogel chains [21]. This is a possible explanation for nanocomposite hydrogels which release water later than pure hydrogel. It is worth noting that the time for swelling of the hydrogels is much longer than for deswelling at the same temperature. The collapse time is shifted toward higher values for samples with clay, especially for PMAA-Salecan-ClNa (138.82 min) versus PMAA-Salecan (79.22 min). The conclusion is that the presence of clay layers acts as a barrier in hydrogel networks restricting the release of water over time. This behavior is beneficial for hydrogels where controlled drug release is crucial.

4.5. Scanning electron microscopy and transmission electron microscopy

For the SEM analysis, the synthesized hydrogel cuts were freeze dried. The necessity of performing SEM on lyophilized hydrogels comes from the idea of having the microstructure and morphology of the samples well-retained.

When the samples (see **Figure 6**) were prepared without Salecan, the microstructure of the PMAA/clay hydrogels consists of nonhomogenous areas. A more detailed analysis shows some differences between the nanocomposites, as a function of clay type. When the unmodified montmorillonite (ClNa) is used, the network is clear and more uniform. This confirms the compatibility of the hydrophilic character of clay with the similar nature of the polymer. As for the modified montmorillonite, the more hydrophobic it became, the worse the compatibility with the polymer. Therefore, it can be noticed in case of Cl30B, Cl20A and Cl15A agglomerates of clay layers [22, 23] within the polymeric structure.

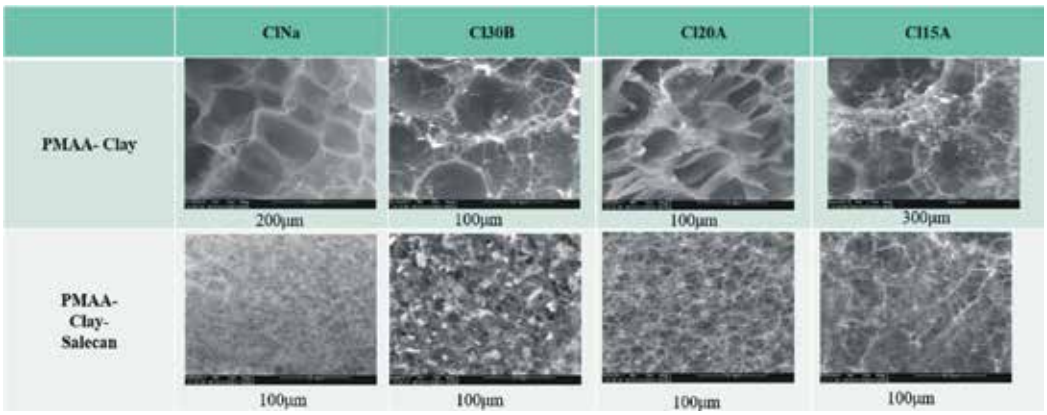

Figure 6. SEM morphology of the PMAA-clay and PMAA-Salecan-clay nanocomposites, respectively. Comparative images obtained for samples with different types of clay.

When analyzing the SIPN prepared with Cloisite and Salecan, the microstructure of the examined surfaces consists of dimensionally equivalent voids separated by thin walls. All hydrogels demonstrated homogeneous and porous architectures with the pore size significantly smaller and the pore number became greater [24]. These observations are supported by swelling studies. Thus, when the pore size and number increased, the specific surface became greater resulting in a higher swelling capacity. Differences can be seen between the samples, as another type of Cloisite is used. The morphology of the sample with unmodified clay (ClNa) is a clear and uniform network (similar to the one analyzed before the sample without Salecan). The morphology changes as the hydrophobic (modified) Cloisites participate in the process of developing the nanocomposites. The main change consists of unorganized, crystalline-luminous aggregates of clay, visible on the surface of the samples. From the analysis of the surface, ClNa seems to have a more intercalated or even exfoliated construction, the presumption being confirmed also by XRD analysis.

TEM analyses (see **Figure 7**) prove the existence of intercalated/exfoliated silica lamella within the hydrogel matrix, which was previously presumed by analyzing the XRD results. The internal intercalated structure of the nanocomposites, with the presence of areas with exfoliated clay nanosheets sustains as well the conclusions from the swelling-deswelling studies that showed superior properties for the PMAA-Salecan-ClNa sample.

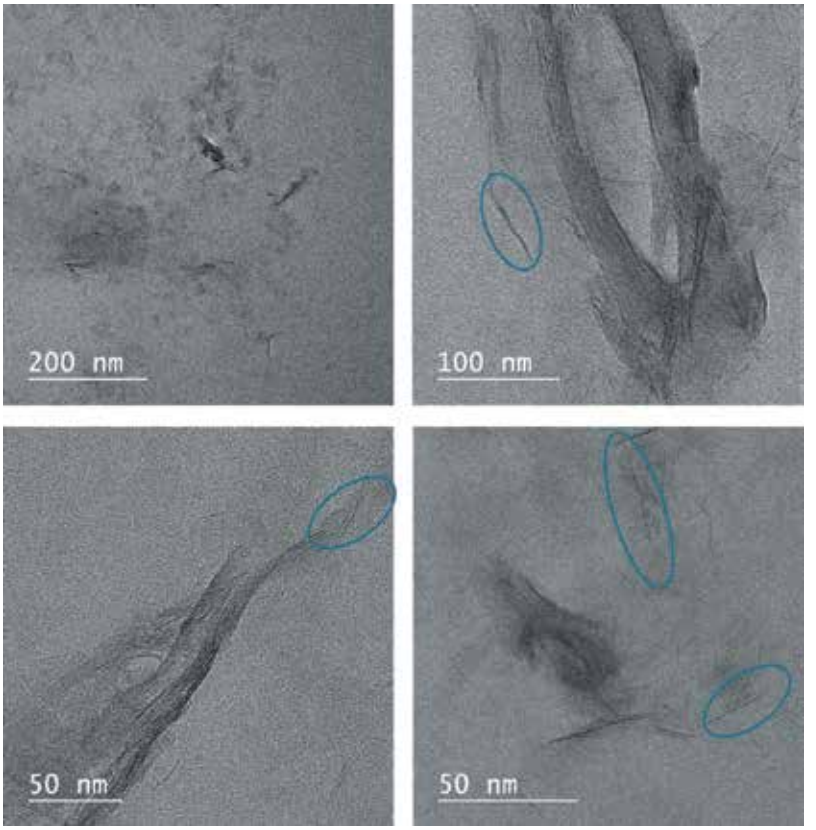

Figure 7. TEM micrographs for PMAA-Salecan-ClNa samples. Exfoliated lamella highlighted with blue circle.

4.6. Thermomechanical properties

In order to appreciate the influence of clay addition, moreover, the effect of clay type upon the mechanical properties of the nanocomposites, dynamic mechanical analyses were performed and are presented in **Figures 8** and **9**. As known from the literature, the storage modulus (G′) is considered a way of appreciation of the extent of gel network formation. Thus, a higher G′ value means a stronger gel structure.

In absence of Salecan, a simple conclusion can be conceived from the data registered (**Figure 8**). In matter of storage modulus, the inclusion of the inorganic filler leads to stronger microstructure of the hydrogels as function of frequency and time, respectively. The presence of montmorillonite increases the intermolecular forces, and the hydrogel nanocomposite behaves as an elastic solid with an enhanced capacity of storing energy and not breaking under the stress applied. For example, the hydrogels obtained in the presence of Cl20A and Cl15A exhibit higher storage modulus than the neat hydrogel. It is worth mentioning that due to unexpected swelling and disintegration phenomenon that occurred in the washing stage, the samples obtained with ClNa and Cl30B could not be analyzed. Moreover, the stiffness increased with the addition of Cl20A and Cl15A clays proving once again the enhanced mechanical stability of nanocomposite hydrogels induced by the hydrophobic modified silicate nanosheets [25]. The same behavior was observed in our recent study that refers to the obtaining of newly advanced nanocomposite hydrogels based on poly(methacrylic acid) with

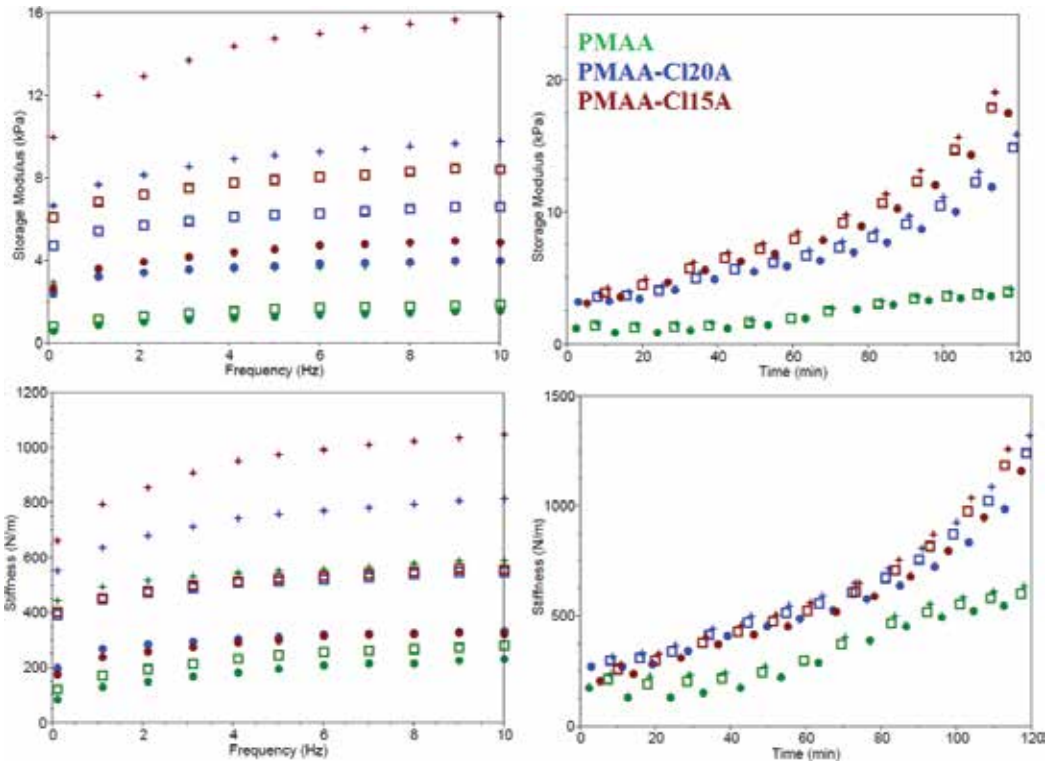

Figure 8. DMA results: storage modulus as a function of frequency and time; stiffness as a function of frequency and time; for: PMAA; PMAA-Cl20A; PMAA-Cl15A.

in house advanced, modified clays by edge covalent bonding [13]. Differences in storage modulus values along frequency-time cycles can be observed due to the hydrogels dehydration.

More challenging to analyze were the results obtained from the samples with Salecan (**Figure 9**). Generally, higher values of storage modulus are noted with the increase in hydrophobicity of the clay used. Thus, even if the storage modulus was lower than for the samples obtained with modified clay, the SIPN containing Cloisite Na were proved to be more stable with frequency and time, in comparison with those obtained with hydrophobic montmorillonites, as observed from the

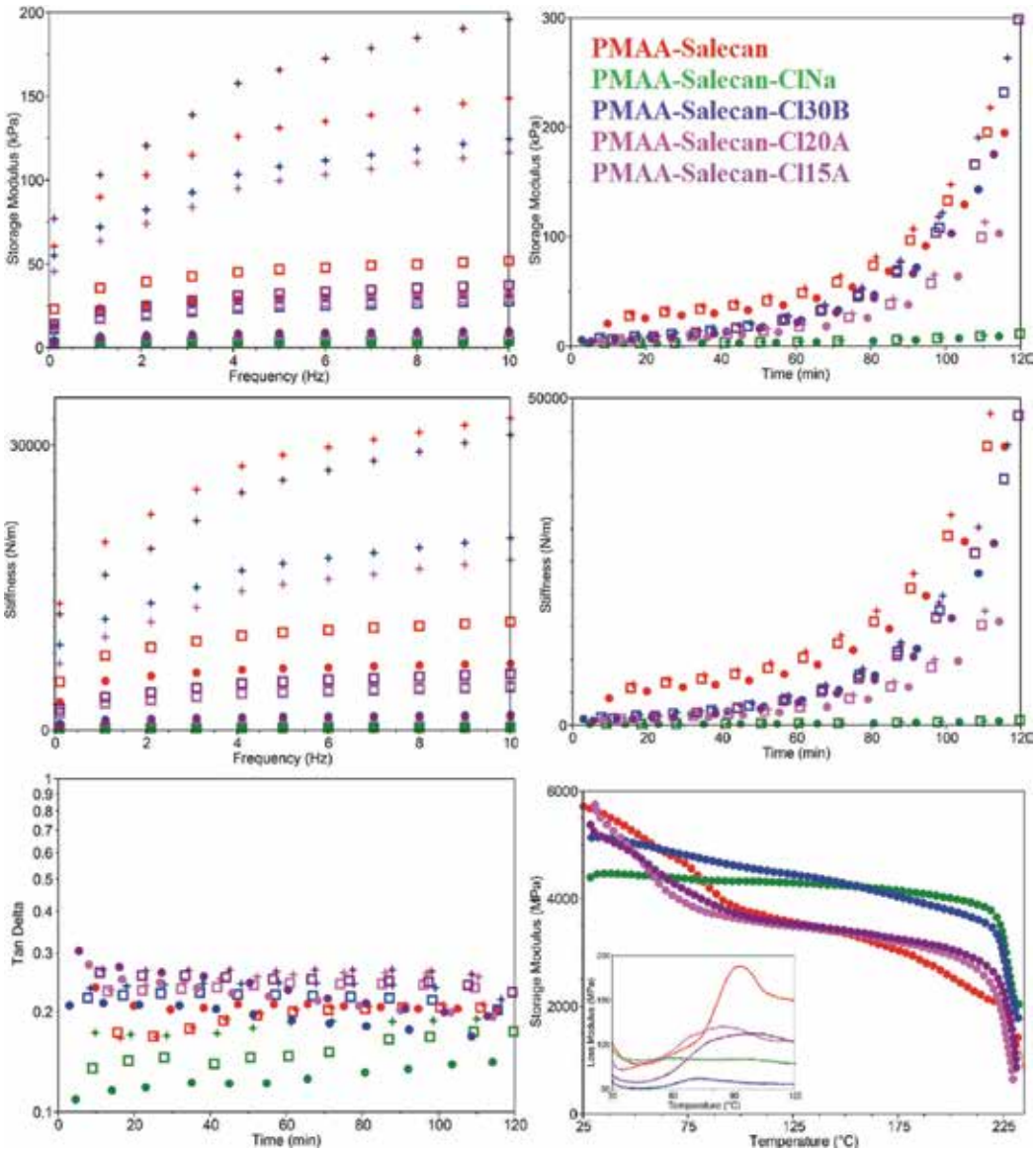

Figure 9. DMA results: storage modulus as a function of frequency and time; stiffness as a function of frequency and time; Tan Delta as a function of time; storage modulus as a function of temperature for: PMAA-Salecan; PMAA-Salecan-ClNa; PMAA-Salecan-Cl30B; PMAA-Salecan-Cl20A; and PMAA-Salecan-Cl15A.

flatness of the specific ClNa curve. These data were in good agreement with swelling-deswelling results where the SIPN with ClNa proved the highest swelling degree and the slowest water release capacity. As a consequence, given the fact that the samples "lose" water when mechanically stressed, the smallest storage modulus values are registered for hydrophilic Cloisites. This phenomenon can also be explained by the presence of a smaller number of silicate sheet in the same volume of the semi-interpenetrated network (the same size of the samples subjected to DMA analysis) as a consequence of the swelling process during washing, which is although an insufficient contribution of silicate lamellae in order to assure an enhanced mechanical behavior.

The DMA analyses obtained for SIPN with Salecan showed increased values for storage modulus and stiffness in comparison with hydrogel nanocomposites. This fact is due to the elastic properties of the Salecan [3, 26, 27] and its –OH groups' interactions with oxygen atoms of the PMAA and the amine protons of the clay as well as between the clay surface hydroxyls and the carbonyl of the polymer. These data are well correlated with FTIR results, peak shifts, respectively, that proved the obtaining of a unique complex structure. Previous studies demonstrated that clay nanoparticles behave as a support for polymer chains which absorb/desorb onto clay sheet by thus inducing a continuous movement in the system [28]. In our case, when applying frequency or time, the whole system reacts trying to withstand, consequently, increased mechanical stability is registered even if the storage modulus was lower than for the samples obtained with modified clay.

For all the hydrogels, tanδ subunitary values indicated that the storage modulus exceeded the loss modulus independent of time, which confirms the elastic solid behavior of the nanocomposites and the dissipation of energy within the whole structure [20].

When temperature increased, the freeze-dried samples evidenced storage modulus changes around 75 and 230°C. These changes are attributed to the movement of methacrylic acid units and are related with the polymer molecular weight. The loss modulus (inset **Figure 9**) registered for SIPN-functionalized clay samples, indicated transition around 70°C due to the melting of quaternary ammonium salts, more obvious in Cl20A and Cl15A cases. The glass transition temperature (around 230°C) does not significantly change when clays were added in the system unlike other cases where the mobility of hydrogel networks was affected, indicating a reinforcing effect of the modified clay [13].

5. Conclusion

Inspired by the recent studies regarding Polymer/Salecan networks and taking into consideration the numerous researches that highlight the outstanding mechanical properties of the clays, we decided to bring an improvement and study the possibility to synthesize PMAA-Salecan hydrogel nanocomposites based on pristine and modified montmorillonite. Further, the effect of the clay type on the final properties of PMAA/Salecan/clay nanocomposites was followed. With the other parameters kept constant, the morphological and compositional analysis performed gave us the possibility of explaining the physicochemical and thermal features of the fabricated materials as function of Cloisite composition.

The designed structures were investigated with the FT-IR technique, which revealed the presence of the specific partner peaks. X-Ray data, supported by TEM images pointed out a

more intercalated structure for the ClNa, which was confirmed by the swelling-deswelling analyses. The presence of exfoliated sheets within the SIPN network prepared with pristine clay was noticed from TEM images. TGA definitely showed that the introduction of Salecan enhanced the thermal stability of the nanocomposites, but no significant distinction was noticed between the samples of different types of inorganic filler. Speaking of mechanical properties, Salecan had a significant impact on the energy dissipation within the semi-IPNs due to its outstanding viscosity properties. The effect of Cloisite and Salecan was expressed by the improved storage modulus and stiffness of the samples.

The more compatible nature of ClNa with the hydrophilic character of PMAA/Salecan hydrogel provided higher swelling capacity, thus slower release in time, which is highly favorable for the designing of a drug release mechanism. As a fact, the smooth architecture of the networks developed with sodium montmorillonite is another reason to believe that the unmodified ClNa would serve as most suitable inorganic filler for the development of an efficient drug release system.

But neither SIPNs obtained with more hydrophobic clays are not to fall and may be employed in controlled *co*-delivery of polar-unpolar drugs. The nontoxicity of the components used sustains the development of semi-IPN architectures with improved mechanical features and adjustable release properties for specific applications in the extensive biomedical domain.

Acknowledgements

This work was supported by a grant of the Romanian National Authority for Scientific Research and Innovation, CNCS/CCCDI-UEFISCDI, project number PN-III-P2-2.1-PED-2016-1896, within PNCDI III.

Conflicts of interest

The authors declare no conflict of interest.

Author details

Tatiana Munteanu[1], Claudia Mihaela Ninciuleanu[2], Ioana Catalina Gifu[2], Bogdan Trica[2], Elvira Alexandrescu[2], Augusta Raluca Gabor[2], Silviu Preda[3], Cristian Petcu[2], Cristina Lavinia Nistor[2], Sabina Georgiana Nitu[2] and Raluca Ianchis[2]*

*Address all correspondence to: ralumoc@yahoo.com

1 Faculty of Applied Chemistry and Materials Science, Politehnica University of Bucharest, Bucharest, Romania

2 National R-D Institute for Chemistry and Petrochemistry ICECHIM, Bucharest, Romania

3 Institute of Physical Chemistry "Ilie Murgulescu", Romanian Academy, Bucharest, Romania

References

[1] Mishra S, Kumar Mishra A. Polymeric hydrogels: A review of recent developments. In: Kalia, Susheel, editors. Polymeric Hydrogels as Smart Biomaterials. Springer Series on Polymer and Composite Materials; 2016. p. 1-17. DOI: 10.1007/978-3-319-25322-0_1

[2] Qi X et al. Development of novel hydrogels based on Salecan and poly(N-isopropylacrylamide-co-methacrylic acid) for controlled doxorubicin release. RSC Advances. 2016;**6**:69869-69881. DOI: 10.1039/C6RA10716H

[3] Qi X et al. Fabrication and characterization of a novel anticancer drug delivery system: Salecan/poly(methacrylic acid) semi-interpenetrating polymer network hydrogel. ACS Biomaterials Science & Engineering. 2015;**1**:1287-1299. DOI: 10.1021/acsbiomaterials.5b00346

[4] Ianchis R et al. Synthesis and properties of new epoxy-organolayered silicate nanocomposites. Applied Clay Science. 2015;**103**(Supplement C):28-33

[5] Nagahama K et al. Self-assembling polymer micelle/clay nanodisk/doxorubicin hybrid injectable gels for safe and efficient focal treatment of cancer. Biomacromolecules. 2015;**16**(3):880-889

[6] Pinnavaia TJ, Beall GW. Polymer-Clay Nanocomposites. Wiley; 2000. 370 p. ISBN: 978-0-471-63700-4

[7] Ianchis R et al. Polymer-clay nanocomposites obtained by solution polymerization of vinyl benzyl triammonium chloride in the presence of advanced functionalized clay. Nanomaterials. 2014;**126**:609-616. DOI: 10.3390/nano7120443

[8] Corobea MC et al. Silica nanowires obtained on clay mineral layers and their influence on mini-emulsion polymerisation. Applied Clay Science. 2014;**95**:232-242

[9] Park JK et al. Controlled release of donepezil intercalated in smectite clays. International Journal of Pharmaceutics. 2008;**359**(1):198-204

[10] Galimberti M et al. Clay delamination in hydrocarbon rubbers. 2007;**19**:2495-2499

[11] Sinha Ray S, Okamoto M. Polymer/layered silicate nanocomposites: A review from preparation to processing. Progress in Polymer Science. 2003;**28**:1539-1641. DOI: doi.org/10.1016/j.progpolymsci.2003.08.002

[12] Ianchis R et al. Implications of silylated montmorillonite on montmorillonite–polyacrylate nanocomposites. Applied Clay Science. 2011;**52**(1):96-103

[13] Donescu D, Ianchis R, Petcu C, Purcar V, Nistor CL, Radovici C, Somoghi R, Pop SF, Perichaud A. Study of the solvents influence on the layered silicates-cation polymer hybrids properties. Digest Journal of Nanomaterials and Biostructures. 2013;**8**(4):1751-1759

[14] Ianchis R, Corobea MC, Donescu D, Rosca ID, Cinteza LO, Nistor LC, Vasile E, Marin A, Preda S. Advanced functionalization of organoclay nanoparticles by silylation and their polystyrene nanocomposites obtained by miniemulsion polymerization. Journal of Nanoparticle Research. 2012;**14**:1233-1244. DOI: 10.1007/s11051-012-1233-6

[15] Ianchis R, Donescu D, Petcu C. Influence of layered silicate on microemulsion polymerization kinetics of butylacrylate with alkoxylane. Materiale Plastice. 2008;**45**(3):265-268

[16] Bajpai SK, Chand N, Mahendra M. In situ formation of silver nanoparticles in poly (methacrylic acid) hydrogel for antibacterial applications. Polymer Engineering & Science. 2013;**53**(8):1751-1759

[17] Qi X et al. Investigation of Salecan/poly(vinyl alcohol) hydrogels prepared by freeze/thaw method. Carbohydrate Polymers. 2015;**118**(Supplement C):60-69

[18] Pretsch E, Bühlmann P, Badertscher M. Structure Determination of Organic Compounds: Tables of Spectral Data. th4 ed. Berlin Heidelberg: Springer-Verlag; 2009. pp. 433-447

[19] Russo P et al. Structure and physical properties of high amorphous polyvinyl alcohol/clay composites. AIP Conference Proceedings. 2015;**1695**:020035. DOI: doi.org/10.1063/1.4937313

[20] Wei W et al. A novel thermo-responsive hydrogel based on salecan and poly(N-isopropylacrylamide): Synthesis and characterization. Colloids and Surfaces. B, Biointerfaces. 2015;**125**:1-11

[21] Zheng S et al. Fast deswelling and highly extensible poly(N-isopropylacrylamide)-hectorite clay nanocomposite cryogels prepared by freezing polymerization. Polymer. 2013;**54**(7):1846-1852

[22] Ianchis R et al. Surfactant-free emulsion polymerization of styrene in the presence of silylated montmorillonite. Applied Clay Science. 2009;**45**(3):164-170

[23] Manfredi L et al. Influence of clay modification on the properties of resol nanocomposites. Macromolecular Materials and Engineering. 2008;**293**:878-886. DOI: 10.1002/mame.200800158

[24] Fathy F. Preparation of carboxymethyl cellulose-g-poly(acrylic acid-2-acrylamido-2-methylpropane sulfonic acid)/attapulgite superabsorbent composite. American Journal of Polymer Science and Technology. 2016;**2**:11-19. DOI: 10.11648/j.ajpst.20160201.12

[25] Han L et al. Mussel-inspired adhesive and tough hydrogel based on nanoclay confined dopamine polymerization. ACS Nano. 2017;**11**(3):2561-2574

[26] Hu X et al. Synthesis and characterization of a novel semi-IPN hydrogel based on Salecan and poly(N,N-dimethylacrylamide-co-2-hydroxyethyl methacrylate). Carbohydrate Polymers. 2014;**105**(Supplement C):135-144

[27] Xiu A et al. Rheological properties of Salecan as a new source of thickening agent. Food Hydrocolloids. 2011;**25**:1719-1725. DOI: doi.org/10.1016/j.foodhyd.2011.03.013

[28] Zhao LZ et al. Recent advances in clay mineral-containing nanocomposite hydrogels. Soft Matter. 2015;**11**(48):9229-9246

Chapter 9

Development of Clay Nanoparticles Toward Bio and Medical Applications

Seyyed Mojtaba Mousavi, Seyyed Alireza Hashemi,
Sarvenaz Salahi, Mojgan Hosseini,
Ali Mohammad Amani and Aziz Babapoor

Additional information is available at the end of the chapter

http://dx.doi.org/10.5772/intechopen.77341

Abstract

Clay nanoparticles are among the most applicable and cost-affordable materials, all of which have a variety of applications in case of medical science. In this chapter, key characteristics of the clay nanoparticles along with their major groups, structure, morphology, and physicochemical properties were evaluated. Thereafter, the applications of clay nanoparticles in the field of nanocomposite, polymeric matrices, and medicine were investigated, while specimen production procedures were also reviewed. The main focus of this chapter is to investigate the applications of clay nanoparticles in bio- and medical science. In fact, organically modified clay nanoparticles (organoclays) are an attractive class of hybrid organic–inorganic nanomaterials with potential applications in case of polymer nanocomposites, rheological properties modification, and drug delivery carrier.

Keywords: clay nanoparticle, bioapplication, medicine, nanocomposite

1. Introduction

Clay nanoparticles are natural materials in nanoscale that originate from clay. They have attracted much attention in recent years due to their widespread applications. The interest in exploiting clay nanoparticles for various purposes is due to their high surface and unique physical and chemical properties.

In 2013, a group of researchers focused on clay nanoparticles as a drug delivery system. Preparation, physical/chemical properties, and bioaccumulation of clay nanoparticles based

on drug delivery systems, as well as their application in the food system as a nanocarrier for vitamins, antioxidants, linoleic acid, and the other foods, were discussed [1]. In addition, studies have shown that nanotechnology will revolutionize the food industry [2]. Nanoscale food control can lead to the correction of micromolecular properties of foods such as taste, aroma, texture, sensory characteristics, processing ability and stability throughout the process, and storage. Nanotechnology applications grow rapidly in the food and ingredient sector. Advanced nanoelectronics, in combination with good nanomaterials and intelligent biological components, are able to develop very specific and selective measuring devices to identify potentially hazardous agents, including viruses, pathogenic microorganisms, as well as inappropriate physical and chemical substances in foods [3–5]. The micro/nanotechnology accelerates the decreasing size of the sensor to the extent appropriate for application (applied field) [6–8].

In addition to ensuring food safety, nanotechnology improves our lives by monitoring quality and nutrition status [9, 10]. Food packaging is another area that has used nanomaterials to increase the shelf life of the food by improving the preserving properties. Nylon-based nanocomposites are currently used to produce beverage bottles in Korea and the United States [11]. Polymer nanoparticles are made by dispersing nanoparticles into a polymer matrix [12]. For example, nylon/silicate nanocomposite containing 2% non-mineral nanoparticle has two times higher tensile strength and thermal stability (at a temperature above 100°C) than pure nylon [12]. Nylon-based nanocomposites are formed by the dispersion of silicate layers on a continuous polymer matrix. This structure significantly reduces the amount of oxygen or carbon dioxide release (diffusion) in encapsulation, since these gases should be distributed through the space between dispersed nano-silicate layers [13]. Properties such as strength and thermal stability make this nanocomposite ideal for packaging food. Several attempts and experiments have been carried out to provide various types of antioxidants, nutrients, minerals, drugs, and other applicable factors through food [14]. Currently, most efforts to develop delivery systems focus on drugs. While safety and cost concerns are one of the most important factors in choosing food for the customer, high production costs of drug delivery systems are still acceptable in medicine. Clay nanoparticles are minerals in clay that have attracted much attention due to the biological application of their abundance in nature, simplicity of construction, and biocompatibility [15–18]. Clay nanoparticles also have a great potential for nutrition because they have been used to treat and protect as a traditional medicine since the beginning of human civilization [19–21]. Clay minerals have been used as laxatives, antidiarrhea, anti-inflammatory agents, blood purification, reducing infections, and healing of stomach ulcers [22]. In addition, biocompatible clay minerals are currently used as oral antioxidants [23, 24]. Clay nanoparticles have unique layer structures, including the accumulation of nanoparticles with metal ions and intracellular ions for charge balancing [25]. The two-dimensional (2D) structure illustrates interesting strategies for the development of new nano-hybrid systems by enhancing active biochemical molecules into space (**Figure 1**). Intrinsically, unstable agents can be protected against processing conditions and hard-working environment and ultimately released with a controlled pattern in a desirable environment [26–28]. Many studies have shown that nano-layered materials can encapsulate DNA [29, 30], nucleotides [31, 32], drugs [33, 34], proteins [35], and even viruses [36]. These nano-hybrid systems are designed to enhance the efficient delivery to cells and the effectiveness of biochemical molecules [37–39]. However, the application of nanoscale materials to nutrients delivery is very limited.

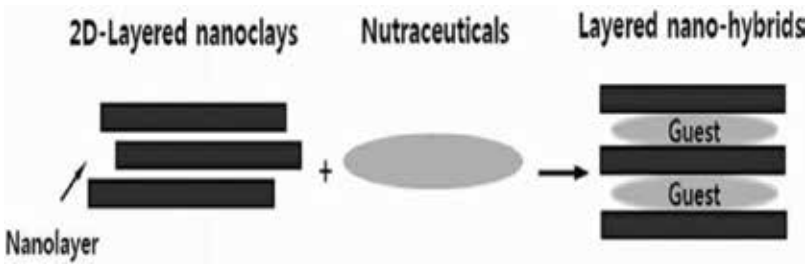

Figure 1. A scheme of clay-layered nanomaterial systems [1].

2. Delivery efficiency and biocompatibility of clay nanoparticles

2.1. Structural and physical properties of nanoclays

Nanoclays are fine-grained crystalline materials. A layer is the basic structural unit of nanoclays, and these layers are prone to arrange themselves over one another like pages of a book. Individual layers are composed of the tetrahedral and/or octahedral sheets, and this arrangement of sheets plays a vital role in defining and distinguishing these clay minerals. In tetrahedral sheet, the silicon-oxygen tetrahedra are linked to neighboring tetrahedra by sharing three corners while the fourth corner of each tetrahedron forms a part to the adjacent octahedral sheet. The octahedral sheet is usually composed of aluminum or magnesium in a sixfold coordination with oxygen from the tetrahedral sheet and with hydroxyl.

2.2. Structural features

Clay layer nanoparticles are divided into two different types of anion and cation depending on the level of layer charge and the types of interlayer ions. Anionic layer nanomaterials typically have been created by double-layered hydroxides (LDHs) with alterable anions in interlayer spaces. LDHs include a wide range of chemical compounds and their layered structure that can be of a great variety to produce poly-types. For example, aluminosilicate cationic nanoparticles like montmorillonite (MMT) have octagonal and quadrilateral plates with high internal surfaces. The main structure of cationic clays is based on a framework, where the unit structure is composed of an octagonal-twisted sheet between two quadrilateral plates. In **Figure 2**, the structure of the double-layer hydroxide and cationic clay (MMT) is presented.

Therefore, cationic and anionic clay nanoparticles can be applied as transfer carriers, which depend on the charge of molecules and essentially on their unique layered structure.

2.3. Biocompatibility

In general, clay nanoparticles are considered as biodegradable materials. In fact, cationic minerals have traditionally been applied in a variety of fields including skin chemotherapy, laxatives, antidiarrhea, and anti-inflammatory agents as well as antimicrobial agents [40–42]. Recently, they are used as lubricants and distributary in pharmaceutical programs to improve chemical, physical, and organoleptic properties [43–45]. MMT can be considered as an

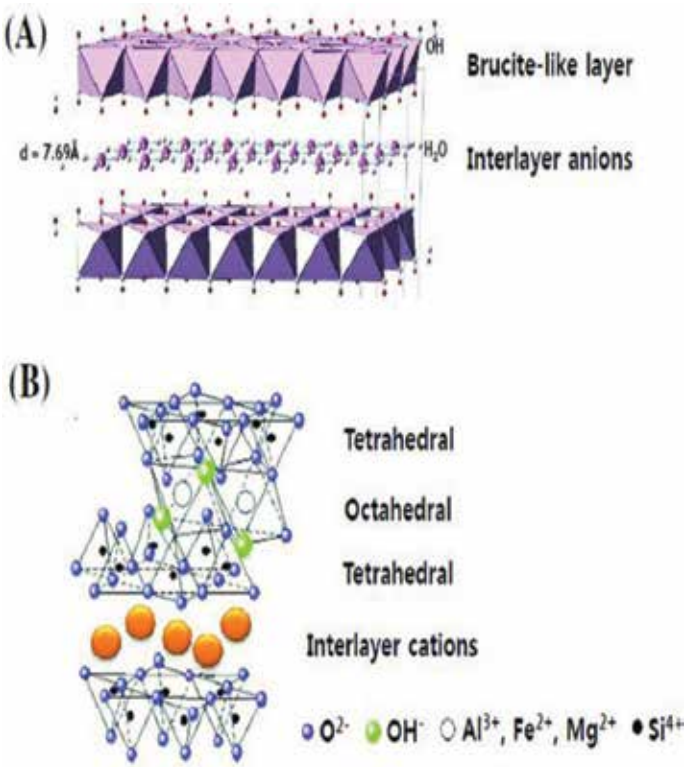

Figure 2. (A) Double-layer hydroxide and (B) cationic clay (MMT) [1].

eco-friendly cationic clay [46], which is commonly used in many pharmaceutical formulations as an active and additive substance [47]. In addition, anionic nanoparticles of LDH in carbonate form are used as an antacid agent (antipepsin) to neutralize gastric acid, which is related to its alkaline properties under physiological pH [48]. The results show that LDH has a lower toxicity compared to single-walled carbon nanotubes and iron oxide and silica nanoparticles.

2.4. Clay nanoparticles for nutrient delivery systems

As previously described, clay nanoparticles are biocompatible materials with a high internal space, a high ion exchange capacity, and a low toxicity that these properties make them ideal for the bioactive compound delivery systems. The nanoclay encapsulation system can be prepared in a relatively simple and inexpensive process compared to other delivery systems. In addition to improving the solubility of the drug or active compounds, the nanoparticle encapsulation system has been considered for oral applications due to its high adhesion properties that are useful for molecules against GI barriers [49]. Choi's research team reports an easy way of encapsulating the strongest antioxidant by MMT with cation exchange reaction (**Figure 3(A)**) [50]. γ-L-glutamyl-L-cysteinylglycine (GSH) is a cellular antioxidant protector (preserver) against reactive oxygen species by neutralizing free radicals. GSH stability can be increased by encapsulating GHS on MMT. The tested GSH-MMT on mice resulted in a significant increase in the bioavailability and high activity of antioxidants in the plasma (**Figure 3(B)**).

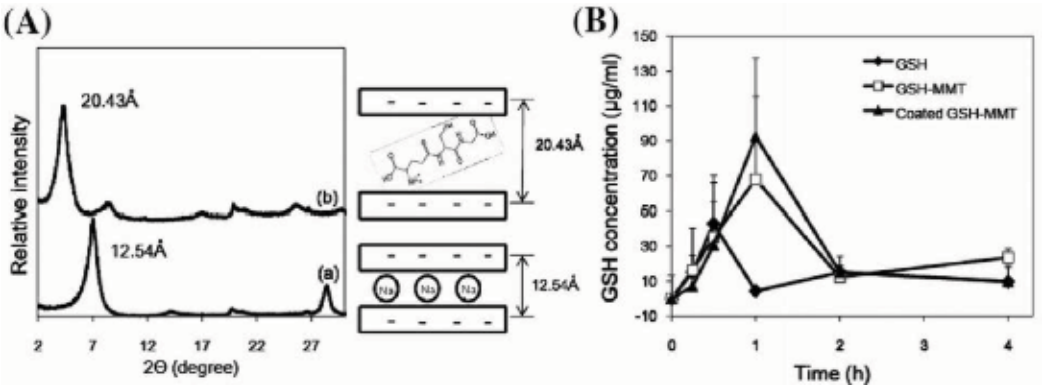

Figure 3. (A) X-ray pattern of (a) MMT and (b) GSH-MMT hybrid; and (B) GSH concentration in mice plasma [1].

Clay nanoparticles have attracted a great deal of attention as a good candidate for packaging of various materials, and it clearly demonstrates the increase in the sustainability and bioavailability of functional molecules.

2.5. The effect of clay mineral nanoparticles on the growth performance of internal organs and blood biochemistry of chickens compared to vaccines and antibiotics

Al-Beitawi et al. [51] investigated the effect of three levels of nanoclay minerals (1, 1.5, and 2%) on the growth performance of internal organs and blood biochemistry of chickens compared to vaccines and antibiotics. The experiment was conducted in nine diets for more than 36 days [51]. Groups 1–3 were fed with diet without clay mineral nanoparticles, and group C1 (positive with vaccines and antibiotics), C2 (positive only with vaccine), and C3 negative and without any of them (as control group). Treating groups with a similar diet to the levels mentioned earlier were done once or twice in a week. Performance of chickens, which fed with 2% clay nanoparticles, significantly improved in terms of body weight and feed conversion rates compared to control groups. With regard to blood biochemistry, high-density lipoprotein that is beneficial to the body was increased. Current results indicate that the mineral clay nanoparticles at certain levels and doses improve the performance of chickens. Nanotechnology is considered as a new potential tool for improving broiler chickens. Researchers believe that the beneficial and positive effects of the use of mineral clay nanoparticles as an additive to the diet of broiler chicks may be due to several factors such as the concentration, dose, and nature of nanoparticles [51]. Desai et al. observed that a nano-supplement form would increase the surface area, which may also increase the absorption and consequently the use of minerals [52]. In addition, Weiss et al. reported that the size of nanoparticles may increase the function or bioavailability of nutrients and compounds [53]. Mushtaq et al. reported that Na^+ is the main cation of extracellular fluids involved in several functions including acid-base balance and amino acid absorption and glucose utilization that is beneficial for body growth, which may have a significant improvement in the growth performance of broiler chickens. On the other hand, the interest in using nanotechnology as a new tool in feeding broiler chicks shows that nanoparticles have very different physical and chemical properties from large particles [54]. In 2013, Sawors et al. suggested that the number of muscle cells returns to genetic, environmental, and nutritional factors [55]. On the other hand, creating more accessible mineral resources,

such as clay nanoparticles, can have positive effects on tissue development. According to the obtained results, it can be concluded that the mineral clay nanoparticles have a favorable effect on total serum protein and its cleft [51]. Nanoparticles have been reported to exhibit several new characteristics of transfer and absorption and also have more effective absorption. The researchers suggested that the superior performance of clay nanoparticles may be due to smaller size and larger surfaces that improve intestinal absorption [56].

2.6. Evaluation of the clay nanoparticles toxicity in epithelial cells

The extending continuous use of products containing nanoparticle for a wide range of applications has raised public health and safety concerns. Although products containing clay nanoparticles cannot be toxic, human contact during its preparation, production, or disposal process can have undesirable effects on health, which makes it necessary to evaluate the biocompatibility of clay nanoparticles. A group of researchers examined the effects of platelet toxicity (Bentone MA, ME-100, Cloisite Na+, Nanomer PGV, and Delite LVF) on human lung [57]. They used automated cells for the first time in real-time impedance imaging compositions and also showed the effect of toxicity on the difference in the dose level and the time-dependent of both types of clay nanoparticles [57]. Clay nanoparticles are used in a wide range of modern products such as electronic, food, clothing, tire, medicine, sunscreen, cosmetics, sports equipment, polymer composites, bone implantation, controlled drug delivery systems, protective coatings (such as anti-corrosion, antibacterial, or antimolding), and for the synthesis of materials [58]. Clay nanoparticles, for example, plastic nanocomposites, are being developed to create unique devices for the next generation of biological applications, including antimicrobial agents, drug delivery, and cancer treatment [59–62].

2.7. Characterization of clay nanoparticles

SEM and TEM images are shown in **Figure 4**. In **Table 1**, a summary of the physiochemical properties of clay nanoparticles such as purity, specific surface area, zeta potential, and so on has been shown, which essentially affects the absorption and toxicity of nanoparticles.

2.8. Application of nanoclay-based composites in bone tissue engineering

The properties of MMT clay, such as its ability to absorb various types of toxins and the ability to cross the digestive tract (stomach and intestines) [60, 63–66], along with the ability to carry and transfer the drug [67–71], encourage human to use it in tissue engineering applications. It is reported that these nanoparticles are removed from the body because they cannot be absorbed by the intestines and they can also be dissolved by the acids in the stomach or intestine [72]. In addition, clay is used as an edible laxative and an antidiabetes [72]. The above suggests that clay is suitable for tissue engineering applications, and decomposed products can be disposed without any effects on the normal body function. The use of MMT clay for bone tissue engineering applications needs further research. In the few studies that have been done in the past, MMT has been used to prepare nano-composites that examine the effect of adding clay on the mechanical and biological properties of polymers [73, 74]. Researchers have used 5-aminovaleric acid-modified MMT clay to prepare polymer composites for bone tissue engineering studies [75].

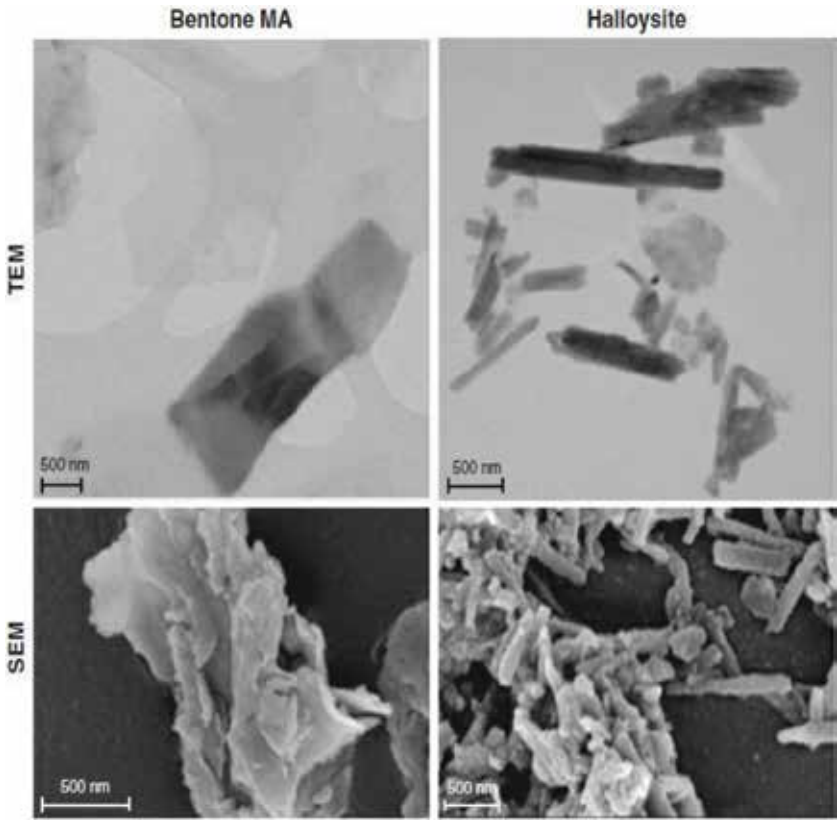

Figure 4. SEM and TEM images [57].

Geometry	Nanoclay	Chemical formula	Purity (%)	Zeta potential (Mv)	Specific surface area (m^2/g)
Tubular	Halloysite MP1	$Al_2Si_2O_5(OH)_4 \times 2H_2O$	90	−41	65
	Halloysite	$Al_2Si_2O_5(OH)_4 \times 2H_2O$	90	−32.1	64
Platelet	Nanomer PGV	$M^+y(Al_{2-y}Mg_y)(Si_4)O_{10}(OH)_2 \times nH_2O$	100	−51.9	ND
	ME-100	$Na_{2x}Mg_{3.0-x}Si_4O_{10}(F_yOH_{1-y})_2$	100	−52.3	9
	Delelite LVF	$(Si,Al)_8(Al,Fe,Mg)_4O_{20}(OH)_4,Xn,m(H_2O)$	100	−45.1	600
	Bentone MA	$Na_{0.4}Mg_{2.7}Li_{0.3}Si_4O_{10}(OH)_2$	98	−36.6	600
	Cloisite Na^+	$(Na,Ca)_{0.33}(Al,Mg)_2Si_4O_{10}(OH)_2$	98	−48.6	800

ND, not tested.

Table 1. Physiochemical properties of clay nanoparticles [57].

2.9. Montmorillonite (MMT) as a carrier for drug delivery

Clay as a carrier for drug delivery is an amazing interdisciplinary field that brings together biology, materials science, and nanotechnology. Composites based on clay minerals have

effect on a variety of fields, especially in pharmaceutical science. The tremendous variety of these natural materials has made the widespread collection of clays and polymers available to researchers [76–84]. The controlled drug delivery system is a method for the development of nanostructures and materials that can encapsulate high concentrations of materials, pass through a cell membrane, and release the drug in the target region for a given period. Clay minerals have exceptional (unique) characteristics such as low toxicity, better biocompatibility, and are guaranteed for a controlled drug release, and thus they are used in biological applications in pharmaceuticals, cosmetics, and even medical purposes [85, 86]. MMT is a natural mineral clay with a layered structure and prominent features such as a high internal surface area and cation exchange capacity (CEC), a high absorption capacity, and low toxicity [64, 87]. MMT with a net charge of the network can well be swollen in the presence of water and hydrophilic solvents, because positive-charged bioactive compounds can be inserted in interlayer (inside layer) spaces by electrostatic interaction. Many attempts have been made to develop MMT as a carrier for drug delivery, for example, to improve the water solubility of insoluble drugs and control the release of bioactive molecules [61, 83, 84, 88–93]. Biochemical properties, which make clay valuable for pharmaceutical applications, include high absorption capacity, high internal surface, high exchange ability, interlayer spatial reactions with drug molecules, chemical moisture, and low toxicity [61, 72, 83, 84, 94–96]. Clay is widely used as an active agent and an additive in pharmaceutical formulations [97–99]. In pharmaceuticals, MMT has found extensive applications as a suspension and a stabilizer, as well as an absorbent and clear factor. Also, MMT has been used as a drug carrier or an additive in pharmaceutical formulations [71, 72, 99–104]. The MMT's ion exchange capacity provides the possibility of replacing Na + with other organic and inorganic cations to increase performance. It also causes the use of MMT and other clay species as a tissue regeneration agent [71, 76–84, 96, 105] (**Table 2**).

The authors have shown that increasing the concentration of silicate nanoparticles increases the mechanical strength of polymer nanoparticles [107]. Wang et al. prepared 2008 complex

Drug	
5-Flurouracil (anticancer)	Ibuprofen (nonsteroidal anti-inflammatory)
Amino acids	BSA (model protein)
Plasmid DNA (gene delivery)	Donepezil (Alzheimer)
Paclitaxel (anticancer drug)	Docetaxel (anticancer drug)
Lidocaine (local anesthetic drug)	5-Fluorouracil (anticancer drug)
Glutathione (antioxidant)	Doxorubicin (anticancer drug)
Ibuprofen (anti-inflammatory)	Buspirone hydrochloride (antianxiety)
Captopril (hypertension)	Timolol maleate (β-adrenergic blocking agent)
Vitamin B1	Ranitidine hydrochloride (antacid)
Quinine (antimalarial drug)	Procainamide hydrochloride (antiarrhythmia drug)
Tamoxifen (anticancer drug)	Epidermal growth factor (tissue engineering)

Table 2. List of drugs used in clay as carrier [106].

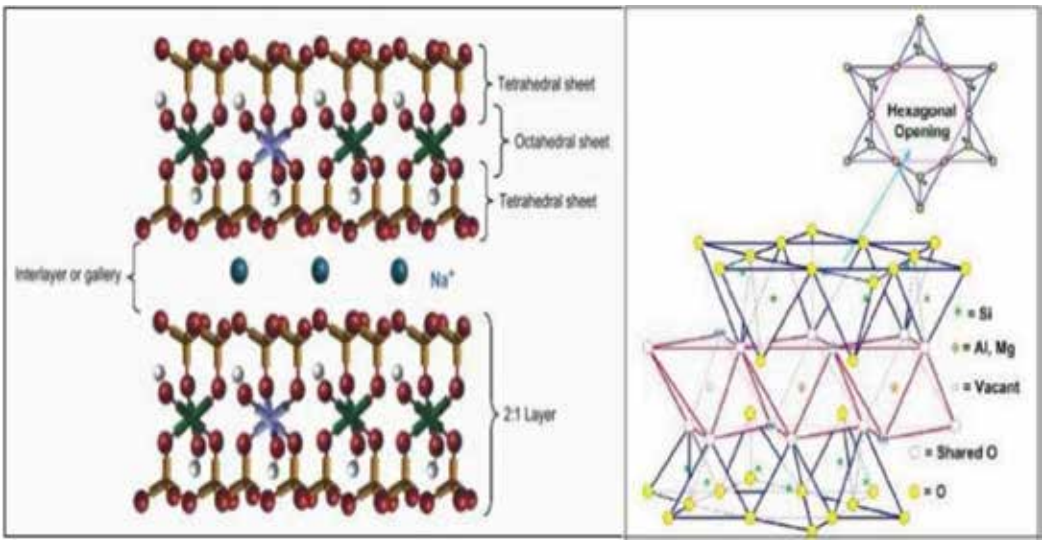

Figure 5. MMT network structure [106].

chitosan-montmorillonite (HTCC/MMT) nanocomposites for the application as protein carriers [103]. In 2010, Shhameli et al. showed a new green color combination for MMT/chitosan nanoparticles (CS) and its antibacterial actions [108]. Lee and Fu found that the properties of the released drug can be controlled by the charge of N-isopropylacrylamide/MMT nanocomposites [109]. In general, the ability to exchange ions, interoperability, and biocompatibility of MMT has made it an ideal candidate for drug delivery. In addition to pharmaceutical use, MMT and its nanocomposites are bioactive agents that have a wide range of applications. MMT can play an important and powerful role in intestinal detoxification, since it can absorb food, microbial, and metabolic toxins and, surprisingly, can increase the hydrogen ions in acidosis. Also, MMT can be used for edible purpose for digestive system detoxification, constipation reduction, internal parasite eradication, strengthening of the immune system, liver detoxification, reduction of stomach pain, and poisoning by bacteria. Revitalizing drugs and tissue engineering programs include bone remodeling as growth agents and wound dressing. The network structure of this is shown in **Figure 5** [106].

MMT is widely used in the treatment of bone pain and damaged muscle, chronic headache, open wounds, special skin conditions (acne, eczema, red seeds on the skin, etc.), diarrhea, hemorrhoids, stomach ulcers, intestinal problems, anemia, rapid recovery of injuries (bruises, stretching, burns, etc.), severe bacterial infections, skin rejuvenation, and various health issues. Therefore, it can be beneficial to health because all its activities are physical and there is no chemical reaction on the body. After taking, no or small amount of MMT is absorbed in the digestive system and the rest is excreted (repulsed) by feces. According to the ISI database, interest in drug delivery by clay shows a significant increase in scientific publications (**Figure 6**) [106].

2.10. Mechanisms of drug-clay interactions

According to the tests conducted, the basis of controlled drug delivery is the use of laminar (layer) interference. Interference may occur by mixing sub-solids (ion converters) with ionic

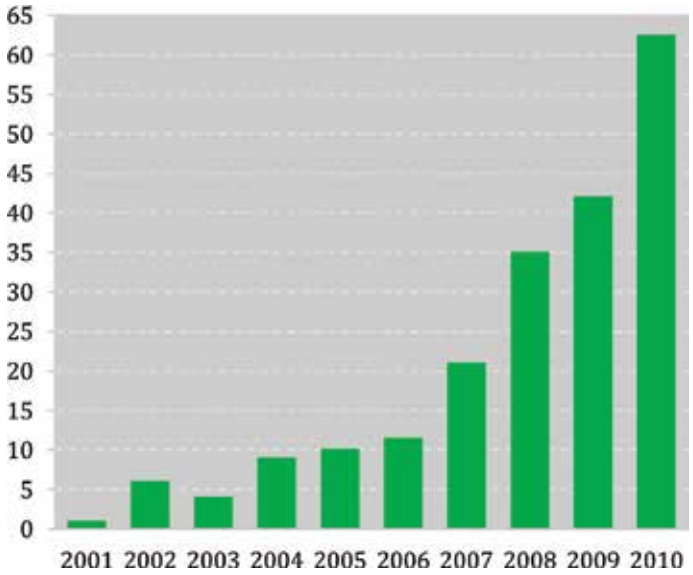

Figure 6. The number of studies on the use of clay nanoparticles as carrier for drug delivery [106].

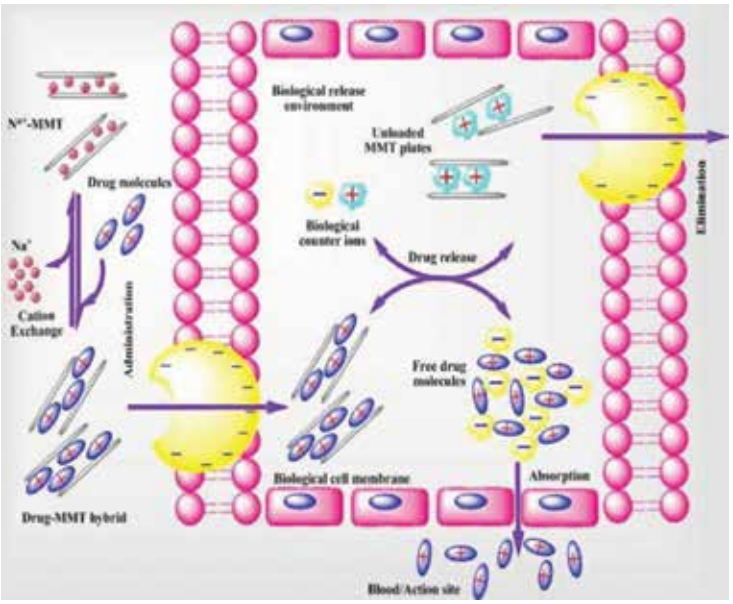

Figure 7. Mechanism of release of MMT and absorption in the body [106].

material in solution. In biological fluids, "anti-ions" can move the drug into the substrate and transfer it to the body, so the converter can be removed or decomposed at the end (**Figure 7**) [106]. Smectites, especially MMT and saponite, have been further studied due to their ionic exchange capacity compared to other silicates (talc, kaolin, and fibrous mineral clay). A specific mechanism depends on factors such as functional groups and chemical physical properties

of organic compounds [109–111]. Silicate-based composites exhibit a good inhibitory (barrier) effect due to complicated intrusive pathways that small molecules need to undergo (pass) in order to clarify the material (**Figure 8**) [112].

2.11. The latest MMT pattern used in drug delivery systems

Lin et al. showed the 5-FU interference on the MMT inner layers [61]. 5-FU-MMT was determined and the successful interference of the drug in MMT was confirmed by opening the inner layer and changing the XRD pattern to the lower 2θ angle, and the results are presented in **Figure 9**. Finally, it can be concluded that the total amount of 5-FU absorbed in MMT is approximately 87.5 mg/g MMT.

Park et al. reported the placement of donepezil molecules on clay (Laponite, LA, saponite, SA and MMT) and provided descriptive information, which confirmed the well-located donepezil molecules in the inner layers of clay (**Figure 10**) [91]. The absorption amount and the donepezil molecular structure depend on the cationic exchange ability of clay, which has designed drug release patterns. The rate of release can be increased easily by using a large cationic polymer. The Eudragit® E-100 hybrid, coated with such a polymer, shows the release of drug at higher speeds over a short period. Therefore, nanoclay materials are proposed as an advanced carrier for drug delivery with a controllable release feature.

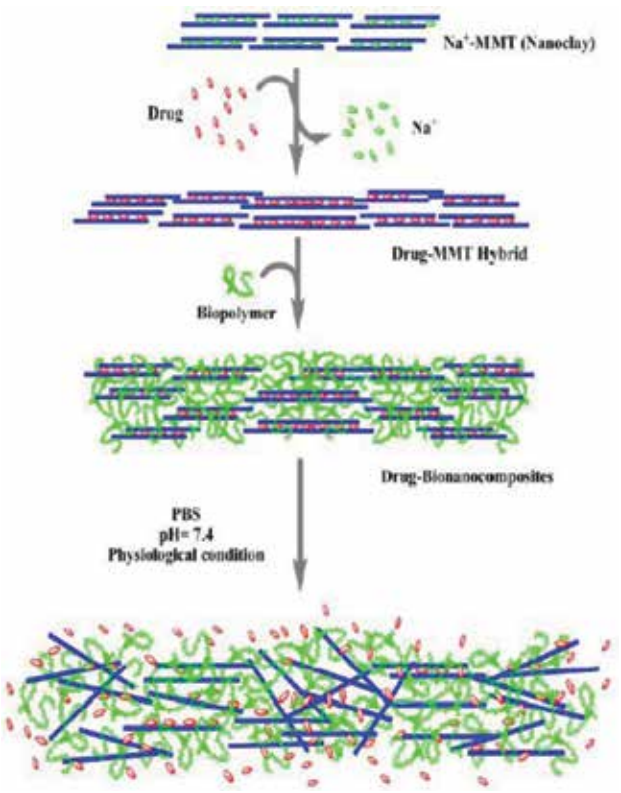

Figure 8. Mechanism of drug release from nanocomposites [106].

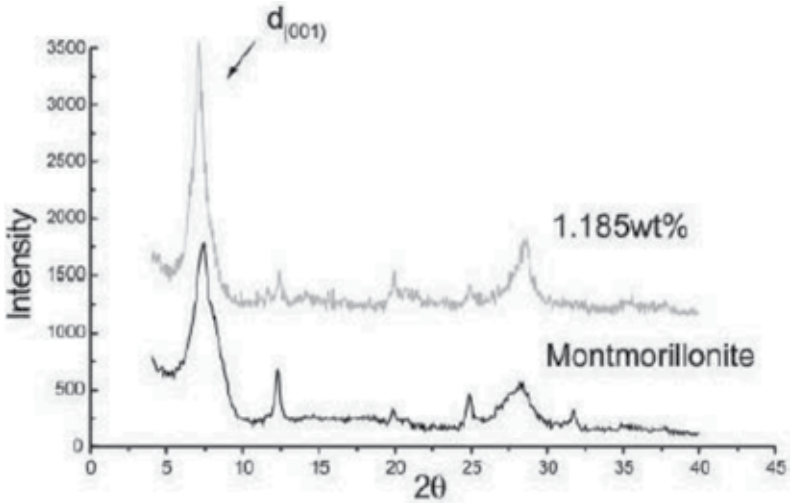

Figure 9. XRD patterns of MMT and 5-FU-MMT [106].

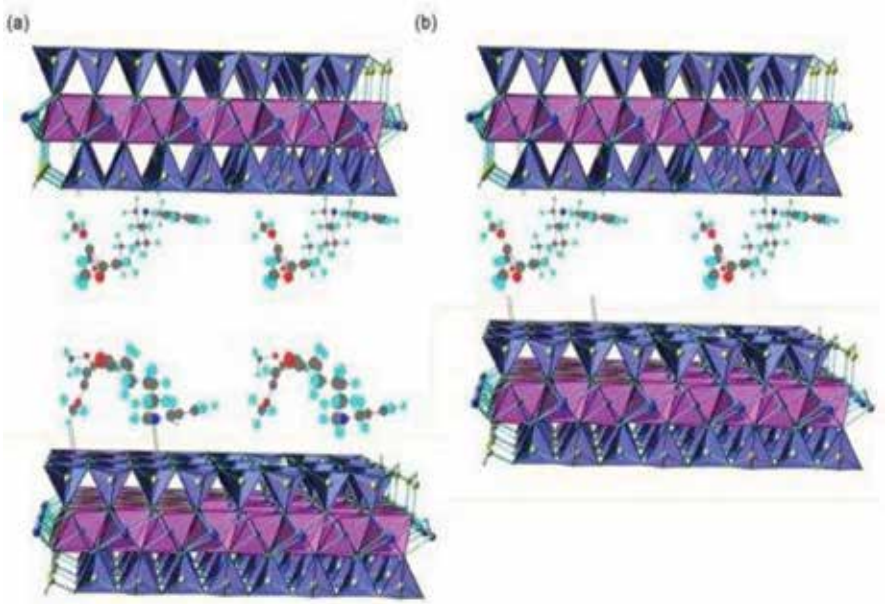

Figure 10. The schematics of donepezil interference in clay nanomaterials: (a) the dual-layer composition and (b) the single-layer composition [106].

2.12. 2D clay nanoparticles for drug delivery in cancer treatment

Two-dimensional kaolinite clay nanoparticles are used in the drug delivery system. The increasing of spacing of the kaolinite nanoparticles from 0.72 to 4.16 nm is due to the interference of guest species with different chain lengths of organic materials that can increase the drug delivery efficiency and reduce the toxicity of doxorubicin (DOX). The kaolinite (Kaolin) and kaolin compounds show a high level of biocompatibility and low toxicity against

pancreatic cancer cells, gastric cancer, prostate cancer, breast cancer, esophageal cancer, and thyroid cancer diagnosis. However, lung cancer and leukemia require structural harder compounds for drug delivery. DOX-Kaolin and its internal contents exhibit more drug release rates in acidic environment than in the neutral environment. The use of two-dimensional clay nanoparticles for a drug delivery system can pave the way for high-performance nanotherapies with superior antitumor efficacy and significant reduction of side effects. As shown in **Figure 11**, it is used for the treatment of tumors [113].

2.13. An overview of clay chemistry

Broadly, clay minerals are structured of two principal units: tetrahedral (T) and octahedral (O) sheets [114, 115]. Each tetrahedron consists of a central cation (mostly Si^{4+}) coordinated to four O^{2-} anions and linked to adjacent tetrahedra through three shared oxygens on the corners (basal oxygens Ob) forming an infinite 2D hexagonal mesh (**Figure 12**). The fourth O^{2-} (apical oxygen Oa) remains unshared, lying perpendicular to the tetrahedral sheet, and is the main site of interaction with the octahedral sheet. Each octahedron consists of a metal cation (M^{n+}) coordinated to six O^{2-} and/or OH^- anions. Adjacent octahedra are linked to each other by sharing edges (two O^{2-} or OH^-), forming an octahedral sheet. If Mn is divalent (Mg^{2+}), a trioctahedral or a brucite-like sheet is produced, if it is trivalent (Al^{3+}), then two out of every three octahedral sites are occupied, leaving a vacant site and the generation of a dioctahedral or a gibbsite-like sheet. Clays can be classified into 1:1 and 2:1 types according to the layering

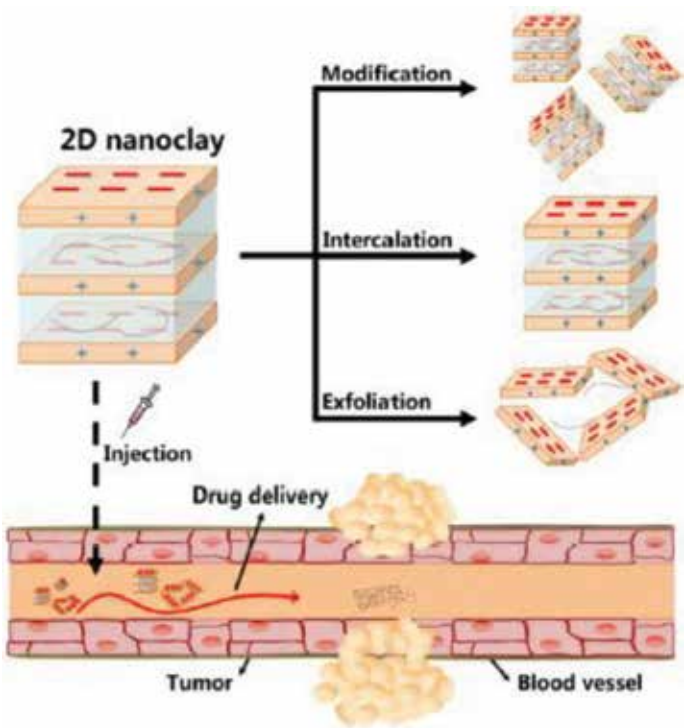

Figure 11. Schematic design and kaolin and kaolin compounds for the treatment of tumors [113].

of T and O sheets. 1:1 (or T-O) clay minerals consist of a single T sheet linked to a single O sheet, and 2:1 (or T-O-T) clay minerals consist of a single O sheet sandwiched between two T sheets (**Figure 12**, **Table 3**).

In the case of smectites, an octahedral sheet of metal oxides (usually Mg^{2+} or Al^{3+}) is sandwiched between two tetrahedral silica sheets. Two types of charges originate on the smectite clay particle: (1) permanent negative charges on the surface due to isomorphous cation substitution in the tetrahedral and/or octahedral sheets (e.g., Li^{+} for Mg^{2+} in Laponite) balanced by exchangeable cations such as Na or Ca^{2+} in the interlayer gallery. (2) Positive (amphoteric) charges on the edges due to broken Si-O, Al-OH, and Mg-OH groups. At pH < Zero Point of Charge (ZPC), these edge charges become positive with anion exchange capacity, while at pH > ZPC, they become negative with a cation exchange capacity. Adapted with permission [116]. Copyright 2014, John Wiley and Sons.

Clay structure and reactivity. The reactivity of clays is largely a function of their swelling capacity. Kaolinite (of the 1:1 clay family) and talc and pyrophyllite (of the 2:1 clay family) possess no structural charges and consequently are non-swelling and of low adsorption capacity. The high-layer charge on vermiculite and illite restricts their swelling and gelling tendency although their surface area and CEC are relatively high. Smectites are characterized by their relatively low-layer charge which allow their particles to undergo complete dissociation in water and give them interesting rheological/gel-forming properties and surface reactivity. Halloysite is formed of hydrated 1:1 layers which role up into nanotubes (alumina sheet on the inside and silica sheet on the outside surface) and sepiolites (and palygorskite) are characterized by their inverted 2:1 ribbon structures. Such arrangements confer large SSA, porosity, and sorptive capacity. Adapted with permission [117].

2.14. Morphology

We focused on the investigation of the potential toxic effects caused by nanoclay particles currently used in tons in several industrial applications. Bentonite, montmorillonite, and

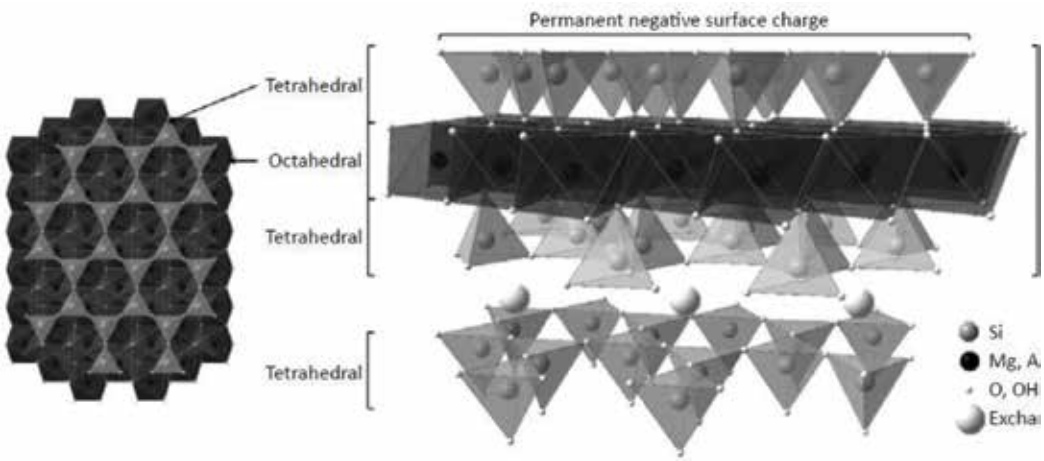

Figure 12. The structure of smectites. Clays are formed of layered tetrahedral (T) and octahedral (O) sheets.

Family group		Species	Chemical formula	Charge/formula unit	CEC	Particle size (nm)
1:1	Serpentine-kaolin	Halloysite	$Al_2Si_2O_5(OH)_4.nH_2O$	~0 [114]	~10 meq/100 g [121, 122]	Nanotube diameter of ~50 nm, lumen of ~15 nm, and length of ~1 mm [119, 126]
2:1	Smectites	Montmorillonite	$Na_m(Al_{2-m}Mg_m)Si_4O_{10}(OH)_2.nH_2O$	~0.2–0.6 [114]	~80–150 meq/100 g [121, 122]	~80–300 nm diameter and ~ 1 nm thickness [127, 129]
		Laponite (synthetic hectorite)	$Na_h(Mg_{3-h}Li_h)Si_4O_{10}(OH)_2.nH_2O$			~25–30 nm diameter and ~ 1 nm thickness [120, 123]
	Sepiolite-palygorskite	Sepiolite	$X^*(Mg, Al, Fe^{3þ})_4(Si,Al)_6O_{15}(OH)_2.nH_2O$	—	~4–40 meq/100 g [124, 125]	Nanofiber diameter of ~15 nm and length of ~200–400 nm [124, 128]

Table 3. Key clay mineral species explored for tissue engineering and regenerative medicine applications with their relevant structural/compositional properties.

kaolin are platy clay particles ranging from nanometers to micrometers, whereas halloysite nanotubes are hollow rod-like particles having a lumen diameter of ~20 nm and a tube length ranging from 300 nm to 2 μm. Spherical silica nanoparticles were also used as a material mimicking the outer silica layer of the clays. Graphene oxide nanosheets having the shape and size close to smectite clays were selected as a material with a relatively high reported toxicity, 30, which was also confirmed in our study. The typical AFM images demonstrating the geometry and sizes of nanoparticles used in this study are given in **Figure 13**.

The nanoparticles used were suspended in water and added to protozoan media at a range of concentrations. Prior to toxicity investigation, the hydrodynamic diameters and surface potential of nanoparticles were determined using dynamic light scattering (DLS) and electrophoretic mobility measurements in water (**Table 4**) [118].

2.15. Ecotoxicological profile

No ecotoxicological studies of nanoclay have been identified as of November 30, 2010. Since clay is a naturally occurring material for which environmental organisms have adapted throughout evolution, the inherent toxicity is expected to be low; however, issues related to small particle sizes may occur [78].

2.16. Toxicological profile

Today, few studies are available, and there is limited knowledge about the toxicity of nanoclays and the chemical derivatives that may be generated during the production and processing of polymer nanoclay composites. However, in general, nanoclay is not considered to pose a major health risk although a possible content of crystalline quartz may constitute a risk.

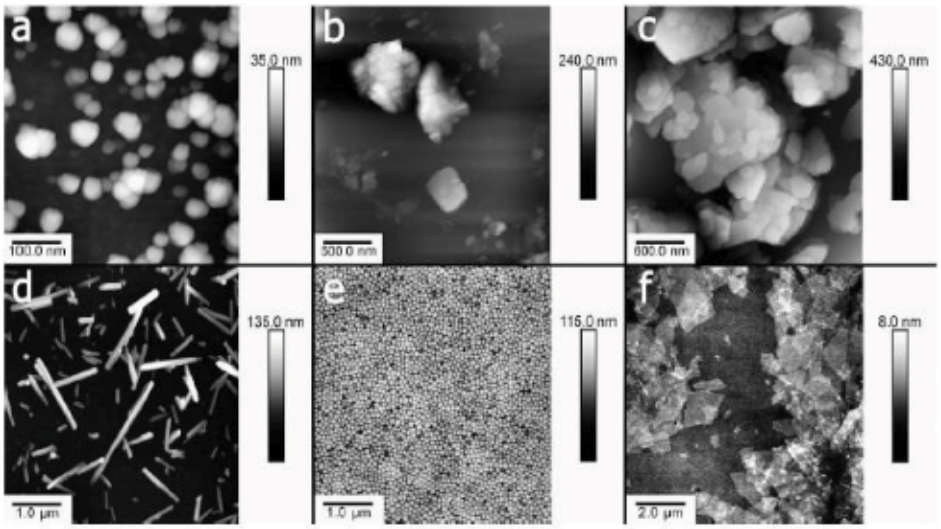

Figure 13. Typical AFM images of (a) bentonite, (b) montmorillonite, (c) kaolin, (d) halloysite, (e) silica, and (f) graphene oxide nanoparticles.

Particles	Hydrodynamic diameter, nm	Zeta-potential, mV	AFM measured dimensions
Halloysite	510 ± 12	−25 ± 3	50 nm diameter, 400–1500 nm length
Kaolin	930 ± 22	−36 ± 1	300–700 nm width, 30–100 nm thick
Montmorillonite	1600 ± 60	−29 ± 1	300–600 nm width, 10–50 nm thick
Bentonite	3040 ± 660	44 ± 2	~4 μm width, ~100 nm thick
Silica	122 ± 3	−39 ± 6	120 nm diameter
Graphene oxide	1940 ± 90	−47 ± 2	2000 nm width, 2–10 nm thick

Table 4. Hydrodynamic diameters, zeta-potential values, and AFM measured sizes of nanoclay particles, silica nanospheres, and graphene oxide nanoflakes.

Furthermore, functionalized nanoclays containing quaternary ammonium or phosphonium functional groups on the surface are described as potentially problematic, as ammonium and phosphonium ions in their pure form can cause asthma symptoms (NFA, 2010) [78].

3. Conclusions

Clay nanoparticles have traditionally been used in many applications such as treatment, skin chemotherapy, and medicine to improve the human health and life. In addition, they have recently been developed as additives, lubricants, and active materials in pharmaceutical formulation. Although their application in food science is relatively limited, they have the potential to

deliver nutrients. Their unique structure is able to place bioactive molecules in the interior space. Nanoparticles that contain nutrients have the ability to protect GI against the environment and control the release features. They can enter the cell and with their adhesion properties facilitate the transfer of GI molecules against barriers. Also, they exhibit low toxicity. Research on the development of clay nanoparticles based on oral delivery systems for nutrients or functional compounds indicates that they are effective in protecting and controlling deliveries and also contributing to the increased bioavailability. The promising potential of the clay nanoparticles makes a new perspectives for the development of nano-based oral delivery systems. The toxicity of nanomaterials is a very important issue. In general, the results show that higher doses of clay nanoparticles result in the death of cells, which is a concern for medical applications. As an important point in the application of clay nanoparticles in delivery systems, to achieve clay-based controlled delivery systems, one of the best ways is to place organic molecules on the underlying layers of mineral clay. Besides, its composites can be used to improve properties.

Author details

Seyyed Mojtaba Mousavi[1,2], Seyyed Alireza Hashemi[1,2], Sarvenaz Salahi[3], Mojgan Hosseini[4], Ali Mohammad Amani[1,2]* and Aziz Babapoor[5]

*Address all correspondence to: amani_a@sums.ac.ir

1 Department of Medical Nanotechnology, School of Advanced Medical Sciences and Technologies, Shiraz University of Medical Sciences, Shiraz, Iran

2 Pharmaceutical Sciences Research Center, Shiraz University of Medical Sciences, Shiraz, Iran

3 Iranian Center of Neurological Research, Tehran, Iran

4 Department of Science, Islamshahr Branch, Islamic Azad University, Sayad Shirazi St. Islamshahr, Tehran, Iran

5 Department of Chemical Engineering,University of Mohaghegh Ardabili, Ardabil, Iran

References

[1] Choi SJ, Kim YR. Bioinspired Layered Nanoclays for Nutraceutical Delivery System. In ACS Symp. Series. 2013. pp. 207-220

[2] Egger S, Lehmann RP, Height MJ, Loessner MJ, Schuppler M. Antimicrobial properties of a novel silver-silica nanocomposite material. Applied and Environmental Microbiology. 2009;**75**(9):2973-2976

[3] Lim MC, Shin YJ, Jeon TJ, Kim HY, Kim YR. Analytical and Bioanalytical Chemistry. 2011;**400**:777-785

[4] Joung CK, Kim HN, Im HC, Kim HY, Oh MH, Kim Y. Sensors and Actuators B: Chemical. 2012;**161**:824-831

[5] Huang Y, Dong X, Liu Y, Li LJ, Chen PJ. Materials Chemistry. 2011;**21**:12358-12362

[6] Batt CA. Science. 2007;**316**:1579-1580

[7] Min J, Kim JH, Lee YS, Namkoong K, Im HC, Kim HN, Kim YH, Huh N, Kim YR. Lab on a Chip. 2011;**11**:259-265

[8] Yager P, Edwards T, Fu E, Helton K, Nelson K, Tam MR, Weigl BH. Nature. 2006;**442**: 412-418

[9] Arora, Amit, Padua GW. Nanocomposites in food packaging. Journal of Food Science. 2010;**75**(1):R43-R49

[10] Malathi AN, Santhosh KS, Nidoni U. Recent trends of biodegradable polymer: biodegradable films for food packaging and application of nanotechnology in biodegradable food packaging. Current Trends in Technology and Science. 2014;**3**(2):73-79

[11] Blasco C, Pico Y. Trends in Analytical Chemistry. 2011;**30**:84-99

[12] Hussain F, Hojjati M, Okamoto M, Gorga RE. Polymer-matrix nanocomposites, processing, manufacturing, and application: an overview. Journal of Composite Materials. 2006;**40**(17):1511-1575

[13] Grunlan JC, Grigorian A, Hamilton CB, Mehrabi ARJ. Applied Polymer Science. 2004;**93**: 1102-1109

[14] Huang Q, Yu H, Ru QJ. Food Science. 2010;**75**:R50-R57

[15] Theng KG. The Chemistry of Clay-Organic Reactions. London, UK: Adam Hilger; 1974

[16] Nemecz E. Clay Minerals. Budapest, Hungary: Akademiai Kiado; 1981

[17] Ogawa M, Kuroda K. Chemical Reviews. 1995;**95**:399-438

[18] Vaccari A. Catalysis Today. 1998;**41**:53-71

[19] Chung HE, Kim IS, Baek M, Yu J, Choi SJ. Long-term cytotoxicity potential of anionic nanoclays in human cells. Toxicology and Environmental Health Sciences. 2011;**3**(2): 129-133

[20] Sanchez CJ, Parras J, Carretero MI. The effect of maturation upon the mineralogical and physicochemical properties of illitic-smectitic clays for pelotherapy. Clay Minerals. 2002;**37**(3):457-463

[21] Veniale F, Barberis E, Carcangiu G, Morandi N, Setti M, Tamanini M, Tessier D. Applied Clay Science. 2004;**25**:135-148

[22] Gorchakov VN, Dragun GN, Kolmogorov YP, Smelova VA, Tikhonova LI, Tysjachnova YV. Nuclear Instruments and Methods in Physics Research Section A. 2001;**470**:437-440

[23] Burzlaff A, Brethauer S, Kasper C, Jackisch BO, Scheper T. Cytometry, Part A. 2004;**62**: 65-69

[24] Peterson CL, Perry DL, Masood H, Lin H, White JL, Hem SL, Fritsch C, Haeusler F. Pharmaceutical Research. 1993;**10**:998-1004

[25] Baes CF, Mesmer RE. The Hydrolysis of Cations. Vol. 95-98. New York: A Wiley-Interscience Publication; 1976. pp. 112-122

[26] Zümreoglu-Karan B, Ay A. Layered double hydroxides—multifunctional nanomaterials. Chemical Papers. 2012;**66**(1):1-10.

[27] Choi SJ, Choy JH. Nanomedicine. 2011;**6**:803-814

[28] Oh, Jae-Min, et al. Cellular uptake mechanism of an inorganic nanovehicle and its drug conjugates: enhanced efficacy due to clathrin-mediated endocytosis. Bioconjugate Chemistry. 2006;**17**(6):1411-1417

[29] Ferencz Z. Mechanochemical Preparation and Structural Characterization of Layered Double Hydroxides and their Amino Acid-Intercalated Derivatives (Doctoral dissertation, szte; 2016

[30] Desigaux L, Belkacem MB, Richard P, Cellier J, Leone P, Cario L, Leroux F, Taviot-Gueho C, Pitard B. Nano Letters. 2006;**6**:199-204

[31] Choy JH, Kwak SY, Jeong YJ, Park JS. Angewandte Chemie: International Edition. 2000; **39**:4042-4045

[32] Wong Y, Cooper HM, Zhang K, Chen M, Bartlett P, Xu ZP. Journal of Colloid and Interface Science;**369**:453-459

[33] Choy JH, Jung JS, Oh JM, Park M, Jeong J, Kang YK, Han OJ. Biomaterials. 2004;**25**: 3059-3064

[34] Choi SJ, Oh JM, Choy JHJ. Physics and Chemistry of Solids. 2008;**69**:1528-1532

[35] Rahman MB, Basri M, Hussein MZ, Rahman RN, Zainol DH, Salleh AB. Applied Biochemistry and Biotechnology. 2004;**118**:313-320

[36] Jin S, Fallgren PH, Morris JM, Chen Q. Science and Technology of Advanced Materials. 2007;**8**:67-70

[37] Oh JM, Park M, Kim ST, Jung JY, Kang YK, Choy JHJ. Physics and Chemistry of Solids. 2006;**67**:1024-1027

[38] Kim JY, Choi SJ, Oh JM, Park T, Choy JHJ. Nanoscience and Nanotechnology. 2007;**7**: 3700-3705

[39] Oh JM, Choi SJ, Lee GE, Han SH, Choy JH. Advanced Functional Materials. 2009;**19**:1-8

[40] Carretero MI, Pozo M. Clay and non-clay minerals in the pharmaceutical industry: Part I. Excipients and medical applications. Applied Clay Science. 2009;**46**(1):73-80

[41] Bolger R. Industrial Minerals. 1995 August:52-63

[42] Ferrand T, Yvon J. Applied Clay Science. 1991;**6**:21-38

[43] Poensin D, Carpentier PH, Féchoz C, Gasparini S. Effects of mud pack treatment on skin microcirculation. Joint Bone Spine. 2003;**70**(5):367-370

[44] Summa V, Tateo F. Applied Clay Science. 1998;**12**:403-417

[45] Cara S, Carcangiu G, Padalino G, Palomba M, Tamanini M. Applied Clay Science. 2000;**16**: 125-132

[46] Gupta G, Gardner WJ. Hazardous Materials. 2005;**118**:81-83

[47] Wang X, Du Y, Luo J. Biopolymer/montmorillonite nanocomposite: preparation, drug-controlled release property and cytotoxicity. Nanotechnology. 2008;**19**(6):065707

[48] Tarnawski A, Pai R, Itani R, Wyle FA. Digestion. 1999;**60**:449-455

[49] Doborozsi D. Oral liquid mucoadhesive compositions. U.S. Patent 6.638.521; 2003

[50] Kim TH, Lee JA, Choi SJ, Oh JM. Polymer coated CaAl-layered double hydroxide nanomaterials for potential calcium supplement. International Journal of Molecular Sciences. 2014;**15**(12):22563-22579

[51] Al-Beitawi NA, Momani Shaker M, El-Shuraydeh KN, Bláha J. Effect of nanoclay minerals on growth performance, internal organs and blood biochemistry of broiler chickens compared to vaccines and antibiotics. Journal of Applied Animal Research. 2017;**45**(1):543-549

[52] Desai MP, Labhasetwar V, Waltwr E, Levy RJ, Amidon GL. The mechanism of uptake of biodegradable microparticles in Caco-2 cells in size dependent. Pharmaceutical Research. 1997;**14**:1568-1573

[53] Weiss J, Takhistov P, McClements J. Functional material in food nanotechnology. Journal of Food Science. 2006;**71**(9):107-116

[54] Ramirez-Mella M, Hernandez-Mendo O. Nanotechnology in animal production. Tropical and Subtropical Agroecosystems. 2010;**12**(3):423-429

[55] Sawors F, Pineda L, Hotowy A, Jaworski S, Prasek M, Sawors E. Nanonutrition of chicken embryos. The effects of silver nanoparticles and ATP on expression chosen genes involved in myogenesis. Archives of Animal Nutrition. 2013;**67**(5):347-355

[56] Ghithrani BD, Chan WC. Elucidating the mechanism of cellular uptake and removal of protein-coated gold nanoparticles of different sizes and shapes. Nano Letters. 2007;**7**:1542-1550

[57] Verma NK, Moore E, Blau W, Volkov Y, Ramesh Babu P. Cytotoxicity evaluation of nanoclays in human epithelial cell line A549 using high content screening and real-time impedance analysis. 2012

[58] Floody MC, Theng BKG, Reyes P, Mora ML. Natural nanoclays: Applications and future trends: A Chilean perspective. Clay Minerals. 2009;**44**:161-176

[59] Suresh R, Borkar SN, Sawant VA, Shende VS, Dimble SK. Nanoclay drug delivery system. International Journal of Pharmaceutical Sciences and Nanotechnology. 2010;**3**:901-905

[60] Dong Y, Feng SS. Poly(D,L-lactide-co-glycolide)/montmorillonite nanoparticles for oral delivery of anticancer drugs. Biomaterials. 2005;**26**:6068-6076

[61] Lin FH, Lee YH, Jian CH, Wong JM, Shieh MJ, Wang CY. A study of purified montmorillonite intercalated with 5-fluorouracil as drug carrier. Biomaterials. 2002;**23**:1981-1987

[62] Nayak PL, Sahoo D. Chitosan-alginate composites blended with cloisite 30B as a novel drug delivery system for anticancer drug paclitaxel. International Journal of Plastics Technology. 2011;**15**:68-81

[63] Forni F, Iannuccelli V, Coppi G, Bernabei MT. Effect of montmorillonite on drug release from polymeric matrices. Archiv der Pharmazie (Weinheim). 1989;**322**(11):789-793

[64] Lee W-F, Fu Y-T. Effect of montmorillonite on the swelling behavior and drug-release behavior of nanocomposite hydrogels. Journal of Applied Polymer Science. 2003;**89**(13):3652-3660

[65] Lin F-H, Chen C-H, Cheng WTK, Kuo T-F. Modified montmorillonite as vector for gene delivery. Biomaterials. 2006;**27**(17):3333-3338

[66] Viseras C, Aguzzi C, Cerezo P, Lopez-Galindo A. Uses of clay minerals in semisolid health care and therapeutic products. Applied Clay Science. 2007;**36**(1-3):37-50

[67] Takahashi T, Yamada Y, Kataoka K, Nagasaki Y. Preparation of a novel PEG-clay hybrid as a DDS material: Dispersion stability and sustained release profiles. Journal of Controlled Release. 2005;**107**(3):408-416

[68] des Rieux A, Fievez V, Garinot M, Schneider Y-J, Préat V. Nanoparticles as potential oral delivery systems of proteins and vaccines: A mechanistic approach. Journal of Controlled Release. 2006;**116**(1):1-27

[69] Sun B, Ranganathan B, Feng S-S. Multifunctional poly_D,L-lactide-co-glycolide/montmorillonite_PLGA/MMT_ nanoparticles decorated by trastuzumab for targeted chemotherapy of breast cancer. Biomaterials. 2008;**29**(4):475-486

[70] Wang X, Du Y, Luo J. Biopolymer/montmorillonite nanocomposite: Preparation, drug-controlled release property and cytotoxicity. Nanotechnology. 2008;**19**(6):065707

[71] Depan D, Kumar AP, Singh RP. Cell proliferation and controlled drug release studies of nanohybrids based on chitosan-G-lactic acid and montmorillonite. Acta Biomaterialia. 2009;**5**(1):93-100

[72] Carretero MI. Clay minerals and their beneficial effects upon human health: A review. Applied Clay Science. 2002;**21**(3-4):155-163

[73] Marras SI, Kladi KP, Tsivintzelis I, Zuburtikudis I, Panayiotou C. Biodegradable polymer nanocomposites: The role of nanoclays on the thermomechanical characteristics and the electrospun fibrous structure. Acta Biomaterialia. 2008;**4**(3):756-765

[74] Zheng JP, Wang CZ, Wang XX, Wang HY, Zhuang H, Yao KD. Preparation of biomimetic three-dimensional gelatin/montmorillonite-chitosan scaffold for tissue engineering. Reactive and Functional Polymers. 2007;**67**(9):780-788

[75] Ambre AH, Katti KS, Katti DR. Nanoclay based composite scaffolds for bone tissue engineering applications. Journal of Nanotechnology in Engineering and Medicine. 2010; **1**(3):031013

[76] Joshi GV, Kevadiya BD, Patel HA, Bajaj HC, Jasra RV. Montmorillonite as a drug delivery system: Intercalation and in vitro release of timolol maleate. International Journal of Pharmaceutics. 2009;**374**:53-57

[77] Joshi GV, Patel HA, Kevadiya BD, Bajaj HC. Montmorillonite intercalated with vitamin B1 as drug carrier. Applied Clay Science. 2009;**45**:248-253

[78] Joshi GV, Kevadiya BD, Bajaj HC. Design and evaluation of controlled drug delivery system of buspirone using inorganic layered clay mineral. Microporous and Mesoporous Materials. 2010;**132**:526-530

[79] Joshi GV, Kevadiya BD, Mody HM, Bajaj HC. Confinement and controlled release of quinine on chitosan–montmorillonite bionanocomposites. Journal of Polymer Science Part B: Polymer Physics. 2012;**50**:423-430

[80] Joshi GV, Pawar RR, Kevadiya BD, Bajaj HC. Mesoporous synthetic hectorites: A versatile layered host with drug delivery application. Microporous and Mesoporous Materials. 2011;**142**:542-548

[81] Kevadiya BD, Joshi GV, Bajaj HC. Layered bionanocomposites as carrier for procainamide. International Journal of Pharmaceutics. 2010;**388**:280-286

[82] Kevadiya BD, Joshi GV, Mody HM, Bajaj HC. Biopolymer-clay hydrogel composites as drug carrier: Host–guest intercalation and in vitro release study of lidocaine hydrochloride. Applied Clay Science. 2011;**52**:364-367

[83] Kevadiya BD, Patel TA, Jhala DD, Thumbar RP, Brahmbhatt H, et al. Layered inorganic nanocomposites: A promising carrier for 5-fluorouracil (5-FU). European Journal of Pharmaceutics and Biopharmaceutics. 2012;**81**:91-101

[84] Kevadiya BD, Thumbar RP, Rajput MM, Rajkumar S, et al. Montmorillonite/poly-(ε-caprolactone) composites as versatile layered material: Reservoirs for anticancer drug and controlled release property. European Journal of Pharmaceutical Sciences. 2012;**47**:265-272

[85] Giannelis EP. Review: Polymer layered silicate nanocomposites. Advanced Materials. 1996;**8**:29-35

[86] Choy JH, Choi SJ, Oh JM, Park T. Clay minerals and layered double hydroxides for novel biological applications. Applied Clay Science. 2007;**36**:122-132

[87] Komine H. Simplified evaluation for swelling characteristics of bentonites. Engineering Geology. 2004;**71**:256-279

[88] Fudala AA, Palinko II, Kiricsi I. Preparation and characterization of hybrid organicinorganic composite materials using the amphoteric property of amino acids: Amino acid intercalated layered double hydroxide and montmorillonite. Inorganic Chemistry. 1999;**38**:4653-4658

[89] Zheng JP, Luan L, Wang HY, Xi LF, Yao KD. Study on ibuprefen/montmorillonite intercalation composites as drug release system. Applied Clay Science. 2007;**36**:297-301

[90] Kollar T, Palinko I, Konya Z, Kiricsi I. Intercalating amino acid guests into montmorillonite host. Journal of Molecular Structure. 2003;**651-653**:335-340

[91] Park JK, Choy YB, Oh JM, Kim JY, Hwang SJ, Choy JH. Controlled release of donepezil intercalated in smectite clays. International Journal of Pharmaceutics. 2008;**359**:198-204

[92] Park M, Kim CY, Lee DH, Choi CL, Choi J, Lee SR, Choy JH. Intercalation of magnesium-urea complex into swelling clay. Journal of Physics and Chemistry of Solids. 2004;**65**:409-412

[93] Baek M, Choy JH, Choi SJ. Montmorillonite intercalated with glutathione for antioxidant delivery: Synthesis, characterization, and bioavailability evaluation. International Journal of Pharmaceutics. 2012;**425**:29-34

[94] Gamiz E, Linares J, Delgado R. Assessment of two Spanish bentonites for pharmaceutical uses. Applied Clay Science. 1992;**6**:359-368

[95] Bolger R. Industrial minerals in pharmaceuticals. Industrial Minerals. 1995;**8**:52-63

[96] Sun B, Ranganathan B, Feng SS. Multifunctional poly(D,L-lactide-coglycolide)/montmorillonite (PLGA/MMT) nanoparticles decorated by trastuzumab for targeted chemotherapy of breast cancer. Biomaterials. 2008;**29**:475-486

[97] Cornejo J, Hermosin MC, White JL, Barnes JR, Hem SL. Role of ferric iron in the oxidation of hydrocortisone by sepiolite and palygorskite. Clays and Clay Minerals. 1983;**31**:109-112

[98] Ferrand T, Yvon J. Thermal properties of clay pastes for pelotherapy. Applied Clay Science. 1991;**6**:21-38

[99] Poensin D, Carpentier PH, Fechoz C, Gasparini S. Effects of mud pack treatment on skin microcirculation. Joint, Bone, Spine. 2003;**70**:367-370

[100] Sposito G, Skipper NT, Sutton R, Park SH, Soper AK, Greathouse JA. Colloquium paper: Surface geochemistry of the clay minerals. Proceedings of the National Academy of Sciences of the United States of America. 1999;**96**:3358-3364

[101] Aguzzi C, Cerezo P, Viseras C, Caramella C. Use of clays as drug delivery systems: Possibilities and limitations. Applied Clay Science. 2007;**36**:22-36

[102] Carretero MI, Pozo M. Clay and non-clay minerals in the pharmaceutical industry. Part I. Excipients and medical applications. Applied Clay Science. 2009;**46**:73-80

[103] Wang X, Du Y, Luo J. Biopolymer/montmorillonite nanocomposite: Preparation, drug-controlled release property and cytotoxicity. Nanotechnology. 2008;**19**:065707 (7pp). DOI: 10.1088/0957-4484/19/6/065707

[104] Takahashi T, Yamada Y, Kataoka K, Nagasaki Y. Preparation of a novel PEG–clay hybrid as a DDS material: Dispersion stability and sustained release profiles. Journal of Controlled Release. 2005;**107**:408

[105] Vaiana CA, Leonard MK, Drummy LF, Singh KM, Bubulya A, Vaia RA, Naik RR, Kadakia MP. Epidermal growth factor: Layered silicate nanocomposites for tissue regeneration. Biomacromolecules. 2011;**12**:3139-3146

[106] Kevadiya BD, Bajaj HC. The layered silicate, montmorillonite (MMT) as a drug delivery carrier. 2013

[107] Cypes SH, Saltzman WM, Giannelis EP. Organosilicate-polymer drug delivery systems: Controlled release and enhanced mechanical properties. Journal of Controlled Release. 2003;**90**:163-169

[108] Shameli K, Ahmad MB, Yunus WMZW, Rustaiyan A, Ibrahim NA, Zargar M, Abdollahi Y. Green synthesis of silver/montmorillonite/chitosan bionanocomposites using the UV irradiation method and evaluation of antibacterial activity. International Journal of Nanomedicine. 2010;**5**:875-887

[109] Browne JE, Feldkamp JR, White JL, Hem SL. Characterisation and adsorptive properties of pharmaceutical grade clays. Journal of Pharmaceutical Sciences. 1980;**69**:816-823

[110] Lagaly G. Pesticide-clay interactions and formulations. Applied Clay Science. 2001;**18**: 205-209

[111] Tolls J. Sorption of veterinary pharmaceuticals in soils: A review. Environmental Science & Technology. 2001;**35**:3397-3406

[112] Yano K, Usuki A, Okada A. Synthesis and properties of polyimide-clay hybrid films. Journal of Polymer Science Part A: Polymer Chemistry. 2000;**35**:2289-2294

[113] Zhang Y, Long M, Huang P, Yang H, Chang S, Hu Y, Tang A, Mao L. Intercalated 2D nanoclay for emerging drug delivery in cancer therapy. 2016

[114] Brigatti MF, Galan E, Theng BKG. Structure and mineralogy of clay minerals. Developments in Clay Science. 2013;**5**:21-81

[115] Brown G, Brindley GW. Crystal structures of clay minerals and their Xray identification. Journal of Minerals Society. 1980;305-356. DOI: 10.1016/j.jenvman.2011.05.031

[116] Dawson JI, Oreffo ROC. Clay: New opportunities for tissue regeneration and biomaterial design. Advanced Materials. 2013;**25**:4069-4086

[117] Mousa M, Evans ND, Oreffo ROC, Dawson JI. Clay nanoparticles for regenerative medicine and biomaterial design: A review of clay bioactivity. Biomaterials. 2018;**159**:204-214

[118] Kryuchkova M, Danilushkina A, Lvo Y, Fakhrullin R. Evaluation of toxicity of nanoclays and graphene oxide in vivo: A *Paramecium caudatum* study. Environmental Science: Nano. 2016;**3**:442

[119] Lvov YM, DeVilliers MM, Fakhrullin RF. The application of halloysite tubule nanoclay in drug delivery. Expert Opinion on Drug Delivery. 2016;**13**:977-986

[120] Neumann BS, Sansom KG. The rheological properties of dispersions of laponite, a synthetic hectorite-like clay, in electrolyte solutions. Clay Minerals. 1971;**9**:231-243

[121] Olphen EHV. Data Handbook for Clay Materials and Other Nonmetallic Minerals. 1979

[122] Drever JI. The Geochemistry of Natural Waters. Englewood Cliffs, NJ: Prentice-Hall, Inc. 1982

[123] Ruzicka B, Zaccarelli E. A fresh look at the Laponite phase diagram. Soft Matter. 2011; **7**:1268

[124] Galan E. Properties and applications of palygorskite-sepiolite clays. Clay Minerals. 1996;**31**:443-453

[125] Jones BF, Galan E. Sepiolite and palygorskite. Reviews in Mineralogy and Geochemistry. 1988;**19**(1):631-674

[126] Lvov YM, Shchukin DG, Mohwald H, Price RR. Halloysite clay nanotubes for controlled release of protective agents. ACS Nano. 2008;**2**:814-820

[127] Li PR et al. Evaluation on cytotoxicity and genotoxicity of the exfoliated silicate nanoclay. ACS Applied Materials & Interfaces. 2010;**2**:1608-1613

[128] Castro-Smirnov FA et al. Cellular uptake pathways of sepiolite nanofibers and DNA transfection improvement. Scientific Reports. 2017;**7**:5586

[129] Rawat K, Agarwal S, Tyagi A, Verma AK, Bohidar HB. Aspect ratio dependent cytotoxicity and antimicrobial properties of nanoclay. Applied Biochemistry and Biotechnology. 2014;**174**:936-944

Edited by Mansoor Zoveidavianpoor

This book presents recent developments and research activities that highlight the importance of clay science and engineering in the environment and medical and civil engineering. The book contains nine chapters separated into three main sections: (1) Clay for the Environment, (2) Clay in Civil Engineering, and (3) Clay in Medical Applications. There are four chapters in the first section and the focus is made on the topics related to an introduction to the natural sources and chemical structure of one of the important clay types, montmorillonite. The application of waste recycling and the removal of arsenic and fluoride are the focus of next two chapters. In addition, a technique for corrosion protection is presented as the fourth chapter within this section. In the second section, special emphasis has been placed on the importance and application of clay in civil engineering, which is demonstrated in two chapters. In the third section, new research and development on utilizing clay minerals in medical applications is presented. Intended for readers wishing to acquire an understanding of the current trends in clay science and engineering and comprehension of the issue, this book addresses exciting topics in this field.

Published in London, UK

IntechOpen

ISBN 978-1-83881-554-7
9 781838 815547